



Tesis Doctoral:

Síntesis y Aplicaciones Catalíticas de Complejos de Rh e Ir con Ligandos Fosfina y Ciclopentadienilo

Jesús Campos Manzano

Sevilla, 2012

UNIVERSIDAD DE SEVILLA
CONSEJO SUPERIOR DE INVESTIGACIONES CIENTÍFICAS

Departamento de Química Inorgánica

Instituto de Investigaciones Químicas



**Síntesis y aplicaciones catalíticas de Complejos de Rh
e Ir con Ligandos Fosfina y Ciclopentadienilo**

**Synthesis and Catalytic Applications of Rhodium and
Iridium Complexes Bearing Phosphine and
Cyclopentadienyl Ligands**

Jesús Campos Manzano

Sevilla, 2012

Síntesis y aplicaciones catalíticas de Complejos de Rh e Ir con Ligandos Fosfina y Ciclopentadienilo

por

Jesús Campos Manzano

Trabajo presentado para aspirar al

Título de Doctor en Química

Sevilla, 2012

Fdo.: Jesús Campos Manzano

El Director:

Ernesto Carmona Guzmán
Catedrático de Química Inorgánica
(Universidad de Sevilla)

A Irene

...porque “cuando tú estás a mi vera, mi otoño ya es primavera”

A mis padres

Como ocurre en ocasiones al empezar un proyecto nuevo, sea en el ámbito que sea, lo más difícil suele dejarse para el final. Después de estos cuatro años de trabajo es precisamente en este momento en el que me veo arrojado a la difícil tarea de agradecer, y recordar, a todos aquellos que me han acompañado en esta aventura. Se trata de una de las labores más complicadas de todo el doctorado, y no por el riesgo que podría correr mi integridad física o emocional si, de manera fortuita o intencionada, omitiera a alguna de estas personas, que también; sino porque será la única parte del manuscrito que gozará del placer de ser leída por más de siete personas (incluyéndome a mí mismo, por supuesto).

El primer reto que se plantea es, ¿por quién empiezo y qué orden sigo? ¿Pensarán aquellos que dejo para el final que son menos importantes? Para evitar confusiones aclaro rápidamente que no existirá ningún orden y que, de existir, es obvio que mi mayor agradecimiento, a años luz de distancia, es para Irene, a quien dedico este trabajo. Ciertamente es que podría haberle dedicado algo más bonito, pero también es cierto que cuando chico yo jugaba al fútbol con Sergio Ramos y ahora él es millonario y yo gano mil euros y desde el INEM ya me están abriendo el expediente. Una segunda cuestión, que imagino que a todos mis compañeros y doctores se les habrá pasado por la cabeza cuando estaban en mi actual situación, es la siguiente: ¿Debería agradecer a todo el mundo con quien mi incipiente vida científica se ha cruzado, o simplemente a los que realmente aprecio? Es más, ¿Sería oportuno desagradecer a aquellos que me han hecho la vida un poquito más difícil? Ser, o no ser, políticamente correcto. Pues bien, intentaré ser lo más franco posible sin polemizar indiscriminadamente, pero no querría dejar de lado a aquellos que siempre estarán conmigo, en mi mente, para

recordarme que un solo gusano es capaz de pudrir todo un arriate de yerbabuena.

En primer lugar querría agradecer el coraje y el valor, la solidaridad, el humanismo y, en definitiva, el más impresionante *enterismo* de todos aquellos hombres y mujeres de ciencia que a lo largo de la historia han puesto su prestigio científico al servicio de las más nobles causas sociales. Personajes como Albert Einstein, Lynn Margulis, Lynus Pauling, Barry Commoner, J. B. S. Haldane, y muchos otros que han servido y servirán como referente científico y ético para anteriores generaciones de científicos, para la mía propia y, con toda seguridad, para las generaciones futuras.

Una de las grandes ventajas de trabajar en ciencia es tener la oportunidad de conocer a tantos y tan buenos colegas de profesión que, en muchos casos, han acabado siendo también grandes amigos. A todos ellos tengo que agradecerle que han hecho de este viaje de cuatro años un paseo inolvidable. Lo haré lo mejor que pueda para intentar acordarme de todos. Empezando por los clásicos, los que ya estaban en Cartuja cuando yo llegué y me recibieron con los brazos abiertos, recuerdo a Mario, que ya se le veía hablando de que el quíntuple estaba casi casi, pó anda que no le quedaba ná. Cuanto me alegro de que haya puesto finalmente la guinda, más bien las guindas, a todos estos años de curro. Y con él trabajaba Irene, que creo que ha sido de las personas más locas que he conocido. Por entonces Jose estaba de estancia, menos mal que no se quedó por tierras nubosas, porque ha sido un colega y compañero de lujo, y siempre recordaré el haber participado en su exitosa aventura cinematográfica y sus fiestas de rancho. Un poco después llegó Cristina, la mejicana que no hablaba así, no ni ná, y menos mal que volvió, porque me pegué dos semanas esperando

que llegara de México para que me enseñara a preparar el iridio-Cp. También me enseñó a manejar la línea de argón y todas esas cosas, lo que le agradezco mucho. La otra cara del laboratorio 1,2 ha estado también llena de gente de la buena, a las que les agradezco su impecable compañerismo estos años: Yohar, Flo, Manolo, Arián, Giovanni, Margarita, Ana y los que me falten. Una segunda generación de artistas inundó de energía este laboratorio en los últimos años: María o Marifé, que aunque sea un poco calladita al final se anima y habla, y con quien espero sellar nuestra estupenda colaboración con algunos papers; Carlos, o el renacimiento de JT, porque ha sido un placer currar con él y enseñarle juntos a las niñas de Abengoa algo de química; y por supuesto, las recién llegadas Natalia y Laura.

Si he hecho un vistazo al resto de laboratorios, está claro que he tenido la suerte de compartir estos años con un buen puñado de mostros. He disfrutado al máximo de las pachangas de basket con Juanfran (un gran teórico y maestro del asunto), Caro, Joaquín, Antonio, Nerea, Alex, Gon, Pablo, Tomás, Empar y muchos más. En esas tardes en que uno acababa harto del laboratorio, ahí estaban las pachangas para dar energías y ánimos renovados. Sin estos amigos y cracks del baloncesto esas tardes épicas habrían sido imposibles.

No puedo olvidar entre las grandes figuras de Cartuja a Álvaro, porque es uno de los tíos más colgaos que he conocido, artista hasta la médula, rebotante de calidad humana y modelo de investigador entusiasmado con lo que hace, lo que hizo y lo que hará próximamente. Y tantos otros compañeros que no enumeraré por no dejarme a muchos otros atrás, pero que han demostrado que en la base de este centro, aunque sólo sea en la base, el compañerismo y el colequeo es lo que prima.

Un cariño muy especial le guardo a mis compañeros del Lab 9. Sería imposible de otra manera. Después de compartir 5 metros cuadrados con cinco personas más durante cuatro años, si hemos salido ilesos, es por algo. En nuestro mini centro de curro tenemos a Crispín, que desde que llegó, y por mucho que le pese, se ha convertido en un andaluz más con el que he pasado unos años de lujo. Nuria, que afortunadamente puso algo de cordura cuando hacía falta y que por lo visto le han reservado ya un panteón mu mono en el cielo por tó lo que ha tenido que aguantar con nosotros. Orestes, compitiendo con Álvaro entre los personajes más grandes con los que he tenido la suerte de cruzarme nunca. Un artistazo con los pies más en el suelo de lo que pudiera parecer y con quien me alegro mucho de haber compartido laboratorio. Marta, exagerao, que voy a decir si la conozco desde la carrera. Pues es una fuera de serie que derrocha buenagentismo y vive en mundos alternativos a los que a veces colegas afortunados podemos entrar. Y me queda Anita, que llegó la última pero al día dos parecía que llevaba ya siete años en el laboratorio. Así son los de Camas, no va a ser tó Curro, Paco y mindundis de medio pelo... Y no me olvido del jefe, de Salva, un maestro del que he podido aprender mucho y un compañero estupendo.

Pero me temo que además de los colegas, que han sido espectaculares, también he tenido la suerte o la desgracia de cruzarme con algunos esperpentos disfrazados de personas o entidades. Cómo no, recordar al brillante Ministerio y su gestión de becas FPU. Espectacular fue el día que nos amenazaron a algunos con arrancarnos la beca si no entregábamos en el plazo de hace tres días el formulario J del anexo H de la Norma 13/24 de la Orden del 2015 del ministro de su hermana, del cuñado de su consejero y de su puñetero padre. Y no han sido los burócratas estatales los únicos, también en nuestro propio centro encontramos la incompetencia en estado puro. Afortunadamente, tanto la

sección de administración del IIQ como la del centro, siempre me han resuelto todas las dudas, papeleo y trámites que he necesitado. A todos ellos les agradezco su impecable trabajo y cordialidad. Sin embargo, aquellos que decidieron administrar el centro como si de su propio patio de recreo se tratara, sin contar ni tan siquiera con la opinión de los afectados por sus nefastas decisiones, a ellos, no tengo nada que agradecerles, simplemente espero que algún día dejen de dar por saco. Pero no sólo los burócratas me han demostrado cómo hacer la vida más difícil. He podido asistir a un mano a mano entre éstos y los políticos, tanto los actuales como los anteriores, que para salvar el país decidieron ahogarlo. Y por supuesto, para empezar, ahoguemos a la ciencia española. En palabras de Bertrand Russell: *Los científicos se esfuerzan por hacer posible lo imposible. Los políticos por hacer lo posible imposible.*

Y ya puestos, me gustaría dedicar un par de frases más. A todos aquellos que padecen un acuciante síndrome de Peter Pan y piensan que el pasado siempre fue mejor, obligándonos a muchos a tener que obviar normas estúpidas, querría dedicarles una reflexión de Isaac Asimov: *Las normas establecidas con razón y con justicia, pueden dejar de ser útiles al cambiar las circunstancias, pero al permitir que continúen vigentes por la fuerza de la inercia, entonces, no sólo es justo, sino también útil, quebrantar aquellas que nos anuncian el hecho de que son inútiles, o incluso realmente perjudiciales.*

También he tenido que cruzarme, como tantos otros compañeros, con aquellos que se ven a sí mismos como mejores que los demás, posiblemente como mecanismo defensivo por su soberana incompetencia. A aquellos que, sin cumplir con sus obligaciones científicas o ni tan siquiera éticas, se dedican a pavonearse

impunemente, les dedico unas palabras de Herman Hesse: *Hay quienes se consideran perfectos, pero es sólo porque exigen menos de sí mismos.*

Y una última dedicatoria a todos y cada uno de los compañeros que con su trabajo diario hacen posible que la ciencia siga avanzando en este centro, a pesar de la mala hierba. En palabras del mismísimo Quijote: *Bien podrán los encantadores quitarme la ventura, pero el esfuerzo y el ánimo será imposible.*

Tengo que agradecer muy especialmente la ayuda que me han brindado algunos compañeros con los que he colaborado directamente en esta Tesis Doctoral, especialmente Miguel y Joaquín. Los resultados descritos en el primer capítulo de este manuscrito sólo han sido posibles gracias al trabajo, codo con codo, con mi colega Migue. Ha sido un placer currar con un tío tan grande y estoy seguro de que seguiremos haciéndolo en el futuro. Trabajar con Joaquín, que se ha encargado de realizar todos los cálculos que aparecen en el manuscrito y otros muchos que ya no cabían, ha sido un gustazo. Currar con un amigo es siempre una suerte, pero si además es un fiero de la química, la situación se torna inmejorable. Otro colaborador de lujo ha sido Riccardo, o el Dr. Peloso, otro máquina de la química y con quien ha sido un gran placer trabajar. También debo agradecer la colaboración de Luis y Eleuterio. El primero por su ayuda en el delicado diseño y montaje de todo el sistema para tritio, así como de otros dispositivos experimentales; el segundo por la resolución de algunas de las estructuras obtenidas por difracción de rayos X que aparecen en la memoria.

Dentro del centro, sólo me falta agradecer a Ernesto, aunque necesitaría mucho tiempo y espacio para escribir unos agradecimientos justos. Como profesor en la facultad fue, sin duda, el mejor de todos. Y aunque no he tenido

tantos jefes como profesores, dudo mucho que su calidad científica y humana pueda llegar a superarse por ningún otro investigador. Tener un maestro como él ha sido sin duda uno de los mayores éxitos y disfrutes de mi doctorado.

Aunque no han compartido vitrina y reactivos conmigo, o nos hemos peleado por el tiempo de RMN, tanto la familia, como todos los colegas, han estado siempre ahí fuera esperando, haciendo de la vida un paseo que merece la pena ser disfrutado al máximo. Como la lista aburriría a cualquiera que haya llegado hasta este punto, recordaré únicamente a mis padres, a quienes dedico esta Tesis, y que desde que tengo uso de razón me han apoyado absolutamente en todo. Porque sin unos cimientos fuertes, como han edificado ellos, cualquier construcción se tambalea.

Para finalizar, mi mayor agradecimiento es para Irene. Todas esas noches en las que salía del laboratorio a las 9, a las 10, a las 10 y media, al llegar a casa, me encontraba con una sonrisa. Porque cada sábado, cada domingo, cada congreso, me lo has pagado con otra sonrisa al volver a casa. Esas vacaciones truncadas y días festivos que no lo fueron, o esos tres meses de estancia, siempre me he encontrado tu comprensión y tu amor como respuesta. A pesar de todos esos momentos que no hemos podido compartir y que he dedicado a mi carrera, siempre has estado ahí, para apoyarme, para animarme y para acompañarme en este periplo. Es por eso, y por mucho más, por lo que te quiero tanto. Preparémonos ahora para la gran aventura que está a punto de empezar, porque todo lo que construyamos juntos será inolvidable.

TABLE OF CONTENTS

Consideraciones Generales	1
Abbreviations	13
Chapter 1. Rhodium–Catalyzed Hydrosilane Chemistry. Catalytic Si–H/D/T Exchanges and D– and T– Silylation of C–X Multiple Bonds.	
I.1 Introduction	19
<i>I.1.1 Isotopic Labeling of Organic Molecules</i>	21
<i>I.1.2 Labeled Hydrosilanes in Organic Synthesis</i>	24
<i>I.1.3 Hydrosilylation Reactions</i>	29
I.2 Results and Discussion	39
<i>I.2.1 Synthesis and Reactivity of the Rhodium Catalyst</i>	41
<i>I.2.2 H/D/T Exchange in Hydrosilanes</i>	45
<i>I.2.3 Hydrosilylation Reactions</i>	61
I.3 Experimental Section	83
I.4 References	125

Chapter 2. Synthesis and Reactivity of Half-sandwich ($\eta^5\text{-C}_5\text{Me}_5$)Ir(III) Complexes of Cyclometalated Aryl Phosphine Ligands

II.1 Introduction	137
II.1.1 C–H Bond Activation, a Brief, General Perspective	139
II.1.2 Half-Sandwich Iridium and Rhodium Complexes for C–H Activation	146
II.1.3 Organometallic Metallacycles and C–H Activation	152
II.1.4 Electrophilic Alkylidenes	155
II.2 Results and Discussion	161
Part A: Study of ($\eta^5\text{-C}_5\text{Me}_5$)Ir(PMe(Xyl)₂)-Derived Compounds	
II.2.A.1 Halide and Pseudohalide Complexes	167
II.2.A.2 Neutral Hydride and Alkyl Complexes	175
II.2.A.3 Hydrogen/Deuterium Exchange Reactions	181
II.2.A.4 Cationic Ir(III) Complexes Generated by Chloride Abstraction from 1–Cl	196
II.2.A.5 Base-catalyzed Intramolecular Dehydrogenative C–C Coupling in 1 ⁺ Leading to the Hydride Phosphine Cation 4 ⁺	202
II.2.A.6 Mechanistic Investigations on the Formation of 4 ⁺	205
II.2.A.7 Synthesis of Iridium (III) Alkylidenes Derived from Compounds 1	215
Summary and Conclusions	234

Part B: Studies on (η^5-C₅Me₅)Ir(PR₂(Xyl)) Units	
<i>II.2.B.1 Synthesis of Chloride Complexes</i>	235
<i>II.2.B.2 Chloride Abstraction from Rh and Ir Halide Complexes</i>	242
<i>II.2.B.3 Reactivity Studies of Hydride-Alkylidene 14⁺</i>	252
<i>Summary and Conclusions</i>	262
II.3 Experimental Section	263
Part A.	265
Part B.	317
II.4 References	363
Conclusiones	373

Table of Contents

CONSIDERACIONES GENERALES

La Química Organometálica se ha desarrollado de forma extraordinaria desde sus comienzos a mediados del siglo XX, como se manifiesta en la enorme cantidad de complejos de muy diversa naturaleza que se han sintetizado hasta la fecha, los cuales exhiben una reactividad química sin precedentes. Estos compuestos se han utilizado en numerosos procesos industriales que en última instancia, han contribuido a mejorar la calidad de nuestra vida. Asimismo, se han empleado complejos organometálicos en procesos relacionados con la vida, en la denominada química bioinorgánica, como agentes antitumorales o con otros fines biológicos, y también en el desarrollo de nuevos materiales y nuevas formas de obtención de energía.

Los resultados que se presentan en esta Memoria se encuadran en una de las líneas de investigación que desarrolla el grupo de Química Organometálica y Catálisis Homogénea del Instituto de Investigaciones Químicas (Centro Mixto Universidad de Sevilla–CSIC), que tiene como objetivo el estudio de las reacciones de ruptura y formación de enlaces C–H, C–O, C–C y otros similares, inducidas de manera selectiva por complejos de los metales del grupo 9 (Rh e Ir, fundamentalmente).

Los experimentos que se describen en esta Tesis Doctoral incluyen la síntesis de compuestos organometálicos que contienen ligandos auxiliares de tipo ciclopentadienilo y fosfinas voluminosas capaces de experimentar

reacciones de ciclometalación. Se describen además los pertinentes estudios de reactividad y de caracterización estructural mediante técnicas espectroscópicas y de difracción de rayos X. Algunas de estas determinaciones cristalográficas se han llevado a cabo de manera independiente a éste trabajo por el Dr. Eleuterio Álvarez, mientras que otras muchas son obras del autor de esta Tesis. Asimismo, se han incluido estudios teóricos desarrollados de manera independiente por el Dr. Joaquín López Serrano. Por motivos de espacio, los datos estructurales detallados derivados de los estudios de rayos X se han incorporado únicamente como Anexo en la versión electrónica de la Memoria.

La Tesis tiene una estructura clásica basada en: **Introducción**, **Resultados y Discusión**, y **Parte Experimental**, para cada uno de los dos capítulos que la componen. Para favorecer su comprensión, el Capítulo 2 ha sido dividido en dos partes (A y B), según la naturaleza de los complejos de iridio que se describen en cada caso. Para facilitar su lectura, la bibliografía aparece tanto a pie de página como al final de cada capítulo, y de forma independiente en cada uno de ellos. Esta distribución hace que algunas referencias aparezcan en ambos capítulos. La numeración de las ecuaciones, los esquemas, las figuras y la numeración de los compuestos es independiente en cada uno de ellos.

Como parte del programa de Formación de Profesorado Universitario (FPU) se ha realizado una estancia breve de tres meses en la *University of North Carolina*, en Chapel Hill (EEUU), bajo la supervisión del Dr. Maurice Brookhart. Por motivos de espacio, los resultados experimentales obtenidos durante dicha estancia no se han incluido en el manuscrito. Estos resultados incluyen la síntesis y reactividad de complejos de iridio con ligandos de tipo

pincer y la polimerización de olefinas mediada por catalizadores Pd conteniendo ligandos diimina. Con el objeto de obtener la mención de *Doctor Internacional* (RD 99/2011; BOE 10-02-2011, Art. 15), la mayor parte de la Tesis, exceptuando el resumen inicial y las conclusiones finales, se ha redactado en inglés.

El objetivo fundamental del primer capítulo de esta Tesis Doctoral es el estudio de las aplicaciones en catálisis de un complejo catiónico de Rh(III) que posee un ligando ciclopentadienilo (C_5Me_5) y una fosfina voluminosa ciclometalada, concretamente la metildixililfosfina, $PMe(Xyl)_2$ ($Xyl=2,6-Me_2C_6H_3$). Este complejo de Rh presenta una estructura de tipo sándwich, que le confiere un interesante comportamiento dinámico en disolución. Su estudio nos ha permitido desarrollar una nueva metodología para la deuteración y tritiación catalítica de hidrosilanos empleando D_2 o T_2 como fuente de deuterio o tritio, respectivamente. El complejo es además muy activo en reacciones de hidrosililación de dobles enlaces $C=X$ ($C = O, N$). Los resultados de esta reactividad se presentan también en el primer capítulo de la Tesis Doctoral. Finalmente, se describe por primera vez en la bibliografía un método muy eficaz para la deuteriosililación y tritiosililación directa de este tipo de grupos funcionales, utilizando un único catalizador para los dos procesos.

En el segundo capítulo de esta Tesis Doctoral se describe la síntesis de complejos de Ir de tipo semisandwich estabilizados con fosfinas voluminosas que tienen tendencia a la ciclometalación. Los estudios de reactividad efectuados con estas especies han proporcionado resultados muy interesantes. El segundo capítulo se ha dividido en dos partes, A y B. En la primera, (A), se discute la síntesis y caracterización de complejos de Ir conteniendo la

fosfina $\text{PMe}(\text{Xyl})_2$. Se hace especial mención a dos procesos de elevado interés desde el punto de vista de la activación y funcionalización de enlaces C–H: (i) reacciones de intercambio C–H/C–D utilizando CD_3OD y operando bajo diferentes mecanismos; (ii) reacción de acoplamiento C–C deshidrogenante y el estudio de su mecanismo. Esta última reacción transcurre a través de un alquilideno de Ir(III), parte por tanto de una familia de especies muy reactivas y raras veces aisladas. Este resultado determinó como nuevo objetivo la síntesis y caracterización de otros alquilidenos catiónicos de este tipo, cuyos resultados constituyen el final de la parte A del Capítulo 2.

En la parte B del segundo capítulo se han preparado complejos de iridio análogos a los de la parte A, pero utilizando cuatro fosfinas voluminosas capaces de ciclometalarse conteniendo un único ligando xililo ($\text{PMe}_2(\text{Xyl})$, $\text{PPh}_2(\text{Xyl})$, $\text{P}^i\text{Pr}_2(\text{Xyl})$ y $\text{PCy}_2(\text{Xyl})$). La elección de estas fosfinas se realizó con el objeto de evitar la reacción de acoplamiento deshidrogenante descrita en la parte A del Capítulo 2, y poder aislar así los deseados alquilidenos catiónicos de Ir(III). Se ha observado que las fosfinas más voluminosas, $\text{P}^i\text{Pr}_2(\text{Xyl})$ y $\text{PCy}_2(\text{Xyl})$, permitieron obtener los esperados alquilidenos, mientras que los complejos basados en fosfinas menos voluminosas ($\text{PMe}_2(\text{Xyl})$, $\text{PPh}_2(\text{Xyl})$) llevaron a la obtención de aductos de diclorometano. Uno de los alquilidenos catiónicos, en concreto el basado en la fosfina $\text{P}^i\text{Pr}_2(\text{Xyl})$, se utilizó como modelo para llevar a cabo estudios de reactividad, cuyos resultados constituyen el final de la parte B del Capítulo 2.

Una parte de los resultados obtenidos se ha publicado en forma preliminar o como trabajo completo, mientras que otras secciones son todavía inéditas. A continuación se relacionan los artículos derivados de esta Tesis

que están ya publicados y se detallan, asimismo, aquéllos cuyos manuscritos están actualmente en fase de preparación. Se indican además otras publicaciones de resultados obtenidos paralelamente a la realización de esta Tesis que, por razones de espacio, no se han incluido en esta Memoria. A esta relación le sigue la de los nuevos compuestos que se han obtenido y caracterizado, y finalmente la lista de abreviaturas utilizadas en la Memoria.

PUBLICATIONS

Research Articles

Cyclometalation and hydrogen/deuterium exchange reactions of an arylphosphine ligand upon coordination to $[Ir(\eta^5-C_5Me_5)]$. Campos, J.; Esqueda, A. C.; Carmona, E. *Chem. Eur. J.* **2010**, 16, 419.

A Cationic Rh(III) Complex that Efficiently Catalyzes Hydrogen Isotope Exchange in Hydrosilanes. Campos, J.; Esqueda, A. C.; López-Serrano, J.; Sánchez, L.; Cossio, F. P.; Cozar, A. de; Álvarez, E.; Maya, C.; Carmona, E. *J. Am. Chem. Soc.* **2010**, 132, 16765.

Synthesis and reactivity of half-sandwich $(\eta^5-C_5Me_5)Ir(III)$ complexes of a cyclometallated aryl phosphine ligand. Campos, J.; Álvarez, E.; Carmona, E. *New J. Chem.*, **2011**, 35, 2122.

Rhodium-Catalyzed, Efficient Deutero- and Tritio-Silylation of Carbonyl Compounds from Hydrosilanes and Deuterium or Tritium. Rubio, M.; Campos, J.; Carmona, E. *Org. Lett.* **2011**, 13, 5236.

Large-Scale Preparation and Labelling Reactions of Deuterated Silanes. Campos, J.; Rubio, M.; Esqueda, A. C.; Carmona, E. *J. Lab. Comp. Radiopharm.* **2011**, 55, 29.

Cationic Ir(III) Alkylidenes are Key Intermediates in C–H Bond Activation and C–C Bond-Forming Reactions. Campos, J.; López-Serrano, J.; Álvarez, E.; Carmona, E. *J. Am. Chem. Soc.* **2012**, 134, 7165.

Synthesis and Characterization of Cationic Ir(III) Alkylidenes Constructed around a Bulky Cyclometalated Phosphine. Campos, J.; Carmona, E. (manuscript in preparation).

Synthesis and Characterization of Cationic Ir(III) Alkylidenes by Reversible α -H Elimination Reactions. Campos, J.; Carmona, E. (manuscript in preparation).

Patents

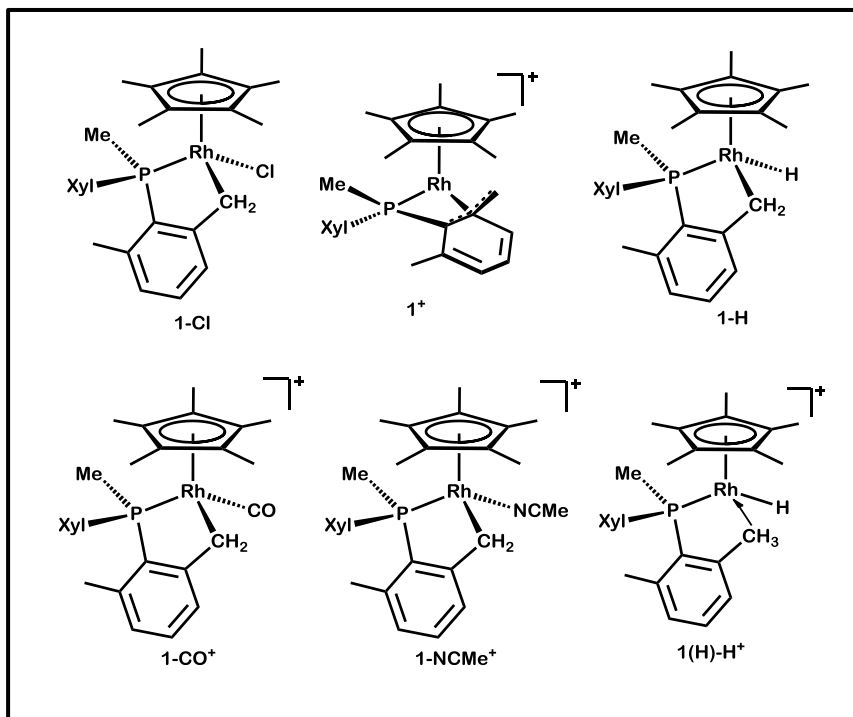
Cationic Complexes Bearing Cyclopentadienyl Ligands and their Use as Catalysts for the Preparation of Deuterated and Tritiated Silanes. Campos, J.; Esqueda, A. C.; Carmona, E. **2010**, España. **P201000507**. Universidad de Sevilla - CSIC.

Other Research Articles not Directly Related with the PhD Thesis

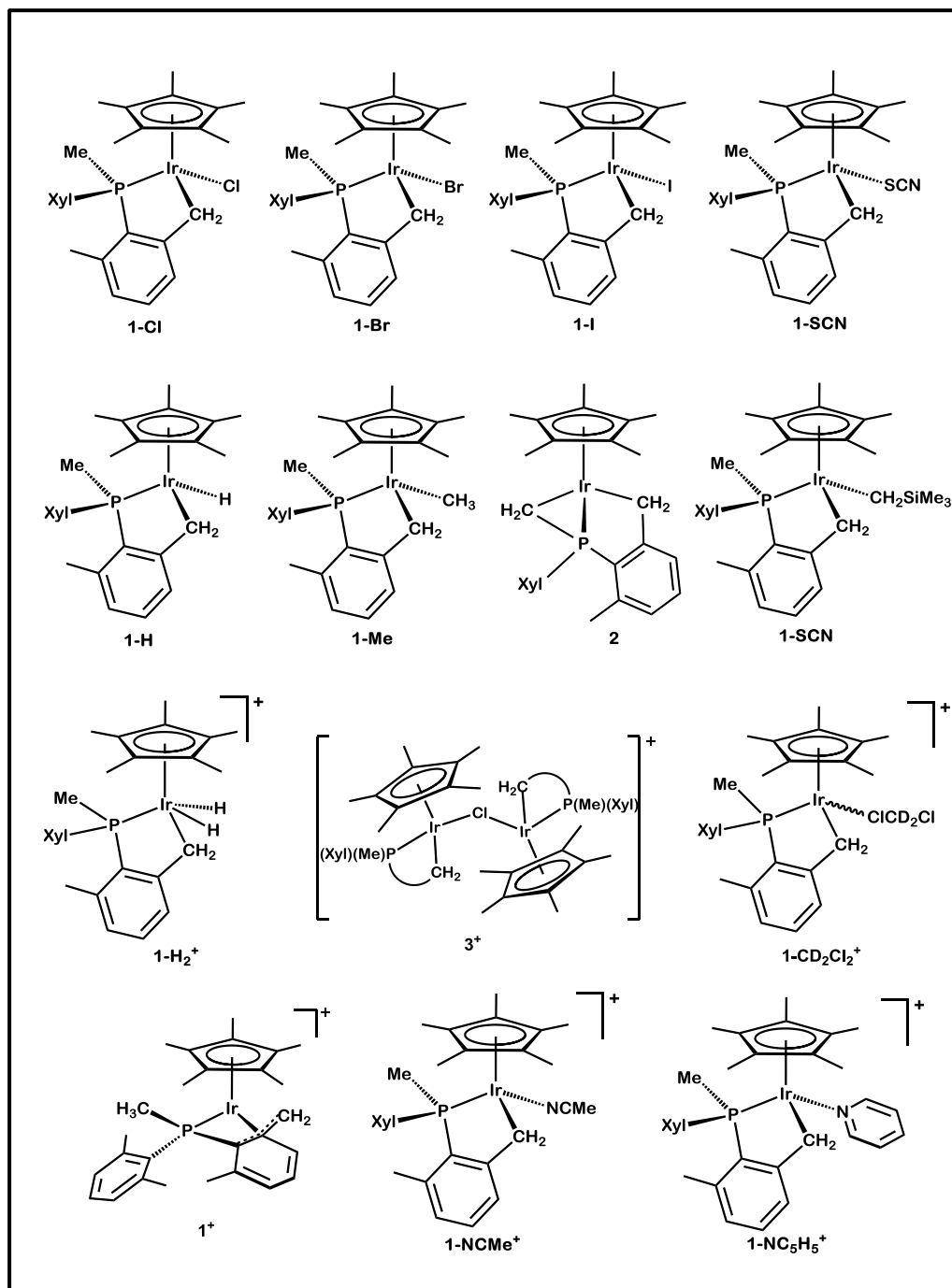
Synthesis and Reactivity of a Cationic Pt(II) Alkylidene Complex. Campos, J.; Peloso, R.; Carmona, E. *Angew. Chem. Int. Ed.* **2012**, accepted.

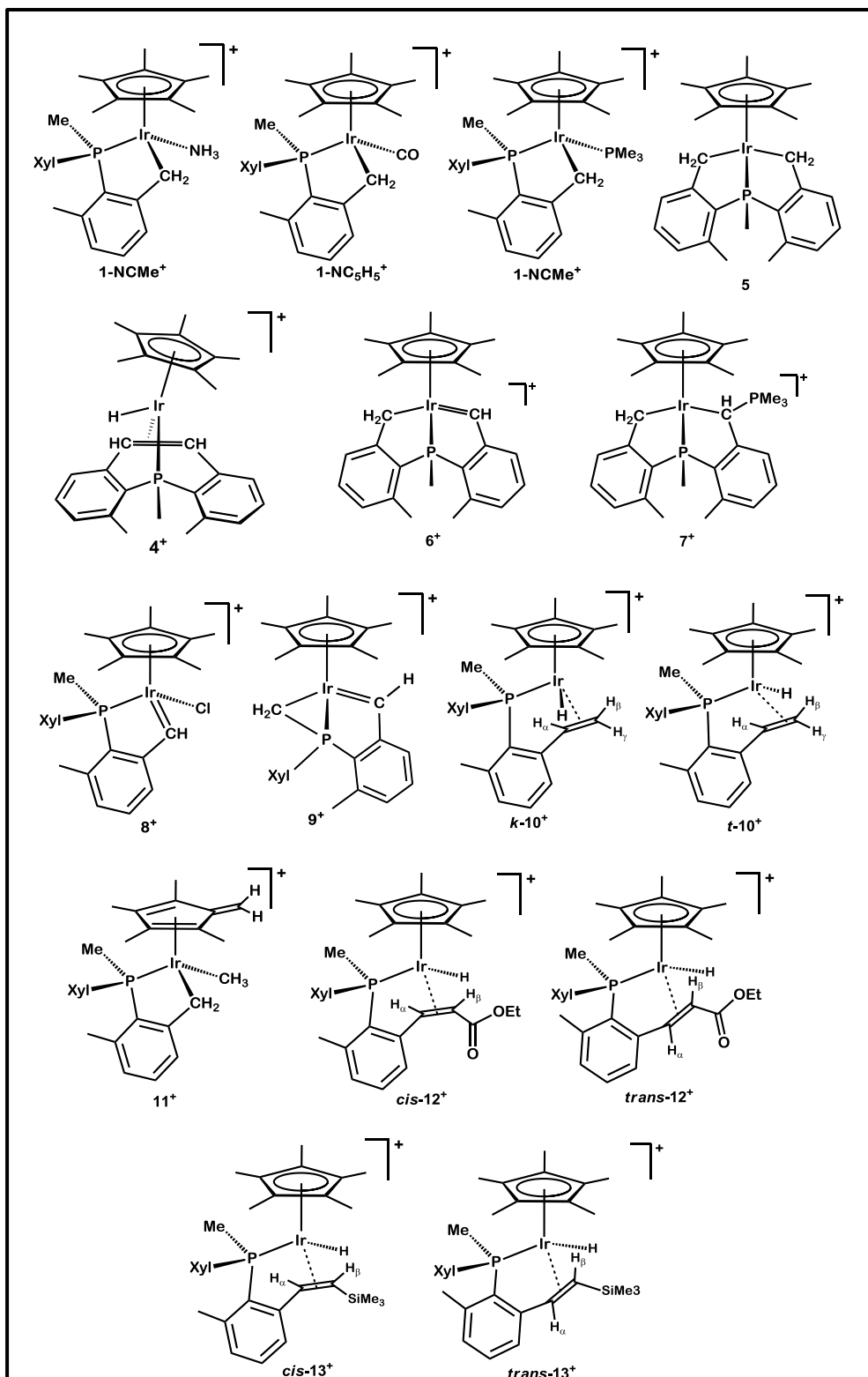
C–C coupling reactions mediated by cationic cyclometalated Pt(II) complexes. Campos, J.; Peloso, R.; Carmona, E. (manuscript in preparation).

Compounds Prepared in Chapter 1

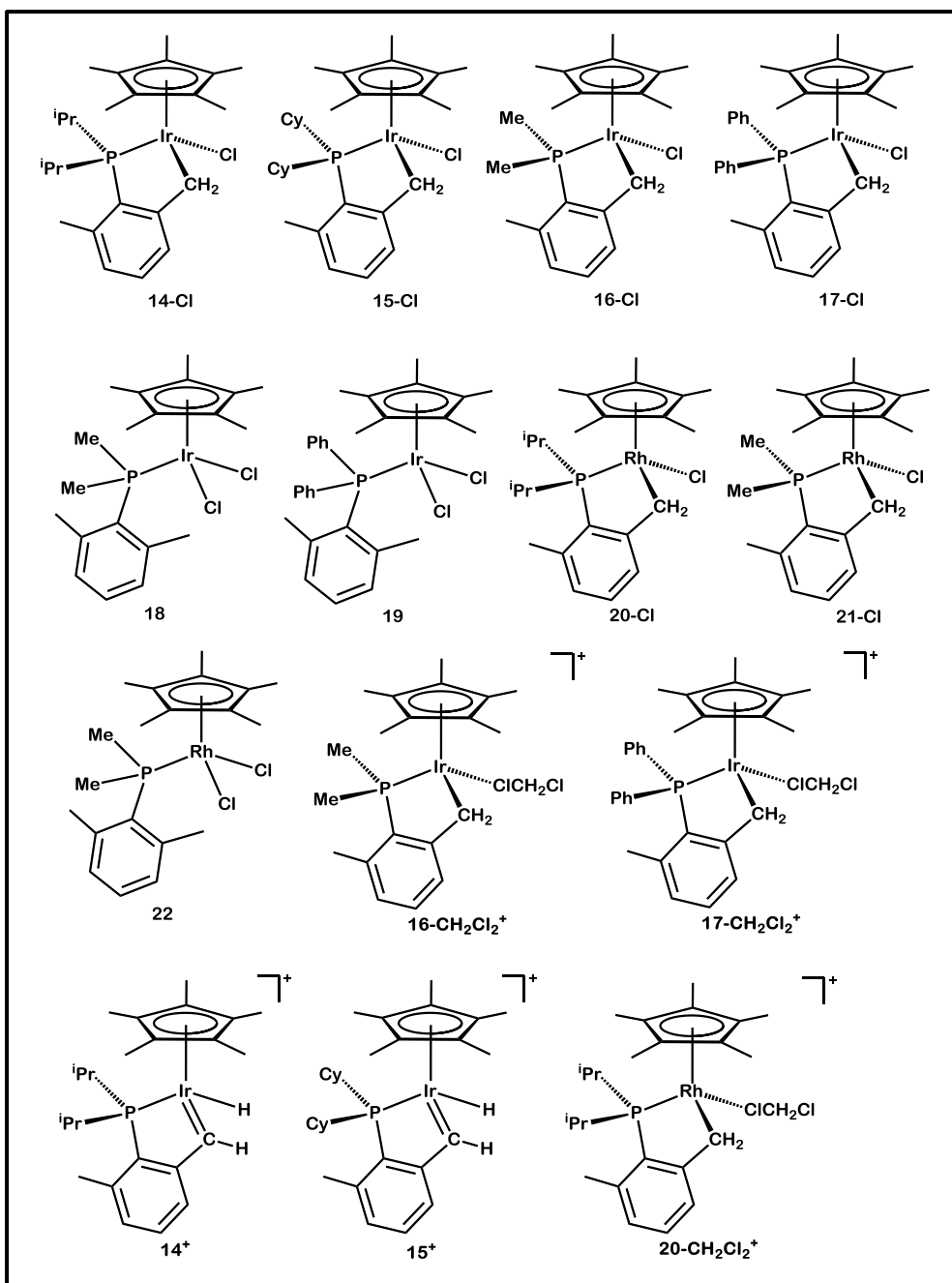


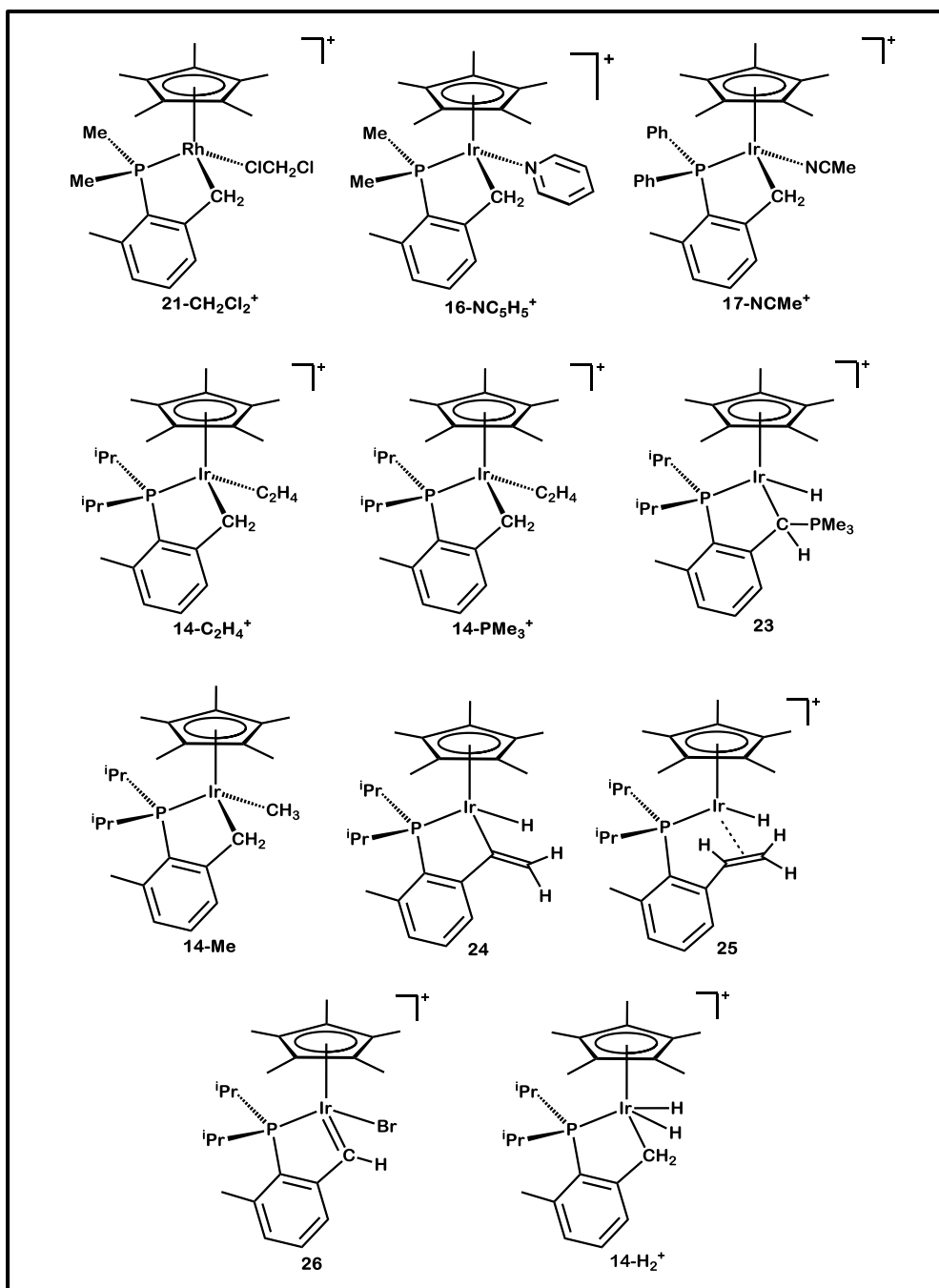
Compounds Prepared in Chapter 2.A





Compounds Prepared in Chapter 2.B





ABBREVIATIONS

Me	methyl, -CH ₃
Et	ethyl, -CH ₂ CH ₃
Pr	propyl, -CH ₂ CH ₂ CH ₃
ⁱ Pr	isopropyl, -CH(CH ₃) ₂
Ph	phenyl, -C ₆ H ₅
Ar	aryl
Xyl	xylyl, 2,6-Me ₂ C ₆ H ₃
^t Bu	<i>tert</i> -butyl, CMe ₃
THF	tetrahydrofuran, C ₄ H ₈ O
Et ₂ O	diethyl ether, CH ₃ CH ₂ OCH ₂ CH ₃
L	2 electron donor ligand
Cp [*]	pentamethyl cyclopentadienilo, C ₅ Me ₅
κ	ligand hapticity
η	number of atoms of a ligand directly bound to a metal center
ν	infrared vibrational frequency (cm ⁻¹)
h	hours
equiv.	equivalents
atm	atmospheres
K _{eq}	equilibrium constant
Anal. Calc.	analysis calculated

Exp.	experimental
[D _n]	number of deuterium atoms in a molecule
g	grams
mmol	millimol
mL	milliliter
cm	centimeter
Å	Amstrong
°	degree
C	Celsius
K	Kelvin
ref.	reference
p	page
vol	volume
ORTEP	crystallographic representation (Oak Ridge Thermal Ellipsoid Program)
IR	infrared
e ⁻	electron
HRMS	high resolution mass spectroscopy
CI	chemical impact
ESI	electrospray
KIE	kinetic isotopic effect
<i>k</i>	rate constant

NMR Abbreviations

NMR	Nuclear Magnetic Resonance
δ	chemical shift in ppm
ppm	parts per million
NOESY	Nuclear Overhauser Enhancement Spectroscopy
COSY	^1H - ^1H correlation spectroscopy
HSQC	^1H - ^{13}C correlation spectroscopy (Heteronuclear Single Quantum Coherence)
HMBC	^1H - ^{13}C correlation spectroscopy (Heteronuclear Multiple Bond Correlation)
s	singlet
d	doublet
t	triplet
q	quartet
sept	septet
m	multiplet
br.	broad
$^nJ_{\text{AB}}$	coupling constant (Hz) between A and B nuclei separated by n bonds
Hz	hertz

CHAPTER I:

Rhodium–Catalyzed Hydrosilane Chemistry.

**Catalytic Si–H/D/T Exchanges and D– and T–
Silylation of C–X Multiple Bonds**

I.1. INTRODUCTION

I.1. INTRODUCTION

I.1.1. Isotopic Labeling of Organic Molecules.

There is increased demand for isotopically labeled compounds as internal standards for mass spectrometric studies, as well as for other modern technologies that include agrochemical, biological, and pharmaceutical investigations of the interaction of small molecules with receptors, enzymes, and other biomolecules.¹ The employment of isotopologues as internal standards for chemical analysis is of particular interest in the investigation of complex systems, such as environmental, animal or human samples. In these cases, impairment of the gradient of response of the instrument due to the

¹ (a) Atzrodt, J.; Derdau, V.; Fey, T.; Zimmermann, J. *Angew. Chem., Int. Ed.* **2007**, *41*, 7744. (b) Elander, N.; Jones, J. R.; Lu, S. -Y.; Stone-Elander, S. *Chem. Soc. Rev.* **2000**, *29*, 239.

presence of diverse components other than the target molecule, which are called matrix effects, can severely interfere the measurement. These effects can be overcome by the use of isotopically labeled internal standards. Furthermore, compounds labeled with both stable and radioactive isotopes are critical to the drug development process and have become essential in many clinical studies.² Since the radioactivity background is negligible, radioisotopes improve the sensitivity of detection of drug molecules in both *in vitro* and *in vivo* studies. Additionally, considering that radioactive drug molecules are generally quantified in terms of their radioactivity, its measurement is not altered by modification of its chemical structure and, also, no standard reference is needed.

The most ubiquitous atom in chemistry is hydrogen and because of its presence in most organic molecules, there is a growing demand for deuterium- and tritium-labeled compounds. As a consequence, the search for efficient and selective catalytic methods that allow efficient isotopic incorporation has been intensified in the last decades. In general, three strategies have been followed for the preparation of ²H- and ³H-labeled organic molecules.

- (i) Using commercially available isotopically labeled precursors.
- (ii) H/D/T exchange at carbon centers.
- (iii) Reduction of C–X multiple bonds (X = C, N, O) with isotopically labeled metal hydrides.

Although the first approach might be seen as the simplest route to obtain labeled organic molecules, the availability of the required labeled starting

² (a) Elmore, C. S.; John, E. M. *Annual Reports in Medicinal Chemistry* **2009**, *44*, 515. (b) Lockley, W. J. S. *J. Labelled Compd. Radiopharm.* **2007**, *50*, 256. (c) Stumpf, W. E. *J. Pharmacol. Toxicol. Methods* **2005**, *51*, 25.

material is not always assured. Moreover, long synthetic routes, along with high costs of labeled compounds need be taken into consideration. In the second alternative, the incorporation of the isotopes can be carried out on the target molecule directly or, at least, on a late intermediate of the synthetic route. In cases in which the acidity of the C–H protons is significant, isotopic exchange can be achieved without the need of a catalyst,^{1a,3} although it usually requires high temperatures (150 – 500 °C) and the resulting selectivities are rather poor. Acid^{1a,4} and base^{1a,5} catalyzed systems have also been reported. However, the best results in terms of versatility have been obtained using homogeneous and heterogeneous transition-metal catalysts,^{1a,2b,6} which in general, feature high functional group tolerance, as well as notable efficiency and regioselectivity.

The last methodology is convenient as it provides high tritium- (T) or deuterium- (D) incorporation at specific positions. However, the use of hydrides derived from boron, aluminum or tin encounters substantial limitations by the chemistry required, such as low functional group tolerance

-
- ³ (a) Werstiuk, N. H.; Ju, C. *Can. J. Chem.* **1989**, 67, 5. (b) Junk, T.; Catallo, W. J. *Tetrahedron Lett.* **1996**, 37, 3445. (c) Perrotin, P. Sinnema, P. –J.; Shapiro, P. J. *Organometallics* **2006**, 25, 2104. (d) Evchenko, S. V.; Kamounah, F. S.; Schaumberg, K.; *J. Labelled Compd. Radiopharm.* **2005**, 48, 209. (e) Shabanova, E. Schaumberg, K. Kamounah, F. S. *J. Chem. Res.* **1999**, 364. (f) de Keczer, S. A.; Lane, T. S. M.; Masjedizadeh, R. *J. Labelled Compd. Radiopharm.* **2004**, 47, 733.
- ⁴ (a) Garnett, J. L.; Long, M. A.; Vining R. F. W.; Mole, T. *J. Am. Chem. Soc.* **1972**, 94, 5913. (b) Seibles, J. C.; Bollinger, D. B.; Orchin M. *Angew. Chem. Int. Ed.* **1977**, 16, 656. (c) Heinkele, G.; Mürdter, T. E. *J. Labelled Compd. Radiopharm.* **2005**, 48, 457.
- ⁵ (a) Berthelette, C.; Scheigetz, J. *J. Labelled Compd. Radiopharm.* **2004**, 47, 891. (b) Coumbarides, G. S.; Dingjan, M.; Eames, J.; Flinn, A.; Northen, J. *J. Labelled Compd. Radiopharm.* **2006**, 49, 903. (c) Elemes, Y.; Ragnarsson, U.; *Chem. Commun.* **1996**, 935.
- ⁶ (a) Junk, T.; Catallo, W. D. *Chem. Soc. Rev.* **1997**, 26, 401. (b) Heys, J. R. *J. Label. Compd. Radiopharm.* **2007**, 50, 770. (c) Skaddan, M. B.; Yung, C. M.; Bergman, R. G. *Org. Lett.* **2004**, 6, 11. (d) Skaddan, M. B.; Bergman, R. G. *J. Label. Compd. Radiopharm.* **2006**, 49, 623. (e) Heys, J. R.; Lockley, W. J. S. *J. Label. Compd. Radiopharm.* **2010**, 53, 635. (f) Allen, P. H.; Hickey, M. J.; Kingston, L. P.; Wilkinson, D. J. *J. Label. Compd. Radiopharm.* **2010**, 53, 731. (g) Chappelle, M. R.; Hawes, C. R. *J. Label. Compd. Radiopharm.* **2010**, 53, 745.

and selectivity (particularly for T-labeling), and by the generation of considerable amounts of waste products.

I.1.2. Labeled Hydrosilanes in Organic Synthesis.

The inherent limitations of metal hydrides for these purposes can be overcome with the employment of hydrosilanes, $\text{SiR}_{4-n}\text{H}_n$ ($n = 1-3$). These reagents provide one of the most powerful tools in synthetic organic chemistry⁷ (Figure 1) and are able to add catalytically to C–C, C–N, and C–O multiple bonds in the widescope hydrosilylation reaction,^{8,9} which will be further discussed below, and to reduce, also catalytically, carbon–halogen bonds,¹⁰ including unreactive C–F bonds.¹¹

⁷ Alonso, F.; Beletskaya, I. P.; Yus, M. *Chem. Rev.* **2002**, *102*, 4009.

⁸ (a) Marciniec B. Ed., *Comprehensive Handbook on Hydrosilylation*, Pergamon, Oxford, **1992**. (b) Marciniec, B. *Silicon Chemistry* **2002**, *1*, 155. (c) Roy, A. K. A. *Adv. Organomet. Chem.* **2007**, *55*, 1; (d) Malacea, E.; Poli, R.; Manoury, E. *Coord. Chem. Rev.* **2010**, *254*, 729. (e) Morris, R. H. *Chem. Soc. Rev.* **2009**, *38*, 2282.

⁹ For selected examples: (a) Calimano, E.; Tilley, T. D. *J. Am. Chem. Soc.* **2009**, *131*, 11161; (b) Park, S.; Brookhart, M. *Organometallics* **2010**, *29*, 6057. (c) Yang, J.; White, P. S.; Brookhart, M. *J. Am. Chem. Soc.* **2008**, *130*, 17509. (d) Tondreau, A. M.; Lobkovsky, E.; Chirik, P. J. *Org. Lett.* **2008**, *10*, 2789. (e) Tondreau, A. M.; Hojilla Atienza, C. C.; Weller, K. J.; Nye, S. A.; Lewis, K. M.; Delis, J. G. P.; Chirik, P. J. *Science* **2012**, *335*, 567. (f) Yang, J.; Tilley, T. D. *Angew. Chem., Int. Ed.* **2010**, *49*, 10186. (g) Blackwell, J. M.; Morrison, D. J.; Piers, W.E. *Tetrahedron* **2002**, *58*, 8247. (h) Buchan, Z. A.; Bader, S. J.; Montgomery, J. *Angew. Chem., Int. Ed.* **2009**, *48*, 4840. (i) Tran, B. L.; Pink, M.; Mindiola, D. J. *Organometallics* **2009**, *28*, 2234.

¹⁰ Karshtedt, D.; Bell, A. T.; Tilley, T. D. *Organometallics* **2006**, *25*, 4471.

¹¹ (a) Aizenberg, M.; Milstein, D. *Science* **1994**, *256*, 359; (b) Yang, J.; Brookhart, M. *Adv. Synth. Catal.* **2009**, *351*, 175. (c) Douvris, C.; Ozerov, O. V. *Science* **2008**, *321*, 1188.

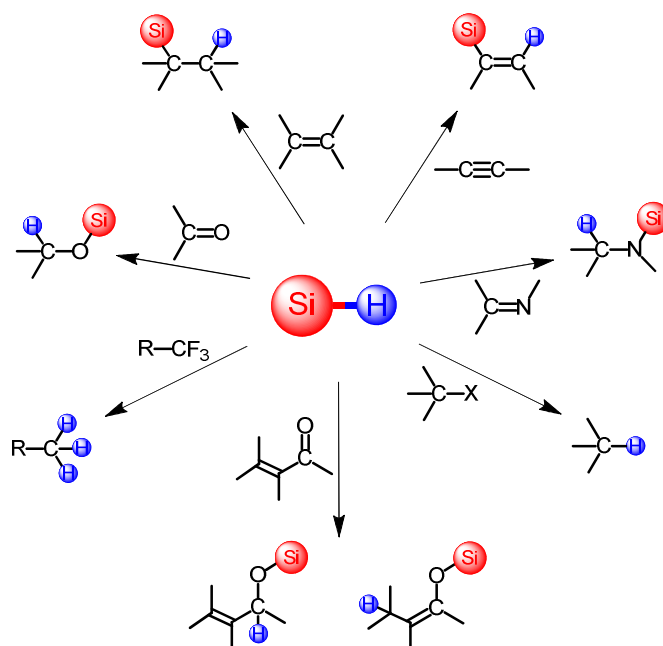


Figure 1. Some synthetic applications of hydrosilanes.

Deuterated and tritiated commonly used silanes, for instance, SiEt_3D and SiEt_3T , or SiPh_2D_2 and SiPh_2T_2 , would therefore offer significant advantages in the solution of chemical and biochemical problems with the use of hydrogen isotopes. In addition, hydrosilanes are environmentally benign, stable to oxygen and moisture, non-toxic and easy to handle.

Despite this great potential, deuterated and tritiated silanes have been hardly exploited as isotopic labeling reagents. Most probably, this is due to the scarcity of information on catalytic H/D (or H/T) exchanges at silicon centers, which leaves reduction of the silicon-halogen bond of halosilanes with NaBD_4 , LiAlD_4 or a similar deuteride agent as the more commonly used

procedure for the synthesis of deuterated silanes.^{1a,12} These strategies require the use of energetic and expensive reagents. Moreover, isolated yields of the labeled compounds are poor and an important amount of waste products is usually generated. Thus conventional methodologies for hydrosilane labeling become unsuitable for high scale preparations, and especially inconvenient for the synthesis of tritiated silanes. Isotopic exchange at silicon centers is known since the early 1960s,¹³ and it has been reported in the literature frequently.¹⁴ Nevertheless, an efficient, widescope catalytic synthesis of deuterated and tritiated hydrosilanes has never been developed.

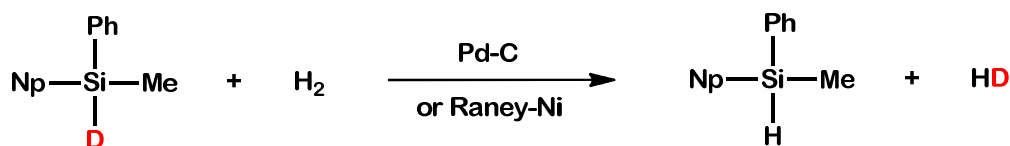
The first attempt to effect the catalytic synthesis of deuterated silanes using D₂ as the deuterium source came from Sommer and co-workers. They showed that heterogeneous catalysts based on group 10 metals (Ni, Pd and Pt), as well as cobalt and iridium homogeneous catalysts, were capable of promoting the exchange of Si–H bonds between molecules of hydrosilanes.^{13c-e} More promising in terms of the preparation of labeled organosilanes, was the Si–H/D exchange observed by the same researchers upon exposure of a deuterated silane to hydrogen gas. The yields of deuterium incorporation were acceptable only with the use of heterogeneous systems (Pd–C and Raney Ni), but the scope of the reaction was extremely limited and only one tertiary hydrosilane (naphthyl-methylsilane) was tested

¹² (a) Prince, P. D.; Bearpark, M. J.; McGrady, G. S.; Steed, J. W. *Dalton Trans.* **2008**, 271. (b) Grant, B. E.; Brookhart, M. *J. Am. Chem. Soc.* **1993**, *115*, 2156. (c) Sousa, S. C. A.; Fernandes, A. C. *Adv. Synth. Catal.* **2010**, *352*, 2218.

¹³ (a) Ponomarenko V. A.; Odabashyan G. V.; Petrov. A. D. *Dokl. Akad. Nauk SSSR.* **1960**, *131*, 321. (b) Ryan J. W.; Speier, J. L. *J. Am. Chem. Soc.* **1964**, *86*, 895. (c) Sommer, L. H.; Lyons, J. E.; Fujimoto, H.; Michael, K. W. *J. Am. Chem. Soc.* **1967**, *89*, 5483. (d) Sommer L. H.; Lyons J. E. *J. Am. Chem. Soc.* **1968**, *90*, 4197. (e) Sommer L. H.; Lyons, J. E.; Fujimoto, H. *J. Am. Chem. Soc.* **1969**, *91*, 7051.

¹⁴ (a) Paonessa, R. S.; Prignano, A. L.; Trogue, W. C. *Organometallics* **1985**, *4*, 647. (b) Liu, X.; Wu, Z.; Cai, H.; Yang, Y.; Chen, T.; Vallet, C. E.; Zuhre, R. A.; Beach, D. B.; Peng, Z.-H.; Wu, Y.-D.; Concolino, T. E.; Rheingold, A. L.; Xue, Z. *J. Am. Chem. Soc.* **2001**, *123*, 8011. (c) Rendler, S.; Oestreich, M. *Angew. Chem. Int. Ed.* **2008**, *47*, 5997.

(Scheme 1). Other heterogeneous systems employing Au,¹⁵ Cu¹⁶ and Zr¹⁷ were reported later. However, they also featured important limitations concerning the nature of the hydrosilane reagent, the need of high catalyst loadings and in some cases the observation of competitive secondary reactions.



Scheme 1. Catalytic Si-H/D Exchange reported by Sommer. (Np = naphthyl)

In homogeneous systems, the groups of Parish¹⁸ and Fryzuk,¹⁹ using Co(I) and Rh(I) complexes, respectively, obtained good results. Parish showed that Co(H)(N₂)(PPh₃)₃ is a useful catalyst for the deuteration of tertiary hydrosilanes (SiR₃H) upon exposure to D₂. Although the catalyst loadings were only of *ca.* 0.3 mole %, deuteration was not complete (30 – 62 % D incorporation) and only four tertiary silanes were tested (R = OEt, Et, Me, F). A series of iridium catalysts were also reported by Parish with poorer results.²⁰ The dimeric rhodium complex reported by Fryzuk allowed deuteration of Ph₂SiH₂ under D₂ atmosphere, although concomitant

¹⁵ Bradshaw, D. I.; Moyes, R. B.; Wells, P. B. *J. Chem. Soc., Chem. Commun.* **1975**, 137.

¹⁶ (a) Bartok, M.; Molnár, A. *J. Organomet. Chem.* **1982**, 235, 161. (b) Bartok, M.; Molnár, A. *J. Chem. Soc., Chem. Commun.* **1982**, 1089.

¹⁷ Coutant, B.; Quignard, F.; Choplin, A. *J. Chem. Soc., Chem. Commun.* **1995**, 137.

¹⁸ Archer, N. J.; Haszeldine, R. N.; Parish, R. V. **1979**, *J. Chem. Soc. Dalton Trans.* 695.

¹⁹ Fryzuk, M. D.; Rosenberg, L.; Rettig, S. J. *Organometallics*, **1991**, 10, 2537.

²⁰ Blackburn, S. N.; Haszeldine, R. N.; Parish, R. V.; Setchfield, J. H. *J. Organomet. Chem.* **1980**, 329.

dimerization of the silane to yield $\text{Ph}_2\text{HSi-SiHPh}_2$ took also place. In addition, metal complexes of Os^{21} and Nb^{22} have been published and their catalytic activities for the deuteration of hydrosilanes tested, using C_6D_6 as the deuterium source. Nevertheless, these systems require higher temperatures and they are not only effective for the activation of Si-H bonds, but also for the exchange of the C-H bonds of the organosilanes.

For the incorporation of tritium into organic molecules, catalytic H/T exchange at carbon^{2b,6} is in general preferred over the use of LiBT_4 , NaBT_4 , LiT and related reagents.^{23,24} This preference is the result of the inconveniences derived from the low functional group tolerance of metal hydrides, as well as the concomitant generation of waste products. Using tritiated silanes would avoid these drawbacks while at the same time allow the selective incorporation of tritium with high specific activity into specific positions of organic molecules (see Figure 1). Indeed, Saljoughian advanced already in 2002²⁵ the high potential of tritiated silanes, such as SiEt_3T , SiPh_2T_2 and $\text{Si}(\text{SiMe}_3)_3\text{T}$, for labeled synthesis, but almost 10 years later, it does not seem to have been accomplished. This fact is most likely due to unsolved problems in the preparation of these tritiating reagents, which have been obtained by reaction of the corresponding chlorosilane with LiT .²⁴ Besides, lithium tritide must be prepared *in situ* by reacting T_2 gas with $^n\text{BuLi}$ in the presence of tetramethylethylenediamine (TMEDA, Scheme 2).

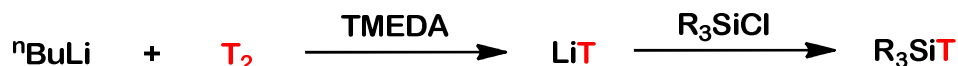
²¹ Berry, D. H.; Procopio, L. J. *J. Am. Chem. Soc.* **1989**, *111*, 4099.

²² Curtis, M. D.; Bell, L. G.; Butler, W. M. *Organometallics* **1985**, *4*, 701.

²³ (a) Than, C.; Morimoto, H.; Andres, H.; Williams, P. G. *J. Org. Chem.* **1996**, *61*, 8771; (b) Zippi, E. M.; Andres, H.; Morimoto, H.; Williams, P. G. *Synthetic Commun.* **1995**, *25*, 2685. (c) Jaiswal, D. K.; Andres, H.; Morimoto, H.; Williams, P. G. *J. Chem. Soc. Chem. Commun.* **1993**, 907. (d) Andres, H.; Morimoto, H.; Williams, P. G. *J. Chem. Soc. Chem. Commun.* **1990**, 627.

²⁴ Neu, H.; Andres, H. *J. Label. Compd. Radiopharm.* **1999**, *42*, 992.

²⁵ M. Saljoughian, *Synthesis* **2002**, 1781.



Scheme 2. Classical synthesis of tritiated silanes (R = Me, Et, Hex, TMS, Ph)

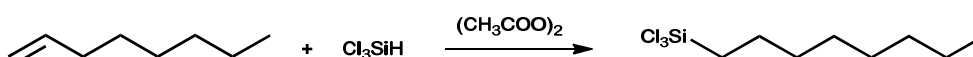
The preparation of triethylsilane, the most commonly used hydrosilane in organic synthesis, presents considerable experimental difficulties. The reaction of Et_3SiCl with LiT is carried out in boiling triglyme and the tritiated silane purified by controlled distillation. However, some TMEDA remaining from the preparation of LiT unavoidably distills together with the silane²⁴ and can poison the catalyst used for the hydrosilylation or any other related reaction subsequently employed to incorporate the tritium atom into organic molecules. To our best knowledge there is no example in the literature for a catalytic tritiation of hydrosilanes. Achieving such a procedure would be highly desirable, since easily prepared tritiated silanes could then be applied for a number of catalytic transformations (see Figure 1) leading to the isotopic labeling of organic compounds of biological and pharmacological interest.

I.1.3. Hydrosilylation Reactions.

As commented above, hydrosilylation refers to the addition of a hydrosilane across a multiple bond ($\text{C}=\text{C}$, $\text{C}=\text{X}$ or $\text{X}=\text{X}$, where $\text{X} = \text{N}, \text{O}, \text{S}$). The first example of this transformation was reported by Sommer in 1947 and consisted in the addition of trichlorosilane to 1-octene catalyzed by acetyl peroxide (Scheme 3).²⁶ However, a great deal of interest interest in this

²⁶ Sommer, L. H.; Pietrusza, E. W.; Whitmore, F. C. *J. Am. Chem. Soc.* **1947**, 69, 188.

transformation grew after the discovery of hexachloroplatinic acid as an efficient hydrosilylation catalyst by Speier and co-workers in 1957.²⁷ During the last 50 years the hydrosilylation reaction has been extensively used for both laboratory and industrial purposes. The reaction can be mediated by free-radicals, nucleophilic-electrophilic catalysts, supported metals and nanoparticles and, predominantly, transition metal complexes.^{8,9}



Scheme 3. First example of hydrosilylation reported by Sommer in 1947.

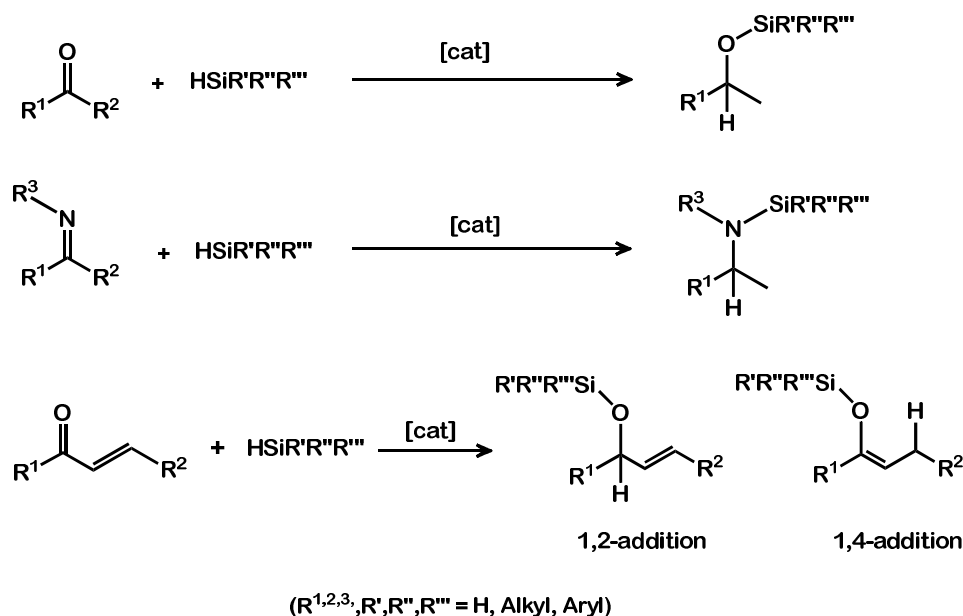
Of all the possible substrates susceptible to undergo hydrosilylation, only a brief introduction regarding those that are directly related to this PhD thesis will be discussed, with emphasis in reactions catalyzed by late transition metal complexes.

Hydrosilylation of C=O and C=N bonds.

Hydrosilylation of carbonyl functionalities and imines is an extensively explored and widely used synthetic methodology that provides a convenient one-step method for converting these substrates into protected alcohols and amines, respectively (Scheme 4). Thus, it circumvents the normal two-step procedure followed in classical organic synthesis, that is, reduction to alcohol or amine followed by silyl protection. If required, silyl ethers and silylamines

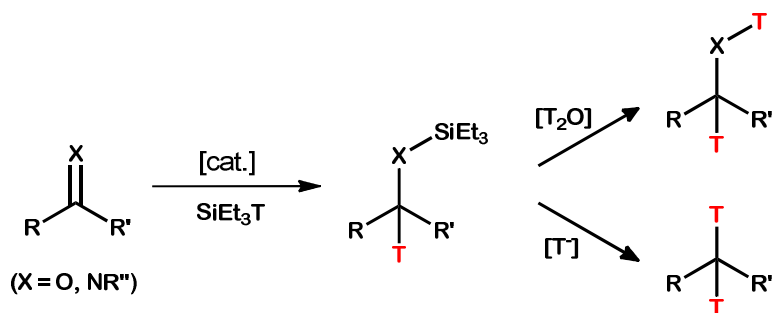
²⁷ Speier, J. L.; Webster, J.A.; Barnes, G.H. *J. Am.Chem. Soc.*, **1957**, 79, 974.

can be easily transformed into alcohols and amines, respectively, *via* an additional hydrolysis step.



Scheme 4. Hydrosilylation of ketones (or aldehydes), imines and α,β -unsaturated enones.

The employment of ²H- and ³H-labeled silanes for such transformations would result in the reduction of C–O and C–N multiple bonds, placing the label at carbon while simultaneously protecting the resulting alcohol or amine moieties. This allows further multistep synthesis, or the direct introduction of a second D or T label by appropriate derivatization of the protected functionality (Scheme 5). The formation of new C–D or C–T bonds could analogously be achieved by catalytic addition of hydrosilanes to alkenes, alkynes or by reduction of carbon-halogen bonds (see Figure 1).



Scheme 5. General, two-step labeling of organic compounds containing C–X (X = O, N) bonds by catalytic tritisilylation.

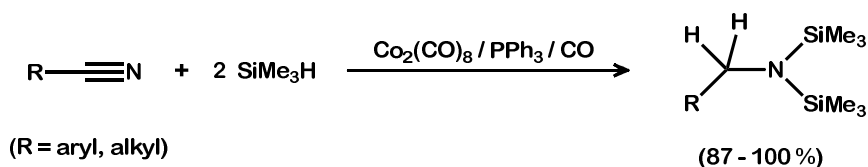
The first hydrosilylation of carbonyl compounds catalyzed by rhodium was reported by Ojima and collaborators in 1972, using Wilkinson's catalyst, $[\text{RhCl}(\text{PPh}_3)_3]$.²⁸ Since that time an enormous progress has been made in the investigation of the hydrosilylation reaction, for which many active catalytic systems based on rhodium have been described.⁸ At present, much effort concentrates on the enantioselective version of this transformation. However, no direct deuterio- or tritisilylation of carbonyl (or any other suitable functionality) has been reported to date, mediated by rhodium or any other metal catalyst.

Hydrosilylation of Nitriles.

Whereas well-known procedures are available for the hydrosilylation of C=X bonds (X = C, N, O), the addition of Si–H bonds to nitriles remains comparatively unexplored because the cyano group behaves as inert under

²⁸ (a) Ojima I.; Nihonyanagi, M.; Nagai I. *J. Chem. Soc. Chem. Commun.* **1972**, 938. (b) Ojima, I.; Kogure, T.; Nihonyanagi, M.; Nagai, Y. *Bull. Chem. Soc. Jpn.* **1972**, 45, 3506.

common hydrosilylation conditions.²⁹ Nevertheless, stoichiometric hydrosilylation of nitriles have been observed in complexes of tungsten³⁰ and ruthenium.³¹ Moreover, efficient hydrosilylation of a wide variety of nitriles, including α,β -unsaturated derivatives, was reported by Murai and co-workers using $\text{Co}_2(\text{CO})_8$ as catalyst (Scheme 6).³² The hydrosilane chosen, SiMe_3H , had to be prepared *in situ* and resulted in the formation of N,N-disilylamines. Subsequently, a heterogeneous, Rh-catalysed process for the hydrosilylation of aromatic aldehydes was developed,^{32b} and more recently, Gutsulyak and Nikonov have reported a very convenient method for the selective monosilylation and disilylation of nitriles, by action of a Ru catalyst.^{32c}



Scheme 6. Hydrosilylation of nitriles using a cobalt catalyst.

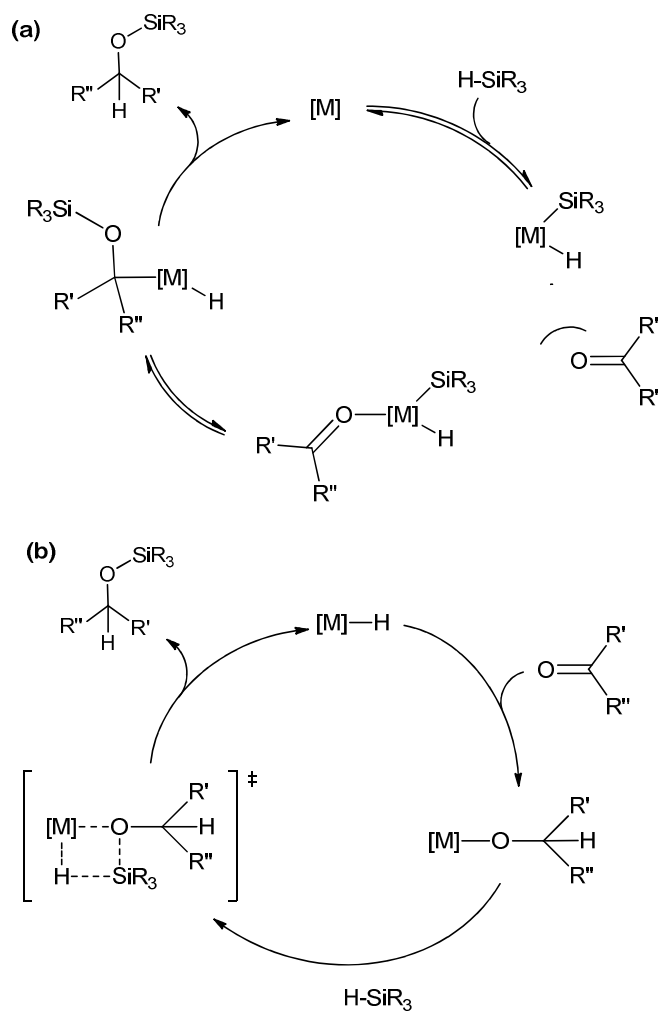
- ²⁹ (a) Addis, D.; Das, S.; Junge, K.; Beller, M. *Angew. Chem. Int. Ed.* **2011**, 50, 6004. (b) Kim, D.; Park, B.-M.; Yun, J. *Chem. Commun.* **2005**, 1755; (c) Belyakova, Z. V. Pomerantseva, M. G.; Chekrii, E. N.; Chernyshev, E. A.; Storozhenko, P. A. *Russ. J. Gen. Chem.* **2010**, 80, 927.
- ³⁰ Watanabe, T.; Hashimoto, H.; Tobita, H. *J. Am. Chem. Soc.*, **2006**, 128, 2176.
- ³¹ Hashimoto, H.; Aratani, I.; Kabuto, C.; Kira, M. *Organometallics*, **2003**, 22, 2199.
- ³² (a) T. Murai, T.; Sakane, S.; Kato, *J. Org. Chem.* **1990**, 55, 499. (b) Caporusso, A. M.; Panziera, N.; Pertici, P.; Pitzalis, E.; Salvadori, P.; Vitulli, G.; Martra, G. J. *J. Mol. Cat. A Chem.* **1999**, 150, 275; (c) Gutsulyak, D. V. Nikonov, G. I. *Angew. Chem. Int. Ed.* **2010**, 49, 7553.

Mechanistic Studies

Several different hydrosilylation mechanisms can be operative depending on the nature of the catalyst and the substrate. We will focus on the hydrosilylation of carbonyl compounds (and the related imine molecules), which generally proceed through one of the three mechanisms discussed below. The most common pathway for late transition metal catalysts, such as rhodium, is the *Chalk-Harrod* mechanism (Scheme 7a). This route was first proposed by Chalk and Harrod for the addition of hydrosilanes to olefins³³ and then extended to the reduction of carbonyl compounds by Ojima and co-workers.³⁴ In this mechanism, and the subsequent related variations, the key step is often the oxidative addition of the silane to a low-valent metal center.

³³ Chalk, A. J.; Harrod, J. F. *J. Am. Chem. Soc.* **1965**, 87, 16.

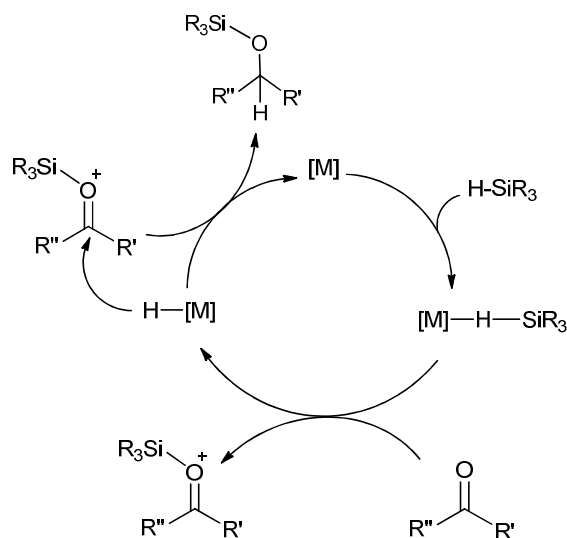
³⁴ Ojima, I.; Kogure, T.; Kumagai, M.; Horiuchi, S.; Sato, Y. *J. Organomet. Chem.* **1976**, 122, 83.



Scheme 7. Proposed catalytic cycles for the hydrosilylation of carbonyl compounds. (a) Chalk-Harrod mechanism; (b) via σ -bond metathesis.

Early metal catalysts, as well as lanthanide and actinide metals, where oxidative addition is disfavored, frequently proceed via a σ -bond metathesis mechanism (Scheme 7b). This pathway is similar to that proposed for hydrogenation reactions catalyzed by these metal centers, although small

differences have been discussed in the literature.³⁵ An alternative mechanism proposed by Piers for the hydrosilylation of ketones using $(\text{C}_6\text{F}_5)_3\text{B}/\text{Ph}_3\text{SiH}$ proceeds by way of silylium (Ph_3Si^+) transfer.³⁶ The same approach was suggested by Brookhart for the addition of hydrosilanes to ketones and aldehydes mediated by an η^1 -silane iridium(III) complex^{9b} (Scheme 8).



Scheme 8. Proposed mechanism for hydrosilylation of carbonyl compounds *via* silylium cation transfer.

³⁵ (a) Haan, K. H.; Wielstra, Y.; Teuben, J. H. *Organometallics* **1987**, *6*, 2053. (b) Nolan, S. P.; Porchia, M.; Marks, T. J. *Organometallics* **1991**, *10*, 1450. (c) Woo, H.-G.; Tilley, T. D. *J. Am. Chem. Soc.* **1989**, *111*, 8043. (d) Molander, G. A.; Dowdy, E. D.; Noll, B. C. *Organometallics*, **1998**, *17*, 3754. (e) Molander, G. A.; Retsch, W. H. *Organometallics*, **1995**, *14*, 4570.

³⁶ (a) Parks, D. J.; Piers, W. E. *J. Am. Chem. Soc.* **1996**, *118*, 9440. (b) Parks, D. J.; Piers, W. E.; Parvez, M.; Atencio, R.; Zaworotko, M. J. *Organometallics* **1998**, *17*, 1369. (c) Parks, D. J.; Blackwell, J. M.; Piers, W. E. *J. Org. Chem.* **2000**, *65*, 3090.

I.2. RESULTS AND DISCUSSION

I.2. Results and Discussion

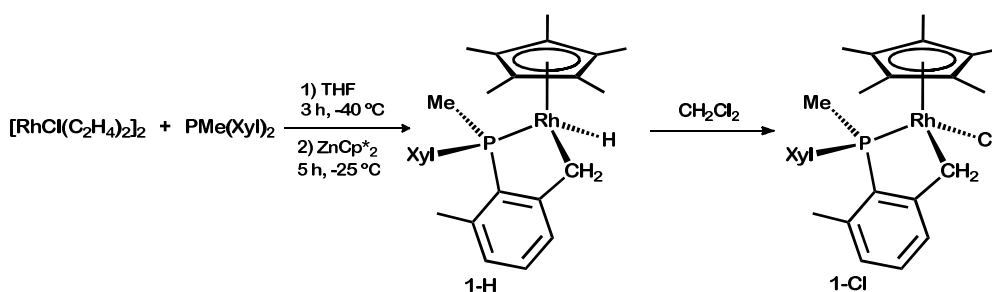
I.2.1. Synthesis and reactivity of the rhodium catalyst.

An impressive milestone in the field of C–H bond activation was accomplished by Bergman and co-workers in the early 1990s, with the report of the selective activation of the C–H bond of alkanes and arenes under unusually mild conditions, using a cationic cyclopentadienyl iridium(III) phosphine complex.³⁷ As discussed in detail in the following chapter, these results attracted our attention and led us in the last years to synthesize a family of related cyclopentadienyl phosphine iridium and rhodium compounds. The cationic rhodium complex **1**⁺ of Scheme 10, utilized as the catalyst for the transformations discussed throughout this chapter, was

³⁷ (a) Burger, P. Bergman, R. G. *J. Am. Chem. Soc.* **1993**, *115*, 10462; (b) Arndtsen, B. A. Bergman, R. G. *Science* **1995**, *270*, 1970.

prepared as part of a parallel project,³⁸ in which a number of rhodium compounds related to Bergman's parent iridium complex was developed.

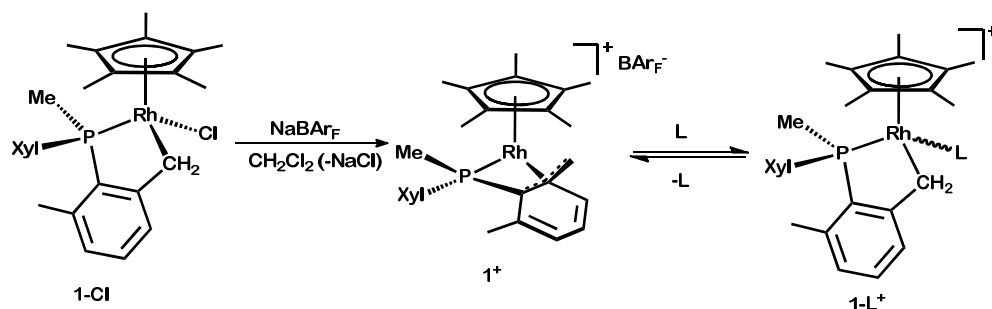
Herein, we will briefly describe the synthesis and properties of the cationic Rh(III) complex **1**⁺, synthesized by the straightforward abstraction of a chloride ligand from **1-Cl**, using NaBAR_F (BAR_F = B(3,5-C₆H₃(CF₃)₂)₄) or AgSbF₆. The neutral chloride precursor was best obtained by chlorination (CH₂Cl₂ or CHCl₃) of hydride **1-H**, which in turn resulted from the stepwise reaction of [RhCl(C₂H₄)₂]₂ with PMe(Xyl)₂ and Zn(C₅Me₅)₂ (Scheme 9).



Scheme 9. Synthesis of rhodium catalyst precursor **1-Cl**.

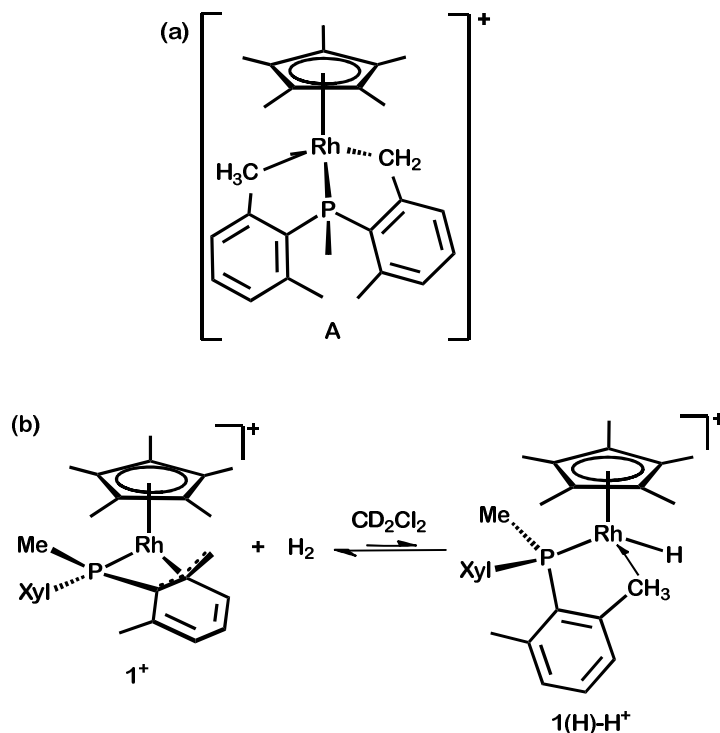
A prominent feature of catalyst **1**⁺ is the ambidentate character of its metalated aryl phosphine ligand, PMe(Xyl)₂ (Xyl = 2,6-C₆H₃Me₂). In the presence of Lewis bases, complex **1**⁺ undergoes a facile, reversible coordination change from κ^4 -P,C,C',C'' to κ^2 -P,C (Scheme 10). For poorly coordinating Lewis bases such as CH₂Cl₂, diethyl ether or methanol, the equilibrium of Scheme 10 shifts to the left and the unusual κ^4 -P,C,C',C'' coordination of the metalated phosphine (**1**⁺) prevails over adduct formation.

³⁸ Esqueda, A. C. *Compuestos de Rh con ligantes de tipo hidrotris(pirazolil)borato y ciclopentadienilo*, **2010**, PhD thesis, Sevilla.



Scheme 10. Synthesis of catalyst $\mathbf{1}^+$ by chloride abstraction from $\mathbf{1-Cl}$ and reversible adduct formation with Lewis bases ($\text{L} = \text{CO}, \text{NCMe}, \text{py}, \text{C}_2\text{H}_4$).

Cation $\mathbf{1}^+$ exhibits a fluxional behavior in solution which implies exchange of the roles of the metalated and non-metalated xylyl rings. Although the fast-exchange limit could not be reached at the highest temperature studied (85 °C), broadening of corresponding methyl and methylene ^1H NMR signals evidenced that the rearrangement involves exchange of the roles of the two phosphine xylyl substituents. Theoretical calculations support that this degenerate exchange occurs through agostic intermediate **A** (Scheme 11a), with an energy of only 9.6 kcal·mol⁻¹ above $\mathbf{1}^+$.³⁸ Indeed, this rearrangement seems to be crucial for the chemical reactivity to be described below, and thus for the catalytic action of complex $\mathbf{1}^+$.

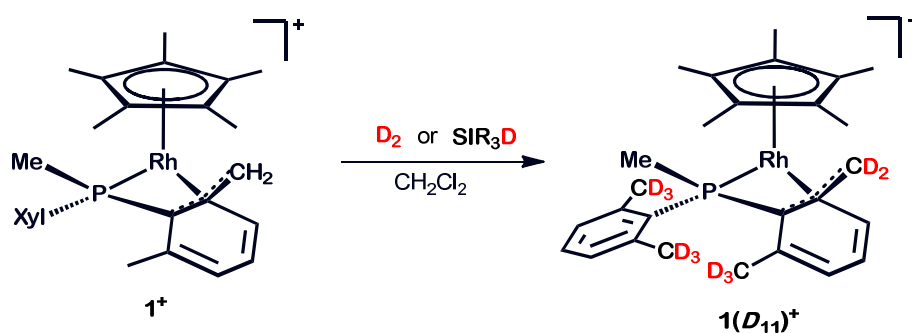


Scheme 11. (a) Agostic intermediate proposed for the exchange of the two xylyl rings of the phosphine moiety; (b) Equilibrium reaction between $\mathbf{1}^+$ and H_2 .

As already mentioned, reactivity studies of $\mathbf{1}^+$ were carried out as part of a different project.³⁸ Of these investigations, the reactivity toward hydrogen and hydrosilanes deserves a brief discussion. At room temperature there is no observable reaction between $\mathbf{1}^+$ and either H_2 or hydrosilanes. However, low-temperature ($-90\text{ }^\circ\text{C}$) ^1H NMR monitoring of the reaction of $\mathbf{1}^+$ and H_2 does not provide experimental evidence for the formation of a $\sigma\text{-H}_2$ complex. Instead, it reveals the existence of a cationic agostic hydride $\mathbf{1(H)-H}^+$ that is in equilibrium with $\mathbf{1}^+$, in a $\mathbf{1}^+ : \mathbf{1(H)-H}^+$ ratio of *ca.* 85:15 (Scheme 11b). Examination of its ^1H NMR spectrum shows a doublet of doublet resonance at -9.43 ppm due to the hydride ligand (with spin-lattice relaxation time $T_1 = 300\text{ ms}$) that undergoes exchange with a signal with $\delta -0.02\text{ ppm}$ attributed to

the agostic methyl protons. A corresponding $^{31}\text{P}\{^1\text{H}\}$ signal at 29.8 ppm can be observed in the range of -90 to -70 °C but disappears above the latter temperature, although cooling at -90 °C restores the original spectrum.

Interestingly, despite the lack of observable reactivity at room temperature between $\mathbf{1}^+$ and H_2 , exposure of solutions of this compound to D_2 yielded $\mathbf{1}(\text{D}_{11})^+$ almost instantly, due to fast H/D exchange of all sp^3 -hybridized C–H bonds of the phosphine xyl units (Scheme 12). Moreover, cation $\mathbf{1}^+$ also underwent exchange with SiEt_3D yielding $\mathbf{1}(\text{D}_{11})^+$, but for this system neither a σ -silane complex nor an agostic silyl related to $\mathbf{1}(\text{H})\text{-H}^+$ formed, according to low-temperature ^1H NMR spectroscopy.

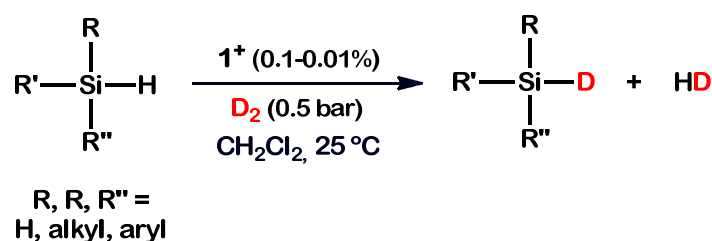


Scheme 12. Deuteration of $\mathbf{1}^+$ to yield $\mathbf{1}(\text{D}_{11})^+$ using D_2 or SiR_3D .

I.2.2. H/D/T exchange in hydrosilanes

The H/D exchange between $\mathbf{1}^+$ and D_2 or SiEt_3D (Scheme 12) suggested that a catalytic synthesis of deuterated silanes could be developed. As discussed in the Introduction section, this is an importance objective, since it

would constitute an improvement of current procedures for the isotopic labeling of organic molecules. With this goal in mind, we performed deuteration of a number of hydrosilanes ($\text{SiR}_{4-n}\text{H}_n$ ($n = 1-3$)) under mild conditions, using D_2 as the deuterium source. Low catalyst loadings of between 1 and 0.001 mol% (Table 1) were needed, denoting the efficiency of the catalyst.



Scheme 13. Deuteration of hydrosilanes ($\text{SiR}_{4-n}\text{H}_n$ ($n = 1-3$)) catalyzed by $\mathbf{1}^+$.

To optimize the conditions of the catalytic system, SiEt_3H was chosen as the model substrate. Screening of solvents showed that the exchange reaction proceeded at higher rates using low coordinating solvents such as CH_2Cl_2 , whereas lower rates were attained using diethyl ether or THF (entries 5, 6 of Table 1). Si–H/D exchange was efficient even in the neat silane, but due to the low solubility of $\mathbf{1}^+$ this strategy was only employed for catalyst loadings below 0.01 mol %. The rate of exchange was also dependent on the pressure of D_2 , since the solubility of the gas is directly related to its pressure. Thus the half-life of the exchange reaction at 0.5 and 3 bar of D_2 was *ca.* 200 and 100 min, respectively, for a reaction carried out at room temperature and with a concentration of $\mathbf{1}^+$ of 0.1 mol %. For the only sake of convenience of handling, we decided to use only 0.5 bar of D_2 for the deuteration of all

hydrosilanes. On the other hand, since the reactants and products in Scheme 13 exist in equilibrium, to ensure complete deuteration of the silanes three loadings with D₂ were routinely employed (see Experimental Section). Thus, the reaction was periodically stopped by cooling at 0 °C, the flask evacuated by application of vacuum (0.1 bar for ~20 s) and the reaction vessel charged again with 0.5 bar of D₂.

Table 1. Optimization of conditions for Si–H/D exchange using SiEt₃H.

Entry	Silane	Cat. (mol %)	Solvent	T (°C)	t (h)	% D
1	SiEt ₃ H	1	CD ₂ Cl ₂	25	3	≥ 99
2	SiEt ₃ H	0.1	CD ₂ Cl ₂	50	5	≥ 99
3	SiEt ₃ H	0.01	-	50	24	≥ 99
4	SiEt ₃ H	0.001	-	60	48	89
5	SiEt ₃ H	0.1	Et ₂ O	50	10	≥ 99
6	SiEt ₃ H	0.1	THF	50	8	≥ 99

The course of the reaction was followed by ¹H and ²⁹Si{¹H} NMR spectroscopy and by IR spectroscopy, to monitor the hydrogen isotope exchange. The ¹H NMR spectrum of SiEt₃H (CD₂Cl₂) exhibits a septet at δ 3.68 ppm that corresponds to the hydrogen atom bonded to silicon. Upon deuteration, this resonance gradually disappears (Figure 2), and it is completely absent in the ¹H NMR of the final product, which shows instead the corresponding signal in the ²H NMR spectrum. Deuteration of the silane ethyl substituents does not occur.

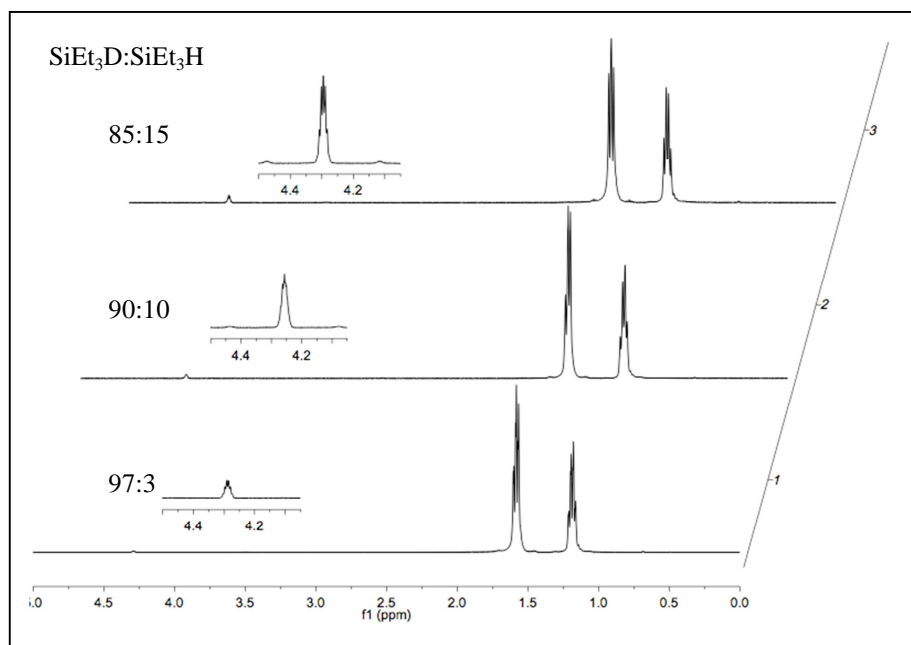


Figure 2. ^1H NMR spectrum of different mixtures of SiEt_3D and SiEt_3H .

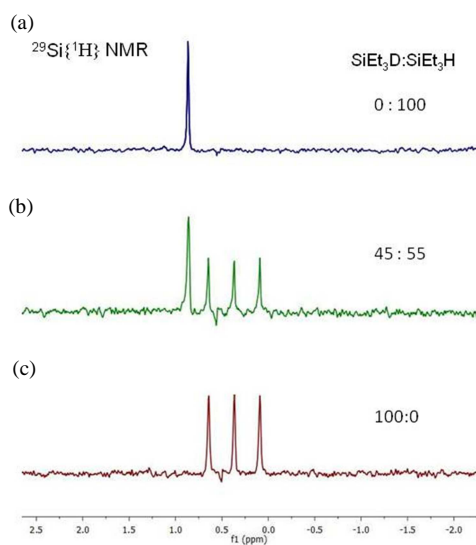


Figure 3. $^{29}\text{Si}\{^1\text{H}\}$ NMR spectrum of mixtures of SiEt_3D and SiEt_3H .

As shown in Figure 3a the $^{29}\text{Si}\{^1\text{H}\}$ NMR spectrum of SiEt_3H is a singlet with δ 0.8 ppm that experiences an isotopic displacement to δ 0.4 ppm ($^1J_{\text{SiD}} = 28$ Hz) upon deuteration (Figure 3c). The spectrum of a *ca.* 45:55 mixture of the two isotopologues is included in Figure 3b. On the other hand, the IR spectrum of SiEt_3H features a band at $\sim 2100\text{ cm}^{-1}$ due to $\nu(\text{Si-H})$ (Figure 4) that shifts to about 1530 cm^{-1} in the spectrum of SiEt_3D . The relative intensities of these IR bands along the course of the H/D

exchange match closely the results obtained from ^1H and $^{29}\text{Si}\{^1\text{H}\}$ NMR studies.

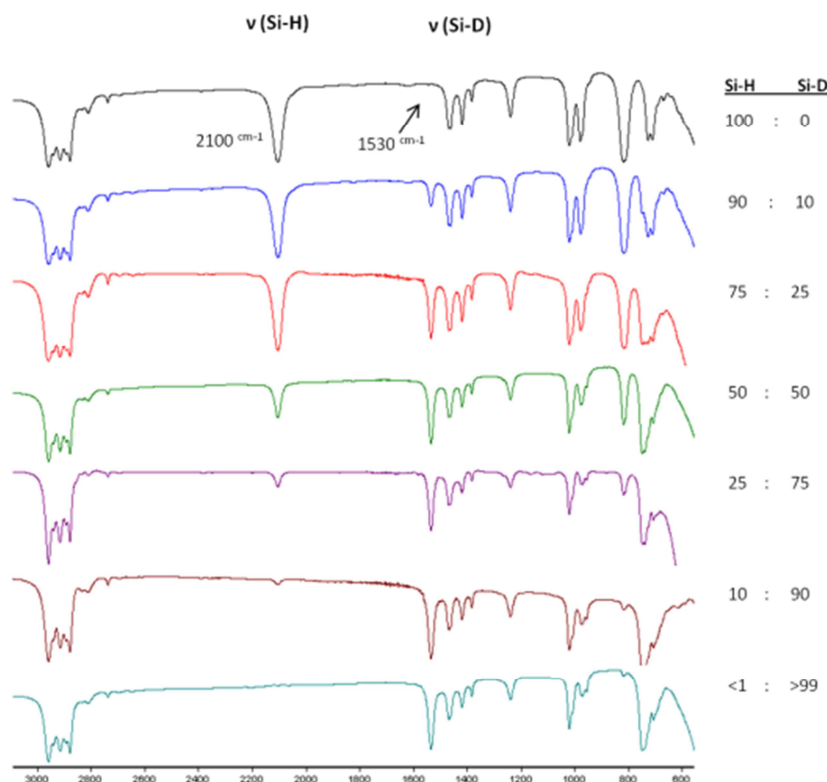


Figure 4. IR spectra (neat silanes) of mixtures of SiEt_3H ($\nu(\text{Si-H}) = 2100\text{ cm}^{-1}$) and SiEt_3D ($\nu(\text{Si-D}) = 1530\text{ cm}^{-1}$).

Table 2 presents a summary of the Si–H/D exchanges catalyzed by $\mathbf{1}^+$ that have been investigated. The deuteration is equally effective for secondary and tertiary silanes (Entries 1 – 4 of Table 2) and even a very reactive primary silane (SiPhH_3 , Entries 5 and 6) has been successfully deuterated. However, attempts to deuterate the explosive gas SiH_4 under strictly controlled conditions were unsuccessful, and decomposition of the

catalyst rapidly took place. It is noteworthy that polymethylhydrosiloxane (PMHS, entries 7 – 9), which is an inexpensive, non-toxic and environmentally benign reagent obtained as a secondary product in the silicon industry,³⁹ became deuterated under the same conditions. Numerous examples have been reported for the catalyzed reduction of a wide range of organic functionalities using PMHS as a *green* reducing reagent.⁴⁰ Thus, access to the deuterated isotopologue is of evident interest. Indeed, two PMHS polymers of different size (390 and 1700-3200 Da) were labeled with identical results.

Table 2. Screening of hydrosilanes.

Entry	Silane	Cat. (mol%)	T (°C)	t (h)	% D	Entry	Silane	Cat. (mol%)	T (°C)	t (h)	% D
1	SiPh ₃ H	1	25	3	≥ 99	13	SiEt ₂ H ₂	0.1	50	5	≥ 99
2	SiPh ₃ H	0.1	50	5	≥ 99	14	SiBzMe ₂ H	1	25	5	≥ 99
3	SiPh ₂ H ₂	1	25	3	≥ 99	15	Si(SiMe ₃) ₃ H ^c	1	25	16	30
4	SiPh ₂ H ₂	0.1	50	5	≥ 99	16	Si(SiMe ₃) ₃ H ^c	2	25	16	98
5	SiPhH ₃	1	25	3	≥ 99	17	Si(ⁿ Pr) ₃ H	1	25	5	≥ 99
6	SiPhH ₃	0.1	50	5	≥ 99	18	Si(ⁱ Pr) ₃ H ^c	1	25	16	80
7	PMHS ^a	1	25	3	≥ 99	19	1,2-C ₆ H ₄ (SiMe ₂ H) ₂	1	25	16	90
8	PMHS ^a	0.1	50	5	≥ 99	20	1,4-C ₆ H ₄ (SiMe ₂ H) ₂	1	25	5	≥ 99
9	PMHS-TMS ^b	0.1	50	5	≥ 99	21	Si(OEt) ₃ H	1	25	5	≥ 99
10	SiMe ₂ PhH	1	25	3	≥ 99	22	Si(OSiMe ₃) ₃ H	1	25	5	≥ 99
11	SiMe ₂ PhH	0.1	50	5	≥ 99	23	SiCl ₃ H ^c	1	25	16	21
12	SiEt ₂ H ₂	1	25	3	≥ 99	24	SiCl ₂ MeH ^c	1	25	16	53

^aPolymethylhydrosiloxane (M_n ca. 1700-3200). ^bPolymethylhydrosiloxane TMS terminated (M_n ca. 390). ^cCatalyst decomposition occurs.

³⁹ Lawrence N. J.; Drew M. D.; Bushell S. M. *J. Chem. Soc., Perkin Trans. 1*, **1999**, 3381.

⁴⁰ For selected examples: (a) Kim, D.; Park, B.-M.; Yun, J. *Chem. Commun.* **2005**, 1755. (b) Jurkauskas, V.; Sadighi, J. P.; Buchwald, S. L. *Org. Lett.* **2003**, 5, 2417. (c) Addis, D.; Das, S.; Junge, K.; Beller, M. *Ang. Chem. Int. Ed.* **2011**, 50, 6004. (d) Maeda, M.; Abe M.; Kojima, M. *J. Fluorine Chem.*, **1987**, 34, 337. (e) Eppstein, D. A.; Marsh, Y. V.; Schryver, B. B.; Larsen, M. A.; Barnett, J. W.; Verheyden J. P. H.; Prisbe, V. *J. Biol. Chem.*, **1982**, 257, 13390.

An important aspect in the development of new catalysts is their recyclability. As revealed by NMR studies, compound **1-BAr_F** is recovered unaltered after the catalytic runs, except in the few cases where catalyst decomposition occurs (Table 2). Furthermore, the catalyst can be recycled at least eight times (tested for deuteration of SiEt₃H) without loss of efficacy. Recycling of the catalyst needs simply a trap-to-trap distillation of the deuterated silane from the reaction crude. The resulting residue, which contained the rhodium catalyst, was dried in a high-vacuum line and used without further purification for the next catalytic cycle. After eight runs the spectrum of the resulting solid residue was identical to that of the starting catalyst precursor, as shown in Figure 5, whereas the fresh triethylsilane added for the last cycle appeared completely deuterated (no ¹H NMR signal due to Si–H at *ca.* 3.7 ppm).

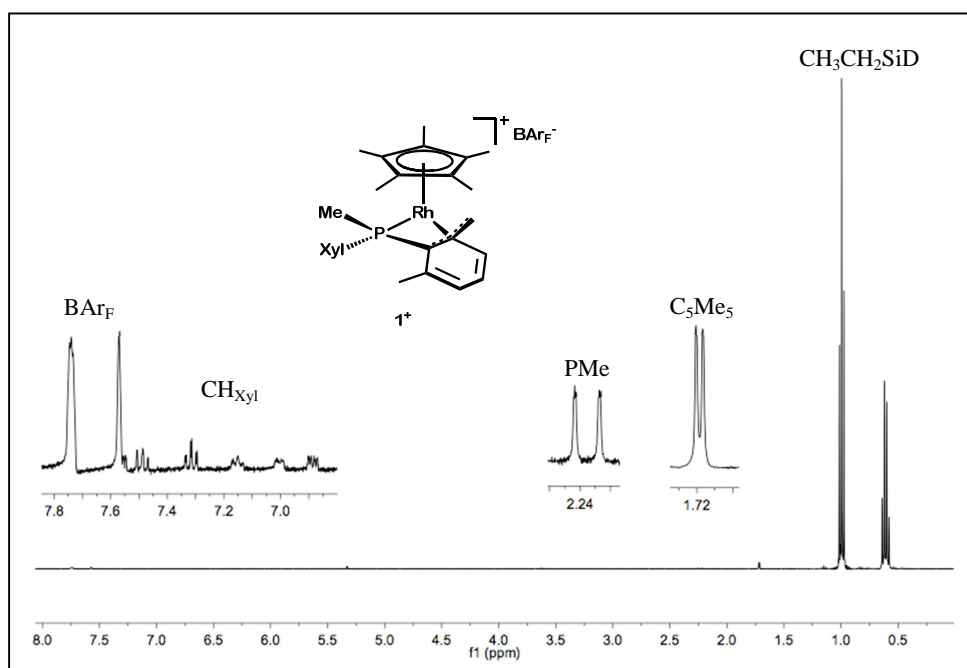


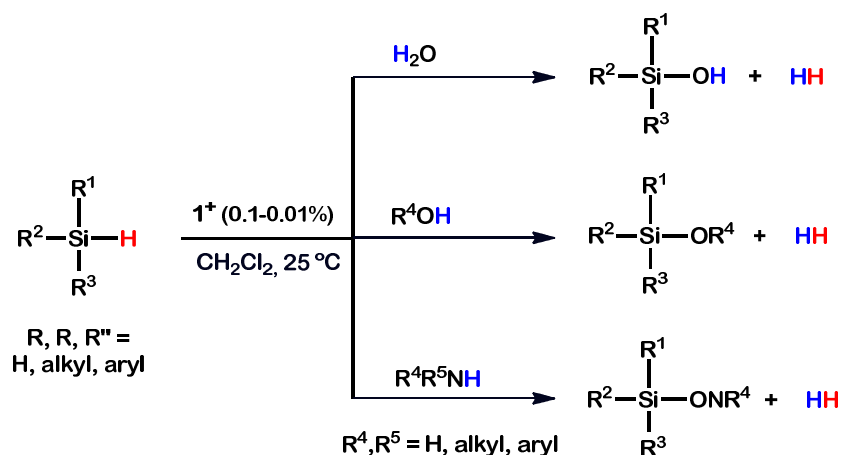
Figure 5. ¹H NMR spectrum of the solid residue after the eighth catalytic cycle (CD₂Cl₂, 25 °C, 400 MHz).

As discussed in the introduction, there are some examples of Si–H/D exchange catalyzed by heterogeneous materials.^{13c-e,15-17} The previous findings concerning the recyclable character of **1-BAr_F** strongly supports a homogeneous active species as the true catalyst. To confirm this hypothesis we performed the mercury test (details can be found in the Experimental Section), to find no loss of activity in the presence of mercury. A final indication that a homogeneous rather than heterogeneous process is responsible for the catalysis was inferred from the use of different catalysts derived from **1**⁺, as summarized in Table 3. In addition to **1-BAr_F** (Entry 1), the neutral complex **1-Cl** (Entry 4) and the cationic adducts, **1-NCMe**⁺ and **1-CO**⁺ (Entries 2 and 3, respectively), were employed, with the observation that the catalytic activity of these complexes was significantly lower than that of **1**⁺, and followed an order that reflects the facility with which **1**⁺ may be generated from these species, by dissociation of their NCMe, CO or Cl[−] ligand. In addition, no precipitation, metal film formation, powder suspension, or even darkening of the reaction mixtures were detected under the exchange conditions. It should be noted that although **1-SbF₆** is also an effective catalyst for the H/D exchange, in this case the process is heterogeneous, at least in part, as demonstrated by the Hg test. In fact, this is discernible from the darkening of the solution and the generation of finely divided metal particles using SbF₆[−] instead of BAr_F[−] as the counterion.

Table 3. H/D Exchange in triethylsilane catalyzed by several complexes.

Entry	Catalyst	Cat. (mol %)	Solvent	T (°C)	t (h)	% D
1	1-BAr_F	1	CD ₂ Cl ₂	25	3	≥ 99
2	1-NCMe ⁺	1	CD ₂ Cl ₂	25	16	95
3	1-CO ⁺	1	CD ₂ Cl ₂	25	16	87
4	1-Cl	1	CD ₂ Cl ₂	25	16	35

Taking into consideration the importance of a methodology for the preparation of isotopically labeled hydrosilanes, we developed a large scale synthesis of deuterated silanes for three commonly employed hydrosilanes, namely, SiEt_3H , SiMe_2Ph and SiPh_2H_2 (3 – 4 g scale). Using SiEt_3H as a representative example, 4.2 mg of compound $\mathbf{1}^+$ (3.1×10^{-3} mmol) were dissolved in 5 mL of SiEt_3H (31.3 mmol; catalyst concentration 0.01 mol %) in a *ca.* 220 mL flask and the mixture stirred at 50 °C, under 0.5 bar of D_2 , for a total time of 16h. Although the H/D exchange is fast at 20 °C in CH_2Cl_2 solution, heating at 50 °C permits complete solubilization of the catalyst into the neat silane, and hence catalysis performance in the absence of solvent. As already discussed, complete deuteration of the silane ($\geq 99\%$) was achieved by successive 0°C/vacuum/ D_2 loading cycles (5 times). Then, SiEt_3D was obtained by trap-to-trap distillation. The same procedure was utilized for the synthesis of SiMe_2PhD and SiPh_2D_2 . Pure SiMe_2PhD was separated by trap-to-trap distillation too, whereas for SiPh_2D_2 a Kugelrohr vacuum distillation apparatus was employed.



Scheme 14. Hydrolysis, alcoholysis and aminolysis of hydrosilanes catalyzed by $\mathbf{1}^+$.

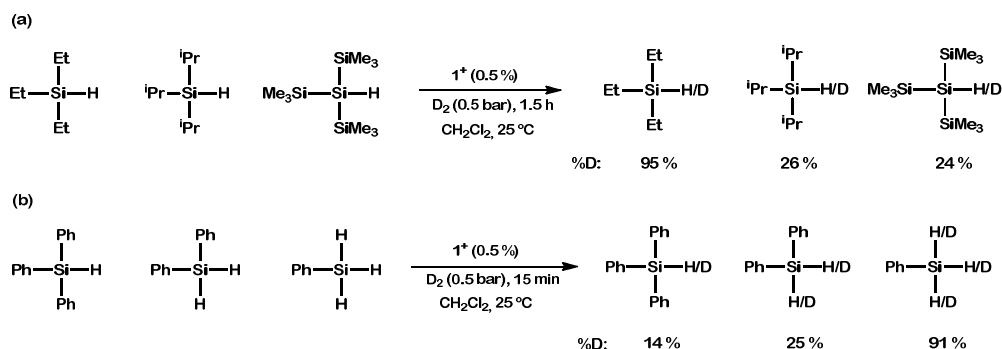
As a general precaution, water must be thoroughly excluded, since compound **1**⁺ also catalyzes, with very high efficiency, the production of H₂ from H₂O and hydrosilanes (see Scheme 14). In fact, the analogous condensation with alcohols or amines is also mediated by **1**⁺. Hydrolysis and alcoholysis of hydrosilanes is a well-known reaction that has been widely exploited in the last decades mainly for two different purposes: production of hydrogen,⁴¹ and alcohol and amine protection by formation of silyl-ethers⁴² and silyl-amines,⁴³ respectively. These transformations are currently being investigated within our research group and the results will be presented in due course.

Competition experiments with different silanes show that SiEt₃H, SiPh₃H and Si(OEt)₃H undergo deuteration with comparable rates. However, Si–H/Si–D exchange for SiEt₃H is considerably faster than for SiⁱPr₃H or Si(SiMe₃)₃H (see Scheme 15a). Similarly, the rate of incorporation of D into phenyl silanes qualitatively follows the order SiPhH₃ > SiPh₂H₂ > SiPh₃H (Scheme 15b). It thus seems that steric effects may be responsible for the observed differences.

⁴¹ (a) Luo, X.-L.; Crabtree, R. H. *J. Am. Chem. Soc.* **1989**, *111*, 2527. (b) Lee, M.; Ko, S.; Chang, S. *J. Am. Chem. Soc.* **2000**, *122*, 12011. (c) Lee, T. L.; Dang, L.; Zhou, Z.; Yeung, C. H.; Lin, Z.; Lau, C. P. *Eur. J. Inorg. Chem.* **2010**, 5675. (d) Mitsudome, T.; Noujima, A.; Mizugaki, T.; Jitsukawaa, K.; Kaneda, K. *Chem. Commun.* **2009**, 5302. (e) Mitsudome, T.; Arita, S.; Mori, H.; Mizugaki, T.; Jitsukawa, K.; Kaneda, K. *Angew. Chem. Int. Ed.* **2008**, *47*, 7938. (d) Tan, T.; Kee, J. K.; Fan, W. Y. *Organometallics*, **2011**, *30*, 4008.

⁴² (a) Mukherjee, D.; Thompson, R. R.; Ellern, A.; Sadow, A. D. *ACS Catal.* **2012**, *1*, 698. (b) Biffis, A.; Braga, M.; Basato, M. *Adv. Synth. Catal.* **2004**, *346*, 451. (c) Corbin, R. A.; Ison, E. A.; Abu-Omar, M. M. *Dalton Trans.* **2009**, 2850.

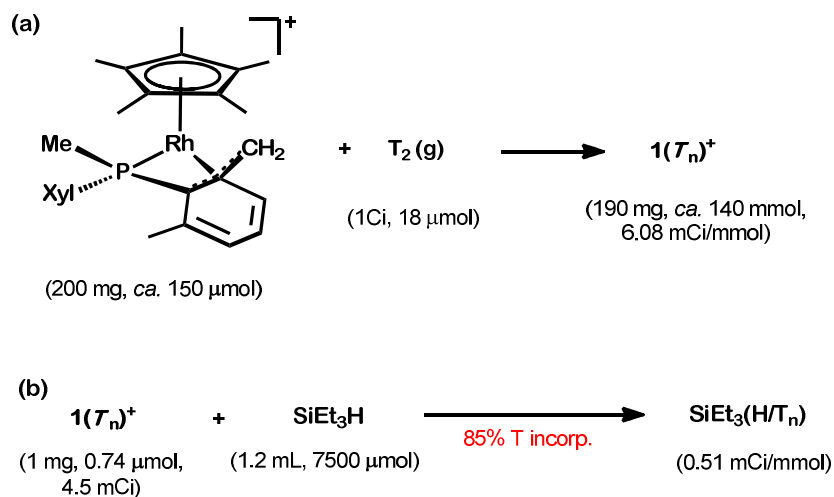
⁴³ (a) Dunne, J. F.; Neal, S. R.; Engelkemier, J.; Ellern, A.; Sadow, A. D. *J. Am. Chem. Soc.* **2011**, *133*, 16782. (b) Buch F.; Harder, S. *Organometallics* **2007**, *26*, 5132. (c)



Scheme 15. Competition studies for Si–H/D exchange.

The deuteration procedures we have just discussed can be extended to the synthesis of tritiated silanes. Despite their great potential, the availability of tritiated silanes is even scarcer than for the related deuterated compounds. We found that catalyst **1**⁺ allows facile tritium incorporation into hydrosilanes under mild conditions overcoming many of the disadvantages of commonly used tritiation methods.^{1b} Although a catalytic procedure similar to that described above for deuterium exchanges may be utilized, to avoid frequent use of tritium gas, which is a radioactive, dangerous and difficult substance to manipulate,^{1b} complex **1**⁺ was used as a tritium carrier for low specific activity tritium labeling. Thus, exposure of CH₂Cl₂ solutions of **1**⁺ (200 mg; 148 μmol) to 1Ci (18 μmol) of T₂ permitted T-incorporation (≥ 85%) into the CH₂ and CH₃(xylyl) sites of the catalyst, to yield **1**(T_n)⁺, which can be stored safely. Then, heating for example 1 mg (0.74 μmol, 4.5 mCi) of the tritiated rhodium complex with an excess of SiEt₃H (1.2 mL, 7.5 mmol; 50 °C, 5 days) permits T transfer to the silane, that can be separated from the catalyst by trap-to-trap distillation; the resulting tritiated silane features specific activity of 0.5 mCi/mmol, which means *ca.* 85 % of tritium incorporation. The specific activity of the resulting tritiated silane can be controlled by varying either the reaction time or the concentration of the

catalyst. Thus, carrying out a similar experiment with one tenth the amount of 1^+ (0.001% molar), the $\text{SiEt}_3(\text{H}/\text{T}_n)$ obtained exhibited 88 % tritium incorporation with specific activity of 0.05 mCi/mmol.

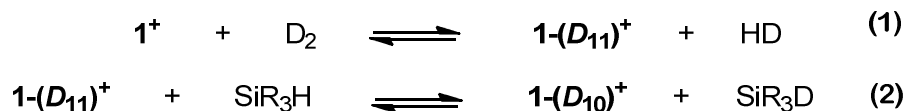


Scheme 16. (a) Tritiation of catalyst 1^+ using T_2 ; (b) Tritiation of SiEt_3H using $1(\text{T}_n)^+$ as the tritium carrier.

Mechanistic Studies

A reasonable mechanism that accounts for the observed Si–H/D exchange results from the simultaneous operation of the exchanges represented in Eqs. 1 and 2, which have been demonstrated experimentally (*vide supra*). A sequential route seems plausible, since deuteration of 1^+ by action of D_2 takes place readily to yield $1-(\text{D}_{11})^+$, which in turn, in the absence of D_2 (naturally, also in its presence), would deuterate the silane. Thus, the catalytic system can proceed through successive deuteration of 1^+

followed by reaction of deuterated $\mathbf{1}^+$ with the silane to afford isotopically labeled products (Scheme 17).



In order to shed light on the two steps of the proposed sequential mechanism, Dr. Joaquín López-Serrano carried out pertinent computational studies. As already mentioned, complex $\mathbf{1}^+$ exhibits a dynamic behavior in solution that results in the exchange of the roles of the two xylyl rings. Approach of a methyl group of the free xylyl ring to rhodium creates an agostic interaction that changes the coordination of the metalated ring to $\kappa^2\text{-}P,C$, with an increase in energy of only $2.9 \text{ kcal}\cdot\text{mol}^{-1}$ (Figure 6). The latter reacts readily with both H_2 and the hydrosilane. H_2 addition produces $\mathbf{1-(H_2)}^+$, which can undergo H–H heterolysis and transfer a proton to the Rh– CH_2 group to form $\mathbf{1(H)-H}^+$. In accordance with the DFT calculations summarized in Figure 6, the overall process is fast and it is entirely reversible, in excellent agreement with the experimental results. The calculations predict that $\mathbf{1(H)-H}^+$ is more stable than the initial $\kappa^2\text{-H}_2$ adduct ($\mathbf{1-(H_2)}^+$), and slightly less stable than $\kappa^4\text{-}\mathbf{1}^+$ plus H_2 (Figure 6), once more in accordance with NMR studies.

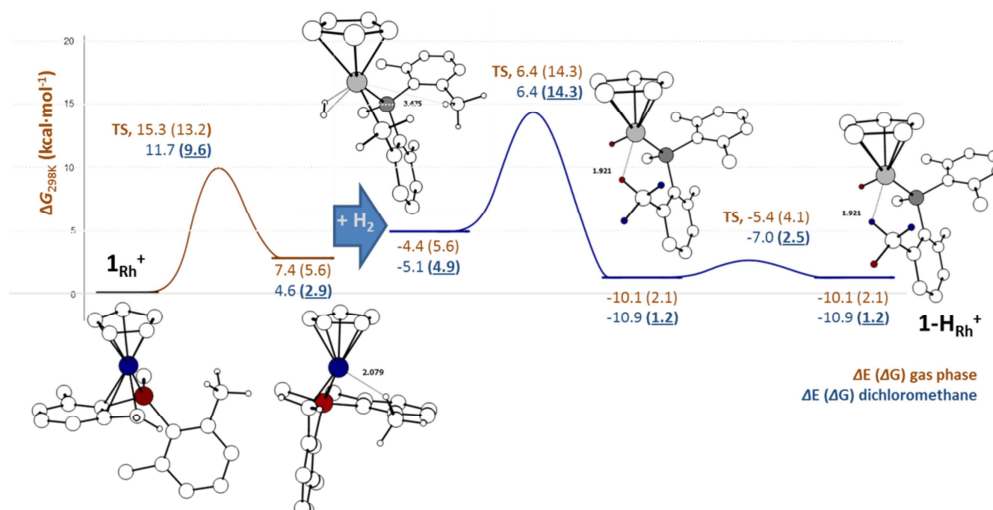


Figure 6. DFT-calculated free energy ($\Delta G_{298.15^\circ}$) profile in dichloromethane for the reaction of $\mathbf{1}^+$ with H_2 ($P = 1\text{ atm}$).

Similar calculations were performed for the reaction of $\mathbf{1}^+$ and silanes, using Me_3SiH as a simplified model silane. The initial product of this reaction is a η^1 -silane adduct ($\mathbf{1}\text{-H-SiEt}_3^+$) analogous to that reported by Brookhart and co-workers,^{9b,44} and situated only $5.7\text{ kcal}\cdot\text{mol}^{-1}$ above $\kappa^4\text{-}\mathbf{1}^+$. Oxidative addition of the Si-H bond leads to a Rh(V) intermediate ($\mathbf{1}\text{-(H)(SiEt}_3\text{)}^+$), for which an overall, readily affordable, free energy barrier of $20.3\text{ kcal}\cdot\text{mol}^{-1}$ was calculated (Figure 7). Slightly higher in energy ($1.6\text{ kcal}\cdot\text{mol}^{-1}$) appears the agostic intermediate $\mathbf{1(H)\text{-SiEt}_3}^+$, which is analogous to the product derived from the reaction with H_2 (i.e. $\mathbf{1(H)\text{-H}}^+$). Considerable steric congestion is observed in these calculated silyl intermediates, in agreement with the results obtained in the competition experiments already discussed, where bulkier hydrosilanes are deuterated at lower rates.

⁴⁴ Yang, J.; White, P. S.; Schauer, C. K.; Brookhart, M. *Angew. Chem. Int. Ed.* **2008**, 47, 4141.

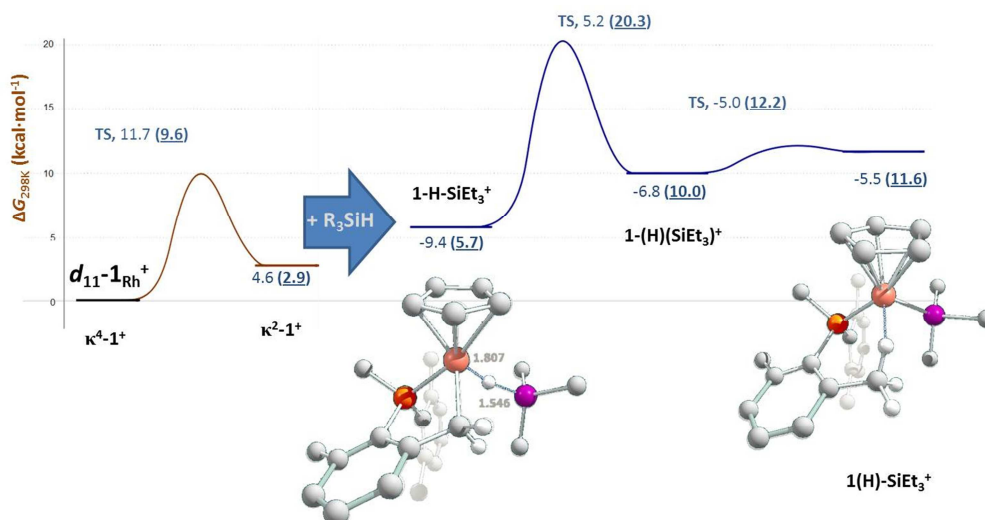
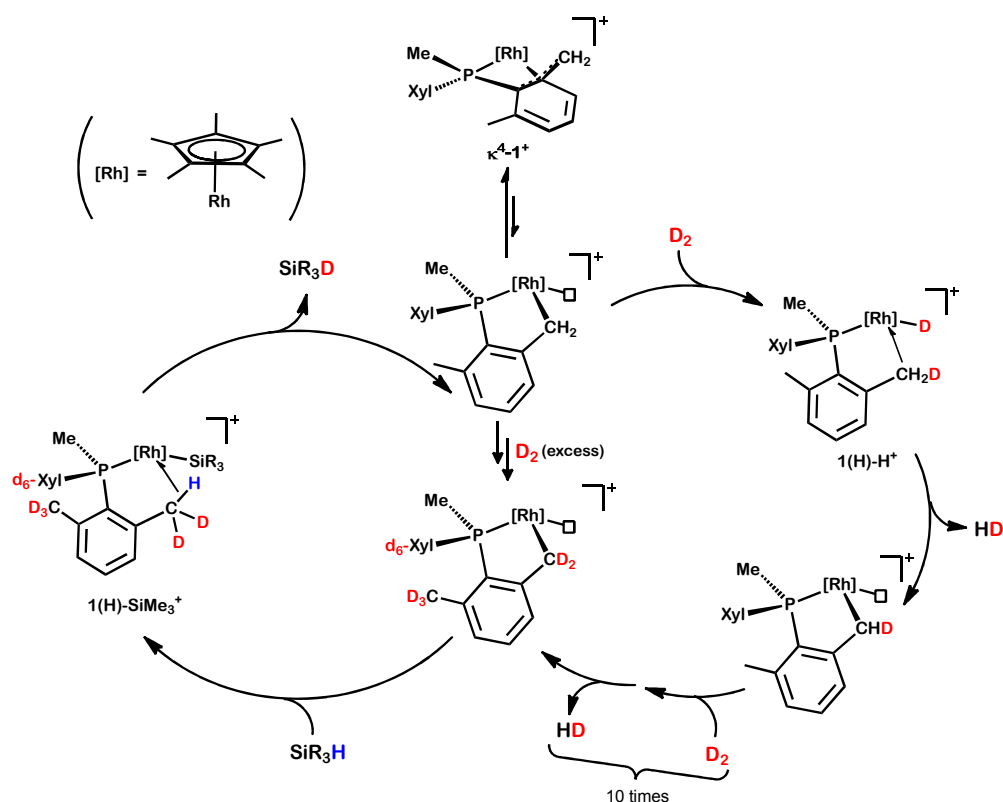


Figure 7. DFT-calculated free energy ($\Delta G_{298.15}$) profile in dichloromethane for the reaction of 1^+ with Me_3SiH ($P = 1 \text{ atm}$).

The two sequential but independent routes provide an overall mechanism that accounts for silane deuteration catalyzed by 1^+ (Scheme 17). C–H/C–D exchange is, as already indicated, a very facile reaction that occurs by addition of D_2 to 1^+ (κ^2 -coordination) followed by elimination of HD. Repetition of this sequence of events leads ultimately to 1-D_{11}^+ , in which all benzylic positions of the two xylyl rings have become deuterated. For simplicity, the Si–H to Si–D conversion of the hydrosilane has been represented in Scheme 17 to involve the fully deuterated compound 1-D_{11}^+ . Most likely, species 1-D_n^+ with intermediate levels of deuteration are also suitable for this purpose. It is worth mentioning that these reaction pathways imply participation of reactive $\sigma\text{-H}_2$ and $\sigma\text{-silane}$ complex intermediates,⁴⁵

⁴⁵ (a) Kubas G. J. *Metal Dihydrogen and Sigma-Bond Complexes. Structure Theory and Reactivity*. (Kluwer Academic, New York, **2001**). (b) Crabtree R. H. *Angew. Chem., Int. Ed.* **1993**, 32, 789. (c) Perutz R. N., Sabo-Etienne S. *Angew. Chem., Int. Ed.* **2007**, 46, 2578.

and constitute a new example of metal-ligand cooperation,⁴⁶ which in this case consists in reversible Rh–C bond cleavage and formation (κ^4 -to- κ^2 coordination change) by action of dihydrogen and hydrosilanes.



Scheme 17. Proposed catalytic cycle for isotopic labelling of hydrosilanes catalyzed by 1^+ .

⁴⁶ Milstein D. *Top. Catal.* **2010**, 53, 915.

I.2.3. Hydrosilylation Reactions

As already indicated, the use of labeled hydrosilanes in chemical synthesis could overcome many of the problems associated with conventional reduction methodologies. We have found that complex **1**⁺ is not only a very effective catalyst for the deuteration and tritiation of hydrosilanes, but also promotes the hydrosilylation of carbonyl compounds, imines, and even the less reactive nitriles. In the following sections the catalytic ability of **1**⁺ to reduce each of these functionalities will be discussed. This reactivity has allowed us to develop a one-flask, two-step procedure for the efficient deuterio- and tritio-silylation of organic compounds, using hydrosilanes under D₂ (0.5 bar) or T₂, at low catalyst loadings (0.1 – 0.5 mol %). The process permits selective regiocontrol by formation of a C–D or C–T bond, with protection of the resulting alcohol or amine as a silyl-ether or silyl-amine, respectively. Therefore it represents a robust and efficient strategy which overcomes the main problems encountered in the synthesis of labeled organic molecules from conventional hydride sources.

Hydrosilylation of Carbonyl Functionalities

As a first step in this development, several hydrosilanes were tested utilizing acetophenone as the reference substrate, with catalyst loadings of 0.1 mol %. The results collected in Table 4 reveal that in most cases (entries 1-4) full conversion to the corresponding silyl-ether resulted after one hour at room temperature. However, the bulky tertiary silanes SiR₃H (R = ⁱPr, SiMe₃, Si(OMe)₃) did not react even at 50 °C overnight (entries 5-7).

Table 4. Screening of silanes^a.

Entry	Silane	T (°C)	t (h)	conv (%)
1	SiEt ₃ H	25	1	99
2	SiEt ₂ MeH	25	1	99
3	SiMe ₂ PhH	25	1	99
4	Si(ⁿ Pr) ₃ H	25	1	99
5	Si(ⁱ Pr) ₃ H	50	12	0
6	Si(SiMe ₃) ₃ H	50	12	0
7	Si(Si(OMe) ₃) ₃ H	50	12	0

^aConditions: acetophenone (0.5 mmol), 0.1 mol % of **1**⁺, 2.2 equiv silane, CD₂Cl₂ (0.5 mL).

With these results in hand, a broad range of ketones (Table 5) and aldehydes (Table 6) were hydrosilylated with SiEt₃H. Excellent activities to the expected silyl ethers were attained at 25 °C, with a reaction time of one hour and a catalyst concentration of 0.1 mol %. Results included in Table 5 point out that increasing the steric properties of the ketone substituents has a detrimental effect in the hydrosilylation reaction. Thus, 2-naphtyl ketone (Entry 8) is quantitatively hydrosilylated after one hour, whereas 1-naphtyl ketone, where the carbonyl functionality is sterically congested due to the condensed phenyl ring, is minimally reduced under the same conditions (15 %). However, at the same temperature and with reduced reaction time (16 vs. 24 h), a catalyst concentration of 1 mol % resulted in the formation of the expected silyl-ether in 75 % yield (Entry 10). A similar effect was observed for the hydrosilylation of di(*iso*-propyl)ketone (Entry 4), whose reduction is

not completed under the conditions employed for less hindered aliphatic ketones (Entries 1 – 3). Other ketones such as benzophenone and cyclohexanone were efficiently hydrosilylated by catalyst **1**⁺ (Entries 11 and 12).

Table 5. Screening of ketones.^a

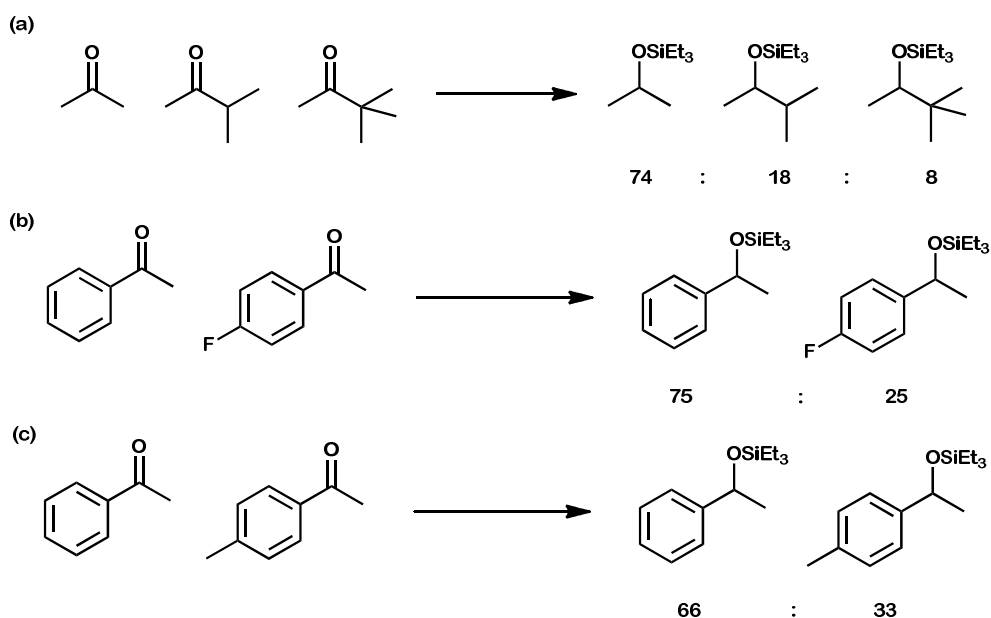
$$\text{R}_1\text{-C(=O)-R}_2 \xrightarrow[\text{SiEt}_3\text{H}]{\text{1}^+} \text{R}_1\text{-CH(OSiEt}_3\text{)-R}_2$$

Entry	R ₁	R ₂	S/C	temp (°C)	t (h)	conv (%)
1	Me	Me	1000	25	1	99
2	ⁱ Pr	Me	1000	25	1	99
3	^t Bu	Me	1000	25	1	99
4	ⁱ Pr	ⁱ Pr	1000	50	24	75
5	Ph	Me	1000	25	1	99
6	4-Me-Ph	Me	1000	25	1	99
7	4-F-Ph	Me	1000	25	1	98
8	2-Naph	Me	1000	25	1	99
9	1-Naph	Me	1000	50	24	15
10	1-Naph	Me	100	50	16	75
11	Ph	Ph	100	25	1	99
12	<i>c</i> -C ₆ H ₁₀ O		100	25	1	99

^a Conditions: 0.1-0.5 mmol substrate, 2.2 equiv SiEt₃H; CD₂Cl₂ (0.5 mL).

As a test for the importance of steric effects, a competition experiment was carried out with equimolar amounts of RC(O)Me (R=Me, ⁱPr, ^tBu) against 1 equiv of SiEt₃H. It resulted in the formation of the expected silyl-ethers (Scheme 18a) in a ratio of 9(Me):2(ⁱPr):1(^tBu), confirming the deleterious effect of bulky groups next to the carbonyl functionality. On the

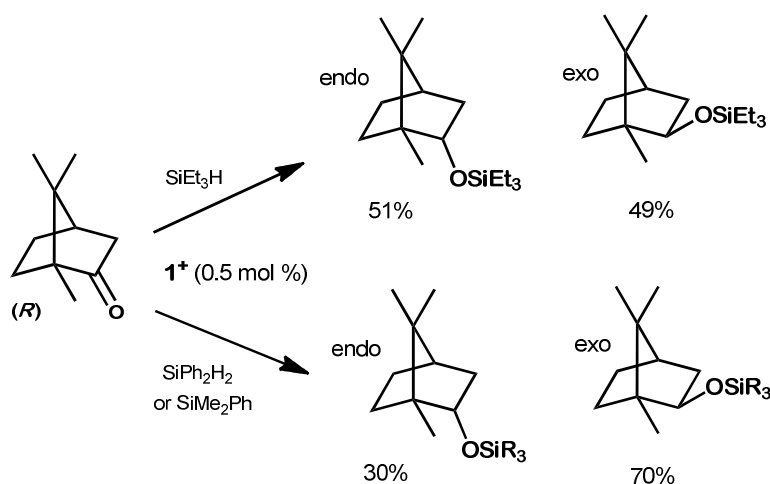
other hand, comparison of the reactivity of the *para*-X acetophenones (X = H, CH₃, F) disclosed a moderate increase in the rate with the basicity of the substrate (Scheme 18b,c), as products formed in the ratio 3(CH₃):1(H) and 2(H):1(F).



Scheme 18. Competition studies for the hydrosilylation of ketones catalyzed by **1**⁺.

The reduction of a common natural product with biological activity, namely the (*R*)-camphor molecule, that contains a sterically congested ketone functionality, deserves some additional comments. Reduction of the carbonyl group of this molecule can give rise to *exo* or *endo* isomers. Due to steric hindrance around the carbonyl group the reaction proceeded at lower rates than for most of the ketones included in Table 5, and to complete the reduction a catalyst load of 0.5 mol % and a reaction temperature of 50 °C during 40 h were needed. The three silanes employed (SiEt₃H, SiPh₂H₂ and SiMePh₂H) led to little or no control of the diastereoselectivity, although

SiPh_2H_2 and SiMe_2Ph favored formation of the *exo* product (*ca.* 7:3 ratio of *exo:endo* in both cases). This selectivity is comparable to that reported when $\text{RhH}(\text{PPh}_3)_4$ was used as a catalyst⁴⁷ (1.8:1 ratio) but is opposite to catalysis by the iridium cation $[\text{IrH}(\text{POCOP})(\text{acetone})]^+$ (POCOP = 2,6-bis(di-*tert*-butylphosphinito)phenyl), that produced an *exo:endo* ratio of 1:4.^{9a} Although our reaction is less efficient than the latter process, which proceeds quantitatively at 0 °C,^{9a} for our system direct deuteriosilylation was achieved by application of the one-flask, two-step procedure that will be described in a subsequent section.



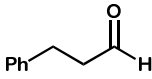
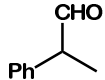
Scheme 19. Hydrosilylation of (*R*)-camphor catalyzed by **1**⁺.

To complete these studies, aldehydes and α,β -unsaturated compounds were also investigated, with excellent results in the reduction of aldehydes (Table 6). For the α,β -unsaturated carbonyl compounds tested (Table 7), 1,2-

⁴⁷ Zheng, G. Z.; Chan, T. H. *Organometallics* **1995**, 14, 70.

and 1,4-addition products were in general observed, with the exception of 2-cyclohexen-1-one (Entry 3) that yielded exclusively the 1,4-addition product.

Table 6. Screening of aldehydes.^a

$ \begin{array}{c} \text{O} \\ \parallel \\ \text{R}_1-\text{C}-\text{H} \end{array} \xrightarrow[\text{SiEt}_3\text{H}]{1} \begin{array}{c} \text{OSiEt}_3 \\ \\ \text{R}_1-\text{C}-\text{H} \end{array} $					
Entry	Substrate	S/C	T (°C)	<i>t</i> (h)	conv (%)
1	CH ₃ (CH ₂) ₅ C(O)H	10000	25	1	99 ^b
2	CH ₃ CH ₂ C(O)H	1000	25	1	99 ^b
3		1000	25	1	99 ^b
4		1000	25	1	99 ^b
5	PhC(O)H	100	25	1	99
6	2-F-PhC(O)H	100	50	8	99
7	4-Cl-PhC(O)H	100	50	12	98
8	4-NO ₂ -PhC(O)H	100	50	72	99

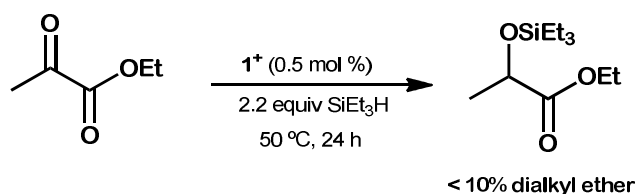
^a Conditions: 0.1-0.5 mmol substrate, 2.2 equiv SiEt₃H, CD₂Cl₂ (0.5 mL). ^b Minor amounts of dialkyl ethers (<10%).

Table 7. Screening of α,β -unsaturated carbonyl compounds.^a

Entry	Substrate	S/C	T (°C)	t (h)	Products and conversion (%)		
					1,2-addition	1,4-addition	
1		20 0	25	1	 6%	 (Z) 63%	 (E) 31%
2		20 0	25	1	 10%	 (Z) 25%	 (E) 65%
3		20 0	25	1		 100%	
4		20 0	25	1	 48%	 (Z) <0,5%	 (E) 52%

^b Conditions: 0.1-0.5 mmol substrate, 2.2 equiv SiEt₃H, CD₂Cl₂ (0.5 mL). Overall conversion of substrates: $\geq 99\%$.

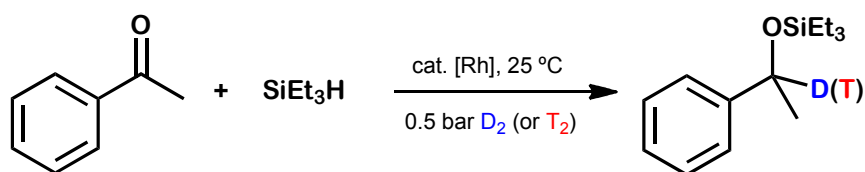
At variance with the above, less reactive carbonyl species like esters, and amides (e. g. ethylbenzoate, ethylbutyrate, benzamide and *N,N*-dimethylacetamide) were unreactive toward several tertiary and secondary silanes (prolongued heating at 60 °C). Profit can, however, be taken from this negative result to achieve the chemoselective reduction of the keto functionality of ethyl pyruvate (Scheme 20) to the corresponding silyl ether.



Scheme 20. Chemoselective hydrosilylation of ethyl pyruvate catalyzed by 1^+ .

Direct Deutero- and Tritio-silylation Reactions of Carbonyl Compounds

The efficiency of complex 1^+ for the hydrosilylation of carbonyl functionalities is noteworthy. Since, as already mentioned, 1^+ is also a very effective catalyst for the hydrogen isotope exchange in hydrosilanes, deutero- and tritio-silanes, e.g. SiEt_3D and SiEt_3T , can be generated *in situ* and used as reagents for deutero- and tritio-silylations, under conditions similar to those employed for Si–H additions. Moreover, as the two catalytic processes are fast at room temperature, a convenient two-step, one-flask method, whereby the labeled silane is generated first from SiEt_3H and D_2 or T_2 in the presence of 1^+ , and then reacted with the organic substrate, can be developed for the efficient, atom-economic deutero- and tritio-silylation reactions of carbonyl compounds (Scheme 21).

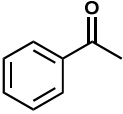
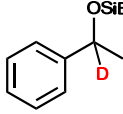
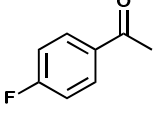
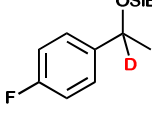
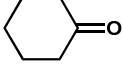
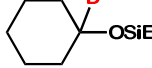
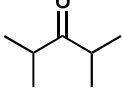
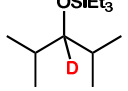
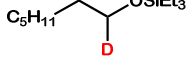

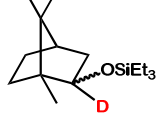
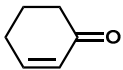
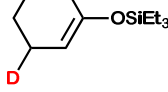
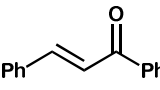
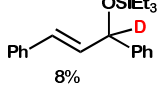
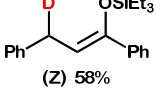
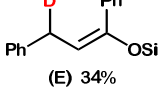
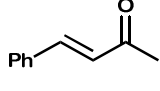
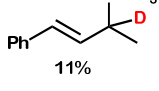
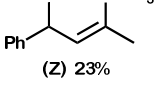
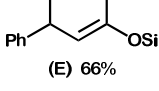
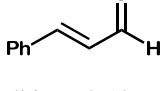
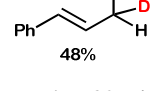
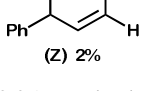
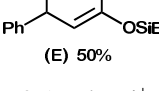


Scheme 21. Direct deutero- and tritosilylation of acetophenone catalyzed by 1^+ .

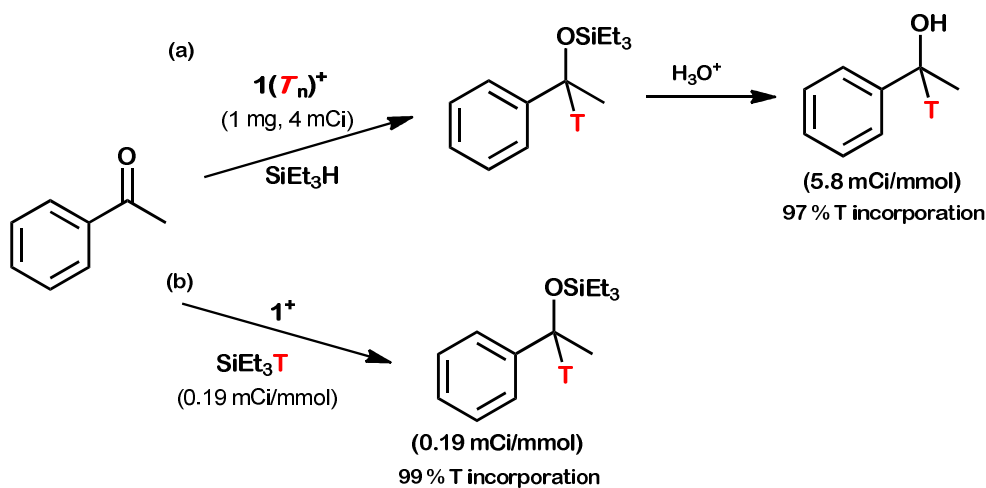
To achieve $\geq 99\%$ D-incorporation into the product, full deuteration of the silane was assured by subjecting the SiEt_3H -plus-catalyst mixture to three D_2 loadings, each involving cooling at $0\text{ }^\circ\text{C}$ / vacuum (0.1 bar) / 0.5 bar D_2 (see Experimental Section). Evidently, these D- (and T-) labeling procedures represent an important simplification of present methods, that require the previous synthesis and isolation of SiEt_3D or SiEt_3T .²⁴ In fact, our catalytic synthesis of SiEt_3T (or SiEt_3D) is clean, rapid and simple, it is performed in one step and permits subsequent use of the silane reagent in the same flask for the silylation reaction. Table 8 summarizes deuteriosilylation reactions in which the substrate is added after SiEt_3D has been formed (from SiEt_3H , D_2 and **1**⁺).

The same concept of labeling was used for tritio-silylations (Table 9). However, considering the very small amounts of the radioisotope needed for the labeling and taking additionally into account reasons of security and convenience of handling, the tritiated complex **1**(T_n), instead of T_2 gas, was employed as a very efficient tritium transferring reagent in the experiment (Scheme 22a). Thus, a mixture of **1**(T_n)⁺ (4 mCi/mg), SiEt_3H and acetophenone yielded the corresponding tritiated silyl-ether with a (non-optimized) reaction time of 8 days to ensure complete T transfer. The resulting silyl-ether was subsequently hydrolyzed and isolated by column chromatography as radioactive 1-phenylethanol, with specific activity 5.88 mCi/mmol (*ca.* 97% T-incorporation).

Table 8. Direct Deuterosilylation of carbonyl compounds.

Entry	Substrate	Conv. (%)	Deuterated Products
1		99	
2		99	
3		99	
4		99	
5	$\text{C}_5\text{H}_{11}\text{CHO}$	99 ^b	
6	 (R)	58 ^c	 ca. 1:1 exo:endo
7		99	
8		99	 8%  (Z) 58%  (E) 34%
9		99	 11%  (Z) 23%  (E) 66%
10		99	 48%  (Z) 2%  (E) 50%

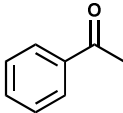
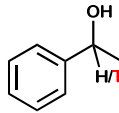
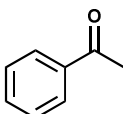
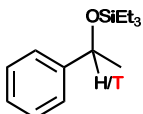
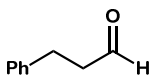
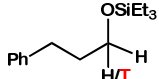
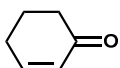
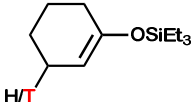
^a Conditions: 0.5 bar D₂ (3 D₂/vacuum cycles, 30 min), 0.25 mmol substrate, 0.5 mol % **1**⁺, 2.2 equiv SiEt₃H, CD₂Cl₂ (0.5 mL), 25 °C, 5 hours. ^b Minor amounts of dialkyl ethers R₁C(O)R₁ (<10%). ^c Conditions: 50 °C, 40 hours.



Scheme 22. Tritiosilylation of acetophenone *via* (a) tritiated complex 1^+ , or (b) tritiated triethylsilane.

From a practical point of view, the same tritiation was performed with previously labeled $\text{SiEt}_3\text{H}(\text{T}_n)$ (0.19 mCi/mmol) and provided 99% tritium incorporation into the resulting silyl-ether (Entry 2) (Scheme 22b). With the latter procedure, the scope of tritiosilylation was also extended successfully to aldehydes and α,β -unsaturated ketones, like hydrocinnamaldehyde (Entry 3), and 2-cyclohexen-1-one (Entry 4), with T-incorporation of 99% into both silyl-ethers.

Table 9. Tritiosilylation of carbonyl compounds.

Entry	Substrate	S/C	t (h)	Conv. (%)	T incorp. (%)	Tritiated Products
1 ^a		1000	192	99	97	
2 ^b		200	24	99	99	
3 ^b		200	24	99	99	
4 ^b		200	24	99	99	

^a Conditions: 2.2 mmol substrate, 0.1 mol % **1**(*T_n*)⁺, 0.9 eq SiEt₃H, CD₂Cl₂ (0.5 mL), 50 °C. ^b 0.44 mmol substrate, 0.5 mol % **1**⁺, 0.9 eq SiEt₃H(*T_n*), CD₂Cl₂ (0.5 mL), 50 °C.

Hydrosilylation of C-N Multiple Bonds

Although the efficacy of catalyst **1**⁺ for the hydrosilylation of C–N multiple bonds is not particularly relevant, there is some interesting catalytic activity that deserves to be discussed. Reaction of N-benzylidene aniline with 2.2 equiv. of SiEt₃H at 50 °C for 2h, in the presence of 1 mol % concentration of **1**⁺, gave the expected silylamine product in quantitative yield (Table 10, Entry 1). Using the procedure described above for direct deuteriosilylation, the D-isotopologue was generated also quantitatively (Entry 2). In this case,

to ensure full deuteriosilylation a non-optimized reaction time of 12h was employed.

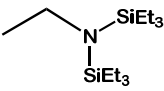
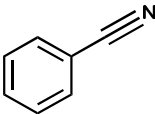
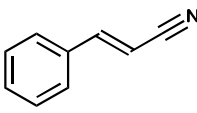
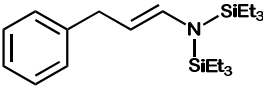
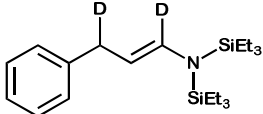
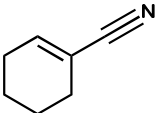
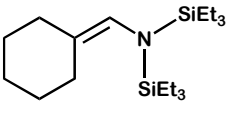
Table 10. Hydrosilylation of imines catalyzed by **1**⁺.

Entry	Substrate	S/C	Silane	t (h)	Conv. (%)	Products
1		100	SiEt ₃ H	2	100	
2		100	SiEt ₃ D	12	100	
3		100	SiEt ₃ H	24	15	 75 % 25 %
4		100	SiEt ₃ H	24	40	

^aConditions: 2.2 equiv. silane, solvent (CD₂Cl₂, 0.5 mL), 50 °C.

The imine hydrosilylation catalyzed by **1**⁺ is very sensitive to steric hindrance around the C=N bond. Thus, hydrosilylation of the bulkier aldimine *N*-benzylidene-*t*-butylamine (Entry 3), and ketimine (*E*)-*N*-(1-phenylethylidene)aniline (Entry 4), occurred with low conversion and in the former case with partial formation of the opposite regioselectivity product (Entry 3).

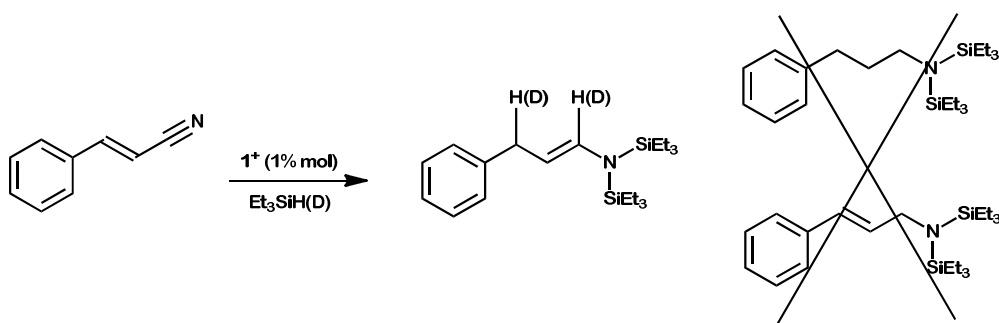
Table 11. Hydrosilylation of nitriles catalyzed by **1**⁺.

Entry	Substrate	S/C	Silane	t (h)	T (°C)	Conv. (%)	Products
1	CH ₃ CN	100	SiEt ₃ H	24	50	38	
2		100	SiEt ₃ H	48	60	-	No reaction
3		100	SiEt ₃ H	6	50	100	
4		100	SiEt ₃ D	36	50	100	
5		100	SiEt ₃ H	7	80	95	

^aConditions: 3 equiv. silane, solvent (ClCH₂CH₂Cl, 0.5 mL).

The related hydrosilylation of C≡N bonds remains comparatively unexplored due to the inertness of the cyano group under common hydrosilylation conditions.²⁹ In fact, acetonitrile (Table 11, Entry 1) underwent only partial conversion (<40%) in the presence of **1**⁺ and SiEt₃H (50 °C, 24h), and benzonitrile remained unaltered under somewhat more forcing conditions (Entry 2). However, α,β-unsaturated nitriles experienced facile hydrosilylation to produce vinylamines protected with two silyl groups (Entries 3-5). This observation finds scarce literature precedent^{32a,b} and

allowed isolation of vinyl bis(silylamines) as stable molecules. The parent vinylamines are usually unstable and decompose gradually even at low temperatures.⁴⁸ Use of this method permitted facile D-labelling of the amine resulting from the double deuteriosilylation of cinnamionitrile (Entry 4). At variance with previous reports,^{32a,b} other possible products of this reaction, like the protected aliphatic amine, or the also protected allylic amine were not observed (Scheme 23). Moreover, the double hydrosilylation of cinnamaldehyde by **1**⁺ is highly regioselective and gives exclusively the *E* isomer.



Scheme 23. Selective hydrosilylation of cinnamionitrile with catalyst **1**⁺. Common by-products found in hydrosilylation of α,β -unsaturated nitriles have not been detected.

⁴⁸ (a) Ripoll, J. L. Lebrun, H. Thuillier, A. *Tetrahedron* **1980**, 36, 2497. (b) Tomoda, S. Matsumoto, Y. Takeuchi, Y. Nomura, Y. *Chem. Lett.* **1986**, 1193.

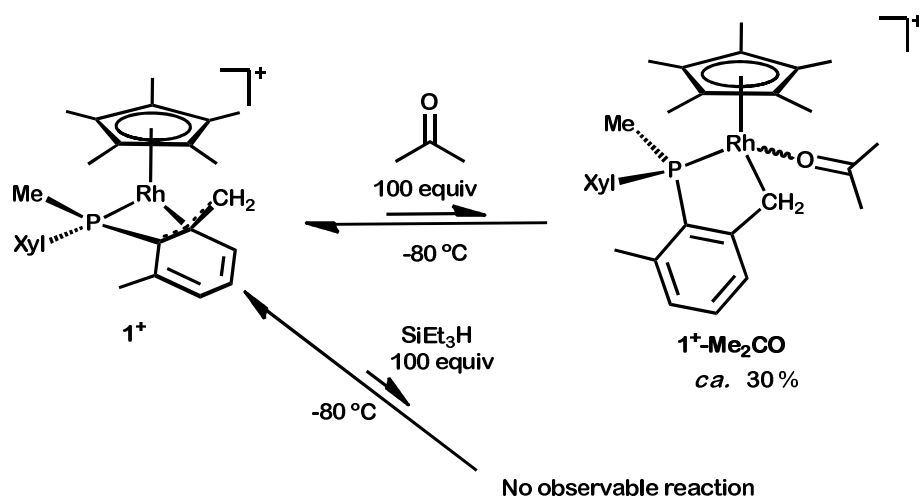
Mechanistic Investigations

The two main mechanistic pathways proposed for the metal-catalyzed hydrosilylation of carbonyl compounds were presented in Scheme 7. Late transition metal catalysts operate usually in accordance with the *Chalk-Harrod* mechanism (Scheme 7a),³⁴ while early transition metal catalysis seems to occur by a σ -bond metathesis route (Scheme 7b).³⁵ In the first instance, oxidative addition of the Si–H bond is key step. A third pathway, first proposed by Piers³⁶ for ketones hydrosilylation by $\text{B}(\text{C}_6\text{F}_5)_3/\text{Ph}_3\text{SiH}$ and later adopted by Brookhart for a cationic iridium-based system,^{9b} implies silylium cation (Ph_3Si^+) transfer (Scheme 8).

To gain mechanistic insight, some additional experiments were developed.

Reactivity of $\mathbf{1}^+$ toward $\text{CH}_3\text{C}(\text{O})\text{CH}_3$ and SiEt_3H

Addition of 20 equiv of either acetone or SiEt_3H to $\mathbf{1}^+$ did not lead to any observable change by NMR in the temperature range from -80 to -40 °C. Increasing the amount of substrate to 100 equiv did not alter this result for SiEt_3H . However, it permitted detection of adduct $\mathbf{1}\text{-Me}_2\text{CO}^+$ at temperatures below -30 °C (Scheme 24). This species gives rise to a broad $^{31}\text{P}\{^1\text{H}\}$ resonance at 47.3 ppm ($^1J_{\text{RhP}} = 155$ Hz) and exists at -80 °C in equilibrium with $\mathbf{1}^+$, in a ratio of *ca.* 1:3. Doubtless, the acetone adduct is favored over the purported silane adduct but the catalyst resting state appears to be complex $\mathbf{1}^+$.



Scheme 24. Equilibrium reactions of **1⁺** with excess acetone and SiEt₃H at -80 °C.

Kinetic Experiments

Kinetic studies by the group of Brookhart for iridium-catalyzed hydrosilylations^{9b} led to the mechanism presented in Scheme 8, which had been proposed earlier by Piers³⁶ for B(C₆F₅)₃ catalysis of the same reaction. Brookhart and co-workers determined that their system was zero-order in ketone and first-order in silane concentration. At variance with this result we ascertained a first-order dependence in the concentration of both the silane and the ketone in the hydrosilylation of acetophenone by SiEt₃H catalyzed by **1⁺** (Figure 8). Additionally, a kinetic isotopic effect (KIE) of 1.9 was measured in the hydrosilylation of acetophenone by SiEt₃H(D).

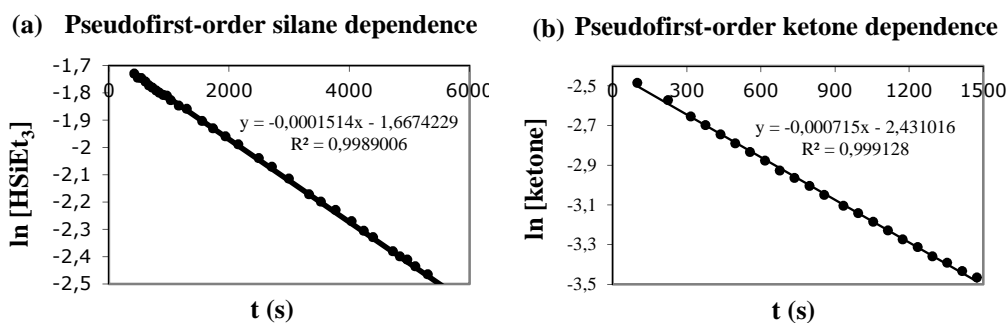
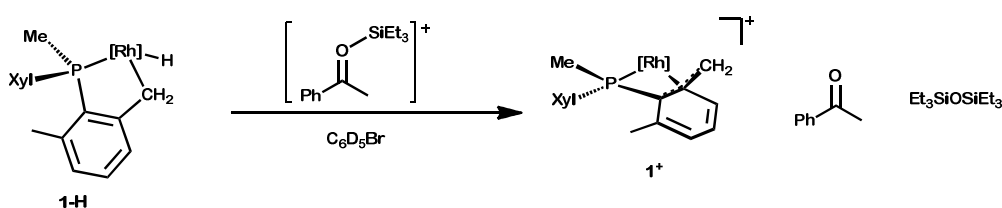


Figure 8. Kinetic studies for the reaction of acetophenone and triethylsilane at 25 °C catalyzed by **1**⁺. (a) Pseudofirst-order consumption of silane. Conditions: [acetophenone]₀ = 1.85M; [HSiEt₃]₀ = 0.18M; [**1**⁺] = 1.4x10⁻⁴M. (B) Pseudofirst-order consumption of acetophenone. Conditions: [acetophenone]₀ = 0.09M; [HSiEt₃]₀ = 2.14M; [**1**⁺] = 1.4x10⁻⁴M.

Hydride character of Complex **1-H**

A key step in the silylium transfer mechanism represented in Scheme 8 is hydride transfer from a metal hydride to the carbonyl carbon of the silylium-ketone adduct. Accordingly, complex **1-H** was treated with the silylium acetophenone adduct, prepared following the procedure described by Lambert.⁴⁹ As shown in Scheme 25 the expected silyl ether did not form and the ketone was recovered unchanged, along with complex **1**⁺ and disiloxane Et₃SiOSiEt₃.

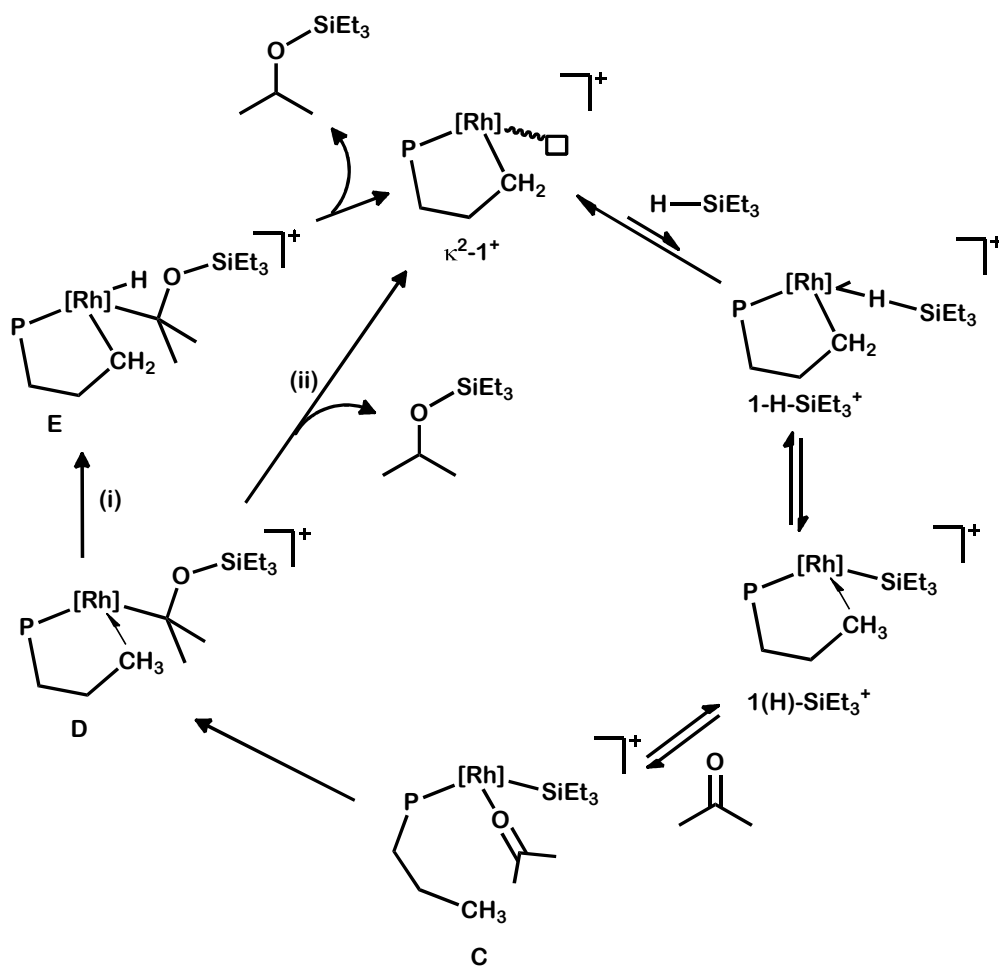


Scheme 25. Reaction of **1-H** with silylium-acetophenone adduct.

⁴⁹ (a) Lambert, J. B.; Zhang, S. Z.; Ciro, S. M. *Organometallics* **1994**, *13*, 2430. (b) Lambert, J. B.; Kania, L.; Schilf, W.; McConnell, J. A. *Organometallics* **1991**, *10*, 2578.

Although these results do not support fully mechanistic pathways involving: (a) a Lewis acid mechanism⁵⁰ initiated by **1**⁺ or (b) silylium ion transfer, they do not allow either to make a definite mechanistic proposal. However, the modified *Chalk-Harrod* mechanism presented in Scheme 26 could be suggested for catalysis by **1**⁺. Reaction could start with formation of the *sigma* silane complex **1-(H-SiEt₃)⁺**, which in accordance with DFT calculations (Figure 7) is energetically accessible under our experimental conditions. Si-H heterolysis would protonate the Rh-CH₂ unit, yielding also accessible **1(H)-SiEt₃⁺** (Figure 7), which would then provide ketone adduct **C**, and agostic species **D**. Two different steps, (i) and (ii), may be envisaged to yield the products. The first implies C-H oxidative cleavage followed by C-H reductive elimination, while in the second a σ -bond metathesis step would be involved.

⁵⁰ (a) Williams, V. C.; Piers, W. E.; Clegg, W.; Collins, S.; Marder, T. B. *J. Am. Chem. Soc.* **1999**, *121*, 3244. (b) Jia, L.; Yang, X.; Stern, C.; Marks, T. J. *Organometallics* **1994**, *13*, 2430.



Scheme 26. Proposed modified *Chalk-Harrod* mechanism to account for the hydrosilylation of carbonyl compounds catalyzed by 1^+ .

Summary and Conclusions

A very productive catalytic procedure for hydrogen isotope exchange in hydrosilanes, Si–H/Si–D/Si–T, has been developed. Catalysis can be carried out in organic solvent solutions or in a solvent-free manner. Low catalyst concentrations are needed and the catalyst may be recycled a number of times. The catalyst is also effective for hydrosilation of C–O and C–N multiple bonds, which permits D or T incorporation into a wide class of organic molecules employing convenient one-flask procedures. All these properties make of the new method an experimentally simple, environmentally benign, technically robust and atom-efficient technology for incorporation of deuterium and tritium into organic molecules.

I.3. EXPERIMENTAL SECTION

I.3. Experimental Section

I.3.1. Materials and methods: General

All operations were performed under an argon atmosphere using standard Schlenk techniques, employing dry solvents and glassware. HRMS data were obtained using a Jeol JMS-SX 102A mass spectrometer at the Analytical Services of the Universidad de Sevilla (CITIUS). Microanalyses were performed by the Microanalytical Service of the Instituto de Investigaciones Químicas (Sevilla, Spain). Infrared spectra were recorded on Bruker Vector 22 spectrometer. The NMR instruments were Bruker DRX-500, DRX-400 and DRX-300 spectrometers. Spectra were referenced to external SiMe₄ (δ 0 ppm) using the residual proton solvent peaks as internal standards (¹H NMR experiments), or the characteristic resonances of the solvent nuclei (¹³C NMR experiments), while ³¹P was referenced to external H₃PO₄. Spectral

assignments were made by routine one- and two-dimensional NMR experiments where appropriate. Radioactivity measurements were made on a Beckman LS 6000 Series Liquid Scintillation System. Liquid Scintillation Cocktails for sample preparation were purchased from Beckman Coulter. Metal complexes $\text{Zn}(\eta^5\text{-C}_5\text{Me}_5)_2$ ⁵¹ and $[\text{RhCl}(\text{C}_2\text{H}_4)_2]_2$,⁵² as well as NaBAr_F ⁵³ were prepared as previously described. All substrates were purchased from commercial sources and were distilled under vacuum from CaCl_2 or MgSO_4 before use. Silanes were purchased from commercial sources and used without further purification. The ^1H and $^{13}\text{C}\{^1\text{H}\}$ NMR spectral data for the BAr_F^- anion ($\text{BAr}_\text{F} = \text{B}[3,5\text{-(CF}_3)_2\text{C}_6\text{H}_3]$) in CD_2Cl_2 are identical for all complexes and therefore are not repeated below. BAr_F^- : ^1H RMN: δ 7.75 (s, 8 H, *o*-Ar), 7.58 (s, 4 H, *p*-Ar). $^{13}\text{C}\{^1\text{H}\}$ RMN: δ 162.1 (q, 37 Hz, *ipso*-Ar), 135.3 (*o*-Ar), 129.2 (q, 31 Hz, *m*-Ar), 124.9 (q, 273 Hz, CF_3), 117.8 (*p*-Ar).

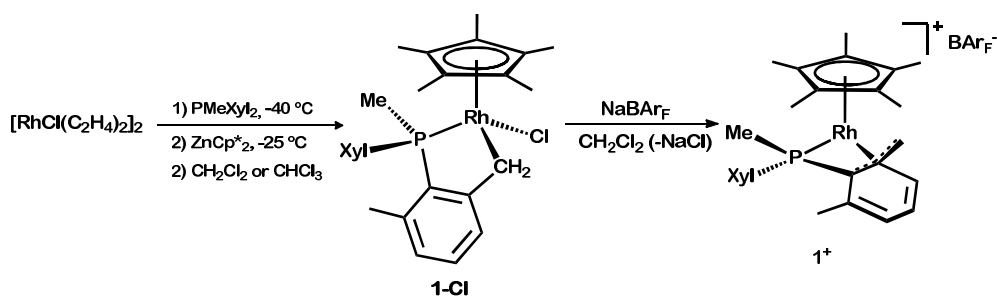
⁵¹ Blom, R.; Boersma, J.; Budzelaar, P. H. M.; Fischer, B.; Haaland, A.; Volden, H. V.; Weidlein, J. *Acta Chem. Scand.* **1986**, A40, 113.

⁵² Cramer, R. *Inorg. Synth.* **1974**, 15, 14.

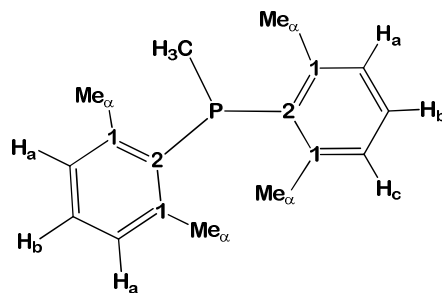
⁵³ Brookhart, M.; Grant, B.; Volpe, A. F. *Organometallics* **1922**, 11, 3920.

I.3.2. Synthesis of rhodium organometallic complexes and the phosphine ligand $\text{PMe}(\text{Xyl})_2$ ($\text{Xyl} = 2,6\text{-C}_6\text{H}_3\text{Me}_2$)

Complexes **1-Cl**, **1⁺** and **1-H**, as well as Lewis adducts **1-CO⁺** and **1-NCMe⁺**, whose synthesis and characterization is described below, have already been reported in the PhD Thesis of Dr. Cristina Esqueda.³⁸ Also, the phosphine ligand contained in all these compounds ($\text{PMe}(\text{Xyl})_2$) has been described in the same PhD Thesis. Nevertheless, we consider that it is worth including the synthesis and characterization of these species due to their important role in the results described in the present Chapter.



Scheme 27. Synthesis of catalyst **1⁺** via precatalyst **1-Cl**.

Synthesis of PMe(Xyl)_2 **Preparation of $\text{Mg(2,6-Me}_2\text{C}_6\text{H}_3\text{)Br}$**

Over a THF suspension of Mg^0 (2.5 g, 102 mmol) in THF (100 mL) placed in a three-necked round-bottom flask equipped with a reflux condenser, 2-bromo-1,3-dimethylbenzene (13 mL, 95.6 mmol) was slowly added under nitrogen using a dropping funnel. The reaction mixture was stirred for 4 hours at room temperature, and the resulting solution filtered and titrated before use.

Preparation of PX(Xyl)_2 , $\text{X} = \text{Cl, Br}$

A solution of PCl_3 (3.55 mL, 40.8 mmol) in THF (30 mL) placed in a three-necked round-bottom flask was cooled down to -78°C . Using a dropping funnel, a THF solution of $\text{Mg(2,6-Me}_2\text{C}_6\text{H}_3\text{)Br}$ (68 mL, 1.2 M, 81.6 mmol) was added to the former solution at this temperature, resulting in the formation of a white precipitate. The reaction mixture was allowed to warm to room temperature and additionally stirred for 12 h. The solvent was removed under reduced pressure and the crude product extracted with pentane (4 x 70 mL). The volatiles were evaporated under vacuum to give a mixture of PCl(Xyl)_2 and PBr(Xyl)_2 in a *ca.* 75:25 ratio.

$\text{PCl}(\text{Xyl})_2$: $^{31}\text{P}\{^1\text{H}\}$ RMN (162 MHz, C_6D_6 , 25 °C) δ : 82.9.

$\text{PBr}(\text{Xyl})_2$: $^{31}\text{P}\{^1\text{H}\}$ RMN (162 MHz, C_6D_6 , 25 °C) δ : 70.9.

Preparation of $\text{PMe}(\text{Xyl})_2$

A mixture of the halophosphines $\text{PCl}(\text{Xyl})_2$ and $\text{PBr}(\text{Xyl})_2$ dissolved in Et_2O (*ca.* 75:25; 4.5 g, *ca.* 21.8 mmol; 80 mL) placed in a three-neck round-bottom flask and MgMeBr (8 mL, 3 M in Et_2O , 24 mmol) added dropwise at -78 °C using a dropping funnel, reacted first at low temperature and then at 25 °C, over a period of 12 h to give the desired product. The solvent was removed under vacuum and the residue extracted with pentane. Concentrating the solution and cooling at -24 °C gave $\text{PMe}(\text{Xyl})_2$ as white crystals (4 g, *ca.* 73 %).

Spectroscopic data

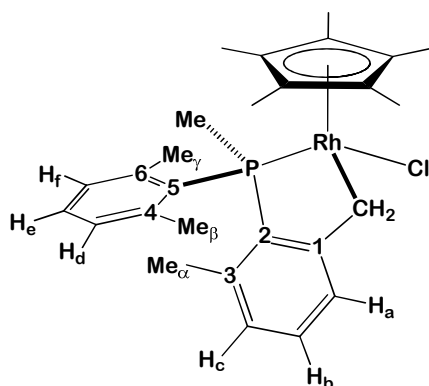
^1H NMR (400 MHz, C_6D_6 , 25 °C) δ : 6.95 (t, 2 H, H_b), 6.83 (dd, 4 H, $^4J_{\text{HP}} = 2.5$ Hz, H_a), 2.25 (s, 12 H, Me_a), 1.63 (d, 3 H, $^2J_{\text{HP}} = 5.7$ Hz, PMe). All aromatic couplings are of *ca.* 7.5 Hz.

$^{13}\text{C}\{^1\text{H}\}$ NMR (100 MHz, C_6D_6 , 25 °C) δ : 141.5 (d, $^2J_{\text{CP}} = 13$ Hz, C_1), 138.7 (d, $^1J_{\text{CP}} = 22$ Hz, C_2), 129.5 (d, $^3J_{\text{CP}} = 2$ Hz, CH_a), 128.0 (CH_b), 23.3 (d, $^3J_{\text{CP}} = 14$ Hz, Me_a), 13.9 (d, $^1J_{\text{CP}} = 17$ Hz, PMe).

$^{31}\text{P}\{^1\text{H}\}$ NMR (162 MHz, C_6D_6 , 25 °C) δ : -33.1.

Synthesis of complex 1-Cl

A solution of PMe(Xyl)_2 (131 mg, 0.5 mmol) in 2 mL of THF was added at $-40\text{ }^\circ\text{C}$ to a solution of $[\text{RhCl}(\text{C}_2\text{H}_4)_2]_2$ (100 mg, 0.25 mmol) in 3 mL of THF. The reaction mixture was stirred for 3 h at this temperature, and then treated with a solution of ZnCp_2^* (84 mg, 0.25 mmol) in 1 mL of THF. The mixture was stirred for 5 h while allowing the temperature to reach $-25\text{ }^\circ\text{C}$. Removal of the solvent under vacuum, extraction of the residue with diethyl ether, further removal of the solvent and addition of 5 mL of CH_2Cl_2 gave a solution that was stirred for 3 h at room temperature. The solvent was removed under vacuum and the crude product washed with pentane to yield complex **1-Cl** as an orange solid in 83% yield.



Analytical and spectroscopic data

Anal. Calc. for $\text{C}_{27}\text{H}_{35}\text{ClPRh}$: C, 61.3; H, 6.7. **Found:** C, 61.2; H, 6.6.

$^1\text{H NMR}$ (400 MHz, C_6D_6 , $25\text{ }^\circ\text{C}$) δ : 7.43 (d, 1 H, H_a), 7.04 (td, 1 H, $^5J_{\text{HP}} = 2.2\text{ Hz}$, H_b), 6.92 (td, 1 H, $^5J_{\text{HP}} = 1.5\text{ Hz}$, H_c), 6.84, 6.64 (m, 1 H each, H_d , H_f), 6.73 (m, 1 H, H_c), 4.11 (dt, 1 H, $^2J_{\text{HH}} = 12.9$, $^2J_{\text{HRh}} = ^3J_{\text{HP}} = 2.5\text{ Hz}$,

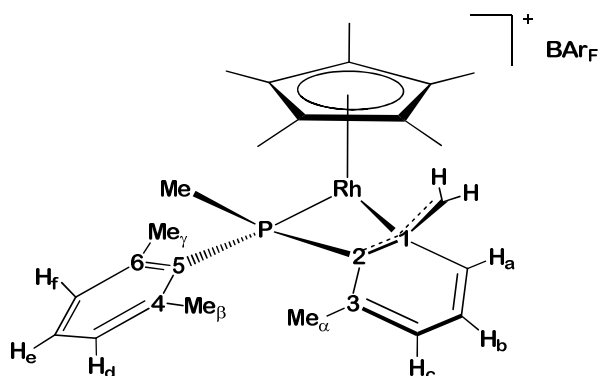
RhCHH), 3.56 (dd, 1 H, $^2J_{\text{HH}} = 12.9$, $^2J_{\text{HRh}} = 3.5$ Hz, RhCHH), 2.32, 1.48 (s, 3 H each, Me $_{\beta}$, Me $_{\gamma}$), 2.22 (d, 3 H, $^2J_{\text{HP}} = 10.5$ Hz, PMe), 1.85 (s, 3 H, Me $_{\alpha}$), 1.30 (d, 15 H, $^4J_{\text{HP}} = 2.5$ Hz, C $_5$ Me $_5$). All aromatic couplings are of *ca.* 7.5 Hz.

$^{13}\text{C}\{^1\text{H}\}$ NMR (100 MHz, C $_6$ D $_6$, 25 °C) δ : 157.7 (d, $^2J_{\text{CP}} = 33$ Hz, C $_1$), 142.0, 140.2 (d, $^2J_{\text{CP}} = 8$ Hz, C $_4$, C $_6$), 139.4 (dd, $^1J_{\text{CP}} = 53$, $^2J_{\text{CRh}} = 3$ Hz, C $_2$), 139.3 (C $_3$), 132.9 (d, $^1J_{\text{CP}} = 32$ Hz, C $_5$), 130.4, 129.9 (d, $^3J_{\text{CP}} = 7$ Hz, CH $_d$, CH $_f$), 129.8 (CH $_b$), 129.4 (CH $_e$), 127.7 (d, $^3J_{\text{CP}} = 17$ Hz, CH $_a$), 127.6 (d, $^3J_{\text{CP}} = 7$ Hz, CH $_c$), 98.2 (dd, $^1J_{\text{CRh}} = ^2J_{\text{CP}} = 3$ Hz, C $_5$ Me $_5$), 34.4 (dd, $^1J_{\text{CRh}} = 24$, $^2J_{\text{CP}} = 7$ Hz, RhCH $_2$), 25.8, 23.7 (d, $^3J_{\text{CP}} = 5$, $^3J_{\text{CP}} = 8$ Hz, resp., Me $_{\beta}$, Me $_{\gamma}$), 20.7 (d, $^3J_{\text{CP}} = 3$ Hz, Me $_{\alpha}$), 20.1 (d, $^1J_{\text{CP}} = 34$ Hz, PMe), 8.7 (C $_5$ Me $_5$).

$^{31}\text{P}\{^1\text{H}\}$ NMR (162 MHz, C $_6$ D $_6$, 25 °C) δ : 47.6 (d, $^1J_{\text{PRh}} = 156$ Hz).

Synthesis of catalyst 1^+ .

To a solid mixture of **1-Cl** (150 mg, 0.28 mmol) and NaBAR_F (252 mg, 0.28 mmol) were added 5 mL of CH₂Cl₂. The reaction mixture was stirred for 10 min at room temperature, after which the solution was filtered and the solvent evaporated under reduced pressure, to obtain an orange solid (350 mg, 95 %). Complex **1⁺** can be crystallized from a 1:1 mixture of CH₂Cl₂:pentane.

**Analytical and spectroscopic data**

Anal. Calc. for C₅₉H₄₇BF₂₄PRh: C, 52.6; H, 3.5. **Found:** C, 53.0; H, 3.3.

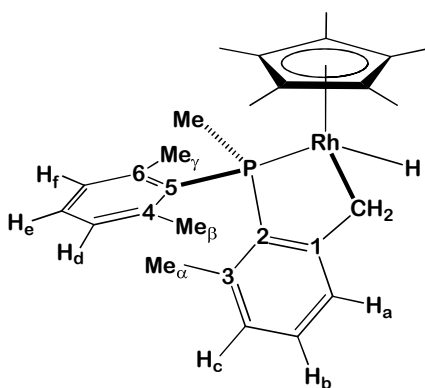
¹H NMR (400 MHz, CD₂Cl₂, 25 °C) δ: 7.54 (m, 1 H, H_c), 7.47 (t, 1 H, H_b), 7.29 (td, 1 H, ⁵J_{HP} = 1.5 Hz, H_e), 7.13, 7.00 (m, 1 H each, H_d, H_f), 6.88 (dd, 1 H, ⁴J_{HP} = 3.5 Hz, H_a), 3.04 (dt, 1 H, ²J_{HH} = 4.5, ²J_{HRh} = ³J_{HP} = 1.5 Hz, RhCHH), 2.63, 2.06 (s, 3 H each, Me_β, Me_γ), 2.55 (s, 3 H, Me_α), 2.22 (d, 3 H, ²J_{HP} = 13.0 Hz, PMe), 1.71 (d, 15 H, ⁴J_{HP} = 2.5 Hz, C₅Me₅), 1.34 (ddd, 1 H, ³J_{HP} = 10.0, ²J_{RhH} = 1.5 Hz, RhCHH). All aromatic couplings are of *ca.* 7.5 Hz.

$^{13}\text{C}\{^1\text{H}\}$ NMR (100 MHz, CD_2Cl_2 , 25 °C) δ : 142.7, 141.8 (s, d, $^2J_{\text{CP}} = 19$ Hz, resp., C_4 , C_6), 137.9 (C_3), 133.1 (CH_b), 132.7 (CH_e), 132.5 (d, $^3J_{\text{CP}} = 6$ Hz, CH_c), 129.9, 129.7 (d, $^3J_{\text{CP}} = 8$ Hz, CH_d , CH_f), 127.8 (d, $^3J_{\text{CP}} = 8$ Hz, CH_a), 120.8 (d, $^1J_{\text{CP}} = 54$ Hz, C_5), 104.3 (dd, $^2J_{\text{CP}} = 13$, $^1J_{\text{CRh}} = 4$ Hz, C_1), 99.5 (dd, $^1J_{\text{CRh}} = 5$, $^2J_{\text{CP}} = 3$ Hz, C_5Me_5), 77.4 (dd, $^1J_{\text{CP}} = 24$, $^1J_{\text{CRh}} = 3$ Hz, C_2), 42.1 (dd, $^1J_{\text{CRh}} = 15$, $^2J_{\text{CP}} = 2$ Hz, RhCH_2), 23.1 (Me_α), 22.4, 21.8 (d, s, $^3J_{\text{CP}} = 17$ Hz, Me_β , Me_γ), 13.3 (d, $^1J_{\text{CP}} = 32$ Hz, PMe), 9.3 (C_5Me_5).

$^{31}\text{P}\{^1\text{H}\}$ NMR (162 MHz, CD_2Cl_2 , 25 °C) δ : -14.7 (d, $^1J_{\text{PRh}} = 138$ Hz).

Synthesis of neutral hydride **1-H**

A solid mixture of **1-Cl** (50 mg, 0.089 mmol) and NaBH₄ (17 mg, 0.45 mmol) was placed in a Schlenk flask and dissolved in a 1:1 mixture of EtOH:THF (5 mL). The reaction was stirred at room temperature until it became clear (*ca.* 6 hours), then evaporated to dryness and co-evaporated with toluene. The residue was extracted with pentane and the solvent removed under vacuum to give **1-H** as a pale yellow powder which was directly used for subsequent experiments. Due to high instability towards chloride solvents and oxygen, it was not possible to obtain analytically pure samples of this hydride.



Spectroscopic data

¹H NMR (400 MHz, C₆D₆, 25 °C) δ : 7.45 (d, 1 H, H_a), 7.06 (td, 1 H, ⁵J_{HP} = 2.8 Hz, H_b), 6.94 (td, 1 H, ⁵J_{HP} = 1.6 Hz, H_c), 6.84, 6.73, 6.71 (m, 1 H each, H_c, H_d, H_f), 3.59 (d, 1 H, ²J_{HH} = 13.6, RhCHH), 3.00 (dd, 1 H, ²J_{HH} = 13.6, ²J_{HRh} = 4.2 Hz, RhCHH), 2.36, 1.63 (s, 3 H each, Me_β, Me_γ), 1.93 (d, 3 H,

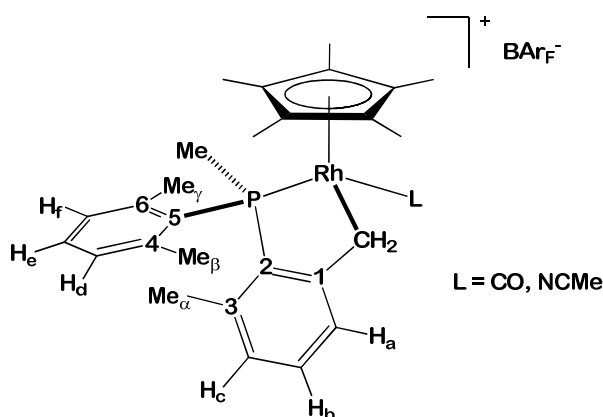
$^2J_{\text{HP}} = 9.0$ Hz, PMe), 1.89 (s, 3 H, Me_a), 1.69 (d, 15 H, $^4J_{\text{HP}} = 1.6$ Hz, C₅Me₅), -13.77 (dd, 1 H, $^1J_{\text{HRh}} = 46.0$, $^2J_{\text{HP}} = 37.0$ Hz, RhH). All aromatic couplings are of *ca.* 7.5 Hz.

$^{13}\text{C}\{^1\text{H}\}$ NMR (100 MHz, C₆D₆, 25 °C) δ : 158.6 (d, $^2J_{\text{CP}} = 33$ Hz, C₁), 141.9 (dd, $^1J_{\text{CP}} = 54$, $^2J_{\text{CRh}} = 4$ Hz, C₂), 141.9, 139.0 (d, $^2J_{\text{CP}} = 8$ Hz, C₄, C₆), 138.8 (C₃), 134.0 (d, $^1J_{\text{CP}} = 27$ Hz, C₅), 129.9, 129.8 (d, $^3J_{\text{CP}} = 7$ Hz, CH_d, CH_f), 129.2 (CH_b), 128.7 (CH_e), 127.3 (d, $^3J_{\text{CP}} = 16$ Hz, CH_a), 127.1 (d, $^3J_{\text{CP}} = 7$ Hz, CH_c), 96.9 (dd, $^1J_{\text{CRh}} = ^2J_{\text{CP}} = 3$ Hz, C₅Me₅), 21.7 (d, $^1J_{\text{CP}} = 38$ Hz, PMe), 25.4, 22.4 (d, $^3J_{\text{CP}} = 4$, $^3J_{\text{CP}} = 9$ Hz, resp., Me _{β} , Me _{γ}), 22.4 (dd, $^1J_{\text{CRh}} = 26$, $^2J_{\text{CP}} = 4$ Hz, RhCH₂), 20.9 (d, $^3J_{\text{CP}} = 3$ Hz, Me_a), 10.6 (C₅Me₅).

$^{31}\text{P}\{^1\text{H}\}$ NMR (162 MHz, C₆D₆, 25 °C) δ : 49.9 (d, $^1J_{\text{PRh}} = 156$ Hz).

Synthesis of Lewis base adducts 1-L⁺ (L = NCMe, CO)

To a solid mixture of **1-Cl** (45 mg, 0.08 mmol) and NaBAR_F (75 mg, 0.08 mmol) placed in a thick-wall vessel were added 5 mL of CH₂Cl₂. The reaction mixture was stirred for 30 min at room temperature under 2 bar of CO (for L = CO), or alternatively treated with 100 μL of NCMe (for corresponding NCMe adduct). The solution was filtered and the solvent was then evaporated under reduced pressure to obtain yellow solids in *ca* 95% yield, as a mixture of diastereomers (98:2, L = CO; 82:18, L = NCMe). The complexes can be recrystallized from a 1:1 mixture of CH₂Cl₂:pentane. Direct reaction of **1⁺** (50 mg, 0.037 mmol) with CO (2 bar) or NCMe (100 μL) led to analogous results.

***Selected spectroscopic data***

1-CO⁺: ¹H NMR (400 MHz, CD₂Cl₂, 25 °C) δ: 3.59 (dd, 1 H, ²J_{HH} = 12.7, ²J_{HRh} = 1.8 Hz, RhCHH), 3.45 (dd, 1 H, ²J_{HRh} = 4.0 Hz, RhCHH), 2.36 (d, 3 H, ²J_{HP} = 10.5 Hz, PMe), 1.68 (d, 15 H, ⁴J_{HP} = 2.5 Hz, C₅Me₅). ¹³C{¹H}

NMR (125 MHz, CD₂Cl₂, 25 °C) δ : 188.8 (dd, $^1J_{\text{CRh}} = 75$, $^2J_{\text{CP}} = 20$ Hz, CO).

$^{31}\text{P}\{^1\text{H}\}$ NMR (162 MHz, CD₂Cl₂, 25 °C) δ : 37.8 (d, $^1J_{\text{PRh}} = 128$ Hz).

1-NCMe⁺: ^1H NMR (500 MHz, CD₂Cl₂, 25 °C) δ : 3.50 (dd, 1 H, $^2J_{\text{HH}} = 13.0$, $^2J_{\text{HRh}} = 3.3$ Hz, RhCHH), 3.37 (dt, 1 H, $^2J_{\text{HRh}} = ^3J_{\text{HP}} = 2.5$ Hz, RhCHH), 2.21 (s, 3 H, NCMe), 2.10 (d, 3 H, $^2J_{\text{HP}} = 9.5$ Hz, PMe), 1.46 (d, 15 H, $^4J_{\text{HP}} = 2.5$ Hz, C₅Me₅). **$^{13}\text{C}\{^1\text{H}\}$ NMR** (125 MHz, C₆D₆, 25 °C) δ : 124.5 (d, $^3J_{\text{CP}} = 17$, NCMe), 3.6 (NCMe). **$^{31}\text{P}\{^1\text{H}\}$ NMR** (162 MHz, CD₂Cl₂, 25 °C) δ : 42.7 (d, $^1J_{\text{PRh}} = 148$ Hz).

I.3.3. Catalytic Si–H/Si–D and Si–H/Si–T exchanges

General low-scale procedure for Si–H/Si–D exchanges.

The screening of all the silanes tested for deuteration was undertaken at low scale without further purification of the deuterated organosilanes. The catalyst **1**⁺ (3 mg, $2.2 \cdot 10^{-3}$ mmol) and the hydrosilane (0.22 mmol) were dissolved in CD₂Cl₂ (0.6 mL) in a Young ampoule (volume *ca.* 50 mL). The solution was cooled to 0 °C and the argon pumped out and replaced by deuterium (0.5 bar). The solution was stirred vigorously at room temperature for 3 hours (although it has been observed that H/D exchange is completed at lower times) and deuterium incorporation determined by IR and ¹H-NMR spectroscopy. Under these conditions only one or two D₂ loading were enough to label the Si–H bond at yields higher than 99%. For experiments with lower amounts of catalyst and/or higher amounts of silane three cycles of 0 °C/vacuum (≈ 0.1 bar, 20 s)/fresh D₂ were routinely employed.

High-scale synthesis of deuteriosilanes.

[1-²H]Triethylsilane (SiEt₃D). Triethylsilane (5 mL, 31.30 mmol) was added under nitrogen to a pressure vessel (volume *ca.* 220 mL) containing catalyst **1** (4.2 mg, $3.1 \cdot 10^{-3}$ mmol). The solution was cooled to 0 °C and nitrogen pumped out. Then the flask was charged with deuterium (0.5 bar) and the mixture was vigorously stirred at 50 °C for 16 hours. In order to exchange quantitatively the Si–H bond, the cooling at 0 °C/vacuum (0.1 bar)/D₂ (0.5 bar) process was repeated five times. The solution was transferred to a Young's ampoule and the deuteriosilane purified by trap-to-trap distillation to obtain SiEt₃D as a colorless liquid (3.49 g, 96% yield; 99%

D incorporation). IR (neat silane): 1530 cm^{-1} . ^1H NMR (500 MHz, C_6D_6 , 25 $^\circ\text{C}$) δ : 0.96 (t, 9 H, $^3J_{\text{HH}} = 7.9$ Hz, 3 CH_3), 0.53 (q, 6 H, $^3J_{\text{HH}} = 7.9$ Hz, 3 CH_2). $^{29}\text{Si}\{^1\text{H}\}$ NMR (99 MHz, C_6D_6) δ : 0.4 (t, $^1J_{\text{SiD}} = 28$ Hz).

[1- ^2H]Dimethylphenylsilane (SiMe_2PhD). The same procedure utilized to deuterate triethylsilane was employed, but using dimethylphenylsilane (5 mL, 32.66 mmol) and catalyst **1** (4.4 mg, $3.2 \cdot 10^{-3}$ mmol). Deuterated dimethylphenylsilane was purified by trap-to-trap distillation and SiMe_2PhD was obtained as a colourless liquid (4.15 g, 93% yield; 99% D incorporation). IR (Neat Silane): 1540 cm^{-1} . ^1H NMR (500 MHz, C_6D_6 , 25 $^\circ\text{C}$) δ : 7.54 (m, 2 H, Ph), 7.28 (m, 3 H, Ph), 0.34 (s, 6 H, 2 CH_3). $^{29}\text{Si}\{^1\text{H}\}$ NMR (99 MHz, C_6D_6) δ : -17.2 (t, $^1J_{\text{SiD}} = 29$ Hz).

[1- $^2\text{H}_2$]Diphenylsilane (SiPh_2D_2). The same procedure utilized to deuterate triethylsilane was employed, but using diphenylsilane (5 mL, 26.86 mmol) and catalyst **1** (7.3 mg, $5.4 \cdot 10^{-3}$ mmol). Deuterated diphenylsilane was purified by Kugelrohr distillation to obtain SiPh_2D_2 as a colourless oil (4.17 g, 84% yield; 99% D incorporation). IR (Nujol): 1550 cm^{-1} . ^1H NMR (500 MHz, C_6D_6 , 25 $^\circ\text{C}$) δ : 7.30 (d, 4 H, $^3J_{\text{HH}} = 7.8$ Hz, *o*-Ph), 6.91 (m, 6 H, *m,p*-Ph). $^{29}\text{Si}\{^1\text{H}\}$ NMR (99 MHz, C_6D_6) δ : -33.8 (quintet, $^1J_{\text{SiD}} = 30$ Hz).

Determination of deuterium incorporation.

The levels of deuteration exchange were checked by ^1H -NMR, ^{29}Si -NMR and IR spectroscopy. The level of deuteration was monitored by ^1H -NMR spectroscopy. Exchange reactions were considered to be complete when no integrable ^1H signal for the Si-*H* atom could be detected. These results were confirmed by the disappearance of the characteristic signals in the ^{29}Si -NMR

and IR spectra. Signals for the hydro- and deuteriosilane appear perfectly well resolved in the ^{29}Si NMR spectra due to the isotope effect on the chemical shift (Figure 3). The calculation of the deuterium percentage by ^{29}Si -NMR is totally in accordance with the results obtained from the ^1H -NMR analysis. The integration of the bands for $\nu(\text{Si-H})$ (*ca.* 2100 cm^{-1}) and $\nu(\text{Si-D})$ (*ca.* 1500 cm^{-1}) match up with the results obtained by ^1H and ^{29}Si NMR.

Synthesis of tritiated silanes.

Tritiation of catalyst 1^+ . Catalyst 1^+ (200 mg, *ca.* 0.15 mmol) was placed in a stainless steel reactor ($V_r = 5.5\text{ mL}$) connected to a stainless steel cylinder containing the tritium gas, (1Ci), a second degassed cylinder filled with activated carbon to trap the excess of radioactive gas and a pressure sensor. The designed system allowed to degas the reactor and dissolve 1^+ in CH_2Cl_2 (2 mL) under argon. The sensitive volume (the volume of gas to be opened to the reactor = V_s , 10.1 mL) was degassed and loaded with 23 torr of T_2 (1Ci), then opened to the steel flask and the reaction stirred vigorously at room temperature for 4 days. At the end of this period the cylinder containing the activated carbon was frozen with liquid nitrogen and opened to the reaction system to trap the rests of HT and T_2 , while the solution was transferred to a *Young's* ampoule from which complex $1(\text{T}_n)^+$ was crystallized by diffusion from CH_2Cl_2 /pentane. The orange crystals were washed with pentane to yield the tritiated compound $1(\text{T}_n)^+$ (190 mg, 95%, 6.08 Ci/mmol).

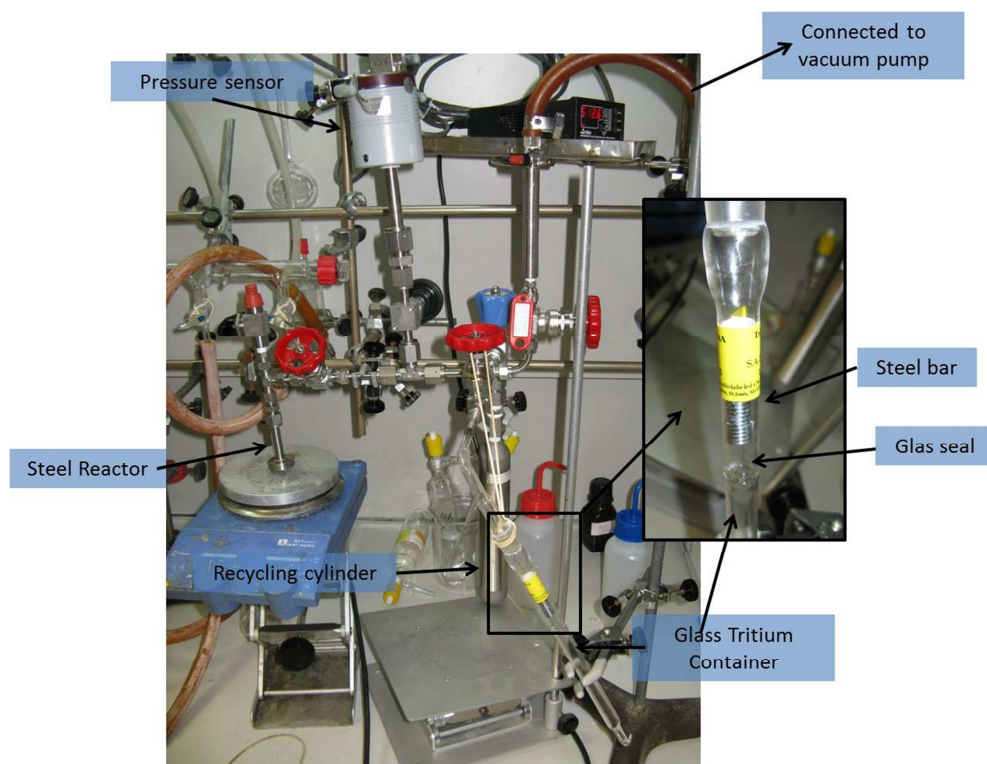


Figure 9. Experimental system for tritiation of catalyst **1**⁺.

A similar experiment was carried out using T₂ (1 Ci) stored in a sealed glass ampoule containing a steel bar for breaking the seal with a magnet. Under the same experimental conditions tritiated complex **1**(T_n)⁺ was obtained as orange crystals (5.42 Ci/mmol).

General procedure for catalytic tritiation of hydrosilanes. Tritiated complex **1**(T_n)⁺ (1 mg, 0.74 μmol, 4.5 mCi) was placed in a *Young's* ampoule and dissolved in SiEt₃H (1.2 mL, 7.5 mmol) under argon. The reaction mixture was heated at 50 °C for 5 days. Tritiated triethylsilane was purified by trap-to-trap distillation (1,1 mL, 92%). The measurement of the specific

activity of the distilled silane showed an incorporation of tritium of 85% (0.51 mCi/mmol). The same experiment was carried out by decreasing the amount of catalyst to 0.001% molar with respect to SiEt_3H . Similar results were obtained (88% of tritium incorporation with specific activity of 0.05 mCi/mmol).

I.3.4. General procedures for the the hydrosilylation and direct deuterio- and tritio-silylation of C–X multiple bonds.

General method for the hydrosilylation of C-O and C-N multiple bonds

In a typical experiment, a 2 mL screw-cap glass vial was charged with catalyst **1**⁺ (0.7 mg, $0.5 \cdot 10^{-3}$ mmol), the hydrosilane (1.1 mmol), the organic substrate (0.5 mmol) and CD₂Cl₂ (0.5 mL) in a glovebox. After stirring for 1 hour, the reaction mixture was transferred to a screw-cap NMR tube and the reaction progress checked by ¹H-NMR spectroscopy.

General method for the direct deuteriosilylation of C-O and C-N multiple bonds.

In a typical experiment, a Young's ampoule was charged with catalyst **1**⁺ (0.7 mg, $0.5 \cdot 10^{-3}$ mmol), triethylsilane (89 µL, 0.55 mmol) and CD₂Cl₂. The solution was cooled to 0 °C, argon pumped out and replaced by D₂ (0.5 bar). The solution was stirred at room temperature for 10 min, then cooled at 0 °C, the gas atmosphere pumped out and replace by D₂ (0.5 bar). After repeating this cycle a total of three times, the organic substrate (0.25 mmol) was added and the mixture transferred to a screw-cap NMR tube. The reaction progress was monitored by ¹H-NMR spectroscopy.

Procedure for the tritio-silylation of acetophenone using $1(T_n)^+$ as the tritiation reagent.

A *Young's* ampoule was charged in a glovebox with catalyst $1(T_n)^+$ (3 mg, 2.2×10^{-3} mmol, 4 mCi/mg), triethylsilane (1.98 mmol) and CH_2Cl_2 (1 mL). The reaction mixture was heated at 50 °C for 3 days and cooled down to room temperature. Then, acetophenone (2.2 mmol) was added and the mixture was heated at 50 °C for an additional period of 8 days. The silyl ether obtained was hydrolyzed to the corresponding alcohol by adding a solution of HCl (2N, 3 mL) and acetone (3 mL) and the mixture was stirred overnight. After removing acetone in the rotary evaporator, the aqueous phase was extracted with dichloromethane (3 x 5 mL). The combined organic layers were dried with Na_2SO_4 . Removal of solvent gave the crude product that was purified by flash chromatography (9:1 hexane-AcOEt). The pure product was dissolved in the liquid scintillation cocktail and its radioactivity measured (5.88 mCi/mmol).

General procedure for the tritio-silylation of C=O bonds with $\text{SiEt}_3\text{H}(T_n)$.

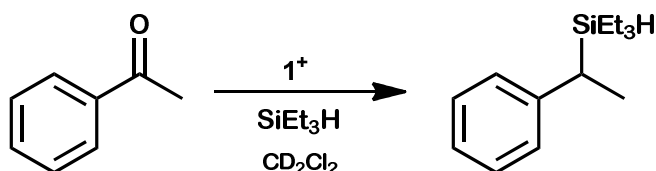
In a typical experiment, a *Young's* ampoule was charged in a glovebox with catalyst 1^+ (3 mg, 2.2×10^{-3} mmol), $\text{SiEt}_3\text{H}(T_n)$ (63 μL , 0.40 mmol, 0.19 mCi/mmol) and the organic substrate (0.44 mmol) and CH_2Cl_2 (1 mL). The reaction mixture was heated at 50 °C for 24 hours and cooled to room temperature. Volatiles were removed under vacuum and the crude mixture was dissolved in hexane and filtered through a short pad of silica. The organic solvent was evaporated and the residue dissolved in the liquid scintillation cocktail and its radioactivity measured.

General procedure for the competition studies.

In a typical experiment, a mixture of catalyst **1**⁺ (1 mg, 1×10^{-3} mmol) and SiEt₃H (0.016 mL, 0.1 mmol) in CD₂Cl₂ (0.5 mL) was added over a mixture of 0.5 mmol of each substrate. The mixture was transferred to a screw-cap NMR tube and the reaction progress was checked by ¹H-NMR spectroscopy.

I.3.5. Kinetic studies.

Hydrosilylation of acetophenone using SiEt_3H was chosen as the model reaction to perform all kinetic studies.

***General procedure for ketone pseudo-first order kinetic measurements.***

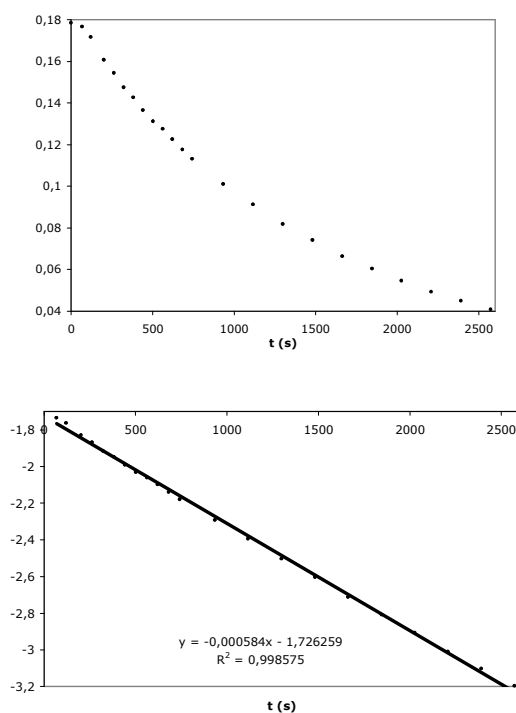
In a general experiment a screw-cap NMR tube was charged with a CD_2Cl_2 solution of 1^+ (0.01 M, 10 μL , 0.1 μmol), SiEt_3H (160 – 240 μL , 1.0 – 1.5 mmol), acetophenone (6 – 15 μL , 0.051 – 0.128 mmol) and CD_2Cl_2 (0.7 mL) at -80°C . Then the reaction was monitored by ^1H NMR at 25°C and k_{obs} were measured from the representation of $\ln[\text{acetophenone}]$ vs time (see for instance Figure 8b).

General procedure for silane pseudo-first order kinetic measurements.

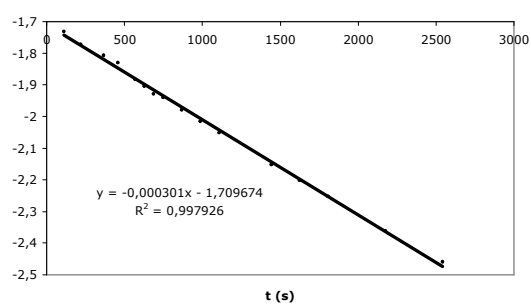
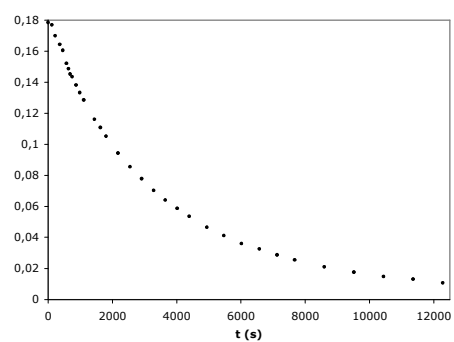
In a general experiment a screw-cap NMR tube was charged with a CD_2Cl_2 solution of 1^+ (0.01 M, 10 μL , 0.1 μmol), SiEt_3H (10 – 30 μL , 0.062 – 0.188 mmol), acetophenone (152 μL , 1.3 mmol) and CD_2Cl_2 (0.7 mL) at -80°C . Then the reaction was monitored by ^1H NMR at 25°C and k_{obs} were measured from the representation of $\ln[\text{silane}]$ vs time (see for instance Figure 8a).

Determination of kinetic isotopic effect (KIE). In a general experiment a screw-cap NMR tube was charged with a CD_2Cl_2 solution of $\mathbf{1}^+$ (0.01 M, 10 μL , 0.1 μmol), acetophenone (20 μL , 0.125 mmol) and CD_2Cl_2 (0.7 mL) at -80 °C. Then SiEt_3H or SiEt_3D (208 μL , 1.3 mmol) were added and the reaction monitored by ^1H NMR at 25 °C. The representation of $\ln[\text{acetophenone}]$ vs time allowed to obtain k_{obs} for the experiment using SiEt_3H ($5.8 \cdot 10^{-4}$) and SiEt_3D ($3.0 \cdot 10^{-4}$), which resulted in a kinetic isotopic effect of $k_{\text{H}}/k_{\text{D}} = 1.9$.

b) Using SiEt_3H $k_{\text{obs}} = 5.8 \times 10^{-4}$



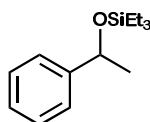
a) Using SiEt_3D $k_{\text{obs}} = 3.0 \times 10^{-4}$



I.3.6. Characterization of organic compounds.

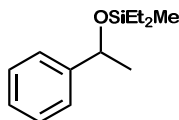
In this section the spectroscopic and analytical data of all organic compounds obtained after hydrosilylation reactions will be summarized, except for those already reported in the literature and whose reference has been included. For simplification, deuterium labeled compounds have not been included, since in all cases the spectroscopic and analytical data were unambiguously consistent with their non-deuterated analogues. The synthetic methods employed to prepare these compounds are, unless otherwise noted, the corresponding general procedures for each case described in section 3.3.

Hydrosilylation of carbonyl compounds.

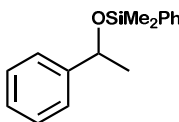


(1-Phenylethoxy)triethylsilane (entry 1, Table 4). Spectroscopic data of the reaction mixture were consistent with previously reported data for this compound.⁵⁴

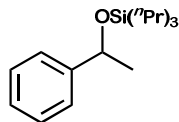
⁵⁴ Field, L. D.; Messerle, B. A.; Rehr, M.; Soler, L. P.; Hambley, T. W. *Organometallics* **2003**, 22, 2387.



(1-Phenylethoxy)diethylmethylsilane (entry 2, Table 4). ^1H NMR (500 MHz, CD_2Cl_2): δ 7.41 (d, 2H, $^3J_{\text{HH}} = 7.5$ Hz), 7.36 (t, 2 H, $^3J_{\text{HH}} = 7.5$ Hz), 7.27 (t, 1 H, $^3J_{\text{HH}} = 7.5$ Hz), 4.94 (q, 1 H, $^3J_{\text{HH}} = 6.3$ Hz), 1.48 (d, 3 H, $^3J_{\text{HH}} = 6.3$ Hz), 0.82 (q, 6 H, $^3J_{\text{HH}} = 7.5$ Hz), 0.79 – 0.32 (m, 4 H), 0.10 (s, 3 H). $^{13}\text{C}\{^1\text{H}\}$ NMR (125 MHz, CD_2Cl_2) δ 147.6 (C_q arom), 128.7 (2 CH arom), 127.4 (CH arom), 125.9 (2 CH arom), 71.2 (CH), 27.6 (CH_3), 7.3 (2 CH_3), 7.2 (2 CH_2), -4.2 (CH_3). **HRMS (CI):** m/z 221.1354 $[\text{M}-\text{H}]^+$ (exact mass calculated for $\text{C}_{13}\text{H}_{21}\text{OSi}$: 221.1362).



(1-Phenylethoxy)dimethylphenylsilane (entry 3, Table 4). Spectroscopic data of the reaction mixture were consistent with previously reported data for this compound.⁵⁵



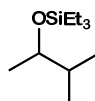
(1-Phenylethoxy)tri-*n*-propylsilane (entry 4, Table 4). ^1H NMR (500 MHz, CD_2Cl_2): δ 7.42 (d, 2 H, $^3J_{\text{HH}} = 7.5$ Hz), 7.37 (t, 1 H, $^3J_{\text{HH}} = 7.5$ Hz),

⁵⁵ Fujita, M.; Hiyama, T. *J. Org. Chem.* **1988**, 53, 5405.

7.28 (t, 1 H, $^3J_{\text{HH}} = 7.5$ Hz), 4.96 (q, 1 H, $^3J_{\text{HH}} = 6.5$ Hz), 1.73 – 1.26 (m, 6 H), 1.08 (t, 9 H, $^3J_{\text{HH}} = 7.2$ Hz), 0.82 – 0.55 (m, 6 H). $^{13}\text{C}\{^1\text{H}\}$ NMR (125 MHz, CD_2Cl_2) δ 147.8 (C_q arom), 128.8 (2 CH arom), 127.4 (CH arom), 126.0 (2 CH arom), 71.4 (CH), 27.9 (CH_3), 19.0 (3 CH_3), 17.6 (6 CH_2). **HRMS (CI):** m/z 277.1993 $[\text{M-H}]^+$ (exact mass calculated for $\text{C}_{17}\text{H}_{29}\text{OSi}$: 277.1988).

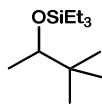


Triethyl(*iso*-propoxy)silane (entry 1, Table 5). Spectroscopic data of the reaction mixture were consistent with previously reported data for this compound.^{9b}



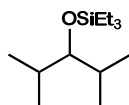
Triethyl(1,2-dimethyl-*n*-propoxy)silane (entry 2, Table 5). Spectroscopic data of the reaction mixture were consistent with previously reported data for this compound.⁵⁶

⁵⁶ Ison, E. A.; Trivedi, E. R.; Corbin, R. A.; Abu-Omar, M. M. *J. Am. Chem. Soc.* **2005**, 127, 15374.



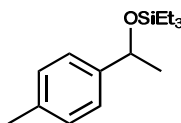
Triethyl(1,2,2-trimethyl n-propoxy)silane (entry 3, Table 5).

Spectroscopic data of the reaction mixture were consistent with previously reported data for this compound.^{9b}



(1-Isopropyl-2-methylpropoxy)triethylsilane (entry 4, Table 5).

Spectroscopic data of the reaction mixture were consistent with previously reported data for this compound.⁵⁷

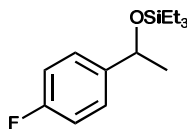


(1-*para*-methylphenylethoxy)triethylsilane (entry 6, Table 5).

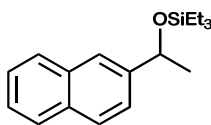
The residue was purified by flash chromatography on silica gel (hexane) to afford the title compound as a colorless oil. ¹H NMR (500 MHz, CDCl₃): δ 7.21 (d, 2 H, ³J_{HH} = 7.8 Hz), 7.10 (d, 2 H, ³J_{HH} = 7.8 Hz), 4.82 (q, 1 H, ³J_{HH} = 6.5 Hz), 2.32 (s, 3 H), 1.40 (d, 3 H, ³J_{HH} = 6.5 Hz), 0.90 (m, 9 H, ³J_{HH} = 8.0 Hz), 0.55 (m, 6 H). ¹³C{¹H} NMR (125 MHz, CDCl₃) δ 143.9 (C_q arom), 136.1 (C_q Arom), 128.7 (2 CH arom), 125.1 (2 CH arom), 70.3 (CH), 27.2 (CH₃), 21.0

⁵⁷ Barden, J.; Fleming, J. *Chem. Commun.* **2001**, 22, 2366.

(CH₃), 6.7 (3 CH₃), 4.7 (3 CH₂). **HRMS (CI):** m/z 249.1672 [M-H]⁺ (exact mass calculated for C₁₅H₂₅OSi: 249.1675).

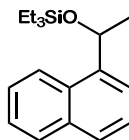


(1-*para*-fluorophenylethoxy)triethylsilane (entry 7, Table 5). ¹H NMR (500 MHz, CD₂Cl₂): δ 7.36 (dd, 2 H, ³J_{HH} = 8.5, ⁴J_{HF} = 5.5), 7.03 (bt, 2 H, ³J_{HH} = ³J_{HF} = 8.0), 4.91 (q, 1 H, ³J_{HH} = 6.6 Hz), 1.44 (d, 3 H, ³J_{HH} = 6.5 Hz), 0.97 (t, 9 H, ³J_{HH} = 8.0 Hz), 0.79-0.55 (m, 6 H). ¹³C{¹H} NMR (125 MHz, CD₂Cl₂) δ 162.4 (d, ¹J_{CF} = 244 Hz, C_q arom), 143.6 (C_q arom), 127.4 (d, ³J_{CF} = 8.0 Hz, 2 CH arom), 115.3 (d, ²J_{CF} = 21.4 Hz, 2 CH arom), 71.8 (CH), 28.9 (CH₃), 7.2 (3 CH₃), 5.4 (3 CH₂). **HRMS (CI):** m/z 253.1418 [M-H]⁺ (exact mass calculated for C₁₄H₂₂FOSi: 253.1424).



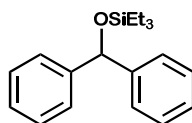
[1-(Naphthalen-2-yl)ethoxy]triethylsilane (entry 8, Table 5). Spectroscopic data of the reaction mixture were consistent with previously reported data for this compound.⁵⁸

⁵⁸ Díez-González, S.; Escudero-Adam, E. C.; Benet-Buchholz, J.; Stevens, E. D.; Slawin, A. M. Z.; Nolan, S. P. *Dalton Trans.* **2010**, 39, 7595.

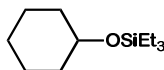


[1-(Naphthalen-1-yl)ethoxy]triethylsilane (entry 9-10, Table 5).

Spectroscopic data of the reaction mixture were consistent with previously reported data for this compound.⁵⁹



(Diphenylmethoxy)triethylsilane (entry 11, Table 2). Spectroscopic data of the reaction mixture were consistent with previously reported data for this compound.⁶⁰

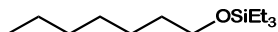


(Cyclohexyloxy)triethylsilane (entry 12, Table 5). Spectroscopic data of the reaction mixture were consistent with previously reported data for this compound.⁶¹

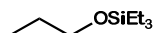
⁵⁹ Kaur, H.; Zinn, F. K.; Stevens, E. D.; Nolan, S. P. *Organometallics* **2004**, 23, 1157.

⁶⁰ Díez-González, S.; Kaur, H.; Kauer, F. Z.; Stevens, E. D.; Nolan, S. P. *J. Org. Chem.* **2005**, 70, 4784.

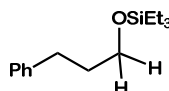
⁶¹ Onaka, M.; Higuchi, K.; Nanami, H.; Izumi, Y. *Bull. Chem. Soc. Jpn.* **1993**, 66, 2638.



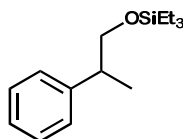
Triethyl(heptyloxy)silane (entry 1, Table 6). Spectroscopic data of the reaction mixture were consistent with previously reported data for this compound.⁵⁵



triethyl(propoxy)silane (entry 2, Table 6). Spectroscopic data of the reaction mixture were consistent with previously reported data for this compound.⁶²



Triethyl(3-phenylpropoxy)silane (entry 3, Table 6). Spectroscopic data of the reaction mixture were consistent with previously reported data for this compound.⁶³

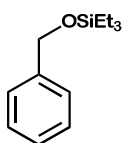


triethyl(2-phenylpropoxy)silane (entry 4, Table 6). ¹H NMR (500 MHz, CD₂Cl₂): δ 7.30 (t, 2 H, ³J_{HH} = 7.3 Hz), 7.24 (d, 2 H, ³J_{HH} = 7.3 Hz), 7.20 (d, 1 H, ³J_{HH} = 7.3 Hz), 3.72 (dd, 1 H, J_{HH} = 9.8, 6.0 Hz, CHH), 3.66-

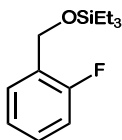
⁶² Lantos, D.; Contel, M.; Sanz, S.; Bodor, A.; Horváth, I. T. *J. Organomet. Chem.* **2007**, 692, 1799.

⁶³ Yeom, C.-E.; Kim, Y. J.; Lee, S. Y.; Shin, Y. J.; Kim, B. M. *Tetrahedron* **2005**, 61, 12227.

3.59 (m, 1 H, CHH), 2.90 (h, 1 H, $^3J_{\text{HH}} = 6.9$ Hz, CH), 1.29 (d, 3 H, $^3J_{\text{HH}} = 6.9$ Hz, CH₃), 1.04-0.90 (m, 9 H), 0.66–0.52 (m, 6 H). $^{13}\text{C}\{^1\text{H}\}$ NMR (125 MHz, CD₂Cl₂) δ 145.4 (C_q arom), 128.8 (2 CH arom), 128.2 (2 CH arom), 126.8 (CH arom), 69.5 (CH₂), 43.3 (CH), 18.1 (CH₃), 8.6 (CH₃), 7.2 (s, CH₃), 5.0 (s, CH₂), 3.1 (CH₂). **HRMS (CI):** m/z 249.1669 [M-H]⁺ (exact mass calculated for C₁₅H₂₅OSi: 249.1675).

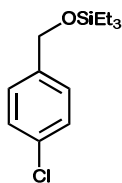


(Benzyloxy)triethylsilane (entry 5, Table 6). Spectroscopic data of the reaction mixture were consistent with previously reported data for this compound.^{9b}

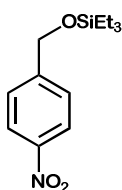


Triethyl(2-fluorobenzyloxy)silane (entry 6, Table 6). Spectroscopic data of the reaction mixture were consistent with previously reported data for this compound.⁶⁴

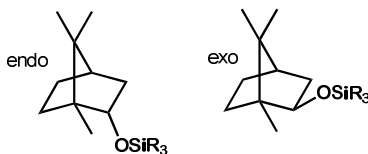
⁶⁴ Tran, B. L.; Pink, M.; Mindiola, D. J. *Organometallics* **2009**, 28, 2234.



Triethyl(4-chlorobenzoyloxy)silane (entry 7, Table 6). Spectroscopic data of the reaction mixture were consistent with previously reported data for this compound.⁶⁴



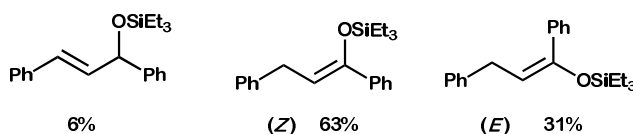
Triethyl(4-nitrobenzyloxy)silane (entry 8, Table 6). Spectroscopic data of the reaction mixture were consistent with previously reported data for this compound.⁶⁵



Hydrosilylation of (*R*)-camphor by hydrosilanes. Using the general procedure at 50 °C, (*R*)-camphor (0.015 g, 0,1 mmol) was hydrosilylated with three different silanes (SiEt₃H, SiPh₂H₂ and SiMe₂PhH). Spectroscopic data of the reaction mixtures were consistent with previously reported data for

⁶⁵ Fernandes, A. C.; Fernandes, R.; Romão, C. C.; Royo, B. *Chem. Comm.* **2005**, 213.

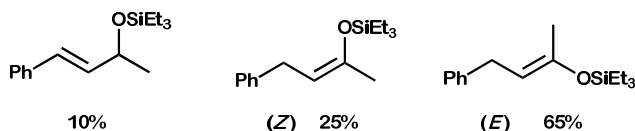
these compounds:^{60,66} **¹H NMR** (500 MHz, CD₂Cl₂, characteristic signals): **SiEt₃H** (51 % *endo*, 49 % *exo*): δ 3.94 (m, 1 H, *endo* isomer), 3.57 (dd, 1 H, $^3J_{\text{HH}} = 7.9, 3.5$ Hz, *exo* isomer). **SiPh₂H₂** (30 % *endo*, 70 % *exo*): δ 4.26 (m, 1 H, *endo* isomer), 3.85 (dd, 1 H, $^3J_{\text{HH}} = 7.8, 3.2$ Hz, *exo* isomer). **SiMe₂PhH** (30 % *endo*, 70 % *exo*): δ 4.03 (m, 1 H, *endo* isomer), 3.65 (dd, 1 H, $^3J_{\text{HH}} = 7.5, 3.0$ Hz, *exo* isomer).



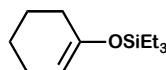
Hydrosilylation of *trans*-chalcone (entry 1, Table 7). Spectroscopic data of the 1,4- and 1,2-addition products were consistent with previously reported data for these compounds.⁶⁷ **¹H NMR** (400 MHz, CD₂Cl₂, characteristic signals): δ 6.66 (d, $^3J_{\text{HH}} = 15.5$ Hz; =CH, 1,2-addition product), 6.32 (dd, $^3J_{\text{HH}} = 15.5, 6.5$ Hz; =CH, 1,2-addition product), 5.35 (t, $^3J_{\text{HH}} = 7.5$ Hz, =CH, *Z*-1,4 addition product), 5.23 (t, $^3J_{\text{HH}} = 7.5$ Hz, =CH, *E*-1,4 addition product), 3.61 (d, $^3J_{\text{HH}} = 7.5$ Hz, CH₂, *Z*-1,4 addition product), 3.47 (d, $^3J_{\text{HH}} = 7.5$ Hz, CH₂, *E*-1,4 addition product).

⁶⁶ b) Bajaj, P.; Babu, G. N. *Indian Journal of Chemistry* **1975**, *13*, 1364. (c) Iida, A.; Horii, A.; Misaki, T.; Tanabe, Y. *Synthesis*, **2005**, *16*, 2677.

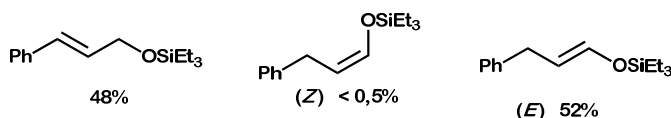
⁶⁷ 1,4-addition products: (a) Ojima, I.; Kogure, T. *Organometallics* **1982**, *1*, 1390. (b) Sumida, Y.; Yorimitsu, H.; Oshima, K. *J. Org. Chem.* **2009**, *74*, 7986. 1,2-addition product: (c) Mahandru, G. M.; Liu, G.; Montgomery, J. *J. Am. Chem. Soc.* **2004**, *126*, 3698.



Hydrosilylation of benzylideneacetone (entry 2, table 7). Spectroscopic data of the 1,2- and 1,4-addition products were consistent with previously reported data for these compounds.⁶⁸ ^1H NMR (400 MHz, CD_2Cl_2 , characteristic signals): δ 6.56 (d, $^3J_{\text{HH}} = 16.0$ Hz; $=\text{CH}$, 1,2-addition product), 6.27 (dd, $^3J_{\text{HH}} = 16.0$, 6.0 Hz; $=\text{CH}$, 1,2-addition product), 4.90 (t, $^3J_{\text{HH}} = 7.5$ Hz, $=\text{CH}$, *E*-1,4 addition product), 4.64 (t, $^3J_{\text{HH}} = 7.0$ Hz, $=\text{CH}$, *Z*-1,4 addition product), 4.52 (m, CH , 1,2 addition product), 3.42 (d, $^3J_{\text{HH}} = 7.0$ Hz, CH_2 , *Z*-1,4 addition product), 3.34 (d, $^3J_{\text{HH}} = 8.0$ Hz, CH_2 , *E*-1,4 addition product).



(Cyclohex-1-en-1-yl)triethylsilane (entry 3, Table 7). Spectroscopic data of the reaction mixture were consistent with previously reported data for this compound.⁶⁹

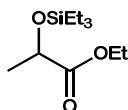


Hydrosilylation of cinnamaldehyde (entry 4, table 7). Spectroscopic

⁶⁸ Charette, A. B.; Lacasse, M.-C. *Org. Lett.* **2002**, *4*, 3351. (b) Ko, C.; Hsung, R. P.; Al-Rashid, Z. F.; Feltenberger, J. B.; Lu, T.; Yang, J.-H.; Wei, Y.; Zifcsak, C. A. *Org. Lett.* **2007**, *9*, 4459. (c) Reich, H. J.; Holtan, R. C.; Bolm, C. *J. Am. Chem. Soc.* **1990**, *112*, 5609.

⁶⁹ Ojima, I.; Donovan, R. J.; Clos, N. *Organometallics* **1991**, *10*, 2606.

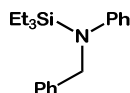
data of the 1,2- and *E*-1,4-addition products were consistent with previously reported data for these compounds.⁷⁰ ¹H NMR (400 MHz, CD₂Cl₂, characteristic signals): δ 6.63 (d, $^3J_{\text{HH}} = 16.0$ Hz; =CH, 1,2-addition product), 6.39 (dt, $^3J_{\text{HH}} = 12.0, 1.2$ Hz; =CH, *E*-1,4-addition product), 6.33 (dt, $^3J_{\text{HH}} = 16.0, 5.2$ Hz; =CH, 1,2-addition product), 5.19 (dt, $^3J_{\text{HH}} = 12.0, 7.5$ Hz; =CH, *E*-1,4-addition product), 4.76 (m, =CH, *Z*-1,4-addition product), 4.37 (dd, $^3J_{\text{HH}} = 5.2, 1.6$ Hz; CH₂, 1,2-addition product), 3.26 (d, $^3J_{\text{HH}} = 7.5$; CH₂, *E*-1,4-addition product).



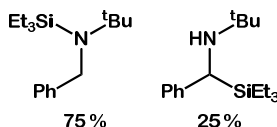
Hydrosilylation of ethyl pyruvate. Spectroscopic data of the reaction mixture were consistent with previously reported data for this compound.⁷¹ ¹H NMR (500 MHz, CD₂Cl₂, characteristic signals): δ 4.30 (q, 1 H, $^3J_{\text{HH}} = 6.8$ Hz, CH₃CH), 4.13 (q, 2 H, $^3J_{\text{HH}} = 7.0$ Hz, OCH₂CH₃), 1.36 (d, 3 H, $^3J_{\text{HH}} = 6.8$ Hz, CH₃CH), 1.26 (t, 3 H, $^3J_{\text{HH}} = 7.0$ Hz, OCH₂CH₃).

⁷⁰ (a) Doyle, M. P.; High, K. G.; Bagheri, V.; Pieters, R. J.; Lewis, P. J. *J. Org. Chem.* **1990**, 55, 6082. (b) Barlow, A. P.; Boag, N. M.; Stone, F. G. A. *J. Organomet. Chem.* **1980**, 191, 39.

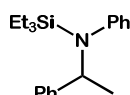
⁷¹ Angle, S. R.; Choi, I.; Tham, F. S. *J. Org. Chem.* **2008**, 73, 6268.

Hydrosilylation of C–N multiple bonds.**Hydrosilylation of N-benzylidene aniline (entry 1, Table 10).**

Spectroscopic data of the reaction mixture were consistent with previously reported data for this compound. ^1H NMR (500 MHz, CD_2Cl_2): δ 7.31 (d, $^3J_{\text{HH}} = 4.3$ Hz, Ph), 7.22 (m, Ph), 7.17 (t, $^3J_{\text{HH}} = 7.9$ Hz, Ph), 6.99 (d, $^3J_{\text{HH}} = 8.1$ Hz, Ph), 6.83 (t, $^3J_{\text{HH}} = 7.3$ Hz, Ph), 4.63 (s, CH_2N), 1.04 (t, 6 H, $^3J_{\text{HH}} = 7.8$ Hz, SiCH_2CH_3), 0.89 (q, 9 H, $^3J_{\text{HH}} = 7.8$ Hz, SiCH_2CH_3).

**Hydrosilylation of N-benzyliden-*t*-butylamine (entry 3, Table 10).**

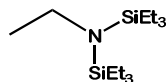
^1H NMR (400 MHz, CD_2Cl_2): characteristic signals, δ 4.14 (s, N-CH-Si, C-Si isomer), 3.75 (s, $\text{CH}_2\text{-NSi}$, C-N isomer), 1.22 (s, ^tBu , C-Si isomer), 1.19 (s, ^tBu , C-N isomer).



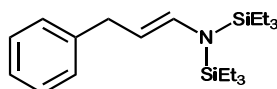
Hydrosilylation of (*E*)-*N*-(1-phenylethylidene)aniline (entry 4, Table 10). Spectroscopic data of the reaction mixture were consistent with previously reported data for this compound.⁷² ^1H NMR (300 MHz, CD_2Cl_2 ,

⁷² Field, L. D.; Messerle, B. A.; Rumble, S. L. *European J. Org. Chem.*, **2005**, 14, 2881.

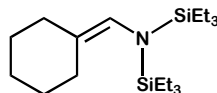
characteristic signals): δ 6.7 (d, $^3J_{\text{HH}} = 8.2$ Hz, N-Ph(*orto*)), 4.52 (q, $^3J_{\text{HH}} = 6.7$ Hz, $\text{CH}_3\text{CH-N}$), 1.62 (d, $^3J_{\text{HH}} = 6.7$ Hz, $\text{CH}_3\text{CH-N}$).



Hydrosilylation of acetonitrile (entry 1, Table 11). ^1H NMR (500 MHz, CD_2Cl_2 , characteristic signals): δ 2.88 (q, 2 H, $^3J_{\text{HH}} = 7.4$ Hz, $\text{CH}_3\text{CH}_2\text{N}$), 0.84 (t, 3 H, $^3J_{\text{HH}} = 7.4$ Hz, $\text{CH}_3\text{CH}_2\text{N}$).



Hydrosilylation of cinnamitrile (entry 3, Table 11). ^1H NMR (400 MHz, CD_2Cl_2): δ 7.29 (t, $^3J_{\text{HH}} = 7.4$ Hz, Ph), 7.19 (m, Ph), 6.05 (d, $^3J_{\text{HH}} = 13.4$ Hz, HC=CH-N), 5.22 (m, 1 H, HC=CH-N), 3.30 (d, 2 H, $^3J_{\text{HH}} = 12.9$ Hz, CH_2), 0.96 (t, 18 H, $^3J_{\text{HH}} = 7.9$ Hz, SiCH_2CH_3), 0.67 (q, 12 H, $^3J_{\text{HH}} = 7.9$ Hz, SiCH_2CH_3). ^{13}C NMR (100 MHz, CD_2Cl_2): δ 142.2 (C(quat), 135.3 (HC=CH-N), 128.6 (*orto*-C), 126.0 (*meta*-C), 120.4 (*para*-C), 37.0 (HC=CH-N), 8.3 (SiCH_2CH_3), 5.2 (SiCH_2CH_3).



Hydrosilylation of cyclohex-1-ene-1-carbonitrile (entry 5, Table 11). ^1H NMR (400 MHz, CD_2Cl_2): δ 5.64 (s, 1 H, C=CH-N), 2.19 (m, 2 H, *orto*-

CH_2), 2.05 (m, 2 H, *orto-CH*₂), 1.55 (m, 6 H, *meta,para-CH*₂), 0.97 (t, 18 H, $^3J_{HH} = 7.6$ Hz, SiCH₂CH₃), 0.64 (q, 12 H, $^3J_{HH} = 7.6$ Hz, SiCH₂CH₃). ^{13}C NMR (100 MHz, CD₂Cl₂): δ 136.7 (C(quat)), 125.4 (C=CH-N), 34.2 (*orto-C*), 28.8 (*orto-C*), 28.2 (*meta-C*), 27.6 (*meta-C*), 27.3 (*para-C*), 8.0 (SiCH₂CH₃), 6.2 (SiCH₂CH₃).

I.4. REFERENCES

I.4. References

- ¹ (a) Atzrodt, J.; Derdau, V.; Fey, T.; Zimmermann, J. *Angew. Chem., Int. Ed.* **2007**, *41*, 7744. (b) Elander, N.; Jones, J. R.; Lu, S. –Y.; Stone-Elander, S. *Chem. Soc. Rev.* **2000**, *29*, 239.
- ² (a) Elmore, C. S.; John, E. M. *Annual Reports in Medicinal Chemistry* **2009**, *44*, 515. (b) Lockley, W. J. S. *J. Labelled Compd. Radiopharm.* **2007**, *50*, 256. (c) Stumpf, W. E. *J. Pharmacol. Toxicol. Methods* **2005**, *51*, 25.
- ³ (a) Werstiuk, N. H; Ju, C. *Can. J. Chem.* **1989**, *67*, 5. (b) Junk, T.; Catallo, W. J. *Tetrahedron Lett.* **1996**, *37*, 3445. (c) Perrotin, P. Sinnema, P –J.; Shapiro, P. J. *Organometallics* **2006**, *25*, 2104. (d) Evchenko, S. V.; Kamounah, F. S.; Schaumberg, K.; *J. Labelled Compd. Radiopharm.* **2005**, *48*, 209. (e) Shabanova, E. Schaumberg, K. Kamounah, F. S. *J. Chem. Res.* **1999**, 364. (f) de Keczer, S. A.; Lane, T. S. M.; Masjedizadeh, R. *J. Labelled Compd. Radiopharm.* **2004**, *47*, 733.

- ⁴ (a) Garnett, J. L.; Long, M. A.; Vining R. F. W.; Mole, T. *J. Am. Chem. Soc.* **1972**, *94*, 5913. (b) Seibles, J. C.; Bollinger, D. B.; Orchin M. *Angew. Chem. Int. Ed.* **1977**, *16*, 656. (c) Heinkele, G.; Mürdter, T. E. *J. Labelled Compd. Radiopharm.* **2005**, *48*, 457.
- ⁵ (a) Berthelette, C.; Scheigetz, J. *J. Labelled Compd. Radiopharm.* **2004**, *47*, 891. (b) Coumbarides, G. S.; Dingjan, M.; Eames, J.; Flinn, A.; Northen, J. *J. Labelled Compd. Radiopharm.* **2006**, *49*, 903. (c) Elemes, Y.; Ragnarsson, U.; *Chem. Commun.* **1996**, 935.
- ⁶ (a) Junk, T.; Catallo, W. D. *Chem. Soc. Rev.* **1997**, *26*, 401. (b) Heys, J. R. *J. Label. Compd. Radiopharm.* **2007**, *50*, 770. (c) Skaddan, M. B.; Yung, C. M.; Bergman, R. G. *Org. Lett.* **2004**, *6*, 11. (d) Skaddan, M. B.; Bergman, R. G. *J. Label. Compd. Radiopharm.* **2006**, *49*, 623. (e) Heys, J. R.; Lockley, W. J. S. *J. Label. Compd. Radiopharm.* **2010**, *53*, 635. (f) Allen, P. H.; Hickey, M. J.; Kingston, L. P.; Wilkinson, D. J. *J. Label. Compd. Radiopharm.* **2010**, *53*, 731. (g) Chappelle, M. R.; Hawes, C. R. *J. Label. Compd. Radiopharm.* **2010**, *53*, 745.
- ⁷ Alonso, F.; Beletskaya, I. P.; Yus, M. *Chem. Rev.* **2002**, *102*, 4009.
- ⁸ (a) Marciniec B. Ed., *Comprehensive Handbook on Hydrosilylation*, Pergamon, Oxford, **1992**. (b) Marciniec, B. *Silicon Chemistry* **2002**, *1*, 155. (c) Roy, A. K. A. *Adv. Organomet. Chem.* **2007**, *55*, 1; (d) Malacea, E.; Poli, R.; Manoury, E. *Coord. Chem. Rev.* **2010**, *254*, 729. (e) Morris, R. H. *Chem. Soc. Rev.* **2009**, *38*, 2282.
- ⁹ For selected examples: (a) Calimano, E.; Tilley, T. D. *J. Am. Chem. Soc.* **2009**, *131*, 11161; (b) Park, S.; Brookhart, M. *Organometallics* **2010**, *29*, 6057. (c) Yang, J.; White, P. S.; Brookhart, M. *J. Am. Chem. Soc.* **2008**, *130*, 17509. (d) Tondreau, A. M.; Lobkovsky, E.; Chirik, P. J. *Org. Lett.* **2008**, *10*, 2789. (e) Tondreau, A. M.; Hojilla Atienza, C. C.; Weller, K. J.; Nye, S. A.; Lewis, K. M.; Delis, J. G. P.; Chirik, P. J. *Science* **2012**, *335*, 567. (f) Yang, J.; Tilley, T. D. *Angew. Chem., Int. Ed.* **2010**, *49*, 10186. (g) Blackwell, J. M.; Morrison, D. J.; Piers, W.E. *Tetrahedron* **2002**, *58*, 8247. (h) Buchan, Z. A.; Bader, S. J.; Montgomery, J. *Angew. Chem., Int. Ed.* **2009**, *48*, 4840. (i) Tran, B. L.; Pink, M.; Mindiola, D. J. *Organometallics* **2009**, *28*, 2234.
- ¹⁰ Karshtedt, D.; Bell, A. T.; Tilley, T. D. *Organometallics* **2006**, *25*, 4471.
- ¹¹ (a) Aizenberg, M.; Milstein, D. *Science* **1994**, *256*, 359; (b) Yang, J.; Brookhart, M. *Adv. Synth. Catal.* **2009**, *351*, 175. (c) Douvris, C.; Ozerov, O. V. *Science* **2008**, *321*, 1188.

- ¹² (a) Prince, P. D.; Bearpark, M. J.; McGrady, G. S.; Steed, J. W. *Dalton Trans.* **2008**, 271.
(b) Grant, B. E.; Brookhart, M. *J. Am. Chem. Soc.* **1993**, *115*, 2156. (c) Sousa, S. C. A.;
Fernandes, A. C. *Adv. Synth. Catal.* **2010**, *352*, 2218.
- ¹³ (a) Ponomarenko V. A.; Odabashyan G. V.; Petrov. A. D. *Dokl. Akad. Nauk SSSR.* **1960**,
131, 321. (b) Ryan J. W.; Speier, J. L. *J. Am. Chem. Soc.* **1964**, *86*, 895. (c) Sommer, L.
H.; Lyons, J. E.; Fujimoto, H.; Michael, K. W. *J. Am. Chem. Soc.* **1967**, *89*, 5483. (d)
Sommer L. H.; Lyons J. E. *J. Am. Chem. Soc.* **1968**, *90*, 4197. (e) Sommer L. H.; Lyons,
J. E.; Fujimoto, H. *J. Am. Chem. Soc.* **1969**, *91*, 7051.
- ¹⁴ (a) Paonessa, R. S.; Prignano, A. L.; Trogue, W. C. *Organometallics* **1985**, *4*, 647. (b)
Liu, X.; Wu, Z.; Cai, H.; Yang, Y.; Chen, T.; Vallet, C. E.; Zuhre, R. A.; Beach, D. B.;
Peng, Z.-H.; Wu, Y.-D.; Concolino, T. E.; Rheingold, A. L.; Xue, Z. *J. Am. Chem. Soc.*
2001, *123*, 8011. (c) Rendler, S.; Oestreich, M. *Angew. Chem. Int. Ed.* **2008**, *47*, 5997.
- ¹⁵ Bradshaw, D. I.; Moyes, R. B.; Wells, P. B. *J. Chem. Soc., Chem. Commun.* **1975**, 137.
- ¹⁶ (a) Bartok, M.; Molnár, A. *J. Organomet. Chem.* **1982**, *235*, 161. (b) Bartok, M.; Molnár,
A. *J. Chem. Soc., Chem. Commun.* **1982**, 1089.
- ¹⁶ Coutant, B.; Quignard, F.; Choplin, A. *J. Chem. Soc., Chem. Commun.* **1995**, 137.
- ¹⁷ Archer, N. J.; Haszeldine, R. N.; Parish, R. V. **1979**, *J. Chem. Soc. Dalton Trans.* 695.
- ¹⁸ Fryzuk, M. D.; Rosenberg, L.; Rettig, S. J. *Organometallics*, **1991**, *10*, 2537.
- ¹⁹ Blackburn, S. N.; Haszeldine, R. N.; Parish, R. V.; Setchfield, J. H. *J. Organomet. Chem.*
1980, 329.
- ²⁰ Berry, D. H.; Procopio, L. J. *J. Am. Chem. Soc.* **1989**, *111*, 4099.
- ²¹ Curtis, M. D.; Bell, L. G.; Butler, W. M. *Organometallics* **1985**, *4*, 701.
- ²² (a) Than, C.; Morimoto, H.; Andres, H.; Williams, P. G. *J. Org. Chem.* **1996**, *61*, 8771;
(b) Zippi, E. M.; Andres, H.; Morimoto, H.; Williams, P. G. *Synthetic Commun.* **1995**,
25, 2685. (c) Jaiswal, D. K.; Andres, H.; Morimoto, H.; Williams, P. G. *J. Chem. Soc.*
Chem. Commun. **1993**, 907. (d) Andres, H.; Morimoto, H.; Williams, P. G. *J. Chem. Soc.*
Chem. Commun. **1990**, 627.
- ²³ Neu, H.; Andres, H. *J. Label. Compd. Radiopharm.* **1999**, *42*, 992.
- ²⁴ M. Saljoughian, *Synthesis* **2002**, 1781.
- ²⁵ Sommer, L. H.; Pietrusza, E. W.; Whitmore, F. C. *J. Am. Chem. Soc.* **1947**, *69*, 188.

- ²⁶ Speier, J. L.; Webster, J.A.; Barnes, G.H. *J. Am. Chem. Soc.*, **1957**, 79, 974.
- ²⁷ (a) Ojima I.; Nihonyanagi, M.; Nagai I. *J. Chem. Soc. Chem. Commun.* **1972**, 938. (b) Ojima, I.; Kogure, T.; Nihonyanagi, M.; Nagai, Y. *Bull. Chem. Soc. Jpn.* **1972**, 45, 3506.
- ²⁸ (a) Addis, D.; Das, S.; Junge, K.; Beller, M. *Angew. Chem. Int. Ed.* **2011**, 50, 6004. (b) Kim, D.; Park, B.-M.; Yun, J. *Chem. Commun.* **2005**, 1755; (c) Belyakova, Z. V. Pomerantseva, M. G.; Chekrii, E. N.; Chernyshev, E. A.; Storozhenko, P. A. *Russ. J. Gen. Chem.* **2010**, 80, 927.
- ²⁹ Watanabe, T.; Hashimoto, H.; Tobita, H. *J. Am. Chem. Soc.*, **2006**, 128, 2176.
- ³⁰ Hashimoto, H.; Aratani, I.; Kabuto, C.; Kira, M. *Organometallics*, **2003**, 22, 2199.
- ³¹ (a) T. Murai, T.; Sakane, S.; Kato, J. *Org. Chem.* **1990**, 55, 499. (b) Caporusso, A. M.; Panziera, N.; Pertici, P.; Pitzalis, E.; Salvadori, P.; Vitulli, G.; Martra, G. J. *J. Mol. Cat. A Chem.* **1999**, 150, 275; (c) Gutsulyak, D. V. Nikonov, G. I. *Angew. Chem. Int. Ed.* **2010**, 49, 7553.
- ³² Chalk, A. J.; Harrod, J. F. *J. Am. Chem. Soc.* **1965**, 87, 16.
- ³³ Ojima, I.; Kogure, T.; Kumagai, M.; Horiuchi, S.; Sato, Y. *J. Organomet. Chem.* **1976**, 122, 83.
- ³⁴ (a) Haan, K. H.; Wielstra, Y.; Teuben, J. H. *Organometallics* **1987**, 6, 2053. (b) Nolan, S. P.; Porchia, M.; Marks, T. J. *Organometallics* **1991**, 10, 1450. (c) Woo, H.-G.; Tilley, T. D. *J. Am. Chem. Soc.* **1989**, 111, 8043. (d) Molander, G. A.; Dowdy, E. D.; Noll, B. C. *Organometallics*, **1998**, 17, 3754. (e) Molander, G. A.; Retsch, W. H. *Organometallics*, **1995**, 14, 4570.
- ³⁵ (a) Parks, D. J.; Piers, W. E. *J. Am. Chem. Soc.* **1996**, 118, 9440. (b) Parks, D. J.; Piers, W. E.; Parvez, M.; Atencio, R.; Zaworotko, M. J. *Organometallics* **1998**, 17, 1369. (c) Parks, D. J.; Blackwell, J. M.; Piers, W. E. *J. Org. Chem.* **2000**, 65, 3090.
- ³⁶ (a) Burger, P. Bergman, R. G. *J. Am. Chem. Soc.* **1993**, 115, 10462; (b) Arndtsen, B. A. Bergman, R. G. *Science* **1995**, 270, 1970.
- ³⁷ Esqueda, A. C. *Compuestos de Rh con ligantes de tipo hidrotris(pirazolil)borato y ciclopentadienilo*, **2000**, PhD thesis, Sevilla.
- ³⁸ Lawrence N. J.; Drew M. D.; Bushell S. M. *J. Chem. Soc., Perkin Trans. 1*, **1999**, 3381.
- ³⁹ For selected examples: (a) Kim, D.; Park, B.-M.; Yun, J. *Chem. Commun.* **2005**, 1755. (b) Jurkauskas, V.; Sadighi, J. P.; Buchwald, S. L. *Org. Lett* **2003**, 5, 2417. (c) Addis, D.;

- Das, S.; Junge, K.; Beller, M. *Ang. Chem. Int. Ed.* **2011**, *50*, 6004. (d) Maeda, M.; Abe M.; Kojima, M. *J. Fluorine Chem.*, **1987**, *34*, 337. (e) Eppstein, D. A.; Marsh, Y. V.; Schryver, B. B.; Larsen, M. A.; Barnett, J. W.; Verheyden J. P. H.; Prisbe, V. *J. Biol. Chem.*, **1982**, *257*, 13390.
- ⁴⁰ (a) Luo, X.-L.; Crabtree, R. H. *J. Am. Chem. Soc.* **1989**, *111*, 2527. (b) Lee, M.; Ko, S.; Chang, S. *J. Am. Chem. Soc.* **2000**, *122*, 12011. (c) Lee, T. L.; Dang, L.; Zhou, Z.; Yeung, C. H.; Lin, Z.; Lau, C. P. *Eur. J. Inorg. Chem.* **2010**, 5675. (d) Mitsudome, T.; Noujima, A.; Mizugaki, T.; Jitsukawaa, K.; Kaneda, K. *Chem. Commun.* **2009**, 5302. (e) Mitsudome, T.; Arita, S.; Mori, H.; Mizugaki, T.; Jitsukawa, K.; Kaneda, K. *Angew. Chem. Int. Ed.* **2008**, *47*, 7938. (d) Tan, T.; Kee, J. K.; Fan, W. Y. *Organometallics*, **2011**, *30*, 4008.
- ⁴¹ (a) Mukherjee, D.; Thompson, R. R.; Ellern, A.; Sadow, A. D. *ACS Catal.* **2012**, *1*, 698. (b) Biffis, A.; Braga, M.; Basato, M. *Adv. Synth. Catal.* **2004**, *346*, 451. (c) Corbin, R. A.; Ison, E. A.; Abu-Omar, M. M. *Dalton Trans.* **2009**, 2850.
- ⁴² (a) Dunne, J. F.; Neal, S. R.; Engelkemier, J.; Ellern, A.; Sadow, A. D. *J. Am. Chem. Soc.* **2011**, *133*, 16782. (b) Buch F.; Harder, S. *Organometallics* **2007**, *26*, 5132. (c)
- ⁴³ Yang, J.; White, P. S.; Schauer, C. K.; Brookhart, M. *Angew. Chem. Int. Ed.* **2008**, *47*, 4141.
- ⁴⁴ (a) Kubas G. J. *Metal Dihydrogen and Sigma-Bond Complexes. Structure Theory and Reactivity.* (Kluwer Academic, New York, **2001**). (b) Crabtree R. H. *Angew. Chem., Int. Ed.* **1993**, *32*, 789. (c) Perutz R. N., Sabo-Etienne S. *Angew. Chem., Int. Ed.* **2007**, *46*, 2578.
- ⁴⁵ Milstein D. *Top. Catal.* **2010**, *53*, 915.
- ⁴⁶ Zheng, G. Z.; Chan, T. H. *Organometallics* **1995**, *14*, 70.
- ⁴⁷ (a) Ripoll, J. L. Lebrun, H. Thuillier, A. *Tetrahedron* **1980**, *36*, 2497. (b) Tomoda, S. Matsumoto, Y. Takeuchi, Y. Nomura, Y. *Chem. Lett.* **1986**, 1193.
- ⁴⁸ (a) Lambert, J. B.; Zhang, S. Z.; Ciro, S. M. *Organometallics* **1994**, *13*, 2430. (b) Lambert, J. B.; Kania, L.; Schilf, W.; Mcconnell, J. A. *Organometallics* **1991**, *10*, 2578.
- ⁴⁹ (a) Williams, V. C.; Piers, W. E.; Clegg, W.; Collins, S.; Marder, T. B. *J. Am. Chem. Soc.* **1999**, *121*, 3244. (b) Jia, L.; Yang, X.; Stern, C.; Marks, T. J. *Organometallics* **1994**, *13*, 2430.

- ⁵⁰ Blom, R.; Boersma, J.; Budzelaar, P. H. M.; Fischer, B.; Haaland, A.; Volden, H. V.; Weidlein, J. *Acta Chem. Scand.* **1986**, *A40*, 113.
- ⁵¹ Cramer, R. *Inorg. Synth.* **1974**, *15*, 14.
- ⁵⁶ Brookhart, M.; Grant, B.; Volpe, A. F. *Organometallics* **1922**, *11*, 3920.
- ⁵⁷ Field, L. D.; Messerle, B. A.; Rehr, M.; Soler, L. P.; Hambley, T. W. *Organometallics* **2003**, *22*, 2387.
- ⁵⁸ Fujita, M.; Hiyama, T. *J. Org. Chem.* **1988**, *53*, 5405.
- ⁵⁹ Ison, E. A.; Trivedi, E. R.; Corbin, R. A.; Abu-Omar, M. M. *J. Am. Chem. Soc.* **2005**, *127*, 15374.
- ⁶⁰ Barden, J.; Fleming, J. *Chem. Commun.* **2001**, *22*, 2366.
- ⁶¹ Díez-González, S.; Escudero-Adam, E. C.; Benet-Buchholz, J.; Stevens, E. D.; Slawin, A. M. Z.; Nolan, S. P. *Dalton Trans.* **2010**, *39*, 7595.
- ⁶² Kaur, H.; Zinn, F. K.; Stevens, E. D.; Nolan, S. P. *Organometallics* **2004**, *23*, 1157.
- ⁶³ Díez-González, S.; Kaur, H.; Kauer, F. Z.; Stevens, E. D.; Nolan, S. P. *J. Org. Chem.* **2005**, *70*, 4784.
- ⁶⁴ Onaka, M.; Higuchi, K.; Nanami, H.; Izumi, Y. *Bull. Chem. Soc. Jpn.* **1993**, *66*, 2638.
- ⁶⁵ Lantos, D.; Contel, M.; Sanz, S.; Bodor, A.; Horváth, I. T. *J. Organomet. Chem.* **2007**, *692*, 1799.
- ⁶⁶ Yeom, C.-E.; Kim, Y. J.; Lee, S. Y.; Shin, Y. J.; Kim, B. M. *Tetrahedron* **2005**, *61*, 12227.
- ⁶⁷ Tran, B. L.; Pink, M.; Mindiola, D. J. *Organometallics* **2009**, *28*, 2234.
- ⁶⁸ Fernandes, A. C.; Fernandes, R.; Romão, C. C.; Royo, B. *Chem. Comm.* **2005**, 213.
- ⁶⁹ b) Bajaj, P.; Babu, G. N. *Indian Journal of Chemistry* **1975**, *13*, 1364. (c) Iida, A.; Horii, A.; Misaki, T.; Tanabe, Y. *Synthesis*, **2005**, *16*, 2677.
- ⁷⁰ 1,4-addition products: (a) Ojima, I.; Kogure, T. *Organometallics* **1982**, *1*, 1390. (b) Sumida, Y.; Yorimitsu, H.; Oshima, K. *J. Org. Chem.* **2009**, *74*, 7986. 1,2-addition product: (c) Mahandru, G. M.; Liu, G.; Montgomery, J. *J. Am. Chem. Soc.* **2004**, *126*, 3698.
- ⁷¹ Charette, A. B.; Lacasse, M.-C. *Org. Lett.* **2002**, *4*, 3351. (b) Ko, C.; Hsung, R. P.; Al-Rashid, Z. F.; Feltenberger, J. B.; Lu, T.; Yang, J.-H.; Wei, Y.; Zifcsak, C. A. *Org. Lett.*

- 2007**, 9, 4459. (c) Reich, H. J.; Holtan, R. C.; Bolm, C. *J. Am. Chem. Soc.* **1990**, 112, 5609.
- ⁷² Ojima, I.; Donovan, R. J.; Clos, N. *Organometallics* **1991**, 10, 2606.
- ⁷³ (a) Doyle, M. P.; High, K. G.; Bagheri, V.; Pieters, R. J.; Lewis, P. J. *J. Org. Chem.* **1990**, 55, 6082. (b) Barlow, A. P.; Boag, N. M.; Stone, F. G. A. *J. Organomet. Chem.* **1980**, 191, 39.
- ⁷⁴ Angle, S. R.; Choi, I.; Tham, F. S. *J. Org. Chem.* **2008**, 73, 6268.
- ⁷⁵ Field, L. D.; Messerle, B. A.; Rumble, S. L. *European J. Org. Chem.*, **2005**, 14, 2881.

CHAPTER 2:

Synthesis and Reactivity of Half-sandwich (η^5 -C₅Me₅)Ir(III) Complexes of Cyclometalated Aryl Phosphine Ligands.

II.1. INTRODUCTION

I.I.1. INTRODUCTION

1.1. C–H Bond Activation, a Brief, General Perspective.

The efficient functionalization of the C–H bonds of alkanes and other common organic molecules remains a difficult and elusive research objective despite its important practical consequences in many industrial and laboratory syntheses.^{1,2} Our use of hydrocarbon feedstocks is inefficient, due mainly to the inertness of their constituent C–C and C–H bonds. The incapacity to transform these compounds into more added-value materials has led to their employment exclusively as fuels, to dispense the energy contained in their C–H and C–C bonds as heat, as a consequence of their

¹ For selected reviews on the topic: (a) Bergman, R. G. *Nature* **2007**, *446*, 391. (b) Crabtree, R. H. *Chem. Rev.* **2010**, *110*, 575. (c) Balcells, D.; Clot, E.; Eisenstein, O. *Chem. Rev.* **2010**, *110*, 749. (d) Labinger, J. A.; Bercaw, J. E. *Nature* **2002**, *417*, 507. (e) Crabtree, R. H. *J. Organomet. Chem.* **2004**, *689*, 4083. (f) Newhouse, T.; Baran, P. S. *Angew. Chem. Int. Ed.* **2011**, *15*, 3362. (g) Wencel-Delord, J.; Dröge, T.; Liu, F.; Glorius, F. *Chem. Soc. Rev.* **2011**, *40*, 4740. (h) Yang, L.; Huang, H. *Catal. Sci. Technol.* **2012**, *6*, 1099.

² Goldberg, K. I.; Goldman, A. S., Eds. *Activation and Functionalization of C-H Bonds*; ACS Symposium Series 885; American Chemical Society: Washington, DC, **2004**.

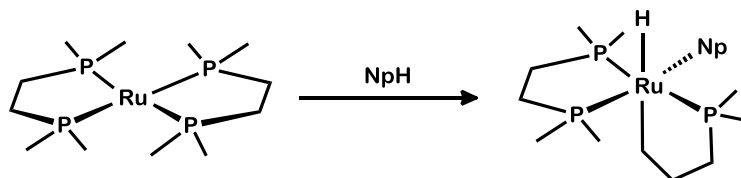
conversion into H₂O and CO₂. The highly detrimental environmental effect derived from the production of large amounts carbon dioxide, as well as the considerable economic impact of using hydrocarbons as raw materials for organic synthesis, have inspired in the last decades investigation of alternative routes to functionalize these molecules. For instance, the activation of the simplest hydrocarbon, CH₄, has attracted the attention of many chemists since the early 1950s. Natural gas is an abundant low-cost feedstock of light hydrocarbons, especially methane. Efficient conversion of the latter into methanol would revolutionize the chemical industry and would have an enormous economic impact. Problems derived from transportation of CH₄, whose location is frequently remote, would be overcome, and moreover, methanol is the starting point for many industrial processes, and it is ultimately added into manufactured products such as plastics and paints.

The utilization of transition metal complexes have led to the activation of C–H bonds with high efficiency and controlled selectivity. Transition metal compounds that are able to promote C–H bond activation with subsequent C–C (or C–X) bond formation (X = O, N, S or other element) hold promise for converting simple and generally available raw materials into complex, elaborated molecules such as pharmaceutical and natural products. Functionalization of alkanes by formation of new C–X bonds opens a plethora of possibilities for a more efficient exploitation of natural hydrocarbon resources, as well as for the preparation of added-value organic molecules.³ On the other hand, selective C–C bond forming reactions⁴ by activation of C–H bonds is an attractive alternative to classical procedures

³ See: Hartwig, J. F. *Nature* **2008**, 455, 314, and references cited therein.

⁴ See: Colby, D. A.; Bergman, R. G.; Ellman J. A. *Chem. Rev.* **2010**, 110, 624, and references cited therein.

such as cross-coupling reactions, which require expensive organohalide and organometallic reagents.⁵



Scheme 1. First example of C–H bond activation reported by Chatt (NpH = naphthalene).

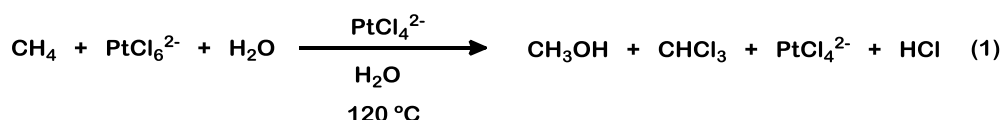
The first example of C–H bond activation was reported by Chatt in 1962 for the oxidative addition of naphthalene to a tetracoordinate ruthenium phosphine complex (Scheme 1).⁶ During the late 60s Garnett and collaborators found that platinum(II) salts were able to catalyze the C–H/D exchange of aromatic polycycles, as well as heterocycles, under acidic conditions.⁷ These ideas were extended by Shilov and co-workers, who published in 1972 the first example of C–H bond functionalization, by means of catalytic alkane oxidation to alcohols and alkyl halides, although inefficiently and using a very energetic reagent as oxidant ($[\text{PtCl}_6]^{2-}$, see Eq 1).⁸

⁵ de Meijere, A.; Diederich, F. *Metal-Catalyzed Cross-Coupling Reactions* **2004**, Eds.; Wiley-VCH: Weinheim.

⁶ Chatt, J.; Watson, H. R. *J. Chem. Soc.*, **1962**, 2545.

⁷ (a) Hodges, R. J.; Garnett, J. L. *J. Phys. Chem.* **1969**, 73, 1525. (b) Hodges, R. J.; Garnett, J. L. *J. Phys. Chem.* **1968**, 72, 1673. (c) Hodges, R. J.; Garnett, J. L. *J. Catal.* **1969**, 13, 83.

⁸ Goldshleger, N.F.; Shteinman, A.A.; Shilov, A.E. Eskova, V.V. *Zh. Fiz. Khim.* **1972**, 46, 1353.



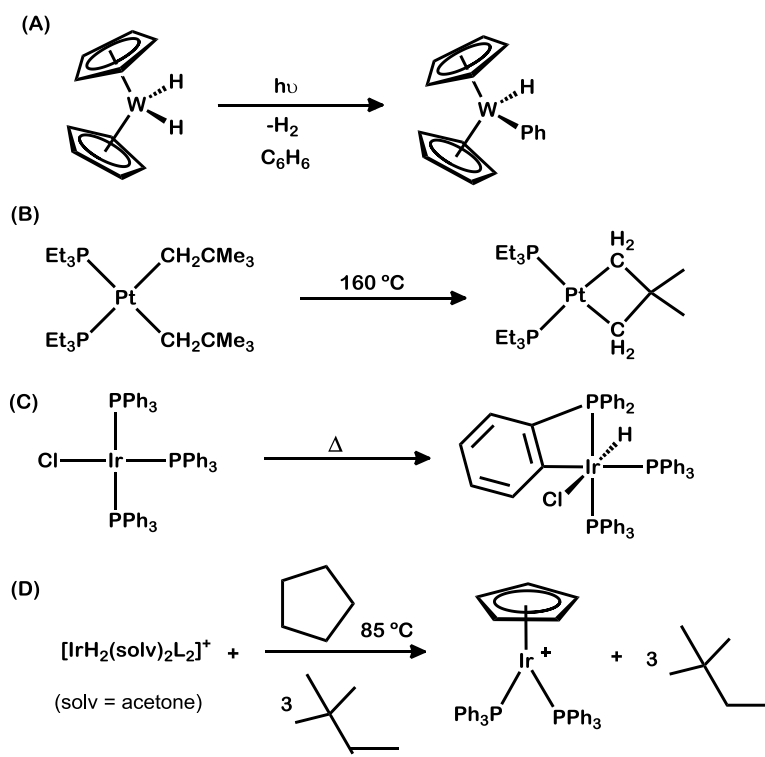
During this decade a number of examples of stoichiometric C–H bond activation also appeared. Scheme 2 contains a selection of these processes.⁹ The work of the groups of Bergman¹⁰ and Graham,¹¹ that demonstrated that intermolecular alkane activation proceeds through the oxidative addition of a C–H bond to a metal center was a milestone in the field. At that time, it was a thought that in the Shilov alkane activation, and also in the reactions reported by Garnett and others, the true catalyst was metallic Pt and Ir, formed by thermal decomposition. However, Bergman and Graham isolated the alkyl hydride complexes resulting from oxidative addition of a C–H bond to an iridium center (Scheme 3), under homogeneous conditions. Many other examples quickly followed¹² and the explosion in C–H bond activation research had continued until today.

⁹ (a) Green, M. L. H.; Knowles, P. J. *J. Chem. Soc. Chem. Commun.* **1970**, 1677; (b) Foley, P.; Whitesides, G. M. *J. Am. Chem. Soc.* **1979**, *101*, 2732. (c) Bennett, M. A.; Milner, D. L. *J. Chem. Soc. Chem. Commun.* **1967**, 581. (d) Crabtree, R. H.; Mihelcic, J. M.; Quirk, J. M. *J. Am. Chem. Soc.* **1979**, *101*, 7738.

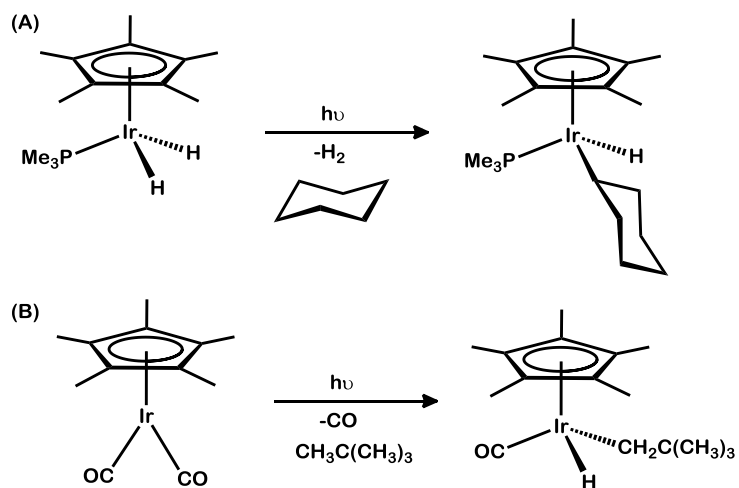
¹⁰ Janowicz, A. H.; Bergman, R. G. *J. Am. Chem. Soc.* **1982**, *104*, 352.

¹¹ Hoyano, J. K.; Graham, W. A. G. *J. Am. Chem. Soc.* **1982**, *104*, 3723.

¹² A review of that achievements can be found in: Shilov, A. E.; Shul'pin, G. B. *Activation and Catalytic Reactions of Saturated Hydrocarbons in the Presence of Metal Complexes*, **2000**, Kluwer Academic, Dordrecht.



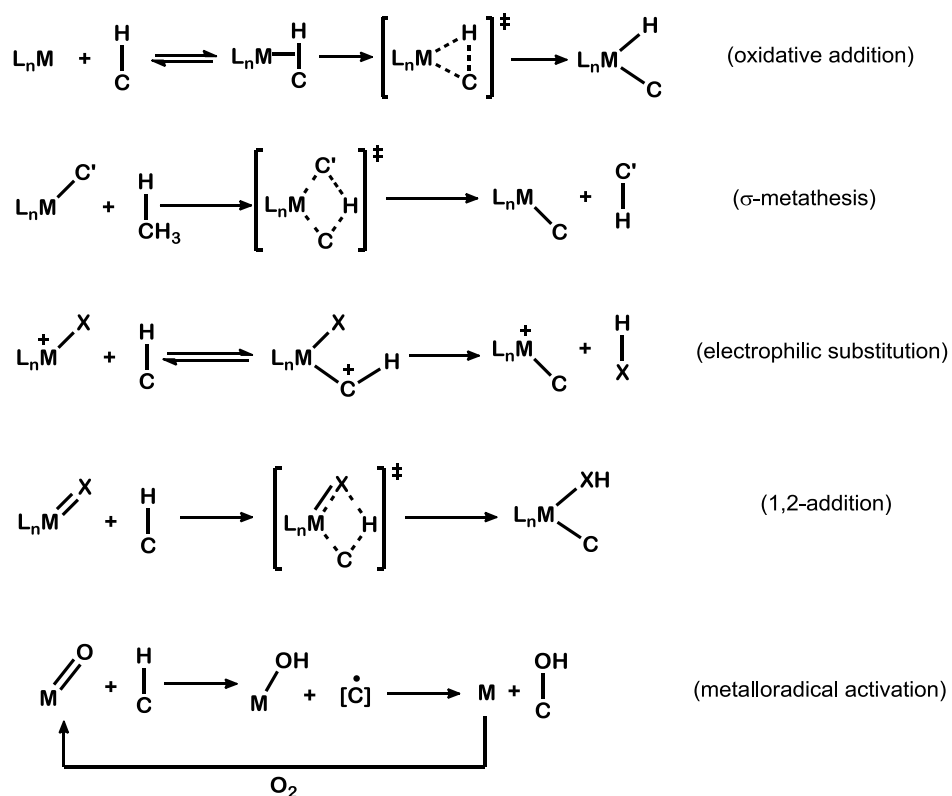
Scheme 2. Early examples of stoichiometric C–H bond activation.



Scheme 3. First examples of intermolecular oxidative addition of an alkane into a metal center reported by (a) Bergman and (b) Graham.

Mechanisms of C–H Bond Activation.

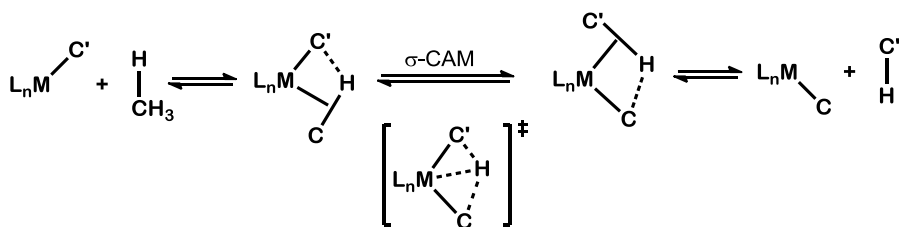
The mechanism of C–H bond activation reactions has been extensively investigated and excellent review articles are available.¹ Scheme 4 summarizes the different proposals of which only the first two will be mentioned briefly.^{1c}



Scheme 4. C–H bond activation mechanisms.

Oxidative Addition is the most common mechanism to account for C–H bond activation. It is preceded by coordination of the C–H bond to a vacant coordination site of the metal to form a σ -complex. Electron-rich, low-valent metal complexes of late transition metals, with an energetically accessible higher oxidation state, usually activate C–H bonds through this mechanism.

σ -Bond Metathesis. This mechanism, that involves an alkyl or hydride metal complex (M–R or M–H, respectively), is the preferred route for C–H activation by early transition metals, as well as lanthanides and actinides, with d^0 electronic configuration. On the basis of previous suggestions by Crabtree on the role of σ -complexes as likely precursors in σ -bond metathesis reactions,¹³ in 2007 Perutz and Sabo-Etienne proposed a new mechanism known as Sigma Complex Assisted Metathesis, or σ -CAM,¹⁴ as shown in Scheme 5. Contrary to classic σ -bond metathesis, this pathway involves discrete σ -complexes as intermediates.



Scheme 5. C–H bond activation through σ -CAM mechanism.

¹³ Crabtree, R. H. *Angew. Chem. Int. Ed.* **1993**, 32, 789.

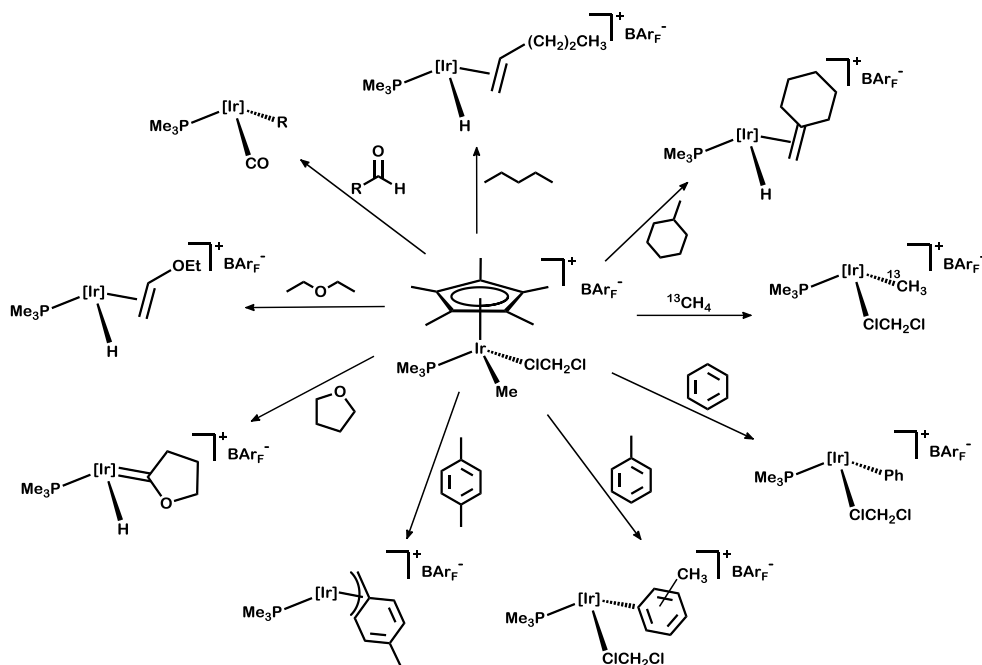
¹⁴ Perutz, R. N.; Sabo-Etienne, S. *Angew. Chem. Int. Ed.* **2007**, 46, 2578.

1.2. Half-Sandwich Iridium and Rhodium Complexes for C–H activation.

Some of the disadvantages of the early systems of Bergman¹⁰ and Graham¹¹ discussed before were soon overcome by the group of Bergman, first with the use of the triflate complex $(\eta^5\text{-C}_5\text{Me}_5)\text{Ir}(\text{PMe}_3)\text{Me}(\text{OTf})$ ¹⁵ ($\text{OTf} = \text{OSO}_2\text{CF}_3$) and subsequently with the isolation and structural characterization of the cationic CH_2Cl_2 adduct,¹⁶ $[(\eta^5\text{-C}_5\text{Me}_5)\text{Ir}(\text{PMe}_3)\text{Me}(\text{CH}_2\text{Cl}_2)]^+[\text{BAr}_\text{F}]^-$ ($\text{BAr}_\text{F} = \text{B}[3,5\text{-C}_6\text{H}_3(\text{CF}_3)_2]_4$). As shown in Scheme 6, this cationic species is capable to activate C_6H_6 ($-30\text{ }^\circ\text{C}$) and even CH_4 ($10\text{ }^\circ\text{C}$). Bergman favored for these C–H activations a mechanism involving a series of oxidative cleavage/reductive coupling steps, and ruled out other possibilities, in particular a mechanism involving Ir–alkylidenes. As we shall discuss in due course, cationic Ir(III) alkylidene complexes play a key role in the chemistry discussed in this Thesis.

¹⁵ Buger, P.; Bergman, R. G. *J. Am. Chem. Soc.* **1993**, *115*, 10462.

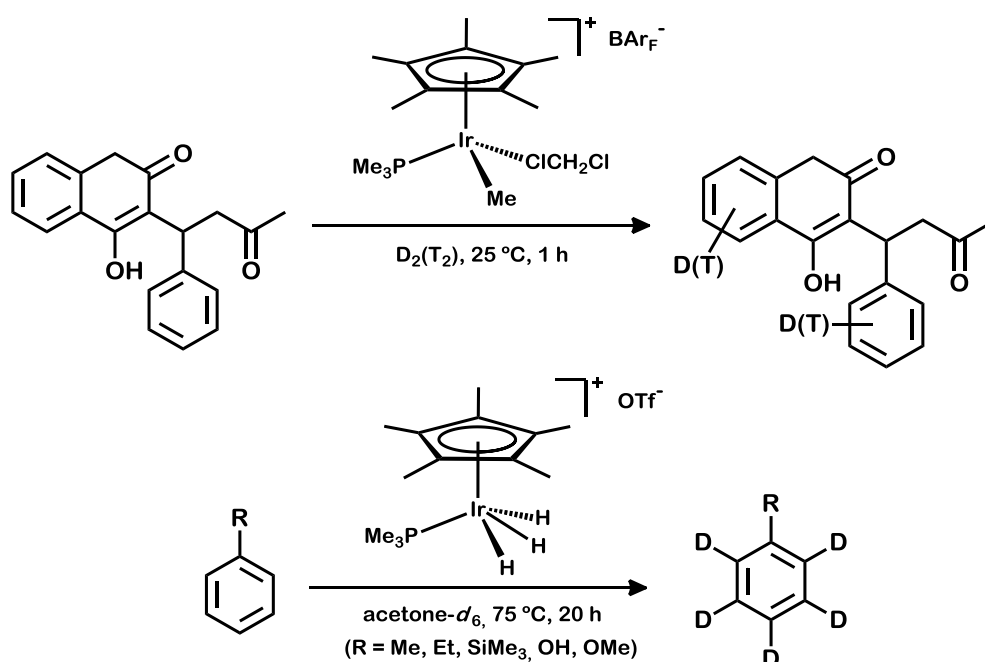
¹⁶ Arndtsen, B. A.; Bergman, R. G. *Science* **1995**, *270*, 1970.



Scheme 6. C–H bond activation reactions mediated by $(\eta^5\text{-C}_5\text{Me}_5)\text{Ir}(\text{PMe}_3)\text{Me}$ cation.

Related also to the work presented herein is the observation of a catalytic hydrogen isotope exchange (H/D and H/T) for a variety of organic molecules¹⁷ under mild experimental conditions (Scheme 7).

¹⁷ (a) Skaddan M. B.; Yung C. M.; Bergman, R. G.; *Org Lett* **2004**, 6: 11. (b) Yung C. M.; Skaddan, M. B.; Bergman R. G. *J. Am. Chem. Soc.* **2004**, 126, 13033. (c) Skaddan, M. B.; Bergman, R. G. *J. Label. Comp. Radiopharm.* **2006**, 49, 623. (d) Klei, S. R.; Golden, J. T.; Tilley, T. D.; Bergman, R. G. *J. Am. Chem. Soc.* **2002**, 124, 2092.

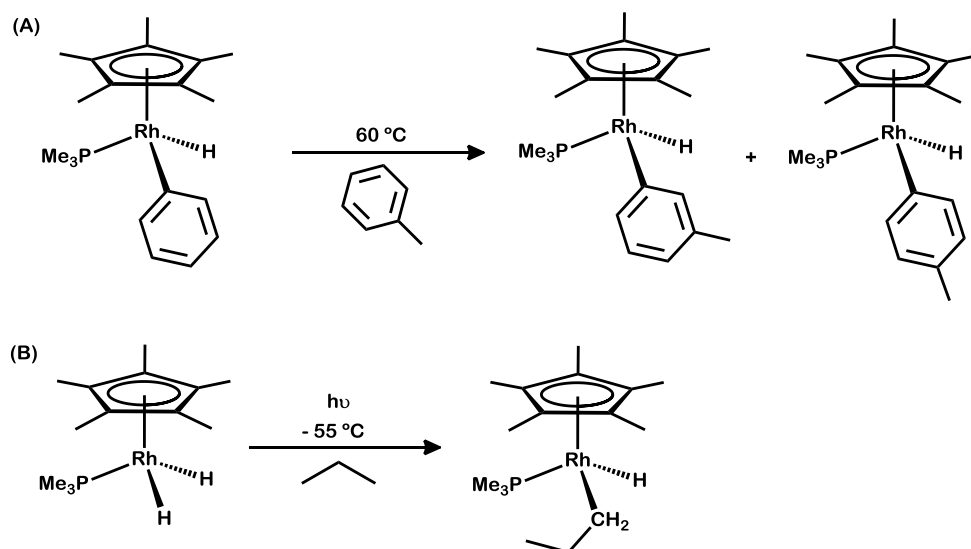


Scheme 7. Catalytic examples of hydrogen isotopic exchange at carbon centers by cationic cyclopentadienyl phosphine Ir(III) complexes.

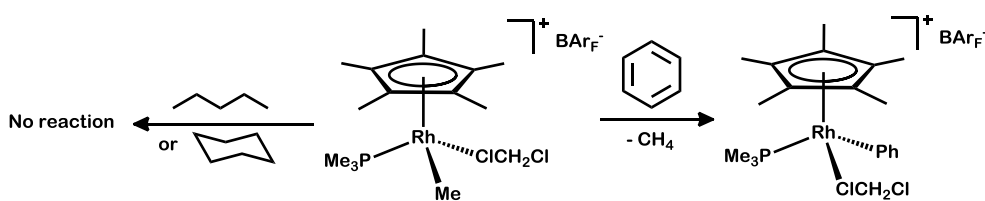
A few months after Bergman's and Graham's original discoveries, Jones described related C–H bond activations by $(\text{C}_5\text{Me}_5)\text{Rh}$ complexes¹⁸ (Scheme 8). The active species was also a $(\text{C}_5\text{Me}_5)\text{M}(\text{I})$ unsaturated species resulting from reductive elimination of C_6H_6 (Scheme 8a) or H_2 (Scheme 8b) from appropriate Rh(III) precursors. At variance with Bergman's results, the related Rh(III), CH_2Cl_2 cationic adduct (Scheme 9) showed inferior capacity

¹⁸ (a) Jones, W. D.; Feher, F. J. *J. Am. Chem. Soc.* **1982**, *104*, 4240. (b) Jones, W. D.; Feher, F. J. *Organometallics*, **1983**, *2*, 562.

to activate C–H bonds,¹⁹ possibly due to the lower accessibility of oxidation state +5 for Rh in comparison with Ir.



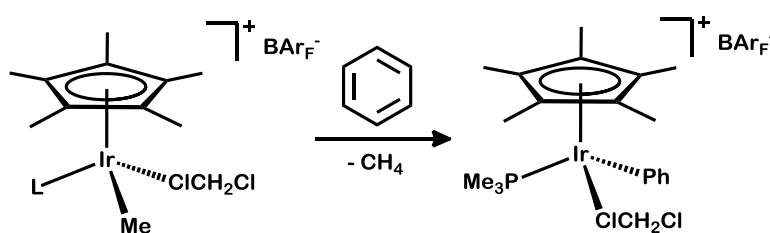
Scheme 8. Arene and alkane C–H bond activation mediated by a $(\eta^5\text{-C}_5\text{Me}_5)\text{Rh}$ complex.



Scheme 9. C–H bond activation mediated by a Rh(III) cationic complex.

¹⁹ (a) Taw, F. L.; Mellows, H.; White, P. S.; Hollander, F. J.; Bergman, R. G.; Brookhart, M.; Heinekey, D. M. *J. Am. Chem. Soc.* **2002**, *124*, 5100. (b) Corkey, B. K.; Felicia, F. L.; Bergman, R. G.; Brookhart, M. *Polyhedron*, **2004**, *23*, 2943.

In the following years many related studies appeared in the literature.²⁰ These included changing the PMe_3 ligand of $[(\eta^5\text{-C}_5\text{Me}_5)\text{Ir}(\text{PMe}_3)\text{Me}(\text{CH}_2\text{Cl}_2)]^+[\text{BAr}_\text{F}]^-$ by P(OMe)_3 , CO, *N*-heterocyclic carbenes and other Lewis bases (Scheme 10), as well as changing the C_5Me_5 ligand by hydrotris(3,5-dimethylpyrazolyl)borate (Tp^{Me_2}). Chen^{20e,f} and Bergman²¹ (among others) utilized also cyclometalated complexes without any significant improvements (Scheme 11).

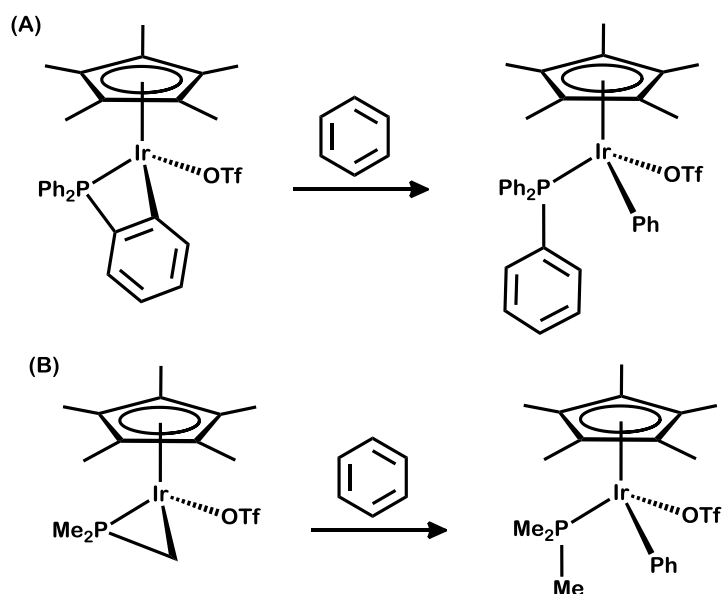


Rate: $\text{L} = \text{PMe}_3 > \text{P(OMe)}_3 > \text{NHC} \gg \text{CO (inactive)}$

Scheme 10. Activation of benzene promoted by the cationic fragment $[(\eta^5\text{-C}_5\text{Me}_5)\text{Ir}(\text{L})\text{Me}]^+$

²⁰ (a) Tellers, D. M.; Yung, C. M.; Arndtsen, B.; Adamson, D. R.; Bergman, R. G. *J. Am. Chem. Soc.* **2002**, *124*, 1400. (b) Meredith J. M.; Goldberg, K. I.; Kaminsky W.; Heinekey, D. M. *Organometallics* **2009**, *28*, 3546. (c) Meredith, J. M.; Robinson Jr., R.; Goldberg, K. I.; Kaminsky, W.; Heinekey, D. M. *Organometallics*, **2012**, *31*, 1879. (d) Tellers, D. M.; Bergman, R. G. *Organometallics* **2001**, *20*, 4819. (e) Hinderling, C.; Plattner, D. A.; Chen, P. *Angew. Chem. Int. Ed.* **1997**, *36*, 243. (f) Hinderling, C.; Feichtinger, D.; Plattner, D. A.; Chen, P. *J. Am. Chem. Soc.* **1997**, *119*, 848

²¹ Luecke, H. F.; Bergman, R. G. *J. Am. Chem. Soc.* **1997**, *119*, 11538.



Scheme 11. Intermolecular C–H activation promoted by cyclopentadienyl iridium complexes.

Besides C–H activation, iridium and rhodium compounds constructed around the $(\eta^5\text{-C}_5\text{Me}_5)\text{M}$ fragment have been utilized for a number of catalytic transformations, such as, for instance, transfer hydrogenation,²² decarbonylation,²³ Diels-Alder²⁴ and cross-coupling reactions.²⁵ Nevertheless, their use in catalysis is still limited, except for transfer

²² (a) Wu, X.; Xiao, J. *Chem. Commun.* **2007**, 2449. (b) Mashima, K.; Abe, T.; Tani, K. *Chem. Lett.* **1998**, 27, 1201. (c) Fujita, K.; Tanino, N.; Yamaguchi, R. *Org. Lett.* **2007**, 9, 109. (d) Tanabe, Y.; Hanasaka, F.; Fujita, K.; Yamaguchi, R. *Organometallics* **2007**, 26, 4618.

²³ Daugulis, O.; Brookhart, M. *Organometallics* **2004**, 23, 527.

²⁴ (a) Carmona, D.; Lamata, M. P.; Viguri, F.; Rodríguez, R.; Lahoz, F. J.; Dobrinovitch, I. T.; Oro, L. A. *Dalton Trans.* **2007**, 1911. (b) Carmona, D.; Lahoz, F. J.; Elipe, S.; Oro, L. A.; Lamata, M. P.; Viguri, F.; Sanchez, F.; Martinez, S.; Cativiela, C.; Lopez-Ram de Viu, M. P. *Organometallics*, **2002**, 21, 5100.

²⁵ (a) Prades, A.; Corberán, R.; Poyatos, M.; Peris, E. *Chem. Eur. J.* **2008**, 14, 11474. (b) Prades, A.; Corberán, R.; Poyatos, M.; Peris, E. *Chem. Eur. J.* **2009**, 15, 4610.

hydrogenation reactions, although as pointed out by Xiao, *it will be only a matter of time before their full potential in catalysis is exploited*.²⁶

1.3. Organometallic Metallacycles and C–H Activation.

Transition metal metallacycles, that result formally from the activation of a C–R bond of an appropriate organic precursor molecule (Scheme 12), constitute an important family of organometallic compounds.²⁷ Complexes of this kind find applications in catalysis,²⁸ bioorganometallic chemistry, including the development of anticancer drugs,²⁹ and material science.³⁰ Some pincer-type iridacycles are outstanding catalysts for processes such as alkane dehydrogenation^{28a} or hydrogen production from aminoborane,³¹ and exhibit great potential as organic light-emitting diodes (OLEDs).³²

²⁶ Liu, J.; Wu, X.; Iggo, J. A.; Xiao, J. *Coord. Chem. Rev.* **2008**, 252, 782.

²⁷ Albrecht, M. *Chem. Rev.* **2010**, 110, 576.

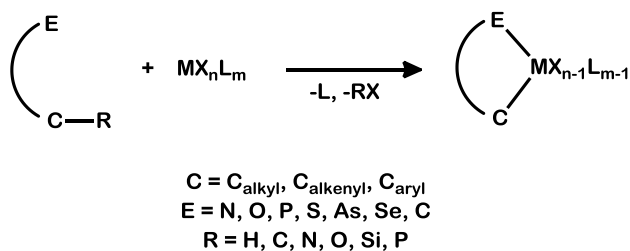
²⁸ (a) Göttker-Schnetmann, I.; White, P.; Brookhart, M. *J. Am. Chem. Soc.* **2004**, 126, 1804. (b) Saidi, O.; Marafie, J.; Ledger, A. E. W.; Liu, P. M.; Mahon, M. F.; Kociok-Köhn, G.; Whittlesey, M. K.; Frost, C. G. *J. Am. Chem. Soc.* **2011**, 133, 19298. (c) Feng, J.-J.; Chen, X.-F.; Shi, M.; Duan, W.-L. *J. Am. Chem. Soc.* **2010**, 132, 5562. (d) Selander, N.; Szabó, K. J. *Dalton Trans.* **2009**, 6267. (e) Bedford, R. B. *Chem. Commun.* **2003**, 1787.

²⁹ (a) Severin, K.; Bergs, R.; Beck, W. *Angew. Chem. Int. Ed.* **1998**, 37, 1634. (b) Dyson, P. J.; Sava, G. *Dalton Trans.* **2006**, 1929. (c) Ryabov, A. D.; Sukharev, V. S.; Alexandrova, L.; Lagadec, R. L.; Pfeffer, M. *Inorg. Chem.* **2001**, 40, 6529.

³⁰ (a) Patoux, C.; Launay, J.-Pierre; Beley, M.; Chodorowski-kimmes, S.; Collin, J.-Paul; James, S.; Sauvage, J.-Pierre *J. Am. Chem. Soc.* **1998**, 120, 3717. (b) Isozaki, K.; Takaya, H.; Naota, T. *Angew. Chem. Int. Ed.* **2007**, 119, 2913. (c) Wadman, S. H.; Lutz, M.; Tooke, D. M.; Spek, A. L.; Havenith, R. W. A.; Klink, G. P. M. V.; Koten, G. V. *Inorg. Chem.* **2009**, 48, 1887. (d) Wadman, S. H.; Kroon, J. M.; Bakker, K.; Lutz, M.; Spek, A. L.; van Klink, G. P. M.; van Koten, G. *Chem. Commun.* **2007**, 1907.

³¹ Denney, M. C.; Pons, V.; Hebden, T. J.; Heinekey, D. M.; Goldberg, K. I. *J. Am. Chem. Soc.*, **2006**, 28, 12048.

³² Chou, P.-T.; Chi, Y. *Chem. Eur. J.* **2007**, 13, 380



Scheme 12. General scheme for cyclometalation reactions.

Some compounds that contain tertiary phosphines which are prone to undergo cyclometalation reactions have provided hybrid olefin-phosphine ligands, following a dehydrogenative C–C bond coupling reaction. Figure 1 contains some of the early examples,^{33,34} whereas Figure 2 collects more recent reports which have found important applications in catalysis.³⁵ While the synthesis of these ligands by conventional methods is time-consuming

³³ (a) Bennett, M. A.; Longstaff, P. *J. Am. Chem. Soc.* **1969**, *91*, 6266. (b) Bennett, M. A.; Clark, P. W. *J. Organomet. Chem.* **1976**, *110*, 367. (c) Bennett, M. A.; Clark, P. W.; Robertson, G. B.; Whimp, P. O. *J. Chem. Soc., Chem. Commun.* **1972**, 1011.

³⁴ (a) Baratta, W.; Herdtweck, E.; Martinuzzi, P.; Rigo, P. *Organometallics* **2001**, *20*, 305. (b) Baratta, W.; Ballico, M.; Del Zotto, A.; Zangrando, E.; Rigo, P. *Chem. Eur. J.* **2007**, *13*, 6701.

³⁵ (a) Shintani, R.; Duan, W.-L.; Nagano, T.; Okada, A.; Hayashi, T. *Angew. Chem. Int. Ed.* **2005**, *44*, 4611. (b) Maire, P.; Deblon, S.; Breher, F.; Geier, J.; Böhler, C.; Rüegger, H.; Schönberg, H.; Grützmacher, H. *Chem. Eur. J.* **2004**, *10*, 4198. (c) Mora, G.; Van Zutphen, S.; Thoumazet, C.; Le Goff, X. F.; Ricard, L.; Grützmacher, H.; Le Floch, P. *Organometallics* **2006**, *25*, 5528. (d) Thoumazet, C.; Ricard, L.; Grützmacher, H.; Le Floch, P. *Chem. Commun.* **2005**, 1592. (e) Thoumazet, C.; Ricard, L.; Grützmacher, H.; Le Floch, P. *Chem. Commun.* **2005**, 1592. (f) Bettucci, L.; Bianchini, C.; Oberhauser, W.; Vogt, M.; Grützmacher, H. *Dalton Trans.* **2010**, *39*, 6509. (g) Bettucci, L.; Bianchini, C.; Oberhauser, W.; Vogt, M.; Grützmacher, H. *Dalton Trans.* **2010**, *39*, 6509. (h) Bettucci, L.; Bianchini, C.; Oberhauser, W.; Vogt, M.; Grützmacher, H. *Dalton Trans.* **2010**, *39*, 6509. (i) Christ, M. L.; Sabo-Etienne, S.; Chaudret, B. *Organometallics* **1995**, *14*, 1082. (j) Douglas, T. M.; Le Nôtre, J.; Brayshaw, S. K.; Frost, C. G.; Weller, A. S. *Chem. Commun.* **2006**, 3408. (k) Lewis, J. C.; Wu, J. Y.; Bergman, R. G.; Ellman, J. A. *Ang. Chem. Int. Ed.* **2006**, *45*, 1589. (l) Lewis, J. C.; Berman, A. M.; Bergman, R. G.; Ellman, J. A. *J. Am. Chem. Soc.* **2008**, *130*, 2493.

and requires many synthetic steps, that usually result in low overall yields, their formation in a metal-induced C–C dehydrogenative coupling is, in no few cases, a straightforward, high-yield process. In the *Results and Discussion* section of this Thesis one such process involving an iridium-bound cyclometalated PMe(Xyl)_2 ($\text{Xyl} = 2,6\text{-Me}_2\text{C}_6\text{H}_3$) ligand will be described.

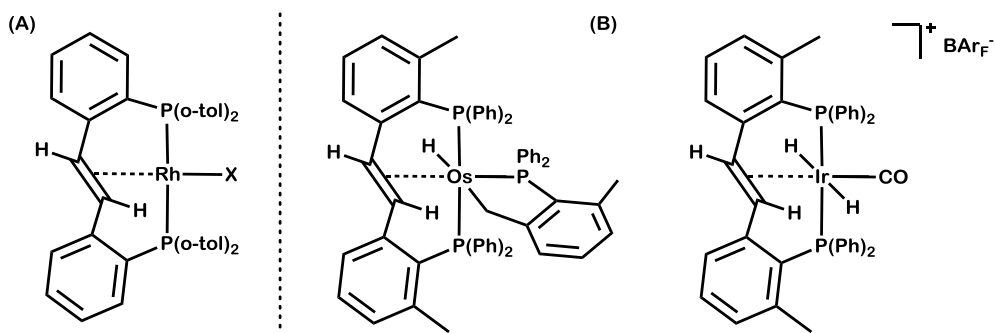


Figure 1. Phosphine-stilbene complexes obtained by C–C bond formation and subsequent dehydrogenation.

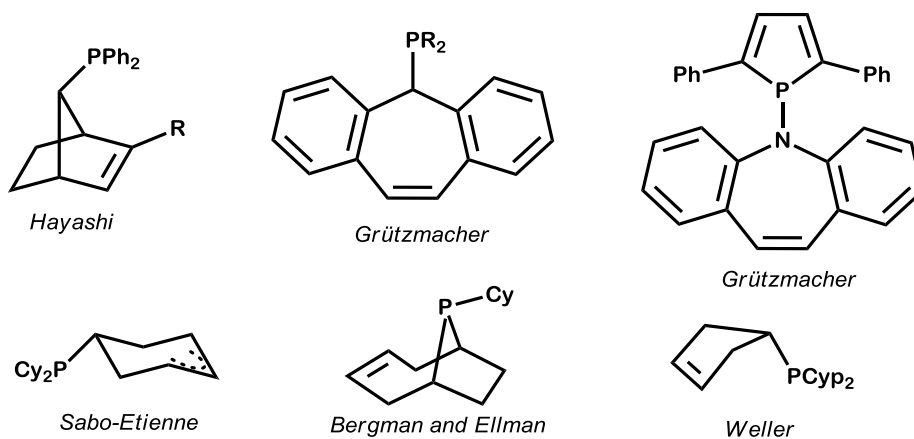


Figure 2. Selected hybrid olefin-phosphine ligands recently used in catalysis.

1.4. Electrophilic Alkylidenes.

During the last decades metal carbenes have become one of the most exploited areas of research in organometallic chemistry due to the almost unlimited reactivity exhibited by this functionality.³⁶ An interesting class of carbenes are alkylidenes, term which refers to those carbenes of formula $L_nM=CR_2$, where $R = H$, alkyl or aryl. Depending on the nature of the metallic fragment, alkylidenes may act either as electrophilic (Fischer type) or nucleophilic carbenes (Schrock type).³⁷ For example, $[(\eta^5-C_5H_5)_2W(=CH_2)Me]^+$ and $(\eta^5-C_5H_5)_2Ta(=CH_2)Me$ are isoelectronic; however the former alkylidene behaves as electrophilic, whereas the latter acts as a Schrock carbene.³⁸

These two types of coordination can be represented by two different binding formulations (Figure 3). The $=CR_2$ ligand is considered to act as a two electrons lone-pair neutral donor ligand (L type) in Fischer carbenes, whereas Schrock analogues are regarded as dianionic four electrons donor ligands (X_2 type). As it is well known, Fischer carbenes are prone to react with nucleophiles and Schrock carbenes with electrophiles.

³⁶ Arduengo, A. J.; Bertrand, G. *Chem. Rev.* **2009**, *109*, 3209.

³⁷ Crabtree, R. H. *The Organometallic Chemistry of the Transition Metals* **2005**, Chap. 11, Ed. John Wiley & Sons, New Jersey.

³⁸ Cooper, N. J. *Pure Appl. Chem.* **56**, 25, 1984.

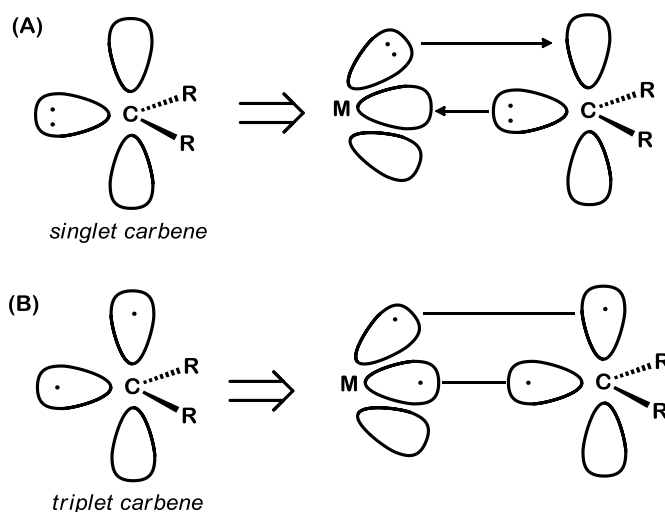
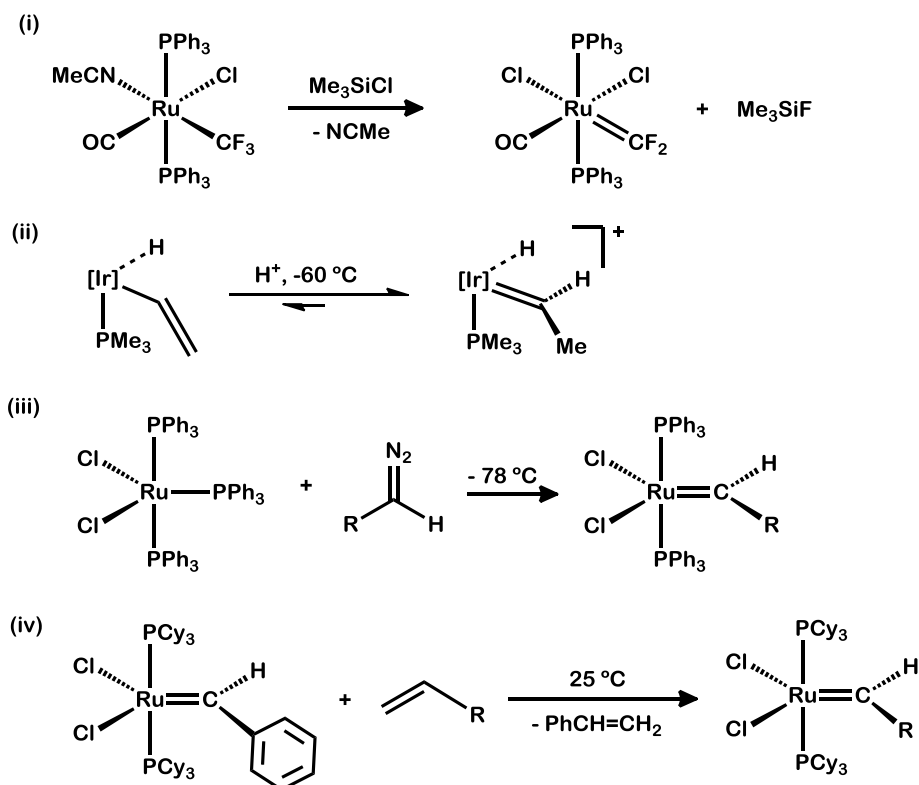


Figure 3. Binding modes of Fischer (a) and Schrock (b) carbenes.

Fischer carbenes are usually found in complexes of the late transition metals in low oxidation states, usually bearing π -acceptor ligands and π -donor substituents on the carbene carbon. In this chapter, work carried out with rhodium and iridium organometallic complexes, which typically form electrophilic carbenes, will be discussed. It is worth recalling that electrophilic alkylidene moieties can be generated by different routes (Scheme 13).^{39,40}

³⁹ (a) Elschenbroich, C. *Organometallics*, Chap 14, Ed. VCH, Weinheim. (b) Astruc, D. *Organometallic Chemistry and Catalysis* **2007**, Chap. 9, Ed. Springer Verlag.

⁴⁰ (a) Clark, G. R.; Hoskins, S. V.; Roper, W. R. *J. Organom. Chem.* **1982**, 234, C9. (b) Alías, F. M.; Poveda, M. L.; Sellin, M.; Carmona, E. *J. Am. Chem. Soc.* **1998**, 120, 5816. (c) Schwab, P.; France, M. B.; Ziller, J. W.; Grubbs R. H. *Angew. Chem. Int. Ed.* **1995**, 34, 2039.



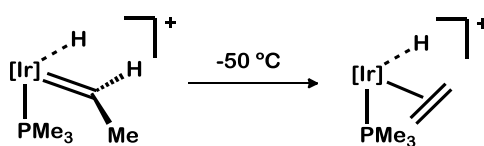
Scheme 13. Examples of procedures for the preparation of electrophilic alkylidenes: (i) Reaction of a Lewis acid with an M-alkyl complex; (ii) Protonation of a M-vinyl complex ($[\text{Ir}] = \text{Tp}^{\text{Me}_2}\text{Ir}$); (iii) Addition of a carbene transfer reagent to a complex with a vacant site. (iv) Cross-metathesis.

Iridium alkylidenes are scarce. A few examples of complexes in which iridium presents the low oxidation state Ir(I), are known.⁴¹ In turn, Ir(III) alkylidenes⁴¹ are rather elusive species, difficult to isolate, although they have been extensively postulated as reactive intermediates.⁴² The first

⁴¹ See for example: (a) Alías, F. M.; Poveda, M. L.; Sellin, M.; Carmona, E.; Gutiérrez, E.; Monge, A. *Organometallics* **1998**, *17*, 4124. (b) Lee, D.-H.; Chen, J.; Faller, J. W.; Crabtree, R. *Chem. Commun.* **2001**, 213-214 (c) Werner, H. *Ang. Chem. Int. Ed.* **2010**, *49*, 4714. (d) Poverenov, E.; Milstein, D. *Chem. Commun.* **2007**, 3189. (e) Fryzuk, M. D.; Macneil, P. A.; Rettig, S. J. *J. Am. Chem. Soc.* **1985**, *107*, 6708.

⁴² See for example: (a) Paneque, M.; Posadas, C. M.; Poveda, M. L.; Rendon, N.; Mereiter, K. *Organometallics* **2007**, *26*, 1900. (b) Luecke, H. F.; Bergman, R. G. *J. Am. Chem. Soc.* **1998**, *120*, 11008. (c) Besora, M.; Vyboishchikov, S. F.; Lledós, A.; Maseras, F.; Carmona, E.; Poveda, M. L. *Organometallics* **2010**, *29*, 2040. (d) Carmona, E.; Paneque,

example of a cationic Ir(III) alkylidene was reported by the group of Carmona in 1998 by protonation of an alkenyl complex with $[\text{H}(\text{OEt}_2)_2][\text{BAr}_\text{F}]$ (Scheme 13(ii)).^{40b} Because of its high reactivity, it readily isomerized at $-50\text{ }^\circ\text{C}$ to its (hydrido)olefin isomer (Scheme 14). One year later Werner and co-workers published an iridium(III) system bearing stabilized aromatic alkylidenes $=\text{CAr}_2$.⁴³ To our knowledge, no other examples of Ir(III) alkylidenes have been reported to date.



Scheme 14. Isomerization of Ir(III) alkylidene at $-50\text{ }^\circ\text{C}$ ($[\text{Ir}] = \text{Tp}^{\text{Me}_2}\text{Ir}$).

M.; Poveda, M. L. *Dalton Trans.* **2003**, 4022. (e) Thorn, D. L.; Tulip, T. H. *J. Am. Chem. Soc.* **1981**, *103*, 5984. (f) Thorn, D. L. *Organometallics* **1982**, *1*, 879. (g) Thorn, D. L.; Tulip, T. H. *Organometallics* **1982**, *1*, 1580. (h) Bell, T. W.; Haddleton, D. M.; McCamley, A.; Partridge, M. G.; Perutz, R. N.; Willner, H. *J. Am. Chem. Soc.* **1990**, *112*, 9212. (i) France, M. B.; Feldman, J.; Grubbs, R. H. *J. Chem. Soc., Chem. Commun.* **1994**, 1307. (j) Bleeke, J. R.; Behm, R. *J. Am. Chem. Soc.* **1997**, *119*, 8503.

⁴³ (a) Ortmann, D. A.; Weberndo, B.; Schoneboom, J.; Werner, H. *Organometallics* **1999**, *18*, 952. (b) Ortmann, D. A.; Weberndo, B.; Kerstin, I.; Laubender, M.; Schoneboom, J.; Werner, H. *Organometallics* **1999**, *18*, 952.

II.2. RESULTS AND DISCUSSION

I.I.2. RESULTS AND DISCUSSION

2. Results and Discussion

As discussed in the *Introduction*, numerous studies of inter- and intramolecular C–H bond activation reactions employing neutral or cationic complexes of the $(\eta^5\text{-C}_5\text{Me}_5)\text{M}$ fragments ($\text{M} = \text{Rh}, \text{Ir}$) have been reported to date,^{10,11,15,19} including a number of catalytic transformations.^{17,26} Considering the high activity and selectivity of the $[(\eta^5\text{-C}_5\text{Me}_5)\text{Ir}(\text{Me})(\text{PMe}_3)(\text{ClCH}_2\text{Cl})]^+$ cation, in C–H activation,¹⁶ it is somehow surprising that information on related complexes with different cyclopentadienyl or P-donor ligands is still scarce.

An important strategy frequently employed in organometallic chemistry to improve metal reactivity in terms of performance, leading to superior

efficiency and selectivity, is modulation of the ligand environment to introduce subtle changes in the steric and electronic properties of the metal center. Bearing in mind the remarkable reactivity of iridium metalacycles, including numerous relevant catalytic applications,^{28a,31,32} we envisaged combining the phosphine and alkyl functionalities of Bergman's cationic Ir(III) complex (Figure 4) into a chelating cyclometalated aryl phosphine. To avoid side reactions like β -H elimination, while at the same time achieving formation of a five-membered metallacycle, aryl phosphines metalated at a benzylic position and, more precisely, phosphines containing at least one Xyl unit (Xyl = 2,6-Me₂C₆H₃), have been chosen. In the first part of this Chapter (Part A), the synthesis and reactivity of cyclopentadienyl iridium complexes constructed around the PMe(Xyl)₂ phosphine will be presented. As discussed later, they feature considerable differences in the chemistry with the analogous rhodium complexes (Chapter 1). The second part of the chapter (Part B) will focus on the effects, in terms of chemical structure and reactivity, that result from subtle changes in the substituents of the metalated phosphine ligand.

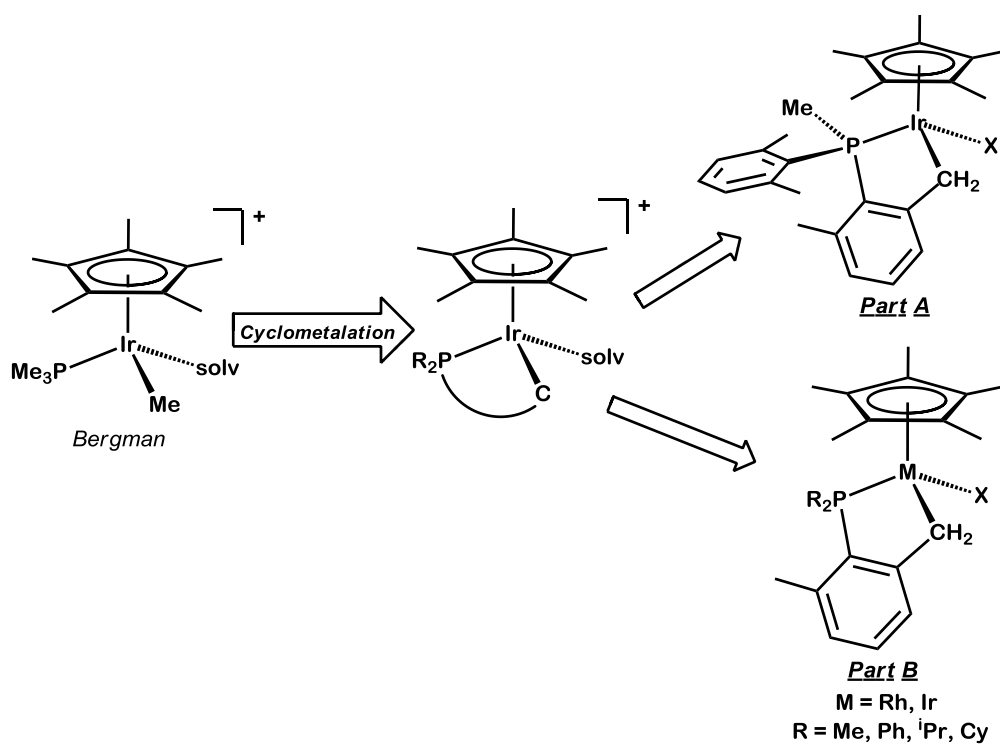


Figure 4. Synthetic plan for the modification of the iridium Bergman's system for C-H activation.

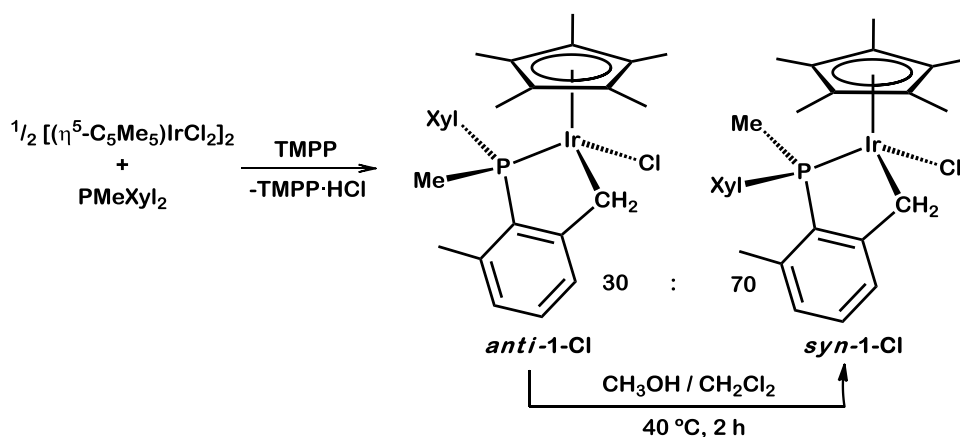
Part A:
**Study of (η^5 -C₅Me₅)Ir(PMe(Xyl)₂)-Derived
Compounds**

2.A. RESULTS AND DISCUSSION

2.A.1. Halide and Pseudohalide Complexes.

Following conventional synthetic procedures, the reaction between equimolar amounts of the Ir(III) dimer [$\{(\eta^5\text{-C}_5\text{Me}_5)\text{IrCl}_2\}_2$] and PMe(Xyl)₂ was attempted. However, instead of the expected phosphine adduct, the cyclometalated complex **1-Cl** formed (Scheme 15) due to fast cyclometalation with concomitant elimination of HCl (trapped as the corresponding phosphine hydrochloride, [HPMe(Xyl)₂]Cl). Consequently,

only half of the starting iridium dimer converted into the desired product. Performing the reaction in the presence of the weakly coordinating base 2,2,6,6-tetramethylpiperidine (TMPP in Scheme 15), gave the desired complex **1-Cl** in the form of two diastereomers (*ca.* 7:3 ratio). Mild heating ($\text{CH}_2\text{Cl}_2/\text{MeOH}$, 40 °C, 2 h) of this mixture caused conversion into its major component as the exclusive product, isolated in 90% yield. The spatial distribution of the ligands in both diastereomers was confirmed by both, NOE experiments of the related methyl complex **1-Me** (*vide infra*) and X-ray analysis (Figure 6). As expected, the major species is the sterically more favorable stereomer, that exhibits a *syn* orientation of chloride and methyl phosphine groups.



Scheme 15. Synthesis of cyclometalated complex **1-Cl** and isomerization to the *syn* diastereomer.

Complex **1-Cl** was obtained as a yellow crystalline solid, which displayed good stability toward oxygen and moisture, particularly in the solid state.

NMR data (Experimental Section and Figure 5) permitted unambiguous characterization of the ligand framework. In the ^1H NMR spectrum there is a prominent doublet at δ 1.32 ($^4J_{\text{HP}} = 1.9$ Hz, 15 H) due to the C_5Me_5 group, as well as three singlets with chemical shifts 1.47, 1.78 and 2.35 ppm (3 H each), that correspond to the non-equivalent methyl aryl protons. The phosphorous-bound methyl group appears as a doublet (δ 2.28, 10.4 Hz), whereas the diastereotopic protons of the methylene group bonded to iridium provide a characteristic pattern of lines which is diagnostic of metalation. This may be identified as the AB part of an ABX spin system, in which only one of the protons features observable coupling to ^{31}P ($\delta_{\text{A}} = 4.15$, $\delta_{\text{B}} = 3.87$ ppm; $^2J_{\text{AB}} = 14.5$, $^3J_{\text{AX}} = 3.8$ Hz). Corresponding signals are found in the $^{13}\text{C}\{^1\text{H}\}$ NMR spectrum. Interestingly, the Ir-CH₂ resonance appears at 20.3 ppm and exhibits negligible coupling to phosphorus, while the two methyl groups of the non-metalated xylyl (δ 22.7 and 25.0) show three-bond couplings with the ^{31}P nucleus of 4 and 8 Hz, respectively. The $^{31}\text{P}\{^1\text{H}\}$ NMR consists of a singlet at 11.3 ppm, that is significantly shifted to higher frequency in comparison with the free ligand (-33.1 ppm). ^1H and $^{31}\text{P}\{^1\text{H}\}$ NMR signals due to the minor isomer are similar to those of the major one.

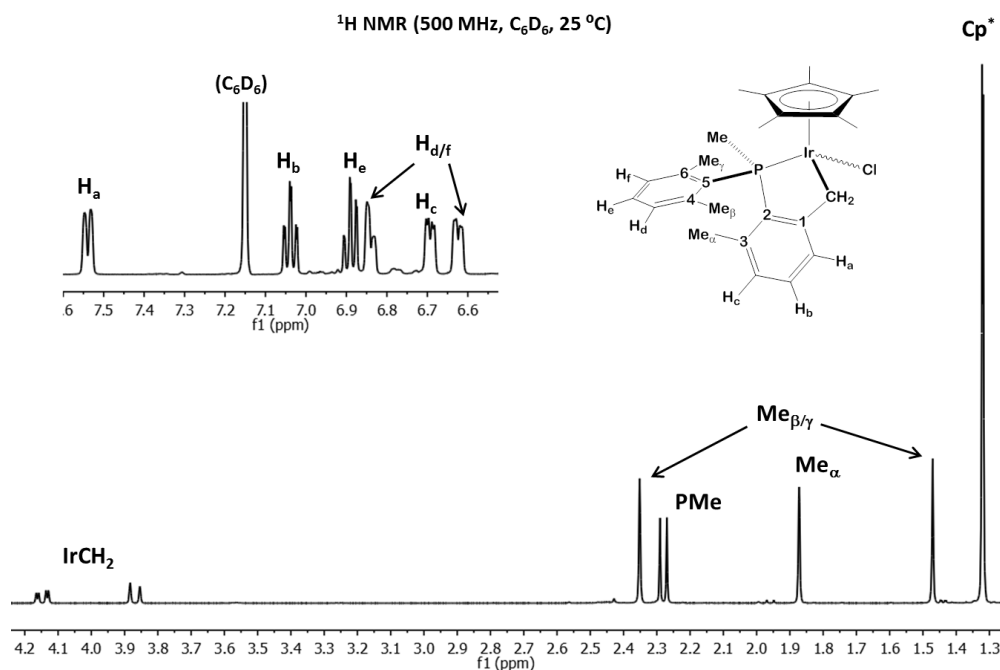


Figure 5. ¹H NMR spectrum (500 MHz, C₆D₆, 25 °C) of **1-Cl**.

Figure 6 collects ORTEP diagrams for complex **1-Cl** and **1-SCN** (*vide infra*). The molecular structure of the complex confirms that cyclometalation of the xylyl-substituted phosphine has occurred at one of the benzylic carbon atoms, giving rise to a five-membered iridacycle. This unit is characterized by Ir–C and Ir–P bonds with lengths of 2.125(8) and 2.246(2) Å, respectively. Bond angles between the P, C and Cl atoms that complete the three-legged piano stool structure are close to the ideal 90° value (in particular the P1–Ir1–Cl angle is 89.55(8)°). The X-ray analysis confirms also the proposed *syn* arrangement of the Cl ligand and phosphine methyl group that leaves the larger, non-metalated phosphine xylyl substituent, on the opposite region of space.

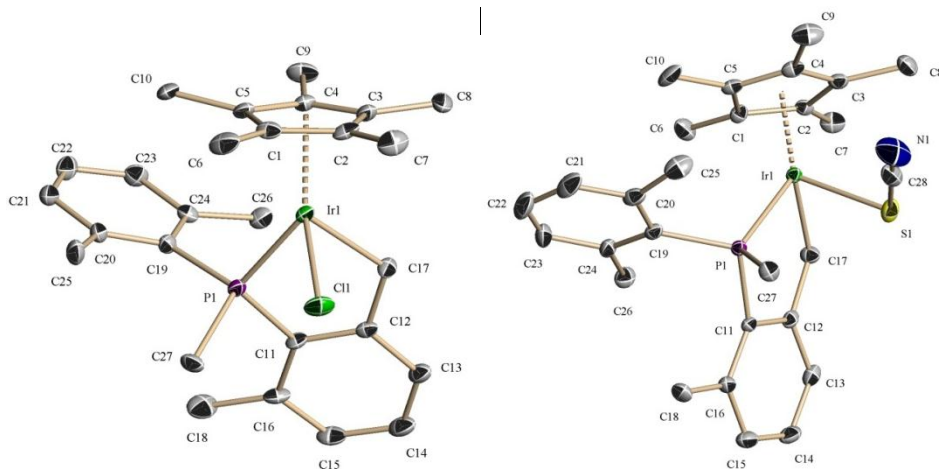
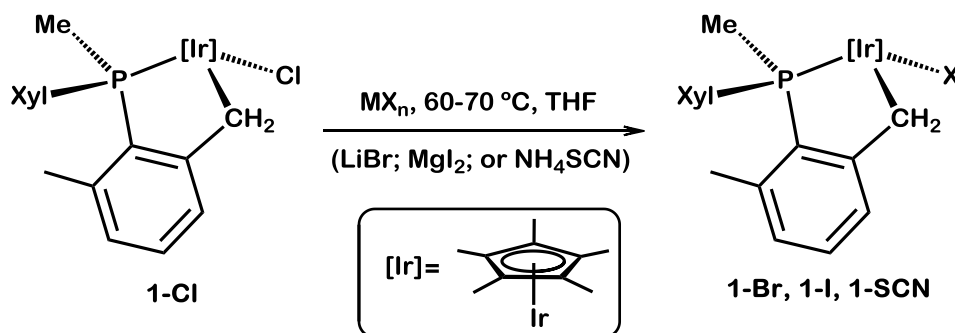


Figure 6. ORTEP diagram for complex **1-Cl** and **1-SCN**. Thermal ellipsoids are drawn at the 50 % probability and hydrogen atoms have been omitted for clarity.

Metathesis reactions of **1-Cl** with LiBr, MgI₂ or NH₄SCN, afforded corresponding complexes **1-X**, as shown in Scheme 16. Under the stated experimental conditions, **1-Br** and **1-I** were produced as single stereomers, whereas **1-SCN** was obtained as a mixture of two isomers in an approximately 6:1 ratio. Similarly to **1-Cl**, the major (or exclusive) reaction product in each case is proposed to be the sterically more favorable isomer, namely that minimizing steric interactions by the adoption of a *syn* distribution of the X and methyl phosphine groups. X-ray studies carried out for complex **1-SCN** confirmed this assumption (Figure 6). Similarly to complex **1-Cl**, Ir–C and Ir–P distances in **1-SCN** are 2.120(4) and 2.254 (1) Å, respectively. Bond angles which characterize the three-legged piano stool conformation are also close to 90°.



Scheme 16. Synthesis of halides and thiocyanate complexes **1-X**.

Compounds **1-X** are orange or yellow crystalline solids that exhibit good solubility properties in common organic solvents. Although they were prepared and manipulated under an inert atmosphere, they are fairly stable toward oxygen and moisture, particularly in the form of crystalline samples. NMR data are in accord with the proposed formulation. For all compounds the $\eta^5\text{-C}_5\text{Me}_5$ ligand yields a doublet in the ^1H NMR spectrum due to weak coupling between the C_5Me_5 protons and the phosphorus nucleus (δ 1.3-1.6 ppm, $^4J_{\text{HP}}$ of *ca.* 2 Hz). Resonances due to the diastereotopic Ir-CH₂ protons are characteristic and evidence their metalated molecular structure (Figure 7). As for **1-Cl**, they appear as two multiplets identified as the AB portions of an ABX spin system ($\text{X} = {}^{31}\text{P}$), where only one of the two ^1H nuclei features observable coupling to ${}^{31}\text{P}$.

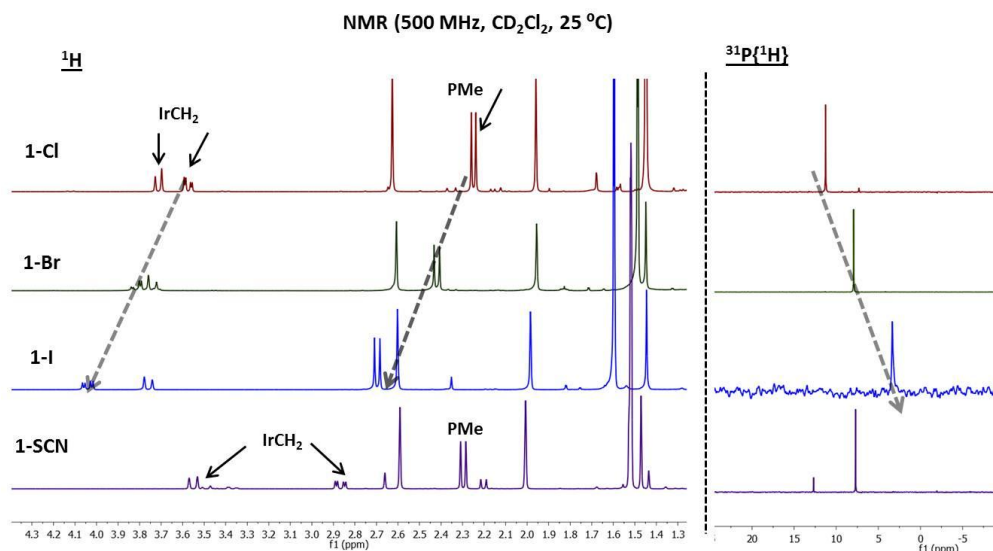


Figure 7. (a) ^1H NMR spectrum (500 MHz, CD_2Cl_2 , 25 °C) of complexes **1-Cl**, **1-Br**, **1-I** and **1-SCN**. (b) $^{31}\text{P}\{^1\text{H}\}$ NMR spectrum (500 MHz, CD_2Cl_2 , 25 °C) of complexes **1-Cl**, **1-Br**, **1-I** and **1-SCN**.

Compound **1-SCN** was prepared with the aim of ascertaining whether it would bind to iridium through the sulfur or the nitrogen donor atoms. S-coordination to the soft $(\text{C}_5\text{Me}_5)\text{Ir}(\text{P}-\text{C})$ fragment would be favored electronically,^{44,45} but N-coordination, with an Ir–N–C–S angle close to 180° would be preferred on steric grounds (Figure 8). IR bands registered at 2100 and 795 cm^{-1} are suggestive of S-binding.⁴⁶ In the X-ray structure the analysis of the size and morphology of the thermal ellipsoids (which sometimes is ambiguous⁴⁷), along with an Ir–X distance of 2.384(1) Å and a

⁴⁴ (a) Pearson, R. G. *J. Am. Chem. Soc.* **1963**, 85, 3533. (b) Schmidtke, H. H. *J. Am. Chem. Soc.* **1965**, 87, 2522.

⁴⁵ Chisholm, M. A.; Rothwell, I. P., *Compreh. Coord. Chem.*, **1987**, Chapter 3.4. Wilkinson, G. W.; Guillard, R. D.; McCleverty, J. A. Eds. Pergamon Press, Oxford.

⁴⁶ Norbury, A. H. *Adv. Inorg. Chem. Radiochem.* **1975**, 17, 231.

⁴⁷ Müller, P.; Herbst-Irmer, R.; Spek, A. L.; Schneider, T. R.; Sawaya, M. R. *Crystal Structure Refinement* **2006**, Chapter 4, Ed. Oxford Univ. Press, New York.

bond angle of 105.9(2) Å demonstrate S-coordination (M–X distances vary between 2.27 and 2.34 Å for S-coordination and between 1.92 and 2.14 for N-bonding)^{48,49}.

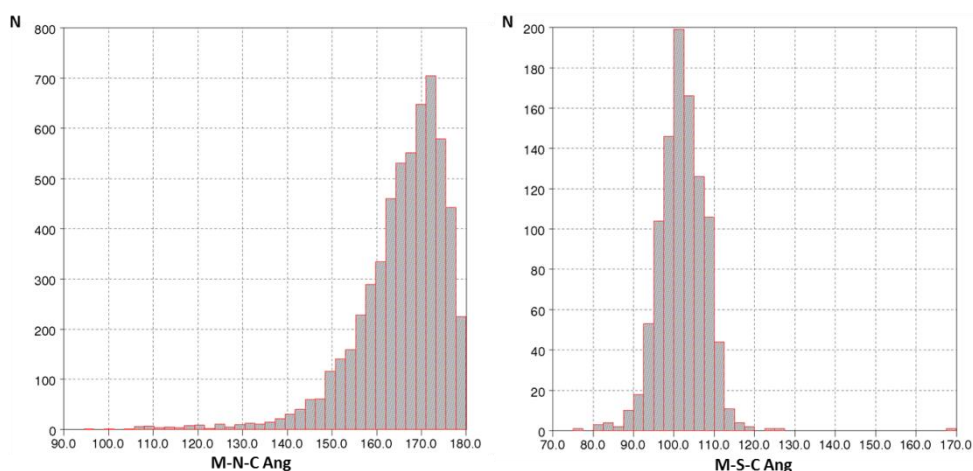


Figure 8. Common angles in transition metal thycyanates: (a) M–N–C; (b) M–S–C (N = number of structures reported in the Cambridge Crystallographic Database for transition metal thycyanates).⁵⁰

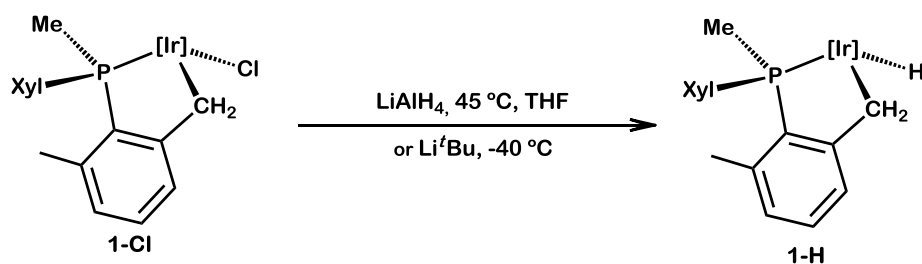
⁴⁸ Data collected from The Cambridge Structural Database (CSD). Cambridge Crystallographic Data Centre, 12 Union Road, Cambridge, England.

⁴⁹ See for example: (a) Comba, P.; Jurisic, P.; Lampeka, Y. D.; Peters, A.; Prikhod'ko, A. I.; Pritzkow, H. *Inorg. Chim. Acta* **2001**, 324, 99. (b) Bernhardt, P. V.; Dyahningtyas, T. E.; Han, S. C.; Harrowfield, J. M.; Kim, I.C.; Kim, Y.; Koutsantonis, G. A.; Rukmini, E.; Thuéry, P. *Polyhedron* **2004**, 23, 869. (c) Majumdar, A.; Pal, K.; Sarkar, S. *Dalton Trans.* **2009**, 1927.

⁵⁰ Data collected from The Cambridge Structural Database (CSD) and analyzed with VISTA software. CCDC (1994). Vista - A Program for the Analysis and Display of Data Retrieved from the CSD. Cambridge Crystallographic Data Centre, 12 Union Road, Cambridge, England.

2.A.2. Neutral Hydride and Alkyl Complexes.

Complex **1-Cl** is a suitable precursor for related complexes that contain Ir–C or Ir–H sigma bonds. Reaction of tetrahydrofuran (THF) solutions of **1-Cl** and LiAlH_4 , at 45 °C for 2 h (Scheme 17) gave iridium hydride **1-H** in the form of a pale yellow powder, which converted into a colorless crystalline material after crystallization from pentane at -25 °C. In an alternative, also high-yield procedure, treatment of a THF solution of **1-Cl** with a cold pentane solution (-40 °C) of Li^tBu , followed by room temperature stirring for a period of 4 h yielded **1-H** too. Monitoring the reaction by ^1H and ^{31}P NMR showed conversion of **1-Cl** into **1-H** with concomitant formation of 1 equiv of isobutene.



Scheme 17. Synthesis of hydride complex **1-H** by addition of LiAlH_4 or Li^tBu to **1-Cl**.

Hydride complex **1-H** is characterized by a medium-weak intensity infrared absorption at 2090 cm^{-1} . The presence of the metal hydride is further demonstrated by the observation of a characteristic ^1H NMR doublet with δ - 17.24 ($^2J_{\text{HP}} = 35.2\text{ Hz}$). Other ^1H , $^{31}\text{P}\{^1\text{H}\}$ and $^{13}\text{C}\{^1\text{H}\}$ NMR signals are

consistent with the structurally similar and previously discussed halide and pseudohalide compounds **1-X**. X-ray analysis demonstrated the *syn* distribution of the metal hydride and the methyl group directly bound to the phosphorous atom (Figure 9).

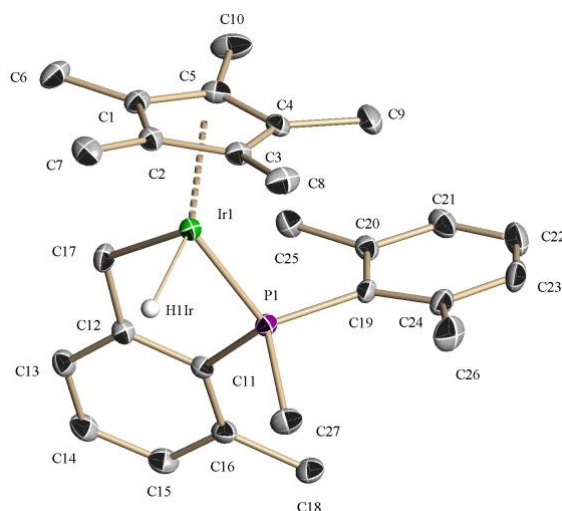
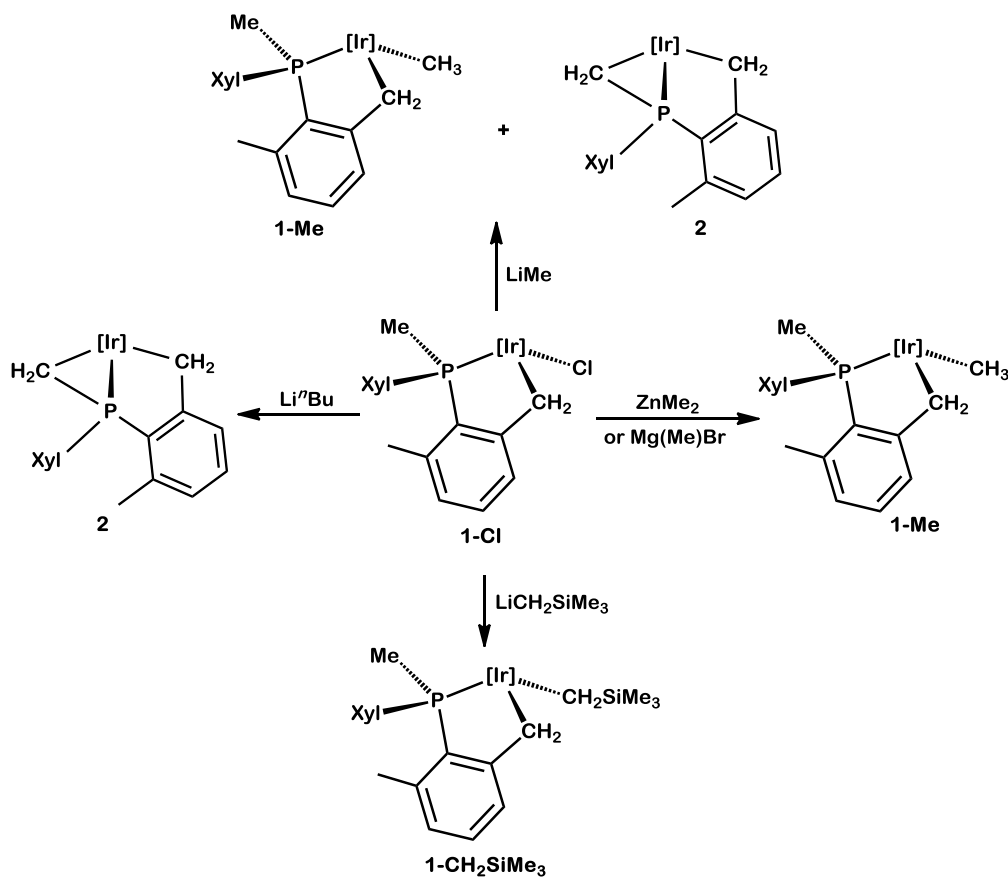


Figure 9. ORTEP diagram for complex **1-H**. Thermal ellipsoids are drawn at the 50 % probability and hydrogen atoms have been omitted for clarity. The metal hydride has been located in the difference electron density map and its Ir–H bond distance restrained.

Three alkyl iridium complexes were prepared by treating **1-Cl** with either lithium, zinc or Grignard reagents. Reaction of **1-Cl** with LiMe yielded the expected methyl derivative **1-Me**, as the major reaction product, albeit, minor amounts (*ca.* 30%) of the somewhat related complex **2**, additionally metalated in the phosphine methyl group, were also produced (Scheme 18). The latter compound did not form in the analogous reactions with the milder dimethyl zinc and methyl Grignard reagents. Thus, the latter provided a straightforward, high-yield route to methyl complex **1-Me**. Notably, Li^{*n*}Bu

gave exclusively doubly metalated compound **2**, whereas reaction with $\text{LiCH}_2\text{SiMe}_3$ produced cleanly alkyl complex **1-CH}_2\text{SiMe}_3.**



Scheme 18. Reactions of compound **1-Cl** to form iridium alkyl complexes.

The NMR data recorded for the C_5Me_5 and cyclometalated phosphine ligands of alkyl compounds **1** are similar to those already discussed for **1-Cl** and **1-H**. The alkyl groups of **1-Me** and **1-CH}_2\text{SiMe}_3** produce high-field ^1H NMR signals, that are observed for the former compound at 0.35 ppm (d, $^3J_{\text{HP}}$

= 5.2 Hz). In the latter, the Ir-CH₂SiMe₃ protons are diastereotopic and appear as multiplets in the chemical shift range of 0.30 – 0.19 ppm. As expected, the ¹³C{¹H} resonances found for these Ir-C units are strongly shielded and appear at -22.9 (**1-Me**) and -29.6 (**1-CH₂SiMe₃**) ppm. ³¹P{¹H} NMR resonances are hardly displaced with respect to previously discussed compounds **1**, and have chemical shifts of 8.4 and 6.4 ppm for **1-Me** and **1-CH₂SiMe₃**, respectively. The *syn* orientation already demonstrated for complexes **1-Cl**, **1-SCN** and **1-H** by X-ray diffraction analysis, was also inferred from NOE studies of alkyl compounds **1** (Figure 10).

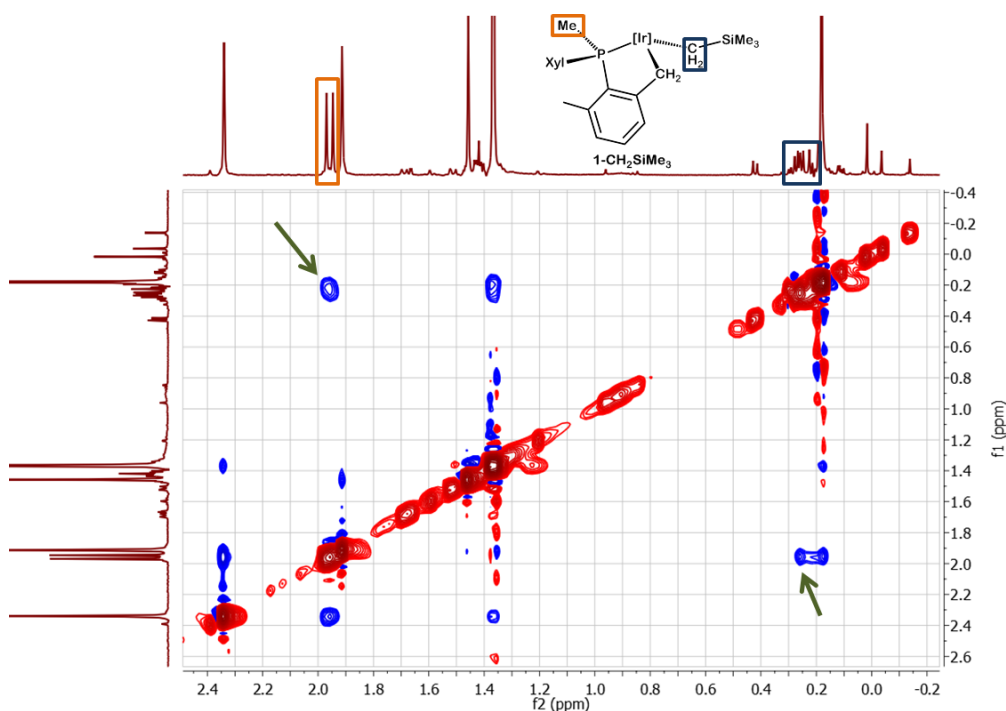


Figure 10. 2D-NOE experiment for **1-CH₂SiMe₃**. Green arrows show NOE cross-peaks for IrCH₂Si and PMe as a result of their *syn* orientation.

In addition, X-ray studies confirmed the molecular structure of **1-Me**. As expected, the two Ir–C bonds, i.e. Ir1–C17 and Ir1–C28, have practically the same length. As shown in Table 1, compounds **1-X** (X = Cl, SCN, H and Me) have a Cp^{*}–Ir–(P–C) skeleton with similar structural parameters.

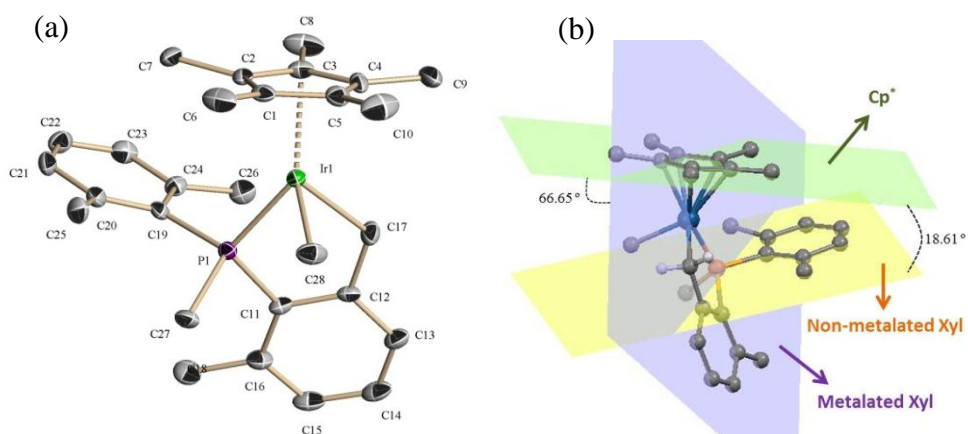


Figure 11. (a) ORTEP diagram for complex **1-Me**. Thermal ellipsoids are drawn at the 50 % probability and hydrogen atoms have been omitted for clarity. (b) Selected common planes of compounds **1**.

Table 1. Selected bond distances and dihedral angles for compound **1**.

Compound	Bond distances (Å)			Dihedral angles (°)	
	<i>Ir1 – C17</i>	<i>Ir1 – P1</i>	<i>Ir1 – X/R</i>	<i>Cp[*] – NM^a</i>	<i>Cp[*] – M^b</i>
1-Cl	2.125(8)	2.246(2)	2.396(2)	20.16	66.38
1-SCN	2.120(4)	2.2537(10)	2.3842(12)	16.01	65.14
1-H	2.165(3)	2.2131(7)	1.59(3) ^c	11.77	69.26
1-Me	2.104(6)	2.2179(17)	2.109(6)	18.61	66.65

^aNM = Non-metalated Xyl ring; ^bM = Metalated Xyl ring; ^cIr–H distance has been restrained.

As discussed above, $^{31}\text{P}\{^1\text{H}\}$ resonances for compounds **1** lie in the narrow range from 11.3 to 3.2 ppm. However, metalation of the P–Me unit (Scheme 18) to give compound **2** causes a $^{31}\text{P}\{^1\text{H}\}$ shift of almost 50 ppm to higher field in comparison with compounds **1** (δ -41.6 ppm, i. e. about 8 ppm to higher field than in the free ligand). In the ^1H NMR spectrum the doublet due to the P–Me group that appears in the vicinity of 2 ppm for compounds **1** is replaced by two multiplets at δ 1.46 and 0.17, due to the diastereotopic IrCH_2P protons. The corresponding $^{13}\text{C}\{^1\text{H}\}$ resonance appears at -18.4 ppm, and features negligible coupling to the ^{31}P nucleus. Only a few other phosphametalacyclopropane species have been reported for Ir,^{21,51} Re⁵² and Os.⁵³

⁵¹ (a) Hinderling, C.; Feichtinger, D.; Plattner, D. A.; Chen, P. *J. Am. Chem. Soc.* **1997**, *119*, 10793. (b) Casalnuovo, A. L.; Calabrese, J. C.; Milstein, D. *J. Am. Chem. Soc.* **1988**, *110*, 6738.

⁵² (a) Wenzel, T. T.; Bergman R. G. *J. Am. Chem. Soc.* **1996**, *108*, 4856. (b) Bergman, R. G.; Seidler, P. F.; Wenzel, T. T. *J. Am. Chem. Soc.* **1985**, *107*, 4358.

⁵³ Shinomoto, R. S.; Desrosiers, P. J.; Harper, G. P.; Flood, T. C. *J. Am. Chem. Soc.* **1990**, *112*, 704.

2.A.3. Hydrogen/Deuterium Exchange Reactions.

Having in mind the importance of H/D exchange reactions,⁵⁴ we have studied the isotopic labeling of the phosphine ligand backbone of compounds **1**. Heating halides and pseudohalides complexes **1-X** in a 1:1 mixture of CH₂Cl₂:CD₃OD at 45 °C in a Young's ampoule for around 24 h, resulted in clean incorporation of deuterium into all sp³-hybridized C-H bonds of the phosphine xylyl substituents only for **1-Cl** (Figure 12) and **1-Br**. Neither **1-I** or **1-SCN** participated in such an exchange, perhaps due to the less polar, more covalent character of the Ir-I and Ir-S bonds in the two complexes. Similarly, alkyl compounds **1-Me** and **1-CH₂SiMe₃** were unable to promote H/D exchange, whereas, interestingly, hydride **1-H** experienced facile D incorporation exclusively at the Ir-H and Ir-CH₂ sites. In the latter case, a CD₃OD concentration of only 10% in the CH₂Cl₂:CD₃OD solvent mixture was needed to promote the scrambling at temperatures as low as 20 °C.

⁵⁴ (a) Rybtchinski, B. Cohen, R. Ben-David, Y. Martin, J. M. L. Milstein, D. *J. Am. Chem. Soc.* **2003**, *125*, 11041. (b) Corberán, R. Sanaú, M Peris, E. *J. Am. Chem. Soc.* **2006**, *128*, 3974. (c) Kloek, S. M. Heinekey, D. M. Goldberg, K. I. *Angew. Chem. Int. Ed.* **2007**, *46*, 4736. (d) Bercaw, J. E. Hazari, N. Labinger, J. A. *Organometallics* **2009**, *28*, 5489. (e) Feng, Y. Lail, M. Barakat, K. A. Cundari, T. R. Gunnoe, B. Petersen, J. L. *J. Am. Chem. Soc.* **2005**, *127*, 14174. (f) Santos, L. L. Mereiter, K. Paneque, M. Slugovc, C. Carmona, E. *New J. Chem.* **2003**, *27*, 107.

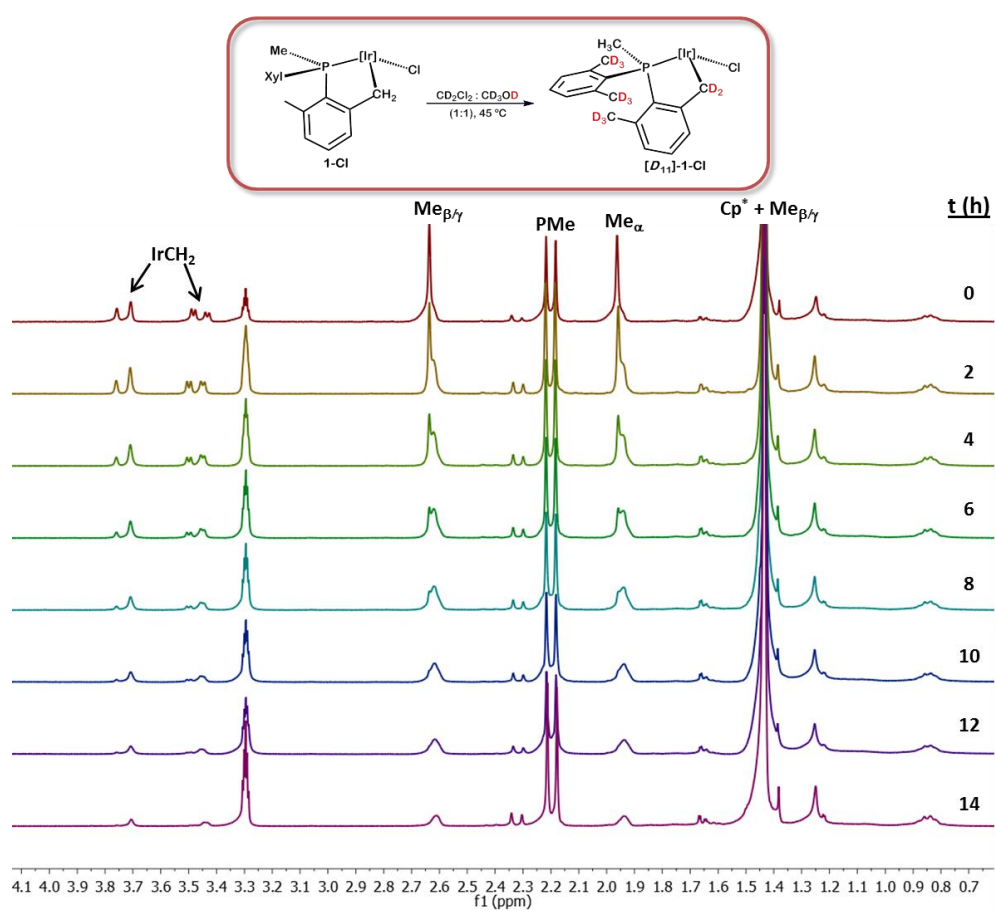
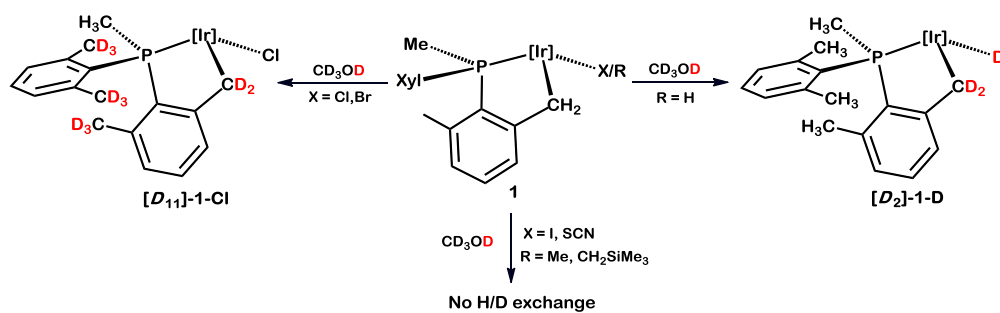


Figure 12. ^1H NMR monitoring of the H/D exchange reaction of **1-Cl** with $\text{CD}_2\text{Cl}_2/\text{CD}_3\text{OD}$ (1:1) at 45°C



Scheme 19. H/D exchange reactions with compounds **1**.

Deuteration of Iridium Halides (1-X)

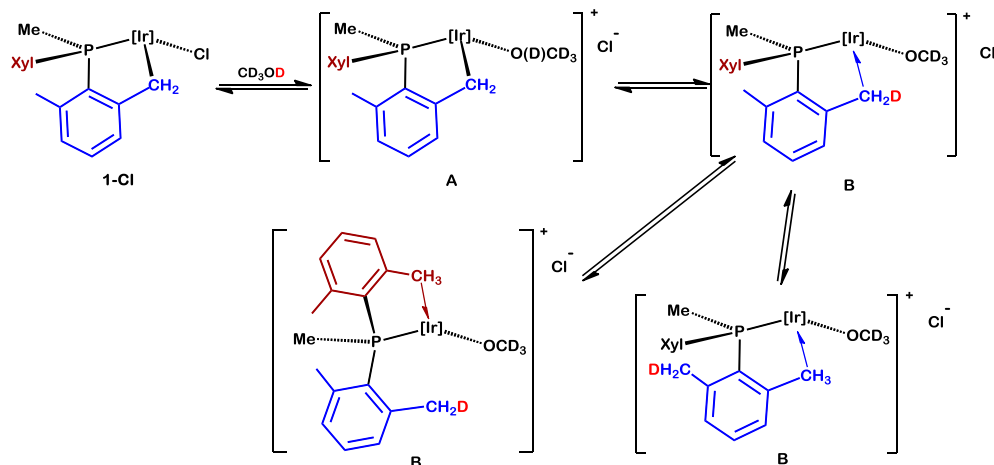
Deuterium incorporation into the methylene and methyl positions of the metalated ligand of **1-Cl** and **1-Br** occurred using CD₃OD as the deuterium source. Due to the poor solubility of iridium halides in this solvent, C₆H₆/CD₃OD, or preferably CH₂Cl₂/CD₃OD, solvent mixtures were employed in practice. Monitoring of the reaction by ¹H NMR spectroscopy evinced that incorporation of deuterium into the CH₂ and CH₃ sites of **1** occurred with the same rate and was characterized by a half-life, $t_{1/2}$ = 490 min (45 °C, CD₃OD/CD₂Cl₂ 1:1). A competition experiment between **1-Cl** and **1-Br** was carried out and resulted in essentially the same rate of deuteration for both complexes. In order to clarify the mechanism of this H/D exchange reaction, a series of parallel experiments was undertaken using **1-Cl** as the model compound (Table 2).

Table 2. H/D exchange reactions of **1-Cl**.^a

Entry	<i>p</i> -TsOH ^b (equiv / mM)	LiCl	$t_{1/2}$ (min) ^c
1	-	-	490
2	-	Sat. ^d	> 3 days
3	0.05 / 1	-	420
4	0.5 / 12	-	270
5	1.0 / 22	-	150
6	2.0 / 44	-	120
7	5.2 / 110	-	40
8	2.0 / 44	Sat. ^d	2100

^aConditions: **1-Cl** (0.013 mmol), solvent mixture CD₂Cl₂/CD₃OD (1:1, 05 mL), 45 °C; ^b*p*-TsOH = *p*-Toluenesulfonic acid; ^cMonitored by ¹H NMR; ^dThe solvent mixture was previously saturated with LiCl (*ca.* 2M).

The deuteration of **1-Cl** slowed down by a factor of ten when the $\text{CD}_2\text{Cl}_2/\text{CD}_3\text{OD}$ solvent mixture was saturated with LiCl (entries 2 and 8). Following related studies by Bergman and Tilley,^{17d} these results may indicate that chloride dissociation and formation of a cationic species **A** (Scheme 20), is likely involved in the H/D exchange. Subsequent incorporation of deuterium onto all benzylic positions of **1-Cl** (or **1-Br**) requires, in all probability, cleavage of the $\text{Ir}-\text{CH}_2$ bond to the cyclometalated carbon. Hence, **A** may undergo deuteration of this bond giving an agostic structure such as **B** in Scheme 20, which would afterwards experience C-H (or C-D) activation at all benzylic sites, by means of P-C bond rotation and exchange of the roles of the two xylyl rings. Failure of **1-SCN** to undergo stereoisomer and H/D exchanges may be due to the lower polarity of the $\text{Ir}-\text{S}$ bond in comparison with the $\text{Ir}-\text{Cl}$ bond, that would render less accessible for **1-SCN** an intermediate alike **A** in Scheme 20.



Scheme 20. Proposed mechanism for H/D exchange in **1-Cl** and **1-Br**.

As shown in Table 2 (entry 5), the deuteration rate is only moderately accelerated by the addition of *p*-toluensulfonic acid ($\text{pK}_a = -2.8$). An increase in the concentration of MeOH results also in faster deuteration (Table 3) and the use of the more polar $\text{CF}_3\text{CD}_2\text{OD}$ considerably speeds up the exchange. All these observations are in accordance with the participation of cationic intermediate species (**A** in Scheme 20) in the H/D exchange reaction.

Table 3. Effect of the deuterium source and its concentration on H/D exchange reactions of **1-Cl**.

Entry	ROD	% ROD	$t_{1/2}$ (min) ^b
1	CD_3OD	25	900
2	CD_3OD	40	560
3	CD_3OD	50	490
4	CD_3OD	60	240
5	CD_3OD	75	180
6	$\text{CF}_3\text{CD}_2\text{OD}$	25	110
7	$\text{CF}_3\text{CD}_2\text{OD}$	50	40

^aConditions: **1-Cl** (0.013 mmol), 45 °C, $\text{CD}_2\text{Cl}_2/\text{ROD}$;
^bMonitored by ^1H NMR

Specific conductivity measurements for **1-Cl**, **1-Me** and **1-H** in different solvents (Table 4) point into the same direction. For comparative purposes, the cationic complex **1-NCMe**⁺ was also investigated. The latter compound undergoes H/D exchange at 45 °C in a 1:1 mixture of CD_2Cl_2 and CD_3OD , with a half-life of only 30 min, clearly demonstrating the key participation of cationic species alike **A** (Scheme 20) in the hydrogen/deuterium exchange reaction.

Table 4. Specific conductivity of solutions of compounds **1** in different solvents.

Compound	Specific Conductivity, L ($\mu\Omega^{-1}$) ^a			
	MeCN	MeOH	CH ₂ Cl ₂	CH ₂ Cl ₂ /MeOH (1:1)
Blank	0.6	0.5	0.08	0.6
1-Cl	3.5	7.5	0.1	3.5
1-Me	0.9	0.9	0.1	0.9
1-H	1.7	22.1 ^b	0.1	15.4 ^b
1-NCMe⁺	85.1	55.2	50.0	52.0

^aConditions: compounds **1** (0.01 M); ^bDecomposition occurs.

Recent work from Goldberg, Brookhart and their co-workers has revealed that an Ir(I)–CH₃ complex stabilized by the pincer ligand PONOP, experiences facile deuterium incorporation in the methyl group in the presence of the acidic deuterated solvents CD₃OD and D₂O.⁵⁵ For this proton-assisted C–D/H activation a mechanism implying generation of an Ir(III) methyl hydride (or deuteride) intermediate, that features reductive coupling and oxidative cleavage reactivity was proposed, with participation of an Ir(I) σ -methane complex intermediate.⁵⁵ In contrast with these observations the Ir(III) compound **1-Me** did not participate in H/D exchanges under the conditions given above for **1-X**, and was recovered unaltered after being heated in CH₂Cl₂:CD₃OD (1:1) at 60 °C for 24 h. The related alkyl complex **1-CH₂SiMe₃** behaves similarly. Thus it seems that methanol is unable to protonate **1-Me** (and **1-CH₂SiMe₃**) to generate a cationic Ir(V) methyl hydride intermediate that could promote H/D scrambling in this compound.

⁵⁵ Bernskoetter, W. H.; Hanson, S. K.; Buzak, S. K.; Davis, Z.; White, P. S.; Swartz, R.; Goldberg, K. I.; Brookhart, M. *J. Am. Chem. Soc.* **2009**, *131*, 8603.

Deuteration Studies of Iridium Hydride (1-H)

As it will be discussed shortly, at variance with **1-Me** and **1-CH₂SiMe₃**, hydride complex **1-H** undergoes deuteration in CD₃OD, albeit exclusively at the Ir–H and Ir–CH₂ sites. However, room temperature EXSY NMR studies gave no indication of this proton exchange.

To gain additional information, the isotopologues **1-D** and [**D**₁₁]-**1-H** were prepared, the former from **1-Cl** and LiAlD₄ (or NaOCD₃/CD₃OD) and the latter from [**D**₁₁]-**1-Cl** and LiAlH₄ (**1-D** features ν (Ir–D) at 1470 cm^{–1}; see Experimental Section for other data for these species). No H/D exchange took place between the Ir–D and Ir–CH₂ positions up to 60 °C, but upon heating above 90 °C the H/D exchange became detectable. Similarly, heating a C₆D₆ solution of [**D**₁₁]-**1-H** at 90 °C resulted in partial incorporation of D into the Ir–H site (no D incorporation from C₆D₆ into **1-H** under similar conditions). However, partial decomposition of **1-H** occurred and therefore this process was not investigated any further.

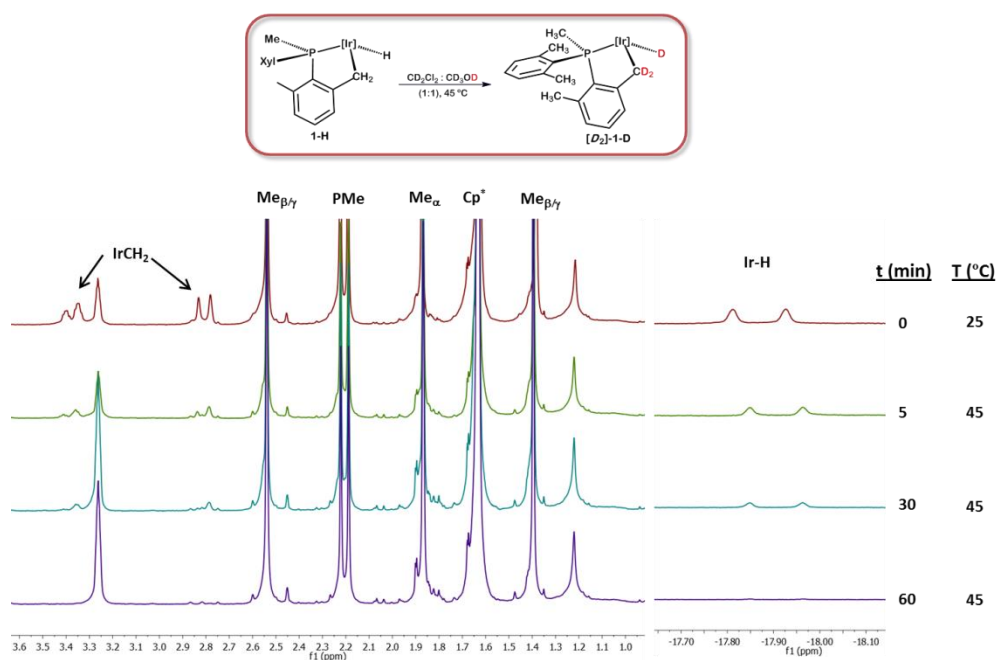


Figure 13. ^1H NMR monitoring of the H/D exchange reaction of **1-H** with $\text{CD}_2\text{Cl}_2/\text{CD}_3\text{OD}$ (1:1) at 45 °C

At room temperature, **1-H** underwent a CD_3OD induced relatively fast H/D exchange (Figure 13 and Table 5; 10% CD_3OD in $\text{CD}_2\text{Cl}_2/\text{CD}_3\text{OD}$ mixtures; $t_{1/2} \sim 130$ min), which became considerably faster in the presence of catalytic concentrations of *p*-toluenesulfonic acid ($t_{1/2} < 3$ min; *ca.* 4 mol%, Table 5, entry 7). In contrast, addition of a base (entries 3 and 4) inhibited the exchange. In the absence of acid, deuteration of the phosphine benzylic positions did not take place, but a sufficiently large concentration of HAcO or HTsO , particularly of the latter (entry 10), yielded **[D₁₁]-1-D**. Use of the more acidic alcohol $\text{CF}_3\text{CD}_2\text{OD}$ resulted in a significant acceleration of the exchange too (entries 11 and 12).

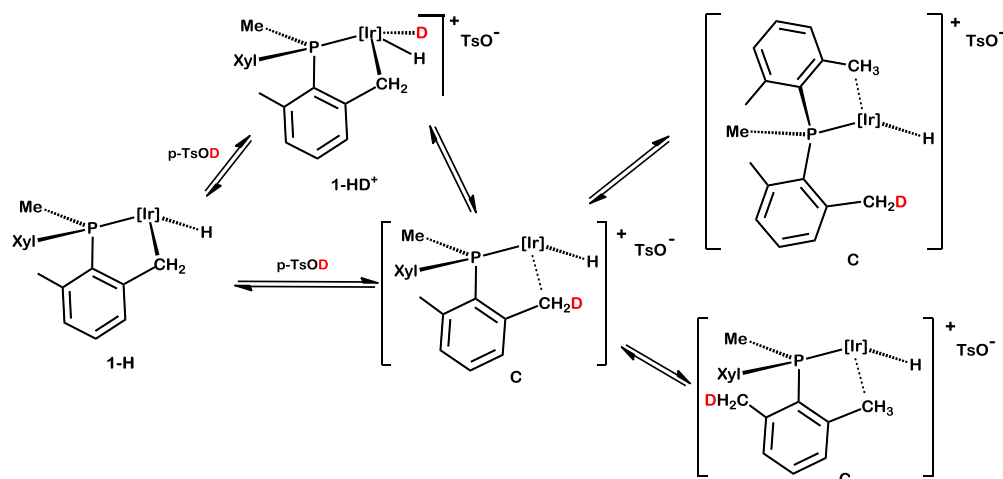
Table 5. H/D exchange reactions of **1-H**.^a

Entry	ROD (%) ^b	Acid ^b (equiv / mM)	Base (M)	<i>t</i> _{1/2} (min) ^c	
				Ir-CH ₂ ; Ir-H	CH ₃ (Xyl)
1	CD ₃ OD (50)	-	-	< 3	-
2	CD ₃ OD (10)	-	-	130	-
3	CD ₃ OD (10)	-	NaOH (0.01)	-	-
4	CD ₃ OD (10)	-	MeONa (0.04)	5 days	-
5	CD ₃ OD (10)	A (0.5 / 12)	-	< 3	1day (7%)
6	CD ₃ OD (10)	A (10 / 250)	-	< 3	1day (15%)
7	CD ₃ OD (10)	B (0.04 / 1)	-	< 3	2.5 days ^d
8	CD ₃ OD (10)	B (0.06 / 1.5)	-	< 3	650
9	CD ₃ OD (10)	B (0.08 / 2)	-	< 3	150
10	CD ₃ OD (10)	B (0.2 / 5)	-	< 3	< 3
11	CF ₃ CD ₂ OD (50)	-	-	< 3	10
12	CF ₃ CD ₂ OD (10)	-	-	< 3	700 ^d

^aConditions: **1-H** (0.013 mmol), solvent mixture CD₂Cl₂/ROD (1:1 or 10:1, 0.5 mL), 25 °C;^bTwo acids were used: A = Acetic acid; B = *p*-Toluenesulfonic acid; ^cMonitored by ¹H NMR; ^dPartial decomposition occurred.

Leaving aside for the time the H/D exchange at the Ir-*H* and Ir-CH₂ sites, incorporation of D at the benzylic positions of the metalated ligand backbone requires (as for **1-Cl**, see Scheme 20) generation of an agostic structure alike **C** in Scheme 21. This species may form by direct protonation of the Ir-CH₂ bond, or through a cationic bis(hydride)intermediate (**1-HD**⁺ in Scheme 21), by intramolecular H⁺ (or D⁺) transfer to the Ir-CH₂ bond. The reversibility of the latter process, that may alternatively be viewed as a classical reductive elimination step, and the already discussed facile exchange of the methyl groups of the phosphine xyllyl substituents, would account for the ready incorporation of D at all sp³-hybridized sites. It is worth noting in this regard

that: (i) the Rh analog of **C** has been described recently by our group; (ii) a related, osmium-based exchange, has also been reported.⁵⁶

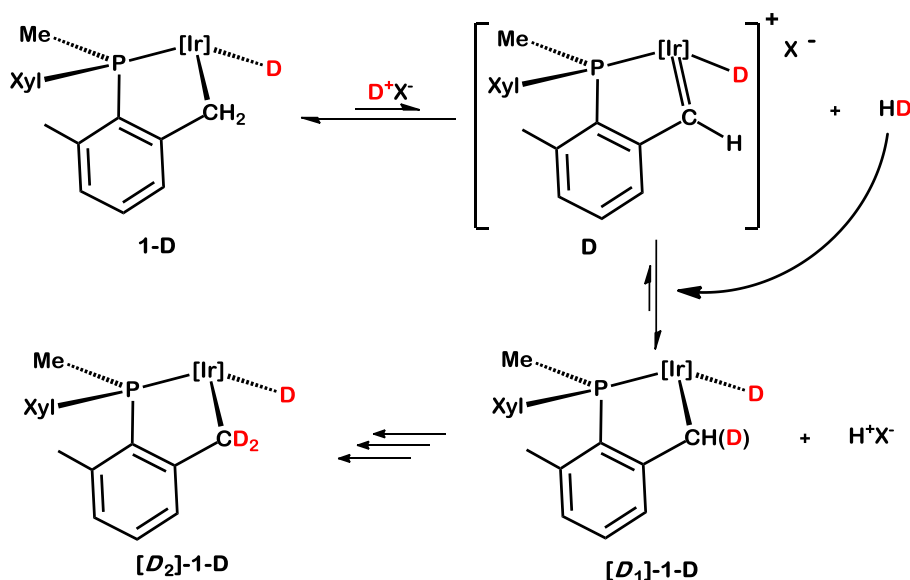


Scheme 21. Proposed mechanism for the CD₃OD deuteration of all benzylic positions of **1-H** catalyzed by *p*-TsOH.

Regarding the more limited, albeit more interesting H/D exchange that implicates only the Ir-H and Ir-CH₂ sites, an alternative route that does not involve cleavage of the Ir-CH₂ bond must be in operation. Ir-H/Ir-D exchange could occur by reversible deuteration (CD₃OD or catalytic DTsO) of **1-H** to yield **1-HD**⁺, as already shown in Scheme 21. But as discussed in a following section, D⁺ can also abstract a H⁺ atom from Ir-CH₂ linkage, to form a cationic iridium alkylidene structure (**D** in Scheme 22), which could either revert to **1-H** releasing H⁺ and incorporating D at a Ir-CH₂ site, or undergo a dihydrogen-induced (HD in Scheme 22) migratory insertion of the

⁵⁶ Baya, M.; Eguillor, B.; Esteruelas, M. A.; Lledós, A.; Oliván, M.; Oñate, E. *Organometallics*, **2007**, 26, 5140.

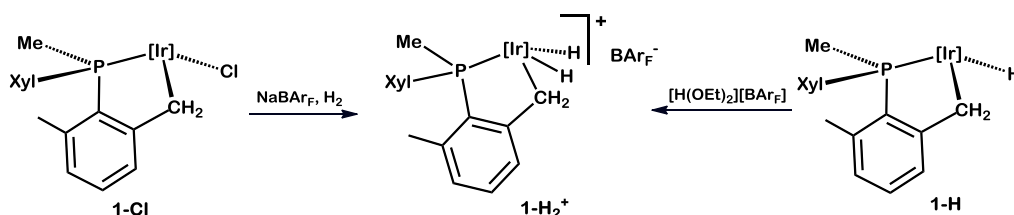
carbene unit into the Ir–D bond, to give the cationic bis(hydride) **1-H₂⁺** (not shown in Scheme 22), which by H⁺ dissociation would render **1-H** with further deuterium incorporation.



Scheme 22. Selective, acid-promoted catalytic deuteration of **1-H** at the hydride and methylene sites.

A key species for the above H/D exchange process is the cationic bis(hydride) Ir(V) complex **1-H₂⁺**. We found that treatment of **1-Cl** with H₂ (1 bar) in the presence of NaBAr_F clearly generated the desired complex (Scheme 23). Moreover, protonation of **1-H** with [H(OEt₂)₂][BAr_F] yielded also **1-H₂⁺**, which reversibly loses H₂ with formation of the cationic compound **1⁺**, whose structure and reactivity will be discussed later. A classical dihydride structure is proposed for **1-H₂⁺** in agreement with the observation at -80 °C of two deshielded ¹H NMR resonances (500 MHz;

CD_2Cl_2) with δ -12.79 (s, 1 H) and -13.37 ppm (d, $^2J_{\text{HP}} = 17.5$ Hz, 1 H), and a spin-lattice relaxation time, $T_1 = 261$ ms (average value for the two hydride resonances at the above temperature). In addition, cation $\mathbf{1-H}_2^+$ features two doublets at 3.93 and 3.38 ppm ($^2J_{\text{HH}} = 14.2$ Hz) each with a relative intensity corresponding to one hydrogen atom, attributable to the diastereotopic Ir- CH_2 protons.



Scheme 23. Synthesis of cationic dihydride compound $\mathbf{1-H}_2^+$.

Compound $\mathbf{1-H}_2^+$ exhibits an interesting dynamic behavior in solution, which is directly related to the H/D exchange reactions discussed for compound $\mathbf{1-H}$ (Figure 14). Upon warming to -60 °C, the two Ir-H and the two Ir- CH_2 resonances broaden and coalesce at -50 °C and -30 °C, respectively. Further broadening of the hydride and methylene resonances is seen upon heating, as a consequence of dynamic exchange of the corresponding protons, with coalescence being reached at *ca.* 0 °C. Lineshape analysis of the corresponding resonances at various temperatures in conjunction with Eyring analysis of the observed rate constants, yield the following activation parameters for the overall process: $\Delta H^\ddagger = 12.6 \pm 0.4$ kcal $\cdot\text{mol}^{-1}$, $\Delta S^\ddagger = 6 \pm 2$ cal $\cdot\text{mol}^{-1}\cdot\text{K}^{-1}$ and $\Delta G^\ddagger_{300\text{K}} = 11 \pm 2$ kcal $\cdot\text{mol}^{-1}$. Upon warming at 25 °C a broad signal due to 4 H appeared at -4.63 ppm. This ^1H

NMR exchange between Ir–H and Ir–CH₂ is consistent with the H/D exchange reaction between **1-H** and CD₃OD described earlier. Moreover, no broadening of the methyl groups of the xylyl rings was observed by ¹H NMR even at 45 °C, which is also in accordance with the discussed H/D exchange reactions of **1-H**.

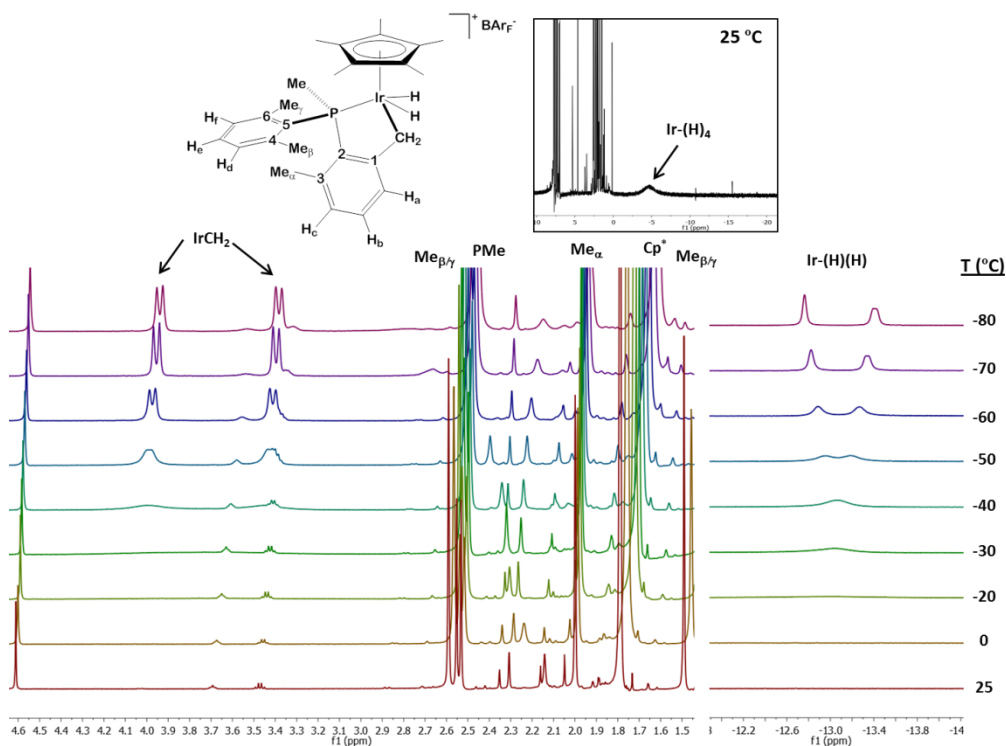
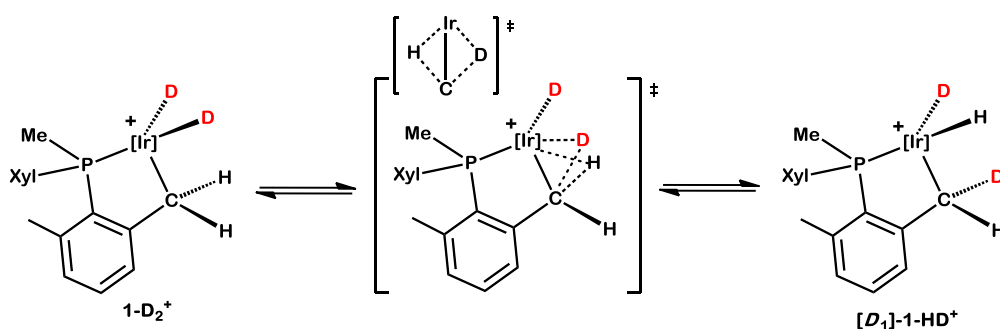


Figure 14. Solution dynamic behavior of **1-H₂⁺** analyzed by ¹H NMR.

Considering the accessibility of **1-H₂⁺** and recent work from Jones and co-workers⁵⁷ regarding C–H and C–C bond activation reactions of nitriles

⁵⁷ Tanabe, T.; Evans, M. E.; Brennessel, W. W.; Jones, W. D. *Organometallics* **2011**, *30*, 834.

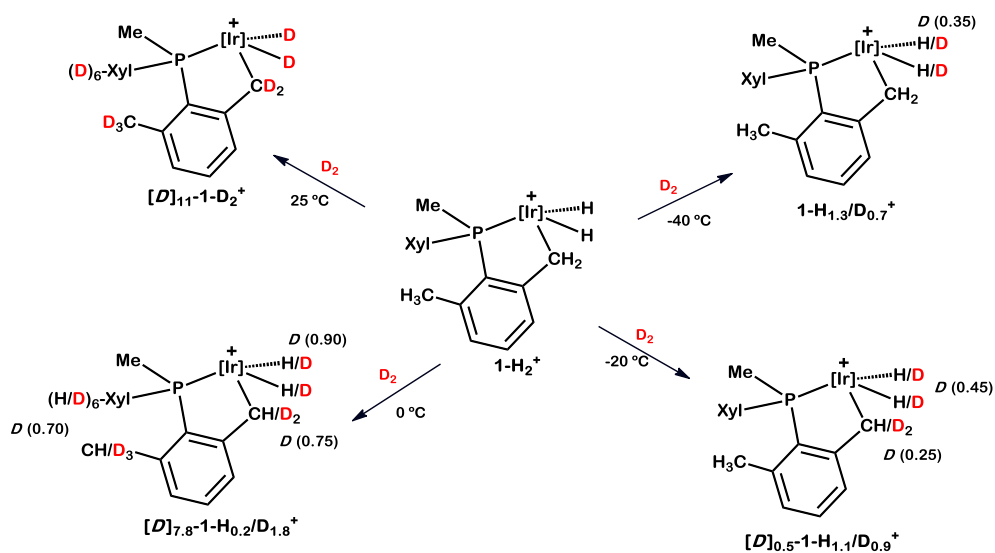
induced by $[\text{Tp}'\text{Rh}(\text{PR}_3)]$ compounds, which propose that hydride and cyano groups may exchange their positions between Rh and a rhodium-bound carbon atom *via* a concerted transition state, an alternative, albeit quite speculative, proposal for the observed H/D exchange in **1-H** might imply the concerted transition state represented in Scheme 24. Theoretical calculations are in progress to ascertain the viability of this concerted state.



Scheme 24. Proposed mechanism for H/D exchange between Ir-H and Ir-CH₂ sites in **1-H₂⁺**.

To complete these studies, the deuteration of **1-H₂⁺**, generated from **1-Cl** and H₂, using D₂ as the deuterium source, was also analyzed (Scheme 25). Interestingly, the positions to be deuterated were highly dependent on the temperature of the H/D exchange reaction. Thus four parallel experiments were undertaken at different temperatures, namely -40, -20, 0 and 25 °C. In all cases, a CD₂Cl₂ solution of **1-H₂⁺** was stirred at the chosen temperature under D₂ (0.5 bar). Whereas no deuteration occurred at -60 °C after stirring for 2 hours, at -40 °C the H/D exchange was effective at the hydride position and deuteration of the methylene site was barely detected. Upon warming to -20 °C deuteration of the Ir-CH₂ also occurred, but deuteration of the methyl

positions was only achieved at 0 °C. Quantitative deuteration of all positions was rapidly accomplished at 25 °C.



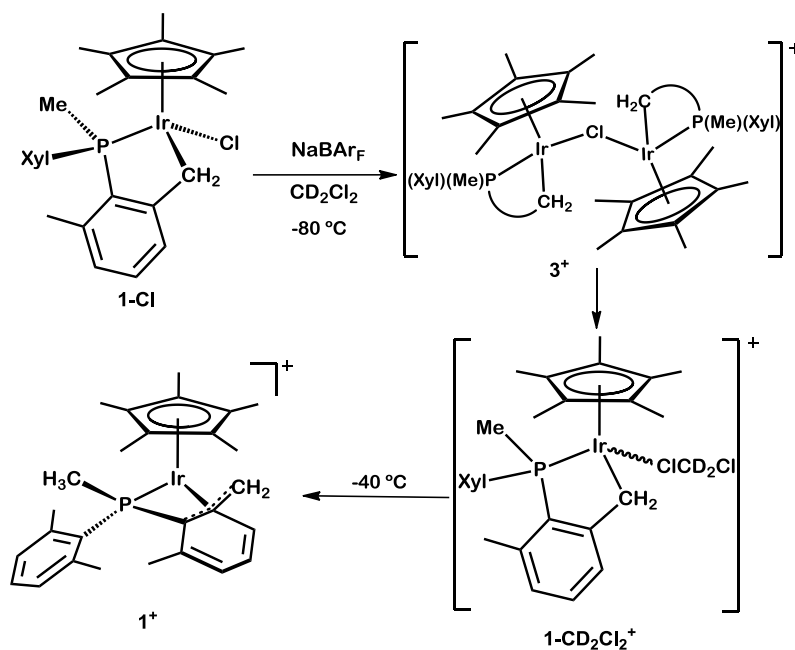
Scheme 25. H/D exchange reactions of **1-H₂⁺** with D₂ at variable temperature. Reaction time: 45 min.

2.A.4. Cationic Ir(III) Complexes Generated by Chloride Abstraction from **1-Cl**.

*Synthesis, Characterization and Reactivity of κ^4 -P,C,C',C'' Compound **1**⁺*

Similarly to the rhodium analogue (Chapter 1), reaction of the neutral compound **1-Cl** with 1 equiv of NaBAr_F in CH₂Cl₂ as the solvent, led to complex **1**⁺ isolated as BAr_F salt (see Scheme 26). Since these results have been published recently in a full paper⁵⁸ only a brief summary will be given here. Details of the chemistry and spectroscopy described in this and the following sections can be found in reference [58] and the corresponding Supporting Information.

⁵⁸ Campos J.; López-Serrano, J.; Álvarez, E.; Carmona, E. *J. Am. Chem. Soc.* **2012**, *134*, 7165.



Scheme 26. Chloride abstraction from **1-Cl** by NaBARF leading to **1⁺** isolated as **1-BArF**.

As represented in Scheme 26, at $-80\text{ }^\circ\text{C}$ two cationic intermediates, **3⁺** and **1-CD₂Cl₂⁺** were detected, that converted cleanly into **1⁺** (Figure 15). Stabilization of the iridium center of the latter species by $\kappa^4\text{-P,C,C',C''}$ coordination of the metalated xylyl-phosphine is probably responsible for its failure to activate C–H bonds (C_6H_6 , THF, Et_2O , etc.).

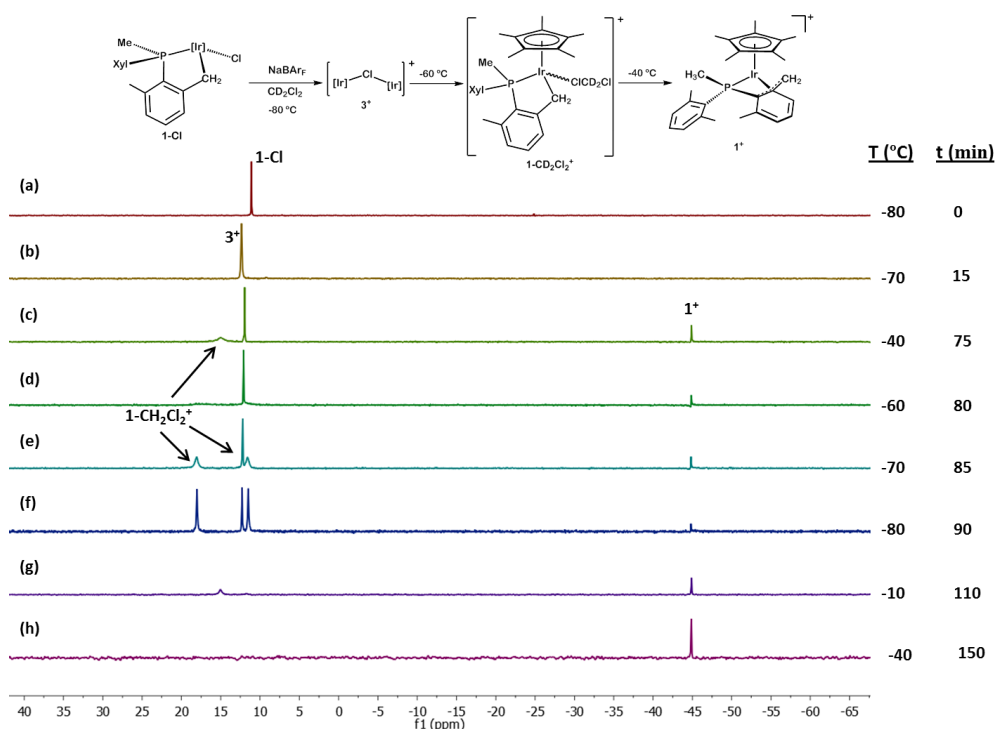


Figure 15. Low-temperature $^{31}\text{P}\{^1\text{H}\}$ NMR (CD_2Cl_2 , 500 MHz) monitoring of the reaction of **1-Cl** with NaBARF . (a) $^{31}\text{P}\{^1\text{H}\}$ NMR of **1-Cl** at -80°C prior to addition of NaBARF ; (b-c) Formation of **3⁺** and evolution to give **1-CH₂Cl₂⁺** and **1⁺**; (d-f) Cooling down below -70°C causes splitting of the broad signal at -15.2 ppm (**1-CH₂Cl₂⁺**) into two peaks (11.2 and 18.1 ppm); (g) Total consumption of **3⁺** at -10°C ; (h) $^{31}\text{P}\{^1\text{H}\}$ NMR showing quantitative conversion to **1⁺** after 15 min at 25°C , then cooled down to -40°C to observe the broad signal at -44.9 ppm.

Inspection of Figure 16 reveals clearly the solution fluxional nature of **1⁺**, which was demonstrated by EXSY and other NMR experiments (Figure 17) and supported by theoretical calculations (Figure 18), to be due to an exchange of the roles of the two aryl groups. Key species for this exchange are a cationic, weakly agostic complex **F** (Scheme 27) and a doubly metalated Ir(V) hydride, **G**, which has energy only $7.2\text{ kcal}\cdot\text{mol}^{-1}$ above **1⁺** (Figure 18).

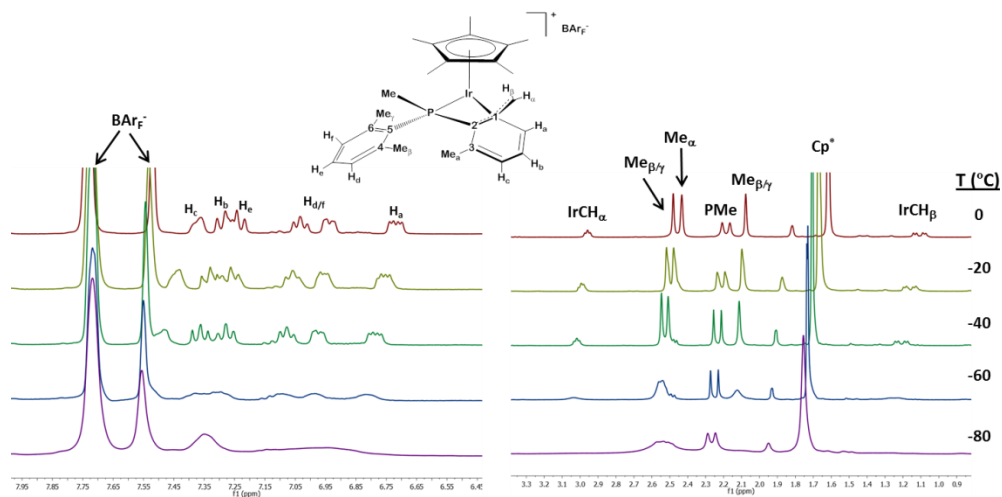


Figure 16. Variable temperature ^1H NMR (300 MHz, CD_2Cl_2) of **1-BArF**.

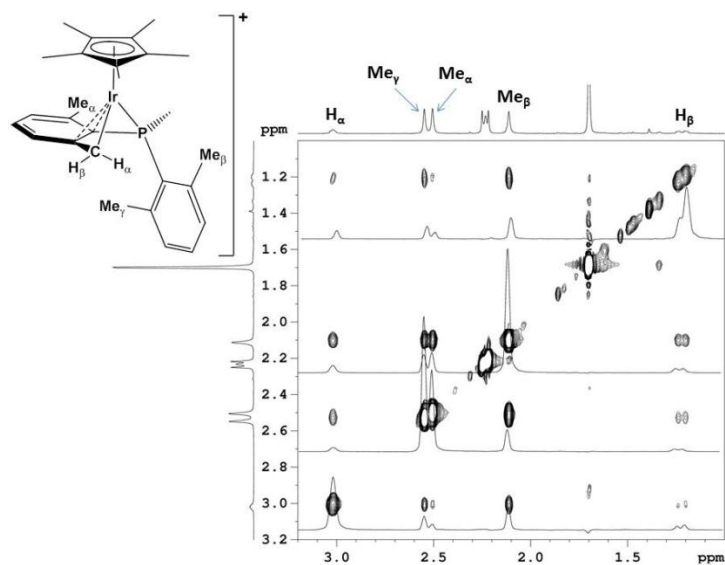
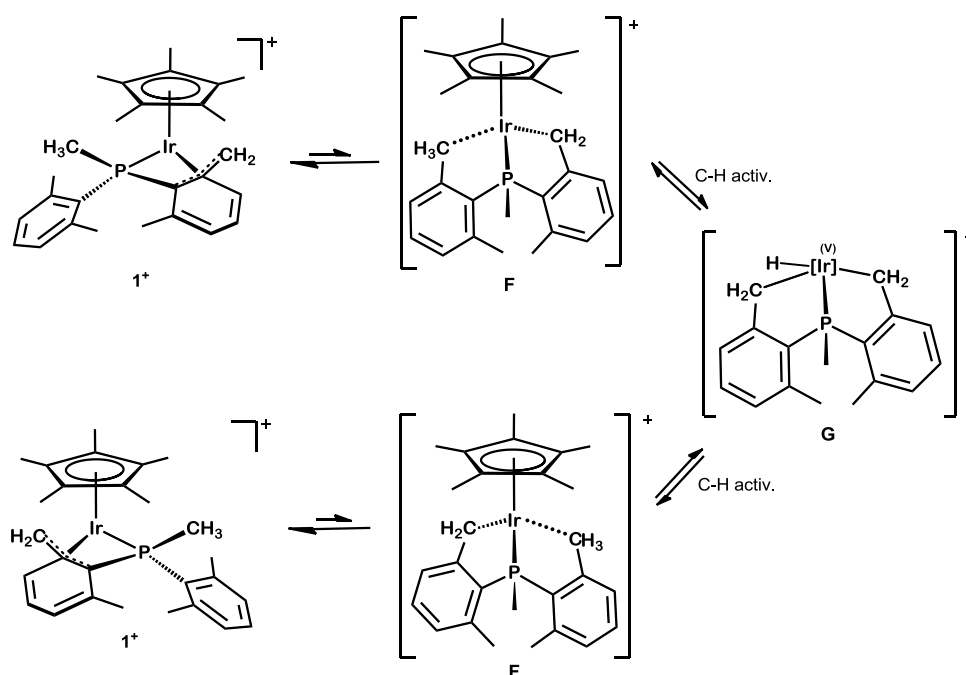


Figure 17. 2D EXSY experiment ($T = 248\text{ K}$, mixing time = 50 ms) showing exchange of all methyl and methylene protons of the phosphine ligand of **1** $^+$. The horizontal traces represent rows extracted from the 2D spectrum.



Scheme 27. Proposed mechanism to account for the solution dynamic behavior of 1^+ .

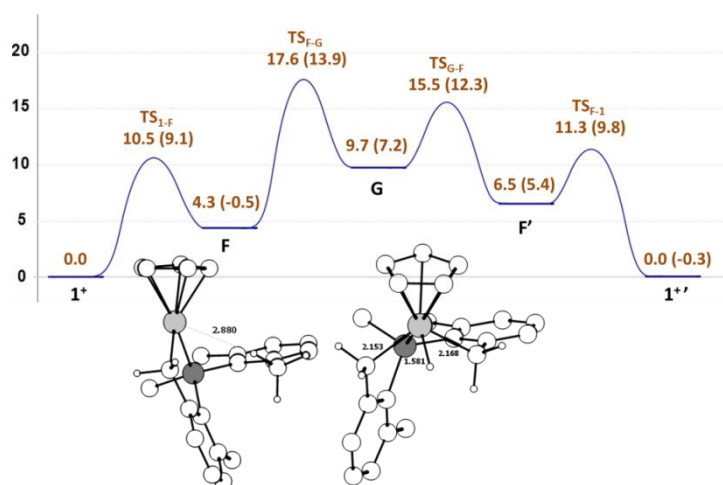
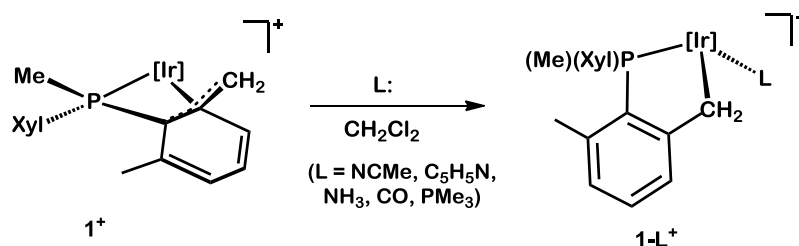


Figure 18. Gas phase Potential Energy profile (in kcal·mol⁻¹) for the degenerate exchange of the roles of the metalated and non-metalated xylyl rings in 1^+ (Free Energy data are also shown in parenthesis). The insets show the optimized geometry for the κ^2 -P,C intermediate **F** (left) and the Ir(V)-hydride **G** (right). Most hydrogen atoms and the methyl fragments of the Cp* ligands have been omitted for clarity.

As expected from the above, compound **1-BAr_F** reacted cleanly with different Lewis bases (L), to form corresponding adducts **[1-L]BAr_F** (Scheme 28). Their characterization by spectroscopy is straightforward.⁵⁸ In addition, the solid-state structures of the BAr_F⁻ salts of **1-NCMe⁺** and **1-PMe₃⁺** were determined by X-ray crystallography (Figure 19).



Scheme 28. Synthesis of cationic adducts **1-L⁺** from reaction of **1⁺** with Lewis bases (L).

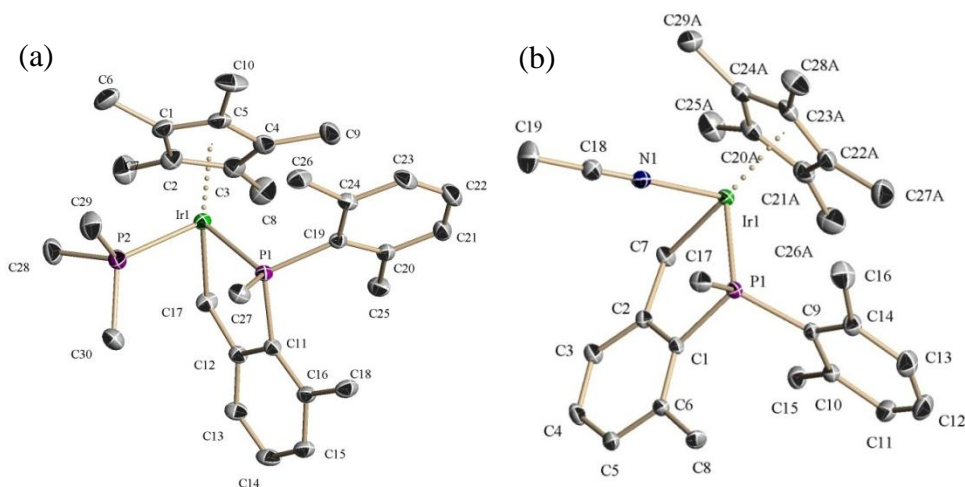
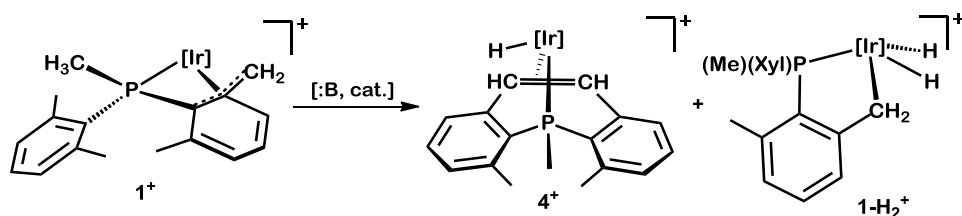


Figure 19. ORTEP diagrams for compounds (a) **1-PMe₃⁺**, and (b) **1-NCMe⁺**. Thermal ellipsoids are drawn at the 50 % probability. Hydrogen atoms and BAr_F⁻ anion have been omitted for clarity.

2.A.5. Base-catalyzed Intramolecular Dehydrogenative C–C Coupling in 1^+ Leading to the Hydride Phosphepine Cation 4^+ .

Although compound **1-BAr_F** is stable in solution and in the solid state for long periods of time, in the course of some of its preparations, and also during unsuccessful attempts to grow single crystals (which required several manipulations, use of different solvents, etc.), small amounts of a new hydride complex that featured ^1H and $^{31}\text{P}\{^1\text{H}\}$ NMR resonances at δ -13.03 (d, $^2J_{\text{HP}} = 25.5$ Hz) and 8.9 ppm, respectively, were observed. Small quantities of bis(hydride) **1-H₂⁺** were detected too. It was soon realized that generation of these complexes was due to the presence of adventitious water that performed a Brönsted-Lowry base catalytic role (Scheme 29). Trace amounts of water acting as an acid catalyst have been reported recently by the groups of Milstein and Brookhart to facilitate the hydrogenation step of reactions of H₂ with Ir complexes of pincer ligands.⁵⁹

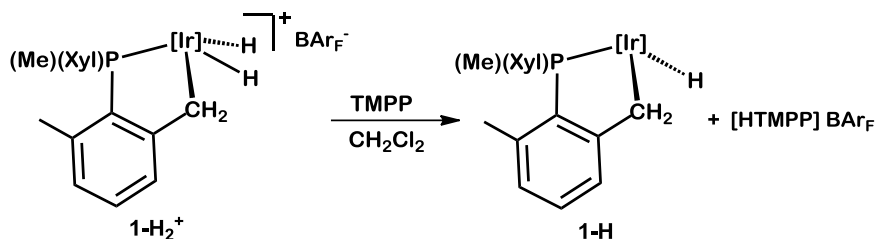


Scheme 29. Base-catalyzed dehydrogenative C–C coupling of 1^+ leading to the hydride phosphepine cation 4^+ .

⁵⁹ (a) Iron, M. A.; Ben-Ari, E.; Cohen, R.; Milstein, D. *Dalton Trans.* **2009**, 9433. (b) Findlater, M.; Bernskoetter, W. H.; Brookhart, M. *J. Am. Chem. Soc.* **2010**, 132, 4534.

Following the screening of different base reagents and solvents, optimal experimental conditions for the formation of the new hydride complex **4**⁺ were determined to involve the reaction of **1-Cl** with NaBAr_F in dichloromethane, in the presence of catalytic amounts of a saturated aqueous solution of NaHCO₃ (*ca.* 30 mol %, 20 °C, 16 h). A buffer solution of piperidinium/piperidine can also be used. The already discussed cationic bis(hydride) complex **1-H₂**⁺ was observed as a side product of this rearrangement. In fact, when the above reaction was effected in a sealed NMR tube, a 1:1 mixture of **4**⁺ and **1-H₂**⁺ was cleanly generated (Scheme 29). In order to isolate **4-BAr_F** in high yields (*ca.* 90 %, see Experimental Section) the above catalyzed reaction was performed for a period of about 16 h, with intermittent vacuum/argon cycles to remove the H₂ generated in the C–C coupling reaction. In accord with these observations and with others previously discussed, strong base catalysts like NaOH gave also rise to the neutral hydride **1-H** as a result of fast deprotonation of **1-H₂**⁺ by the base. The proposed Brönsted-Lowry acidity of the cationic Ir(V) bis(hydride) complex **1-H₂**⁺ finds ample literature precedent, not only for electrophilic transition metal hydrides but also for related dihydrogen complexes.⁶⁰ Indeed, treatment of **1-H₂**⁺ with NEt₃ or with 2,2,6,6-tetramethylpiperidine, TMPP, afforded the neutral hydride **1-H** (Scheme 30).

⁶⁰ See for example: (a) Crabtree, R. H. *Angew. Chem. Int. Ed.* **1993**, 32, 789. (b) Kubas, G. J. *Metal Dihydrogen and sigma-Bond Complexes*; Publishers, K. A., Ed.; New York, **2001**. (c) Kubas, G. J. *Chem. Rev.* **2007**, 107, 4152.



Scheme 30. Deprotonation of $\mathbf{1-H}_2^+$ by action of TMPP (TMPP = 2,2,6,6-tetramethylpiperidine).

Compound $\mathbf{4-BAr_F}$ was isolated as a crystalline solid with low reactivity toward oxygen and water. Its spectroscopic properties are in agreement with the proposed structure⁵⁸ which was unequivocally confirmed by X-ray studies (Figure 20). As discussed in the *Introduction*, hybrid phosphine-olefin ligands find ample use in homogeneous catalysis³⁵ and some of them have been generated in metal-induced processes similar to that presented herein.^{33,34} Clearly, a mechanistic understanding of the reaction pathway leading to cation $\mathbf{4}^+$ was desirable. Accordingly, some experimental and theoretical studies toward this aim were performed and are described in the following two sections.

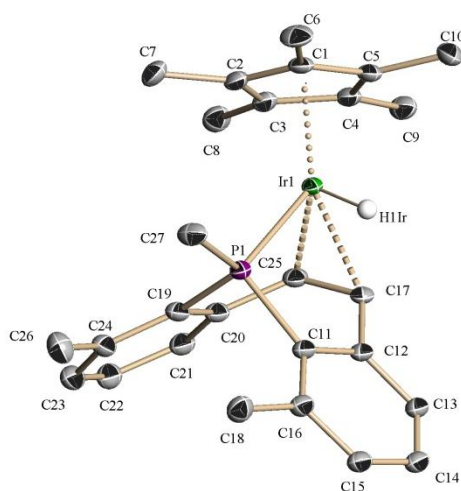
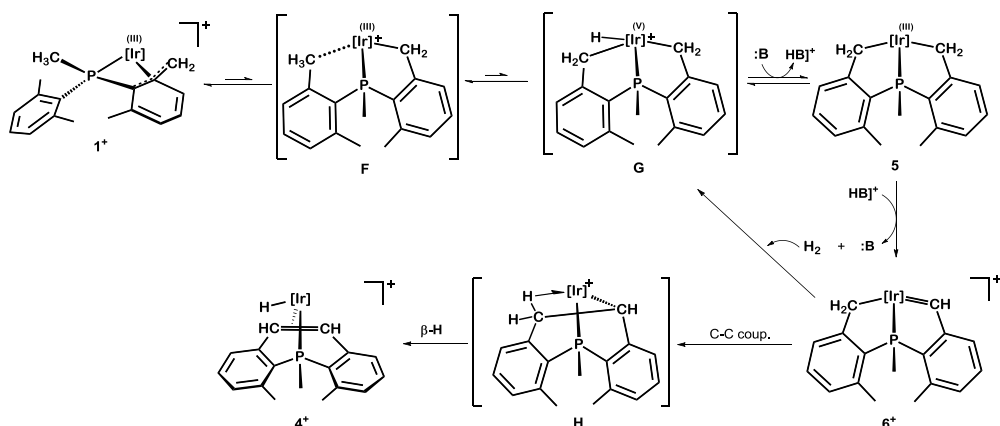


Figure 20. ORTEP diagrams for compound 4^+ . Thermal ellipsoids are drawn at the 50 % probability. Hydrogen atoms and BAR_F anion have been omitted for clarity.

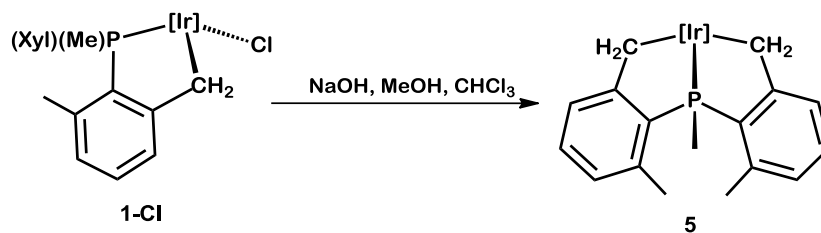
2.A.6. Mechanistic Investigations on the Formation of 4^+ .

The chemical and spectroscopic properties of 1^+ discussed in the preceding sections led us to formulate the mechanistic hypothesis presented in Scheme 31 for the formation of the hydride phosphepine cation 4^+ . Fundamental steps in this transformation are: (i) the base-promoted conversion of the cationic acidic Ir(V) hydride complex **G** (*vide supra*) into the neutral dimetalacycle **5**; (ii) hydride abstraction from an Ir–CH₂ unit by the conjugate acid of :B to yield alkylidene 6^+ . Once the latter is formed, well-known migratory insertion and β -H elimination steps would account for the generation of 4^+ (Scheme 31). The other reaction product, namely the cationic 1-H_2^+ , would result from the interaction of still unreacted **F** with the hydrogen liberated in the **5**-to- 6^+ reaction step.



Scheme 31. Proposed mechanism for the base-catalyzed dehydrogenative C–C bond coupling that leads to complex **4**⁺.

To gain experimental support, these key intermediates **5** and **6**⁺ were synthesized. As shown in Scheme 32 the former resulted from the reaction of **1-Cl** with NaOH in a 1:1 mixture of MeOH and CHCl₃. Once again, compound **5** was characterized by spectroscopy and by X-ray studies (Figure 21).



Scheme 32. Synthesis of doubly metalated compound **5**.

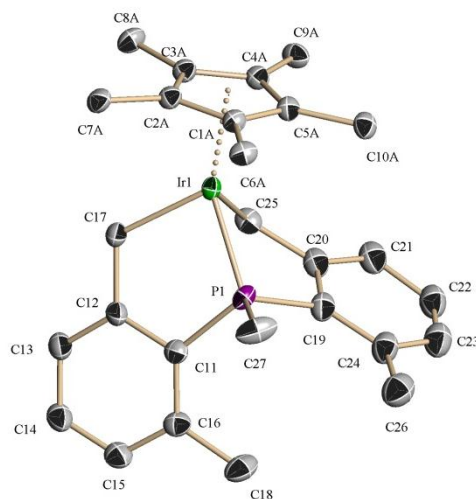
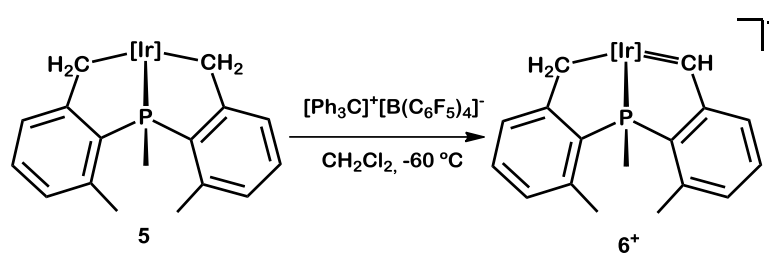


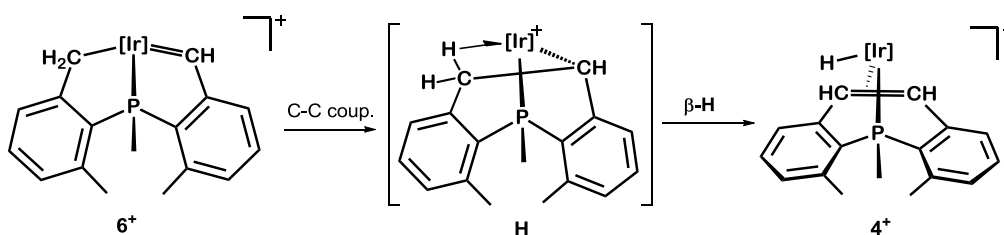
Figure 21. ORTEP diagrams for compound **5**. Thermal ellipsoids are drawn at the 50 % probability and hydrogen atoms have been omitted for clarity.

In turn, the cationic alkylidene **6**⁺ responsible for the C–C coupling reaction was successfully generated (Scheme 33) by the low-temperature (–60 °C) reaction of **5** and [Ph₃C][B(C₆F₅)₄] in CH₂Cl₂ solution. Hydride abstraction was instantaneous at this temperature and yielded an alkylidene unit characterized by NMR resonances with δ 15.91 ppm (¹H) and 258.3 ppm (¹³C{¹H}).



Scheme 33. Synthesis of alkylidene **6**⁺ by hydride abstraction from **5**.

As mentioned in the *Introduction*, species of this type are rarely isolable or even observable,⁴² in particular those of Ir(III). Indeed, upon warming to room temperature a freshly prepared solution of **6**⁺ in CD₂Cl₂ at -60 °C, the hydride phosphepine **4**⁺ was formed in essentially quantitative yield (by NMR) in less than an hour (Scheme 34). The rate of formation of **4**⁺ according to Scheme 34 was measured by ³¹P{¹H} NMR spectroscopy at 0 °C, using CD₂Cl₂ solutions of **6**⁺ generated *in situ* at -60 °C from **5** and [Ph₃C]⁺[PF₆]⁻. A first-order dependence on the concentration of **6**⁺ was disclosed (see Figure 42 in the Experimental Section), with a calculated rate constant of 2.2·10⁻⁴ s⁻¹ and an associated energy barrier, Δ*G*[‡] = 20.5 kcal mol⁻¹. The alkyl/alkylidene C–C coupling reaction that leads to **4**⁺ may be viewed as a model for the key step of several catalytic processes, including C1 polymerization of diazocompounds.⁶¹

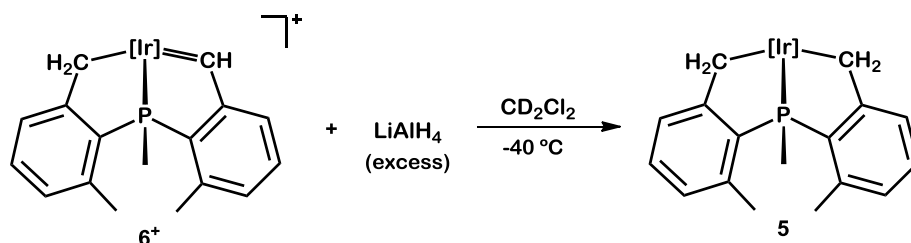


Scheme 34. C–C bond coupling from alkylidene **6**⁺.

The hydride abstraction reaction that converts compound **5** into the metalacyclic alkylidene **6**⁺ can actually be reversed. As depicted in Scheme

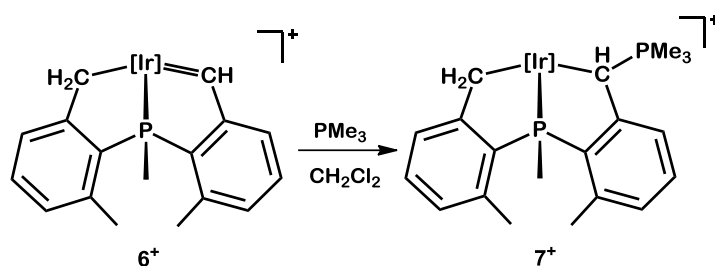
⁶¹ Jellema, E.; Jongerius, A. L.; Reek, J. N. H.; de Bruin, B. *Chem. Soc. Rev.* **2010**, *39*, 1706.

35, treatment of CD_2Cl_2 solutions of $\mathbf{6}^+$ with LiAlH_4 at $-40\text{ }^\circ\text{C}$ produced cleanly the neutral dimetalacycle $\mathbf{5}$.



Scheme 35. Hydride addition to alkylidene complex $\mathbf{6}^+$.

Additional support for the structure proposed for cation $\mathbf{6}^+$ was obtained with the generation of the phosphonium ylid $\mathbf{7}^+$, that resulted when solutions of PMe_3 were added to $\mathbf{6}^+$ at $-60\text{ }^\circ\text{C}$. A dramatic shift of the methylenidene proton from 15.91 in $\mathbf{6}^+$ to 3.72 ppm (d, $^2J_{\text{HP}} = 21\text{ Hz}$) in $\mathbf{7}^+$ was observed, accompanied by the appearance of a $^{13}\text{C}\{^1\text{H}\}$ doublet at 2.5 ppm ($^1J_{\text{CP}} = 26\text{ Hz}$). Two doublets were detected in the $^{31}\text{P}\{^1\text{H}\}$ NMR spectrum at 33.3 (Ir–P) and 26.8 ppm (PMe_3 ; $^3J_{\text{PP}} = 3\text{ Hz}$).

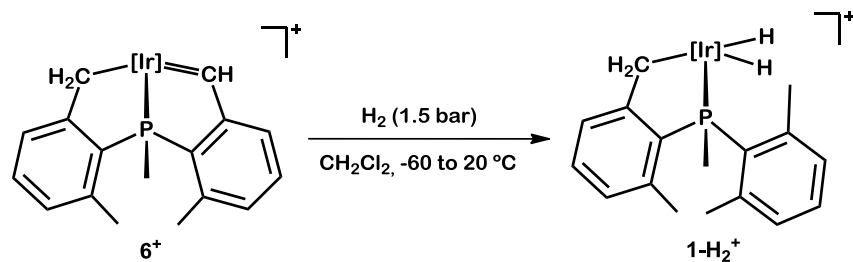


Scheme 36. PMe_3 addition to alkylidene $\mathbf{6}^+$ and formation of ylid $\mathbf{7}^+$.

To gain additional information on key steps of Scheme 31 that involve species **5** and **6**⁺, some additional experiments were performed. These consisted in hydrogenation of the latter and protonation of the former.

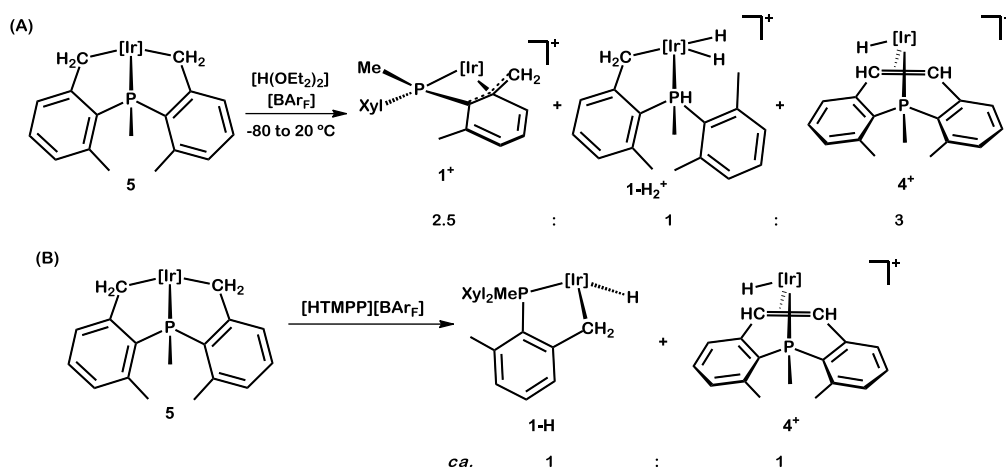
As discussed above, hydride abstraction from dimetalacycle **5** by HB⁺ yields equimolar amounts of **6**⁺ and H₂. The highly electrophilic character of the benzyldiene terminus of **6**⁺ is evidently responsible for the migratory insertion reaction that produces ultimately the hydride phosphepine cation **4**⁺. Nonetheless, interaction of **6**⁺ with H₂ to afford **1**⁺ (through intermediates **G** and **F**), and subsequently **1-H₂**⁺ if sufficiently H₂ is available, is also expected to be a facile process.

When a solution of **6**⁺ (generated by the procedure of Scheme 33) was treated with a large excess of H₂ (1.5 bar) and the mixture allowed to reach slowly room temperature with intense stirring, clean quantitative transformation into **1-H₂**⁺ was achieved (Scheme 37). Hence, under these conditions alkylidene hydrogenation is much faster than benzyl-benzyldiene coupling and subsequent β-H elimination. However, as discussed already in detail,⁵⁸ an analogous NMR tube reaction afforded slightly different results, most probably due to slow diffusion of H₂. After mixing of the reagents at -80 °C, monitoring of the reaction by ¹H NMR in the temperature range from -80 to -20 °C ascertained formation of a 1:4 mixture of **4**⁺ and **1-H₂**⁺. Clearly, the low solution concentration of H₂ retarded hydrogenation and allowed partial formation of the C–C coupling product.



Scheme 37. Reaction of alkylidene 6^+ with an excess of H_2 .

Protonation reactions of the dimetalacycle **5** have also been discussed in detail.⁵⁸ Scheme 38A summarizes the results of the reaction between complex **5** and $[H(OEt)_2][BAr_F]$ (from -80 to 20 °C). As can be seen a 2.5:1:3 mixture of compounds 1^+ , $1-H_2^+$ and 4^+ is obtained which may be taken as indicative that protonation of **5** occurs in both, the **5** to **G** and the **5** to 6^+ directions in Scheme 31. Seemingly, the former is kinetic favored over the latter.

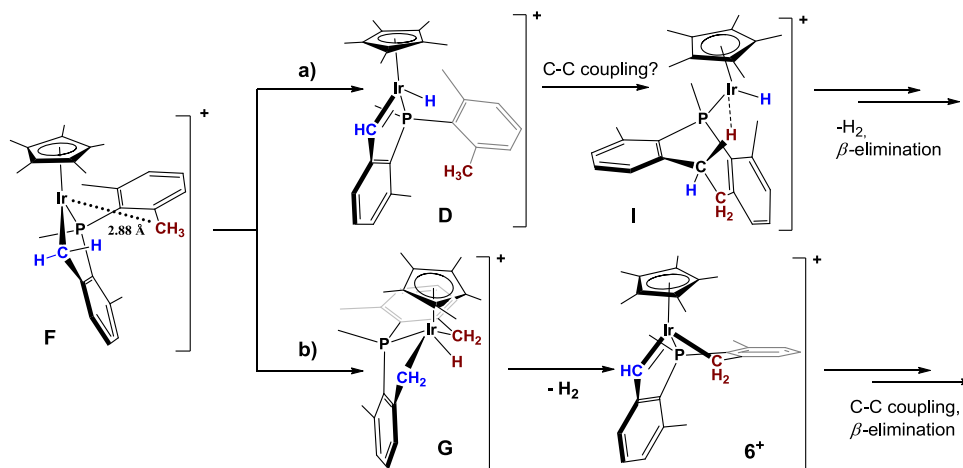


Scheme 38. Protonation reactions of **5**.

As a further test for this hypothesis one last acid-promoted hydride abstraction reaction from **5** was effected utilizing 1 equiv of [HTMPP][BAr_F] (HTMPP = 2,2,6,6-tetramethyl piperidinium). In terms of reactivity, this is similar to the base-catalyzed conversion of **1**⁺ into a 1:1 mixture of **1-H**₂⁺ and **4**⁺. However, in this case 1 equiv of the base, rather than a catalytic amount, would be produced. Hence, a 1:1 mixture of the hydride-phosphepine compound **4**⁺ and the neutral hydride **1-H** should be expected (the latter resulting from deprotonation of **1-H**₂⁺ according to Scheme 5), which is in excellent agreement with the experimental results shown in Scheme 38B.

Independent work by Dr. Joaquín López-Serrano provided a theoretical basis for the experimental results already discussed. Two mechanistic pathways, *a* and *b* in Scheme 39, were considered, both starting from the κ²-*P,C* isomeric structure of **1**⁺ (**F**), which at variance with the Rh analog⁶² features a very weak (if any) agostic interaction (*d*[Ir-CH₃] = 2.90 Å). It should be recalled that **F** is instrumental in the solution dynamic behavior of **1**⁺ and it plays also a key role in the formation of the hydride phosphepine complex **4**⁺ (Schemes 27 and 31, respectively).

⁶² Campos, J.; Esqueda, A. C.; López-Serrano, J.; Sánchez, L.; Cossio, F. P.; de Cózar, A.; Álvarez, E.; Maya, C.; Carmona, E. *J. Am. Chem. Soc.* **2010**, *132*, 16765.



Scheme 39. Initial steps in the two mechanisms considered for the C–C bond formation reaction leading to hydride phosphepine 4^+ .

Route *a* was discarded⁵⁸ as the suggested C–C coupling must overcome a barrier higher than $55 \text{ kcal}\cdot\text{mol}^{-1}$. Contrary to this situation, the highest barrier for route *b* (Figures 22 and 23), which is associated with the C–C coupling reaction, amounts $27.9 \text{ kcal}\cdot\text{mol}^{-1}$. Surpassing this barrier gives access to intermediate **F** in Figure 23, whose transformation into complex 4^+ requires three almost barrierless steps, the latter being a β -H elimination reaction.

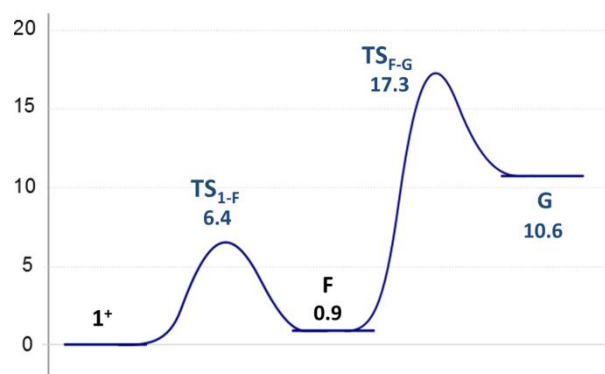


Figure 22. Potential energy profiles in dichloromethane (in $\text{kcal}\cdot\text{mol}^{-1}$) for the formation of the Ir(V) hydride **G**.

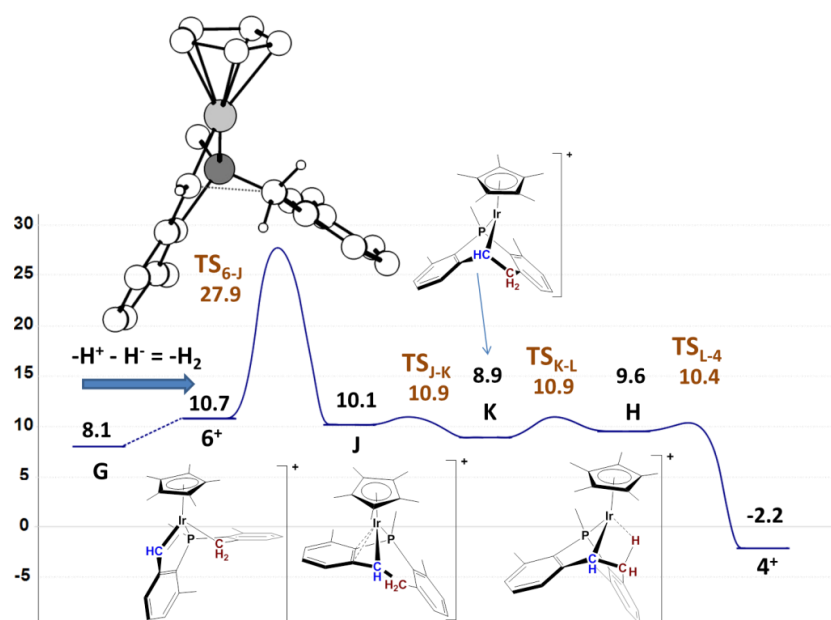


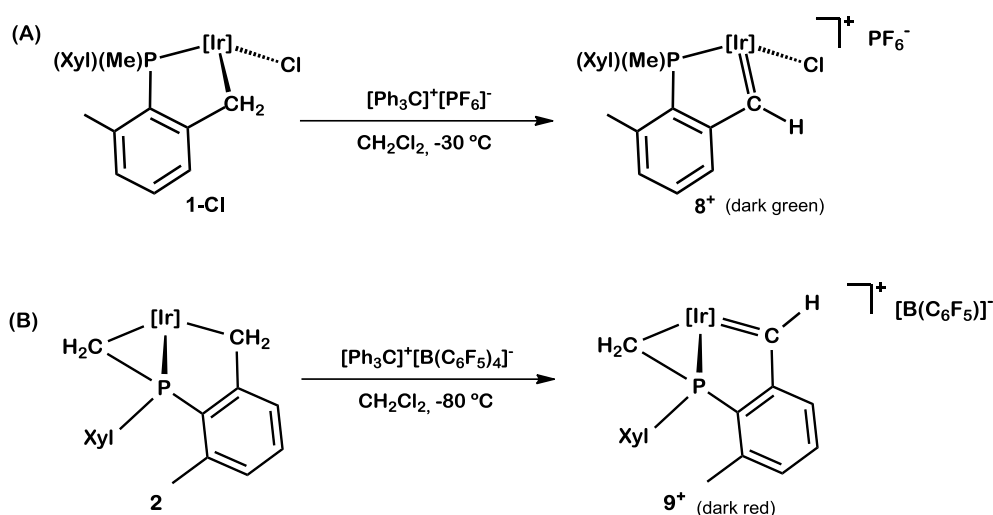
Figure 23. Free energy profile in dichloromethane (in $\text{kcal}\cdot\text{mol}^{-1}$) for the formation of the hydride phosphepine **4**⁺ from the alkyl alkylidene derivative **6**⁺ (note **1**⁺ is the origin of free energies). The inset shows the calculated geometry for $\text{TS}_{6\rightarrow\text{J}}$ indicating the forming C–C bond with a dotted line

2.A.7. Synthesis of Iridium (III) Alkylidenes Derived from Compounds **1**.

As already discussed, reaction of the neutral, doubly metalated complex **5** with $[\text{Ph}_3\text{C}]^+[\text{B}(\text{C}_6\text{F}_5)_4]^-$, quantitatively produces the cationic alkylidene **6**⁺ (Scheme 33). Considering the very few reported examples of electrophilic Ir(III) alkylidenes,^{30b,43} as well as the intriguing C–C bond formation reactivity that stems from **6**⁺, we have extended this chemistry to other related neutral compounds **1**. In addition, we have studied the reaction of **1**⁺ with diazocompounds.

Reactions of 1-Cl and 2 with Trityl Cation (Ph_3C^+)

Reaction of neutral compounds **1-Cl** and **2** with $[\text{Ph}_3\text{C}]\text{X}$ ($\text{X} = \text{PF}_6^-$ or $\text{B}(\text{C}_6\text{F}_5)^-$), led to quantitative formation of the corresponding cationic Ir(III) alkylidenes **8**⁺ and **9**⁺, respectively (Scheme 40). Formation of these cationic species was instantaneous at -30 °C and resulted in characteristic dark and intense green and red color solutions of compounds **8**⁺ and **9**⁺, respectively.



Scheme 40. Synthesis of Ir(III) alkylidenes by hydride abstraction from **1-Cl** and **2**.

Compound **8⁺** is characterized by a deshielded ^1H NMR signal at 16.61 (d, $^3J_{\text{HP}} = 0.9\text{ Hz}$), which is shifted by *ca.* 12 – 13 ppm with respect to the peaks due to the diastereotopic Ir– CH_2 protons of **1-Cl**. The corresponding $^{13}\text{C}\{^1\text{H}\}$ signal is found at 262.4 ppm and features a one-bond C–H coupling constant of 153 Hz. Other NMR data are in agreement with those of the neutral chloride precursor **1-Cl**. A characteristic alkylidene ^1H NMR signal is found for **9⁺** at 14.9 ppm, with a related $^{13}\text{C}\{^1\text{H}\}$ NMR resonance at 243.7 ppm ($^2J_{\text{CP}} = 28\text{ Hz}$).

Hydride abstraction from compound **2** might be expected to implicate either of the two different Ir– CH_2 groups, thereby forming distinct cationic alkylidenes. 2D-NOE studies revealed chemoselective abstraction from the five-membered metalacyclic moiety and this was also confirmed by X-ray diffraction studies (see below).

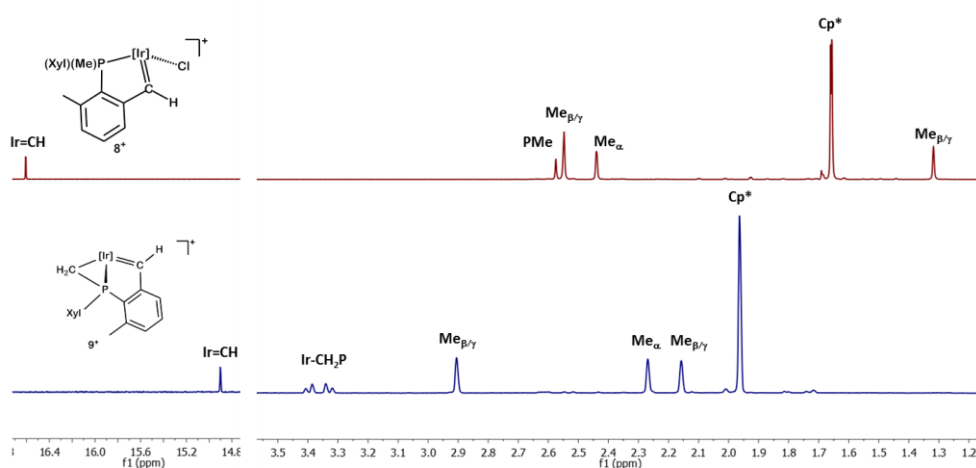
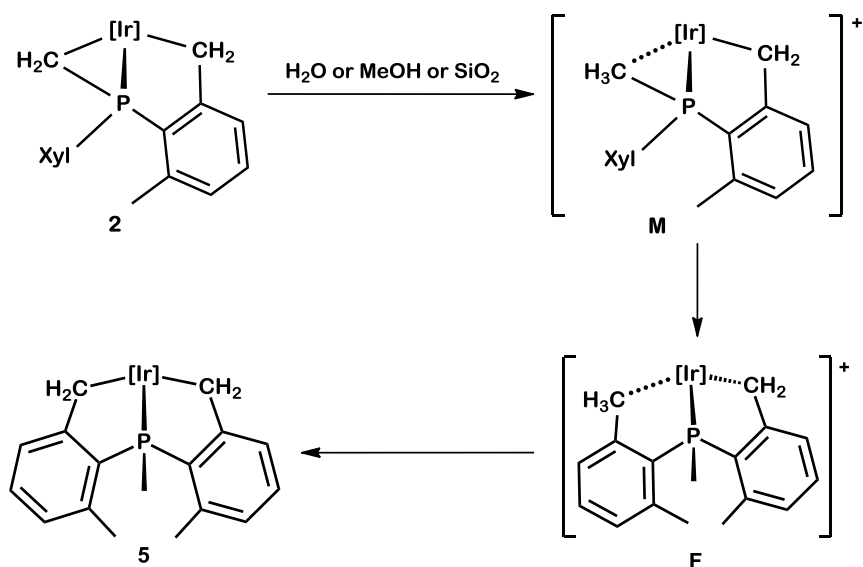


Figure 24. ^1H NMR (500 MHz, CD_2Cl_2 , 25 $^\circ\text{C}$) spectra of cationic alkylidenes $\mathbf{8}^+$ and $\mathbf{9}^+$.

Compound $\mathbf{8}^+$ is stable in the solid state for long periods of time, although it slowly decomposes in dichloromethane solution at room temperature ($t_{1/2}$ *ca.* 4 days). Alkylidene $\mathbf{9}^+$ exhibits also fair thermal stability, both as a solid and in solution; however it rapidly decomposes in the presence of adventitious water. It has been observed that traces of water, as well as exposure to SiO_2 , cause isomerization of the 3/5 dimetallacycle $\mathbf{2}$ into the more stable 5/5 dimetallacycle $\mathbf{5}$ (Scheme 41).



Scheme 41. Acid catalyzed isomerization of **2** into **5**.

Single crystals of **8**⁺ and **9**⁺ suitable for X-ray studies were obtained by slow diffusion of pentane into a dichloromethane solution of the complexes at -20 °C. A characteristically short Ir1–C17 bond distance was measured in both compounds (1.899(5) Å, (**8**⁺); 1.905(4) Å, (**9**⁺)), whereas the average Ir–C distance in previously discussed neutral and cationic compounds **1** is significantly longer (*ca.* 2.12 Å), as expected for a single Ir–C bond. As shown in Figure 25B, X-ray crystallography unequivocally confirms that hydride abstraction from **2** occurred from the Ir–CH₂ methylene group within the five-membered ring, whereas the metalated P–Me group remained unaltered. The P1–C27 bond distance (1.750(4) Å) is slightly shorter than the other two P1–C bonds (*ca.* 1.80 Å), most likely due to the partial double-bond character of the P1–C27 unit. The strain within the three-membered metallacycle is clearly reflected by the acute P1–Ir1–C27 angle of 46.84°,

less than half the value that would correspond to a tetrahedral environment around the P1 atom.

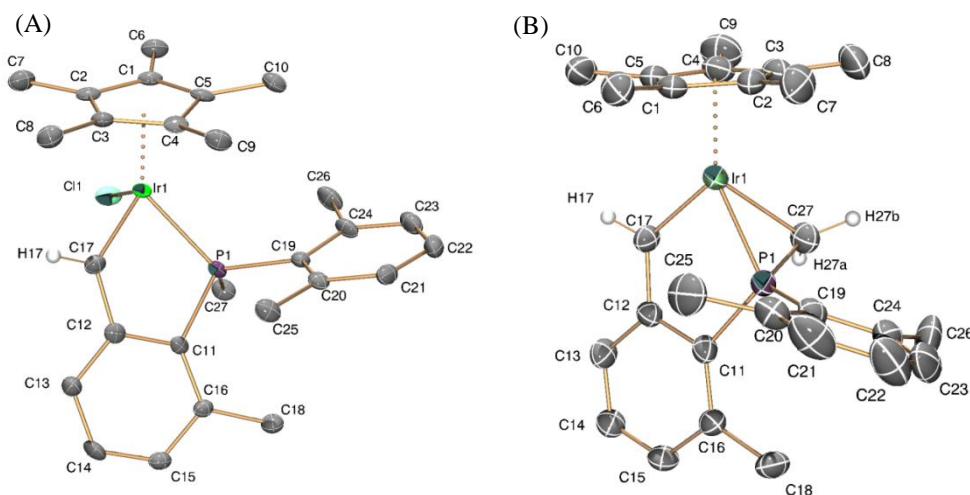
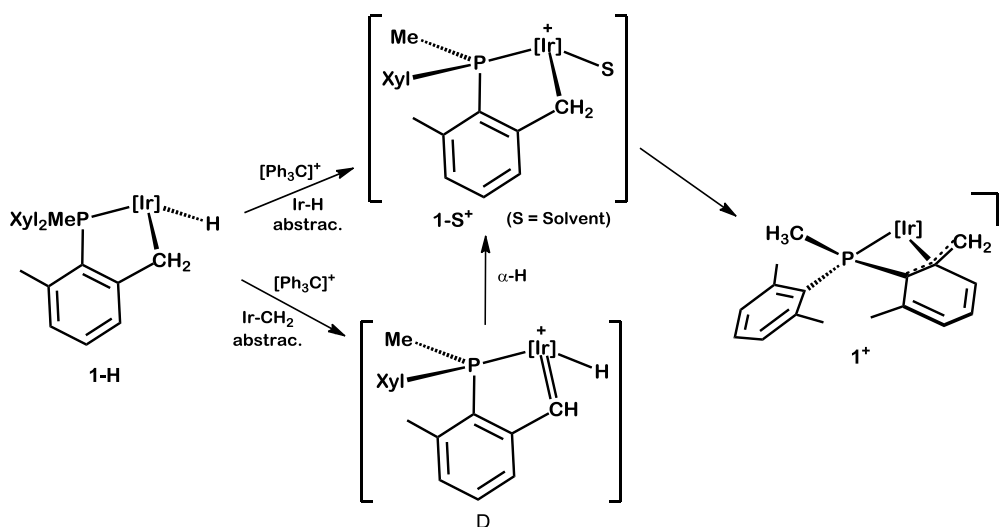


Figure 25. ORTEP diagrams for complexes 8^+ (a) and 9^+ (b). Thermal ellipsoids are drawn at the 50 % probability. Hydrogen atoms and counterions have been omitted for clarity.

Contrary to the C–C bond coupling observed for alkylidene 6^+ that leads to hydrophosphepine 4^+ , species 9^+ does not undergo analogous reactivity even at 50 °C. Possibly, the rigidity of the three-membered metallacycle hinders approach of the Ir–CH₂ to the Ir=CH unit and achievement of an energetically accessible transition state for the C–C coupling reaction to occur.

Reaction of 1-H with Trityl Cation (Ph_3C^+)

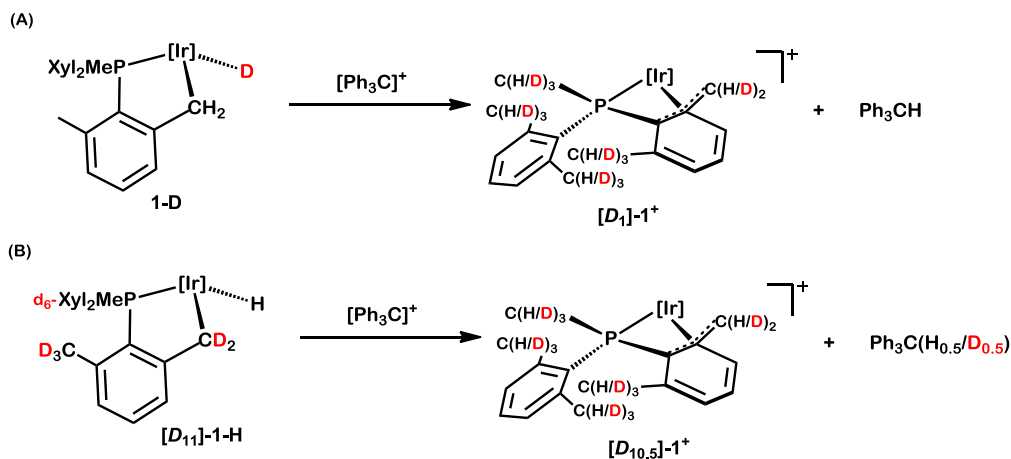
Addition of the trityl cation to a dichloromethane solution of **1-H** led to immediate and quantitative formation of the κ^4 -complex **1**⁺. Even though hydride abstraction could occur at the Ir-H or Ir-CH₂ sites, the reaction product would be the same (Scheme 42).



Scheme 42. Possible routes for the hydride abstraction from **1-H** to give **1**⁺.

To gain a better understanding of the mechanism of hydride abstraction from **1-H** two experiments with deuterated samples were undertaken (Scheme 43). Hydride abstraction from **1-D** using one equiv of $[\text{Ph}_3\text{C}]^+$ resulted in formation of exclusively Ph_3CH (no D incorporation was detected). The deuteride of **1-D** probably became incorporated into the ligand back-bone (benzylic H atoms of the two xylyl groups), but its very low concentration (one D over eleven positions) along with broadness of the ^1H

NMR resonances of $\mathbf{1}^+$ created by its dynamic behavior, made its detection difficult. These results strongly suggest that hydride abstraction occurs selectively from the Ir–CH₂ methylene site.

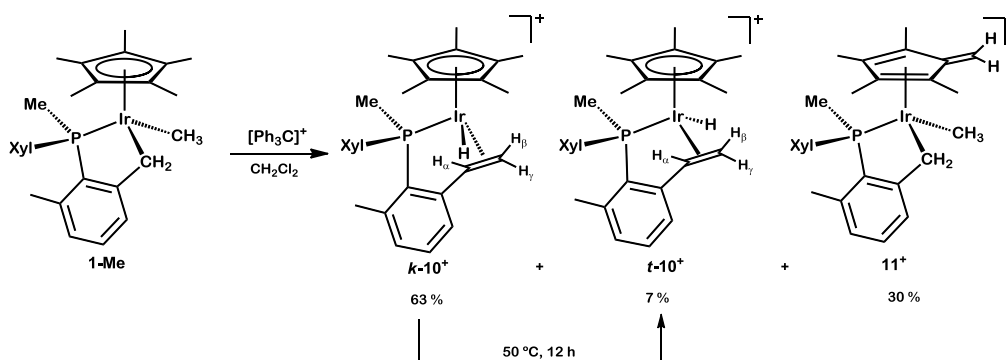


Scheme 43. Hydride abstraction with $[\text{Ph}_3\text{C}]^+$ from $\mathbf{1-D}$ and $[\text{D}_{11}]\text{-}\mathbf{1-H}$ isotopologues.

However, reaction of compound $[\text{D}_{11}]\text{-}\mathbf{1-H}$ with one equiv of cation $[\text{Ph}_3\text{C}]^+$ yielded partially deuterated (*ca.* 50 %) $\text{Ph}_3\text{CH/D}$, with hydrogen incorporation (*ca.* 5 %) into all benzylic sites of $\mathbf{1}^+$. These observations suggest that hydride abstraction from Ir–CH₂ and Ir–H occur with comparable rates, with the former being somewhat faster than the latter. Primary kinetic isotope effects (mostly Ir–CH₂/Ir–CD₂) are probably responsible for the above differences.

Reaction of Trityl Cation (Ph_3C^+) with **1-Me**

Reaction of **1-Me** with $[\text{Ph}_3\text{C}]^+[\text{B}(\text{C}_6\text{F}_5)_4]^-$ resulted in the coupling of the Ir–CH₂ and Ir–Me groups and formation of a hydride alkene complex **10**⁺ in the form of a 1:9 kinetic mixture of two diastereomers that differ in the *syn* (**t-10**⁺, the thermodynamic isomer) or *anti* (kinetic isomer, **k-10**⁺) distribution of the Ir–H and P–Me groups (Scheme 44). Besides compound **10**⁺, a different complex **11**⁺ derived from H⁺ abstraction from the C₅Me₅ appeared in the reaction mixture (*ca.* 30 %). Conversion of coordinated C₅Me₅ into a 1,2,3,4-tetramethylfulvene is not uncommon.⁶³ Compound **11**⁺ could not be isolated in a pure form, but an almost pure sample of **t-10**⁺ was obtained after isomerization of **k-10**⁺ and several fractional crystallizations steps. The two stereoisomers of **10**⁺ have been characterized by X-ray crystallography.



Scheme 44. Reaction of **1-Me** with $[\text{Ph}_3\text{C}]^+$ and isomerization of **10**⁺.

⁶³ (a) Klahn, A. H.; Moore, M. H.; Perutz, R. N. *J. Chem. Soc. Chem. Commun.* **1992**, 1699. (b) Fairchild, R. M.; Holman, K. T. *Organometallics* **2008**, 27, 1823. (c) Fan, L.; Turner, M. L.; Hursthouse, M. B.; Malik, K. M. A.; Gusev, O. V.; Maitlis, P. M. *J. Am. Chem. Soc.* **1994**, 116, 385. (d) Fan, L.; Wei, C.; Aigbirhio, F. I.; Turner, M. L.; Gusev, O. V.; Morozova, L. N.; Knowles, D. R. T.; Maitlis, P. M. *Organometallics* **1996**, 15, 98. (e) Kölle, U.; Kang, B.-S.; Thewalt, U. *J. Organomet. Chem.* **1990**, 386, 267. (f) Yamamoto, Y.; Arakawa, T.; Itoh, K. *Organometallics* **2004**, 23, 3610.

As represented in Figure 26, the two diastereoisomers of **10**⁺ present similar molecular structures, with the only discernible difference of the *syn* (**k-10**⁺) or *anti* (**t-10**⁺) orientation of the Ir–H and P–Me units. Other geometrical parameters are in agreement with previously discussed molecular structures and do not need further discussion.

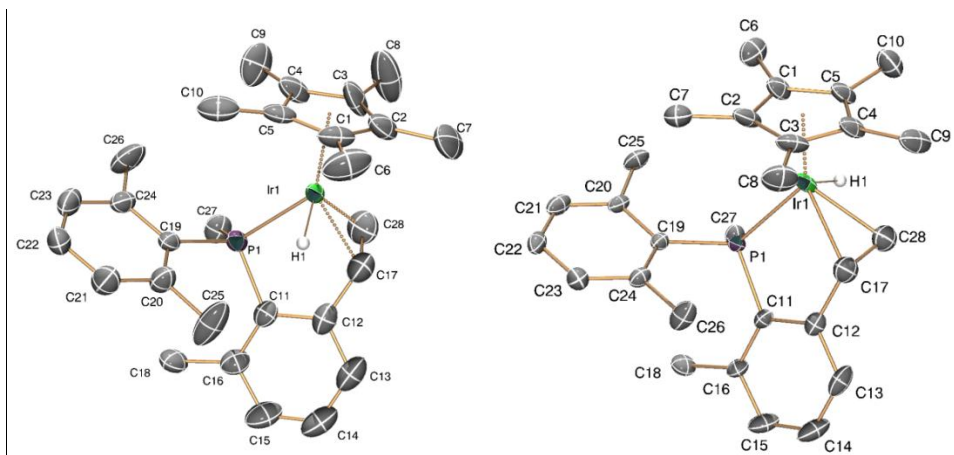


Figure 26. ORTEP diagrams for complexes for the two diastereoisomers of compound **10**⁺: (a) kinetic isomer **k-10**⁺; (b) thermodynamic isomer **t-10**⁺. Thermal ellipsoids are drawn at the 50 % probability. Hydrogen atoms (except Ir–H) and counterions have been omitted for clarity.

Compounds **t-10**⁺ and **k-10**⁺ are characterized by ¹H NMR signals at -15.77 (d, ²J_{HP} = 30.1 Hz) and -14.31 (d, ²J_{HP} = 28.5 Hz) ppm, respectively, due to the iridium hydride group. In the ³¹P{¹H} NMR spectra peaks at -0.1 and -9.8 ppm appear due to the thermodynamic and kinetic isomers, respectively. For the former, the olefin moiety features three ¹H NMR signals at 4.27 (dd), 2.83 (dt) and 2.64 (dd) ppm, due to H_α, H_γ and H_β, respectively. Coupling constants are in agreement with the formulation depicted in Scheme 44, with values of 10.5 and 8.6 Hz for the three-bond H–H coupling of *trans*

(H_α-H_γ) and *cis* (H_α-H_β) protons, whereas the geminal $^2J_{\text{HH}}$ coupling between H_β and H_γ amounts 2.4 Hz. No coupling to the phosphorous nucleus is observed, except for H_γ, which exhibits a three-bond coupling of *ca.* 2.4 Hz. Corresponding $^{13}\text{C}\{^1\text{H}\}$ NMR signals appear strongly deshielded with respect to **1-Me** (which exhibits resonances at 16.9 and -22.9 ppm for Ir-CH₂ and Ir-CH₃, respectively), with values of 62.7 (CH_α) and 34.1 (CH_βH_γ) ppm, as expected for olefinic carbon¹³ nuclei. ^1H and $^{13}\text{C}\{^1\text{H}\}$ NMR signals due to the kinetic isomer are similar to those of the thermodynamic one. The formulation depicted in Scheme 44 for both diastereomers have been inferred from 2D-NOE experiments. Compound **t-10⁺** exhibits an intense NOE cross-peak between Ir-H and PMe, thus suggesting that both groups lie in a *syn* conformation. However, this cross-peak is absent in **k-10⁺**, which indicates an *anti* rearrangement of both functionalities. Figure 27 shows the ^1H NMR spectrum in the region *ca.* 3 – 0.5 ppm for a *ca.* 6:4 mixture of **t-10⁺** and **11⁺**. Since the latter compound has not been isolated in a pure form we will not discuss it any further. Other NMR data can be found in the Experimental Section.

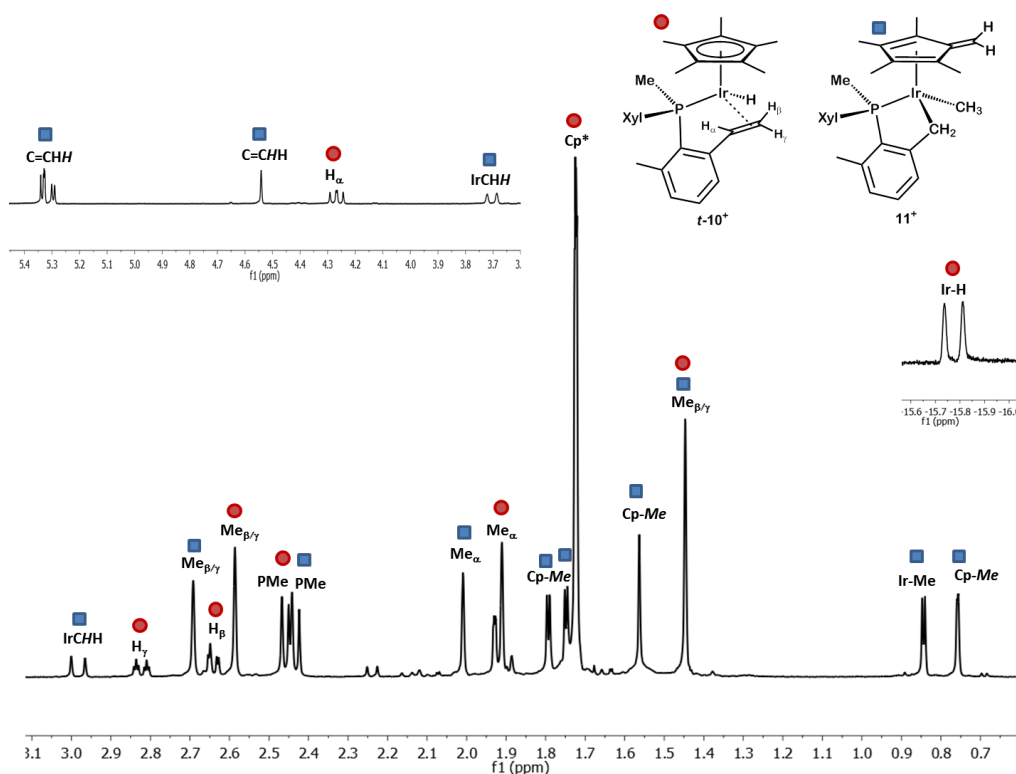


Figure 27. ^1H NMR (400 MHz, CD_2Cl_2 , 25 °C) spectrum of a mixture of $t\text{-}10^+$ and 11^+ (ca. 6:4).

The kinetic isomer $\mathbf{k}\text{-}10^+$ (around 90 % of 10^+) can be converted into the thermodynamic isomer, $t\text{-}10^+$, by heating the reaction mixture at 50 °C for 12 hours. This isomerization monitored by $^{31}\text{P}\{^1\text{H}\}$ NMR at 40 °C gave a first order rate constant of $1.4 \cdot 10^{-5} \text{ s}^{-1}$ (see Figure 28), which corresponds to a $\Delta G^\ddagger = (25.3 \pm 0.1) \text{ kcal} \cdot \text{mol}^{-1}$.

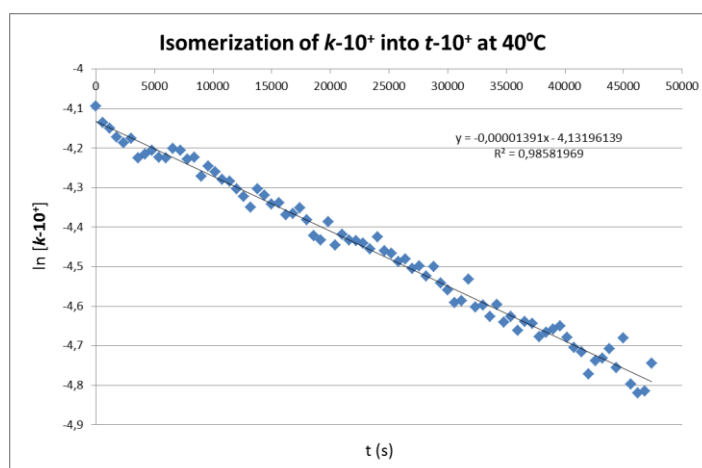
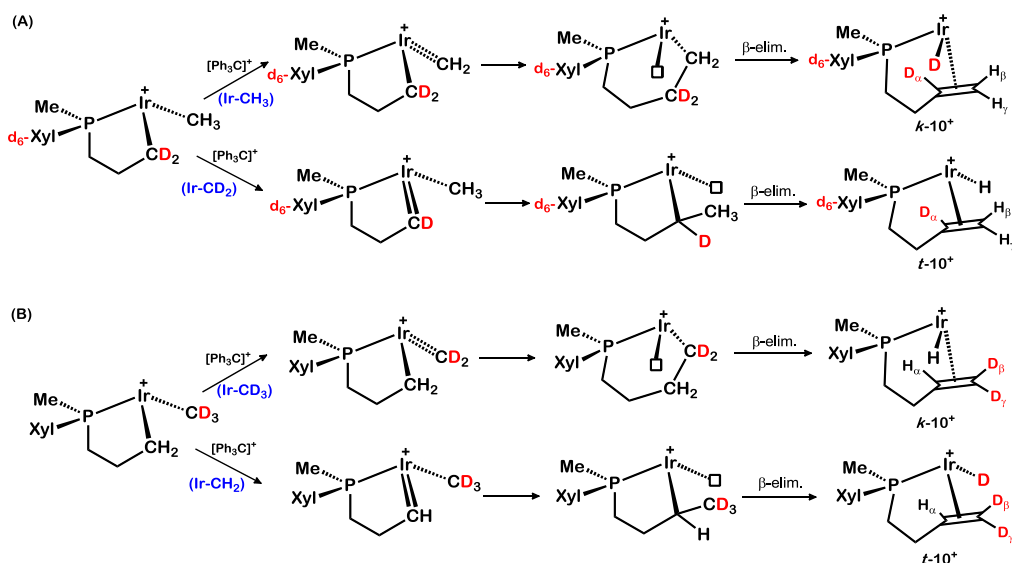


Figure 28. First-order kinetic representation for the isomerization of $k\text{-}10^+$ into $t\text{-}10^+$ at 40°C .

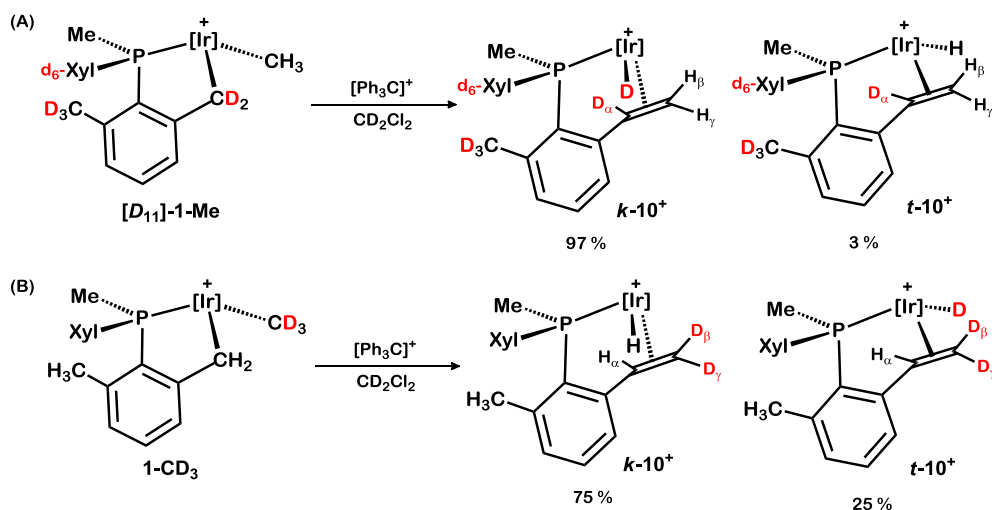
To understand the mechanism of formation of 10^+ , some experiments were undertaken using different isotopologues of **1-Me** (Scheme 45). Abstraction of a hydride from either the Ir-CH₂ or Ir-CH₃ sites of **1-Me**, would be followed by migratory insertion of the alkyl group into the alkylidene functionality and β -hydrogen elimination. These two steps are reminiscent of those involved in the already discussed C-C coupling reaction of alkylidene **6**⁺ to yield hydride-phosphepine **4**⁺ (Scheme 31). Scheme 45 shows the labeled products expected from deuterated samples [*D*₁₁]-**1-Me** and **1-CD**₃, for either of these reaction routes, i.e. Ir-CH₃ (*A-top* and *B-top*) and Ir-CH₂ (*A-bottom* and *B-bottom*).



Scheme 45. Expected deuteration patterns of the products ($\mathbf{10}^+$) resulting from Ir-CH₃ or Ir-CH₂ hydride abstraction of isotopologues $[D_{11}]\text{-1-Me}$ (A) and 1-CD_3 (B). Molecular structures have been simplified for clarity.

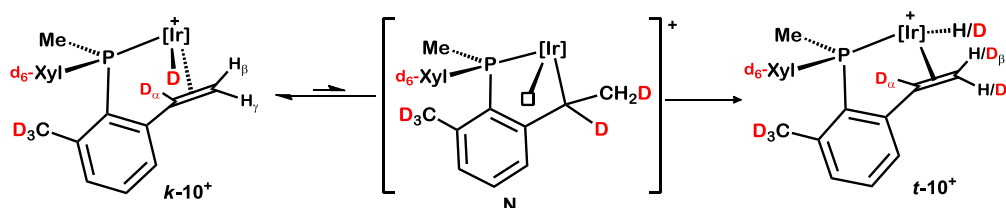
Complex $[D_{11}]\text{-1-Me}$ was readily prepared employing the procedure utilized for the synthesis of 1-Me but with deuterated $[D_{11}]\text{-1-Cl}$ instead of 1-Cl (which in turn was labeled by treating 1-Cl with CD_3OD). On the other hand, compound 1-CD_3 was best synthesized by reacting $\mathbf{1}^+$ with the Grignard reagent $\text{Mg}(\text{CD}_3)\text{I}$ (see Experimental Section for details). The results depicted in Scheme 46 confirmed that not unreasonably, there is a competition between abstraction of the hydride from the two alkyl positions, Ir-CH₂ and Ir-CH₃, with the latter, that lead to the kinetic isomer $k\text{-10}^+$, being preferred. Primary kinetic isotopic effects are noticeable: hydride abstraction from the protio isotopologue, 1-Me , yields a 90:10 mixture of $k\text{-10}^+:\text{t-10}^+$, whereas $[D_{11}]\text{-1-Me}$ increases the ratio of the k -isomer (abstraction

from Ir–CH₃) at the expense of the *t*-isomer (abstraction from Ir–CD₂), with a *k*:*t* proportion of *ca.* 97:3. The opposite effect is detected when **1-CD₃** undergoes hydrogen abstraction (*k*:*t* \approx 75:25).



Scheme 46. Reaction of trityl cation with deuterated compounds **[D₁₁]-1-Me** (A) and **1-CD₃** (B).

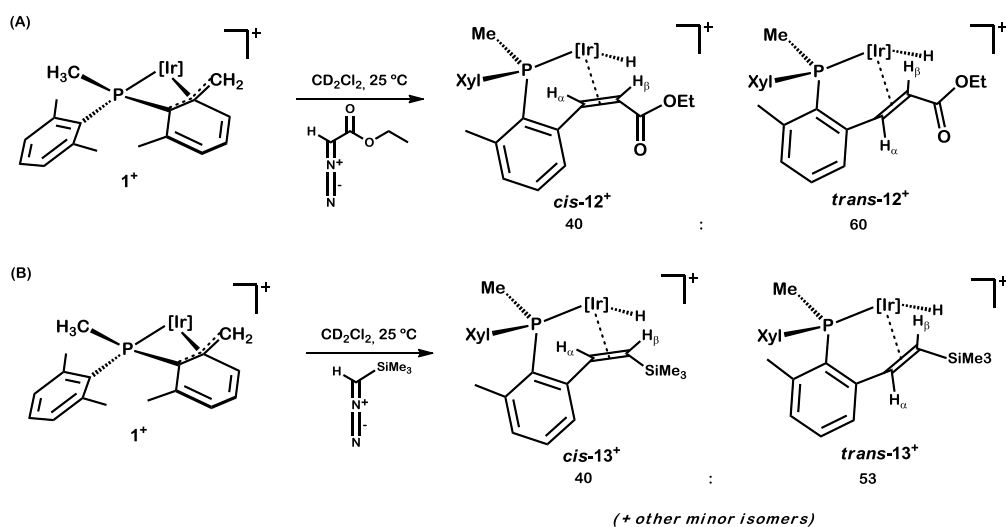
Finally the isomerization of ***k*-10⁺** into ***t*-10⁺** can be proposed to proceed through the intermediacy of the five-membered metallacycle **N** of Scheme 47, which is structurally related to species **F** derived from **1⁺** (Scheme 27). When the isomerization of ***k*-10⁺** resulting from **[D₁₁]-1-Me** is considered, concomitant H/D exchange implicating the Ir–H, H_β and H_γ, but nor the H_α, sites should occur, in agreement with the experimental results presented in Scheme 47.



Scheme 47. Isomerization of 10^+ by formation of intermediate N and subsequent H/D exchange process.

Reaction of 1^+ with Diazocompounds

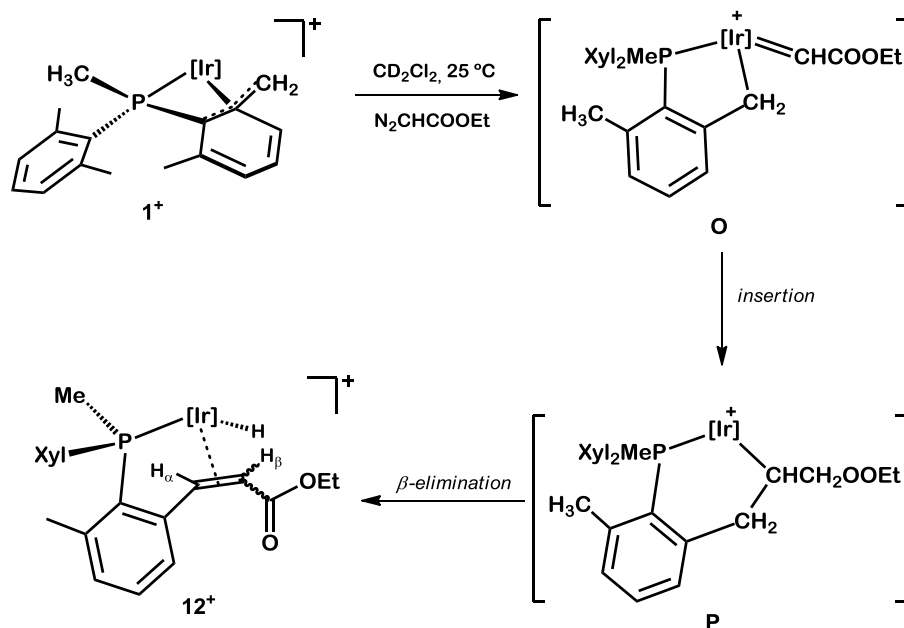
To complete these studies we investigated the reaction of 1^+ with two diazocompounds (Scheme 48) as carbene transfer reagents. Addition of either EDA (EDA = ethyldiazoacetate, $N_2CHCOOEt$) or (trimethylsilyl)diazometane ($N_2CHSiMe_3$) resulted in the expected C–C coupling reaction that led to complexes 12^+ and 13^+ , respectively. These compounds were obtained as mixtures of *cis* and *trans* isomers of the newly formed olefinic ligand. The identification of geometric isomers was achieved by 2D-COSY and NOESY studies. A slight preference for the *trans* isomer was found for the formation of both 12^+ and 13^+ . In fact, the proportion of the *trans*- 12^+ increased to *ca.* 75 % after carrying out the reaction of 1^+ with EDA at $-80^\circ C$ and allowing the mixture to reach slowly room temperature.



Scheme 48. Reaction of **1**⁺ with diazocompounds EDA (A) and N₂CHSiMe₃ (B).

No intermediates were detected by low-temperature ¹H NMR monitoring, but in view of the chemistry already discussed the reaction involves, in all probability, a highly reactive cationic alkylidene species (**O** in Scheme 49) that rearranges by migratory insertion and β-H elimination elementary steps.⁶⁴

⁶⁴ (a) Braga, A. A. C.; Caballero, A.; Urbano, J.; Díaz-Requejo, M. M.; Pérez, P. J.; Maseras, F. *ChemCatChem* **2011**, 3, 1646. (b) Hansen, J. H.; Parr, B. T.; Pelphrey, P.; Jin, Q.; Autschbach, J.; Davies, H. M. L. *Angew. Chem. Int. Ed.* **2011**, 50, 2544.



Scheme 49. Proposed mechanism for the reaction of **1**⁺ with diazocompounds.

Compounds **12**⁺ and **13**⁺ were characterized by NMR spectroscopy. The iridium-hydride groups exhibit characteristic ¹H NMR doublets between -15 and -17 ppm, with a two-bond coupling to the phosphorous nucleus of around 29 Hz. Their corresponding infrared bands appear between 2150 and 2175 cm⁻¹. Two deshielded doublets at 4.73 and 3.72 ppm in the ¹H NMR spectrum of *trans*-**12**⁺ are due to olefinic protons H_α and H_β, respectively, and exhibit a three-bond coupling constant of 9.3 Hz. The corresponding ¹³C{¹H} NMR signals for CH_α and CH_β appear at 59.5 and 40.9 ppm, respectively, the former presenting a small coupling to phosphorous of 4 Hz. The methylene protons of the ethoxy group (OCH₂CH₃) are diastereotopic and give two multiplets at 4.29 and 4.14 ppm, whereas the methyl group displays a triplet (³J_{HH} = 7.1 Hz) at 1.32 ppm. 2D-NMR analysis (HSQC, HMBC, COSY and NOESY) are consistent with the formulation depicted in Scheme 48A. ¹H and

$^{13}\text{C}\{^1\text{H}\}$ NMR data due to *cis*-**12**⁺ are in agreement with those of the *trans* isomer (see Experimental Section for details).

The olefinic protons of *cis*-**13**⁺ exhibit ^1H NMR doublets at 4.85 (H_α) and 2.38 (H_β) ppm, with a three-bond coupling constants of 11.7 Hz. The corresponding $^{13}\text{C}\{^1\text{H}\}$ peaks appear at 71.6 (d, $^2J_{\text{CP}} = 4$ Hz) and 44.4 (s) due to CH_α and CH_β , respectively. The trimethylsilyl group is responsible for a singlet in the ^1H NMR spectrum at 0.13 ppm. Similarly to compounds **12**⁺, the formulation depicted in Scheme 48B has been inferred from two-dimensional homonuclear and heteronuclear studies.

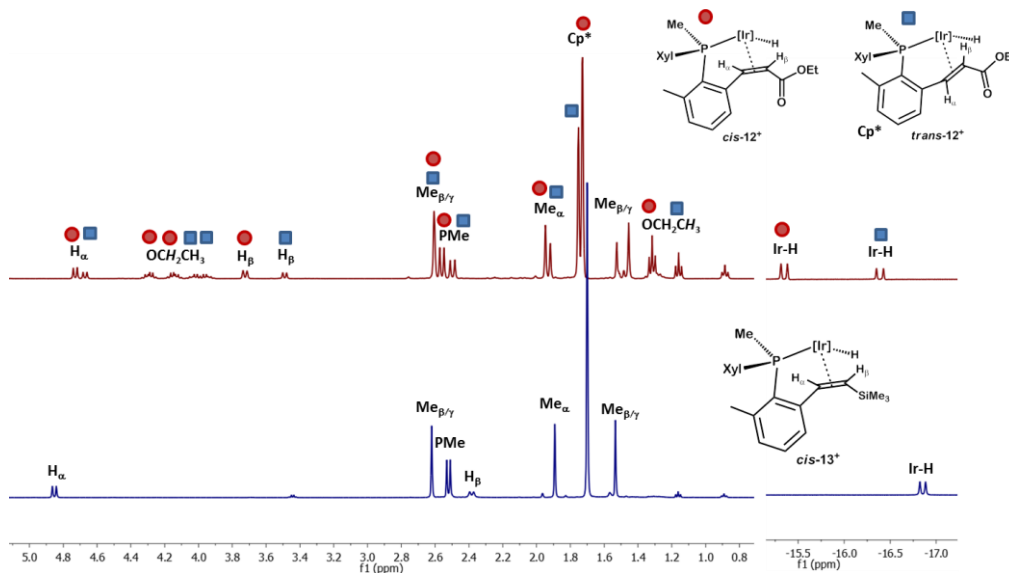
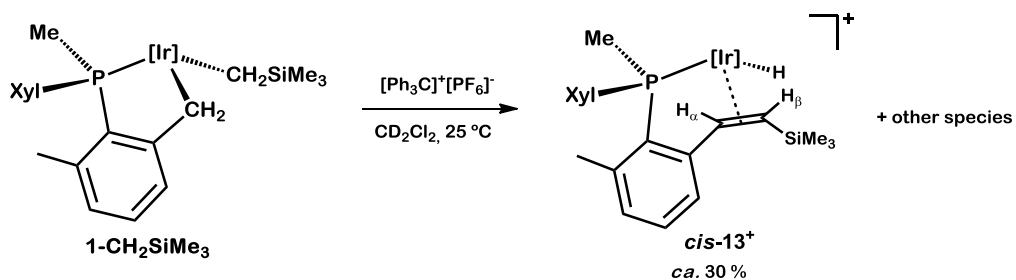


Figure 29. ^1H NMR (400 MHz, CD_2Cl_2 , 25 °C) spectra of compounds **12**⁺ (*cis* and *trans* isomers, around 4:6) and *cis*-**13**⁺.

To confirm further the molecular structure proposed for **13**⁺ (Scheme 48), we attempted its synthesis from alkyl compound **1-CH₂SiMe₃** and

$[\text{Ph}_3\text{C}]^+[\text{PF}_6]^-$. Although compound **13**⁺ formed in only *ca.* 30 % yield (other four unidentified species exhibiting iridium-hydride signals were also detected), this result supports the formulation proposed for compounds **12**⁺ and **13**⁺ and their likely formation *via* alkylidene species.



Scheme 50. Reaction of **1-CH₂SiMe₃** with $[\text{Ph}_3\text{C}]^+[\text{PF}_6]^-$.

Summary and Conclusions

*In summary, we have demonstrated that the readily prepared cyclometalated complex **1-Cl** is an excellent precursor for the synthesis of related halide (or pseudohalide), hydride and alkyl derivatives. Compounds **1-Cl** and **1-Br** feature H/D scrambling in the presence of CD₃OD that affects all benzylic sites, whereas for the hydride **1-H** an unusual acid-catalyzed reaction permits D incorporation exclusively into the Ir–H and Ir–CH₂ units.*

*Abstraction of the chloride from **1-Cl** yielded Ir(III) cation **1**⁺, that contains a monometalated xylyl phosphine coordinated in a κ^4 -P,C,C',C'' fashion through the phosphorus and three benzylic carbon atoms. This molecule experiences a base-catalyzed C–C dehydrogenative coupling that results in equimolar mixtures of hydride phosphine complex **4**⁺ and the cationic, bis(hydride) Ir(V) derivative **1-H**₂⁺. The former derives from a cationic alkyl-alkylidene intermediate **6**⁺ which experiences migration of the iridium-alkyl onto the iridium-alkylidene, accompanied by β -H elimination. Other related Ir(III) alkylidenes have been prepared and fully-characterized, and their reactivity has been investigated.*

Part B: Studies on $(\eta^5\text{-C}_5\text{Me}_5)\text{Ir}(\text{PR}_2(\text{Xyl}))$ Units

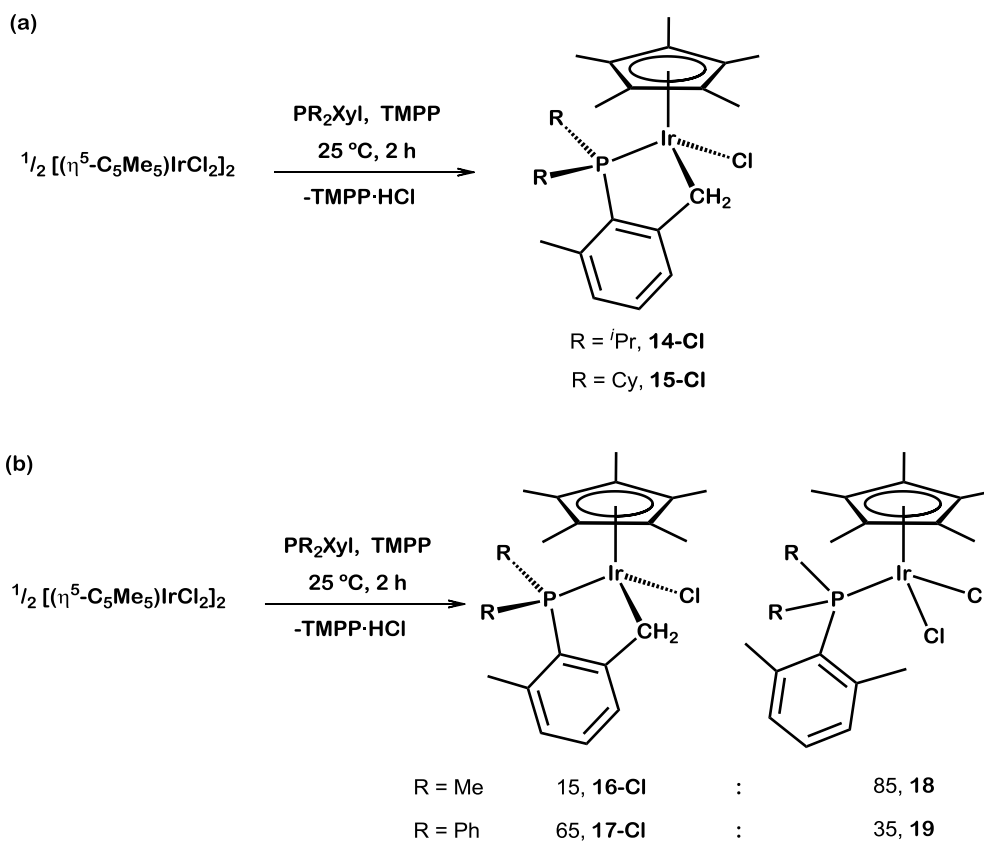
2.B. RESULTS AND DISCUSSION

2.B.1. Synthesis of Chloride Complexes.

The facile synthesis of the unusual Ir(III) cationic alkylidenes described in Part A led us to prepare other compounds of this kind with different phosphine ligands. Above $-20\text{ }^\circ\text{C}$, alkylidene **6**⁺ underwent spontaneously above $-20\text{ }^\circ\text{C}$ a facile C–C coupling between the two *o*-methyl groups of the two xylyl rings of the phosphine, with formation of a hydride phosphepine complex **4**⁺. To prevent this transformation, we have synthesized

cyclometalated iridium and rhodium chloride complexes related to **1-Cl**, but containing only one xylyl substituent on the phosphine ligand (see Figure 4, page 165).

Four different phosphines containing a single xylyl substituent, namely $P^iPr_2(Xyl)$, $PCy_2(Xyl)$ (Cy = cyclohexyl), $PMe_2(Xyl)$ and $PPh_2(Xyl)$, were prepared by conventional procedures (see Experimental Section for details). By the same method employed for the synthesis of **1-Cl**, we obtained related halide complexes from the reactions of the Ir(III) dimer $[\{(\eta^5-C_5Me_5)IrCl_2\}_2]$ and the phosphines $P^iPr_2(Xyl)$ (**14-Cl**), $PCy_2(Xyl)$ (**15-Cl**), $PMe_2(Xyl)$ (**16-Cl**) and $PPh_2(Xyl)$ (**17-Cl**), in the presence of TMPP to trap the HCl produced (Scheme 51). Stirring the reaction mixtures for two hours at room temperature was sufficient to obtain compounds **14-Cl** and **15-Cl** as single isomers in yields around 90 % (Scheme 51a). However, under these conditions, complex **17-Cl** was accompanied by the corresponding non-metalated bis(chloride) species **19** (Scheme 51b) in *ca.* 35 % spectroscopic yield, possibly due to the smaller size of the phenyl ring in comparison with the iPr and Cy substituents. Indeed, under the same conditions the major product of the reaction between the Ir(III) dimer and the less-hindered phosphine $PMe_2(Xyl)$, was the non-metalated compound (**18** in Scheme 51b, *ca.* 85 %), whereas the desired complex **16-Cl** appeared as a minor component in the reaction mixture (*ca.* 15 %). Performing the same reaction at 0 °C for 30 min in the absence of TMPP led to quantitative formation of **18**, isolated as a bright orange powder stable to air and moisture.



Scheme 51. Synthesis of cyclometalated iridium halide complexes.

Mild heating of dichloromethane solutions of the non-metallated compounds **18** (45 °C, 16 h) and **19** (45 °C, 6 h), in the presence of 1 equiv of TMPP, caused quantitative conversion into the corresponding cyclometalated species **16-Cl** and **17-Cl**, respectively. Similarly to previously discussed related complexes, chloride compounds (**14-17**)-Cl feature characteristic ^1H NMR signals due to diastereotopic Ir-CH₂ protons between *ca.* 3 and 4 ppm, with a two-bond ^1H - ^1H coupling constant of around 14 Hz. In all cases, only one of the two proton signals revealed coupling to the phosphorous nucleus, with a corresponding $^3J_{\text{HP}}$ of *ca.* 4-5 Hz. Corresponding $^{13}\text{C}\{^1\text{H}\}$ resonances

appear at around 17 ppm and present a two-bond coupling to phosphorous of 3 Hz. The C_5Me_5 ring leads to doublets ($^4J_{HP} \approx 1.5$ Hz) with δ *ca.* 1.7 ppm, whereas the non-metalated methyl group of the xylyl ring gives a resonance around 2.5 ppm. 1H NMR spectra of the bis(chloride) compounds **18** and **19** demonstrated their non-metalated structure. The two equivalent *o*-methyl groups of the xylyl ring give a singlet (relative intensity 6 H) at 2.59 (**18**) and 2.31 (**19**) ppm, and no resonances due to the Ir-CH₂ unit were detected.

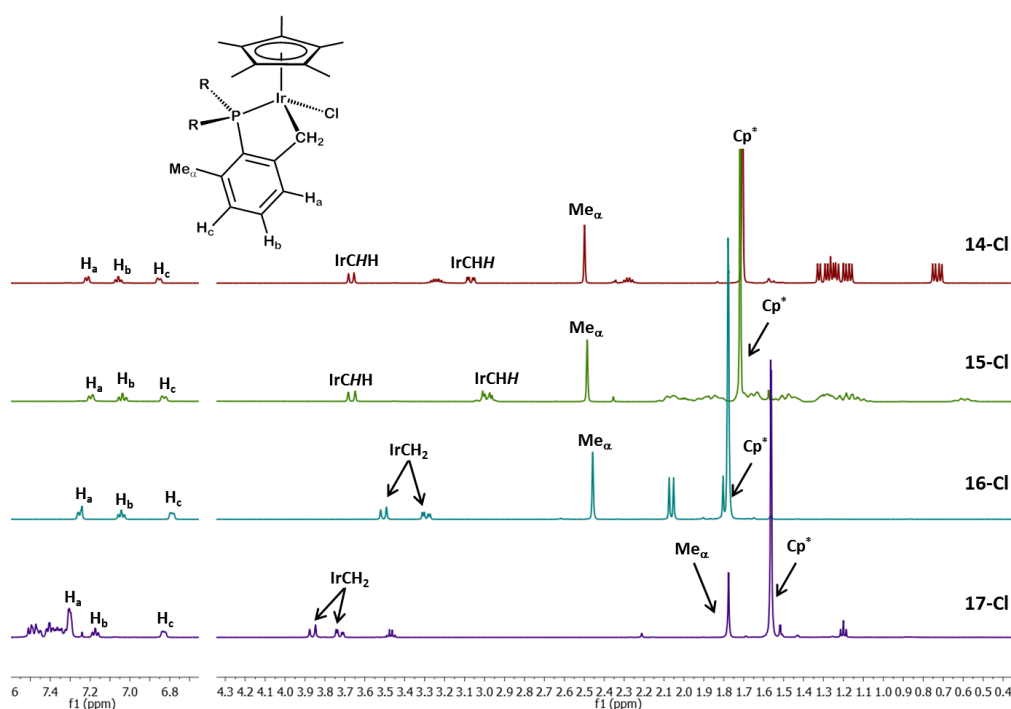


Figure 30. 1H NMR spectra of iridium halide complexes **14-Cl**, **15-Cl**, **16-Cl** and **17-Cl**.

Slow diffusion of pentane into concentrated dichloromethane solutions of compounds **14-Cl** and **16-Cl** provided suitable crystals for X-ray studies

(Figure 31). In accordance with ^1H NMR data, the molecular structures of these complexes confirm that cyclometalation of the xyl-yl-substituted phosphine gave rise to a five-membered iridacycle. The Ir–C, Ir–P and Ir–Cl bond distances of the two compounds are similar to corresponding values for **1-Cl** (around 2.10, 2.25 and 2.40 Å, respectively). Similarly to related complexes of the $\text{PMe}(\text{Xyl})_2$ ligand, bond angles for the three-legged piano stool are close to the ideal 90° .

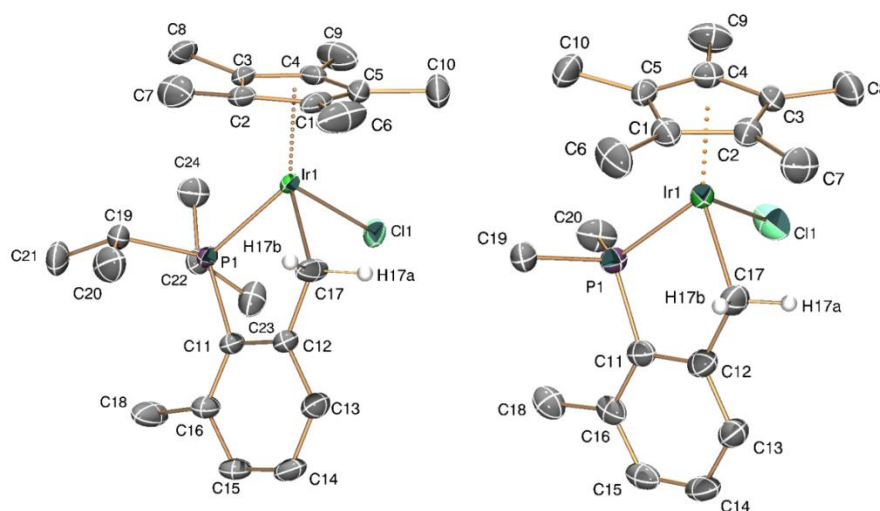
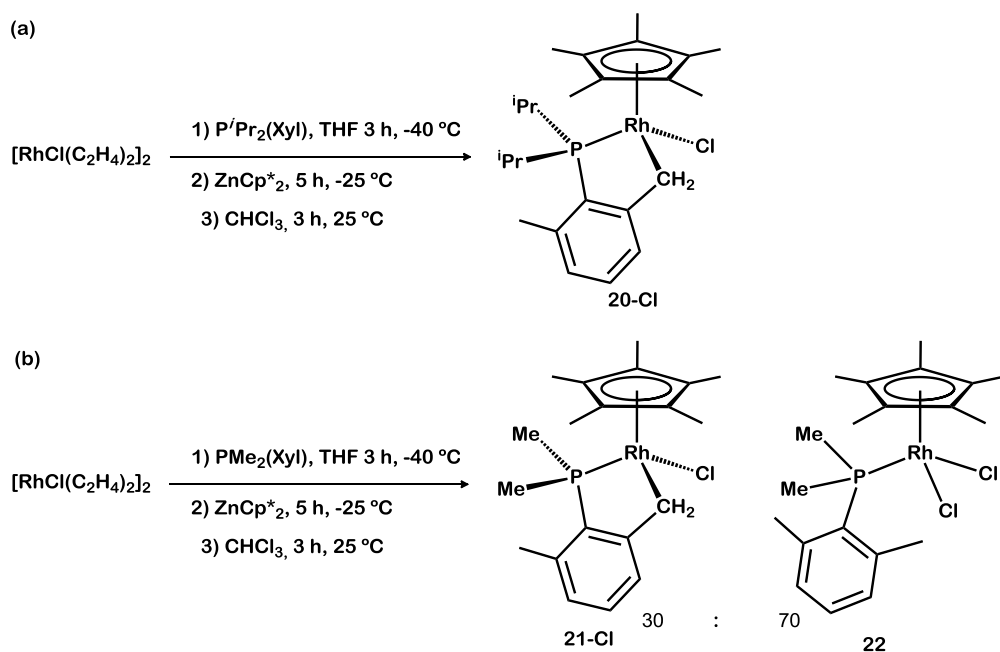


Figure 31. ORTEP diagrams for compound **14-Cl** and **16-Cl**. Thermal ellipsoids are drawn at the 50 % probability and most hydrogen atoms have been omitted for clarity.

Reactions of the Rh(III) dimer $[\{(\eta^5\text{-C}_5\text{Me}_5)\text{RhCl}_2\}_2]$ with phosphines $\text{P}^i\text{Pr}_2(\text{Xyl})$ and $\text{PMe}_2(\text{Xyl})$ in the presence of TMPP, required harsher conditions to proceed (the rhodium dimer remained unaltered after heating a $\text{ClCH}_2\text{CH}_2\text{Cl}$ solution at 80°C). Nevertheless, refluxing a toluene solution of the phosphine and the Rh precursor for several days led to the formation of

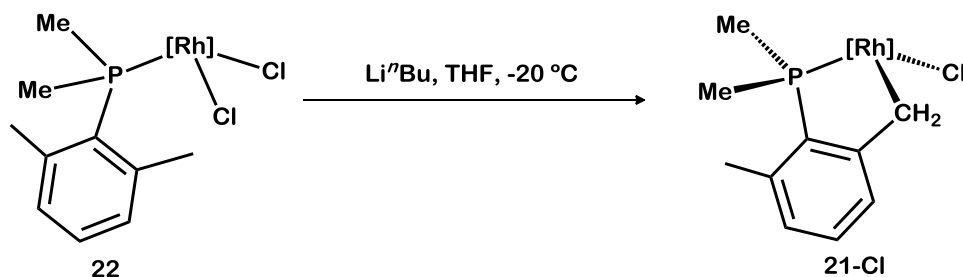
the expected halide complexes (< 50 % yield), along with other unidentified species. However, these cyclometalated rhodium compounds ($P^iPr_2(Xyl)$, **20-Cl**; $PMe_2(Xyl)$, **21-Cl**) were best obtained by the stepwise reaction of $[RhCl(C_2H_4)_2]_2$ with the phosphine, followed by treatment with $Zn(C_5Me_5)_2$ at $-25\text{ }^\circ\text{C}$, and subsequent chlorination of the resulting hydride species by the addition of $CHCl_3$ (Scheme 52).



Scheme 52. Synthesis of rhodium halide complexes.

As found for the iridium analog **16-Cl**, cyclometalated rhodium complex **21-Cl** based on $PMe_2(Xyl)$ was the minor product of the reaction depicted in Scheme 52b, whereas most of the rhodium dimer converted into the non-metalated bis(chloride) complex **22**. Cyclometalation of the latter was not

achievable under mild conditions, and needed instead treatment with Li^nBu at $-20\text{ }^\circ\text{C}$. Minor amounts of unidentified by-products were produced in this reaction. Other reagents like TMPP, KO^tBu or NaOH did not promote cyclometalation. In any case, compounds **21-Cl** and **22** were separated by column chromatography and obtained as analytically pure samples.



Scheme 53. Cyclometalation of **22** by reaction with Li^nBu .

These rhodium compounds feature a characteristic $^{31}\text{P}\{^1\text{H}\}$ NMR doublet with a one-bond $^{31}\text{P}-^{103}\text{Rh}$ coupling constant of around 160 Hz (**20-Cl** and **21-Cl**), and 140 Hz for non-metallated complex **22**. ^1H and $^{13}\text{C}\{^1\text{H}\}$ NMR data are in full agreement with the proposed structure. Interestingly, the diastereotopic $\text{Rh}-\text{CH}_2$ protons of **20-Cl** and **21-Cl** do not exhibit detectable coupling to the rhodium center, whereas their corresponding $^{13}\text{C}\{^1\text{H}\}$ NMR signals appear as doublet of doublets at 30.5 and 28.9 ppm, respectively ($^1J_{\text{CRh}} \approx 23\text{ Hz}$ and $^2J_{\text{CP}} \approx 8\text{ Hz}$). The molecular structure of **20-Cl** was confirmed by X-ray diffraction studies of crystals obtained from slow diffusion of pentane into a CH_2Cl_2 solution of the complex. Bond distances and angles around the rhodium metal center are identical, within the experimental error, to those of its iridium analog **14-Cl**.

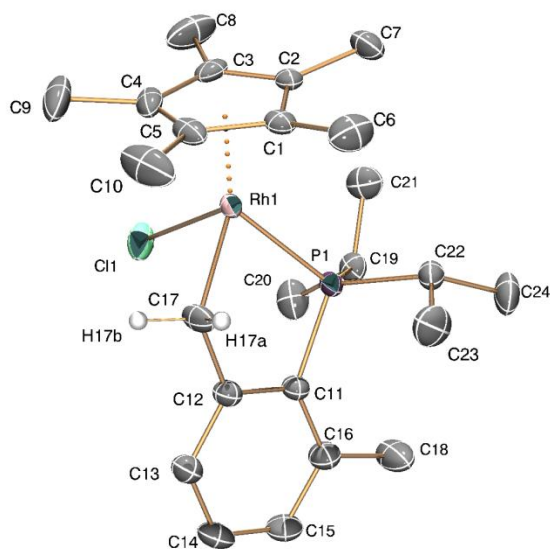
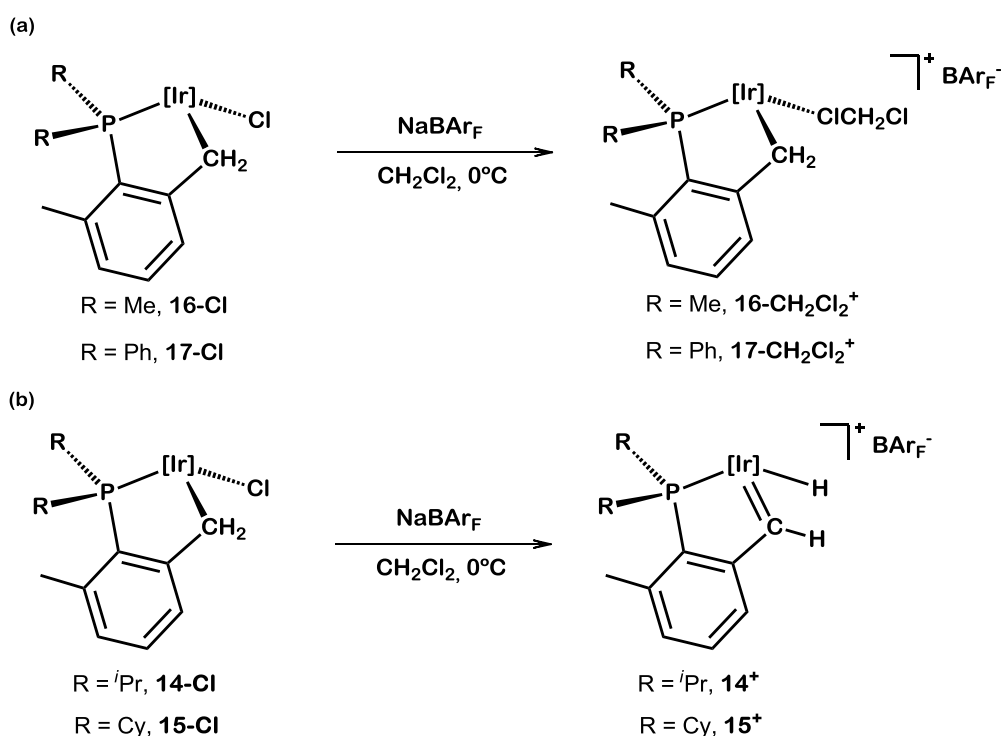


Figure 32. ORTEP diagram for compound **20-Cl**. Thermal ellipsoids are drawn at the 50 % probability and most hydrogen atoms have been omitted for clarity.

2.B.2. Chloride Abstraction from Rh and Ir Halide Complexes.

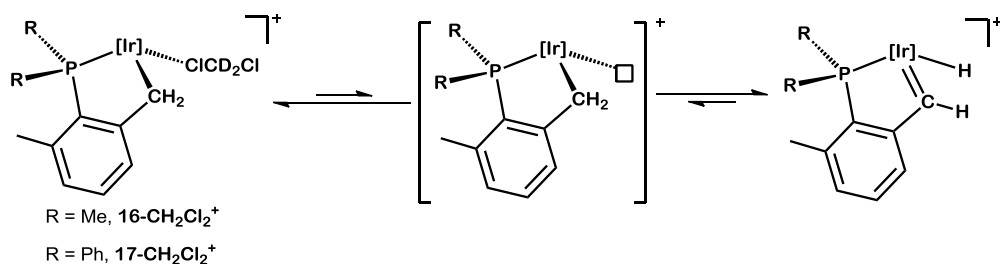
As stated at the beginning of this chapter, we carried out these reactivity studies with the main objective of isolating and characterizing stable cationic Ir(III) alkylidenes (and if possible the Rh analogs). Starting, once more, with Ir complexes, we found that the reaction of **16-Cl** (derived from $\text{PMe}_2(\text{Xyl})$) and **17-Cl** ($\text{PPh}_2(\text{Xyl})$ analog) with NaBAR_F in CH_2Cl_2 , at 0 °C, led to the formation of the cationic CH_2Cl_2 adducts, **16-CH₂Cl₂⁺** and **17-CH₂Cl₂⁺**, respectively (Scheme 54a). It is intriguing that NMR studies provided no

indication for the formation of a $\kappa^4\text{-P,C,C',C''}$ structure analogous to that of $\mathbf{1}^+$, suggesting that two Xyl substituents are needed to stabilize this kind of electronic interaction between the metalated Xyl unit and the metal center. At variance with Bergman original observations,^{15,16} the two adducts are stable at room temperature and do not undergo decomposition. Moreover, despite the lability of the coordinated molecule of CH_2Cl_2 (*vide infra*), α -H elimination to yield the desired cationic hydride alkylidene was not observed either. Regarding the formation of these carbene species, it is instructive to discuss briefly first the dynamic behavior exhibited in solution by the dichloromethane adducts $\mathbf{16}\text{-CH}_2\text{Cl}_2^+$ and $\mathbf{17}\text{-CH}_2\text{Cl}_2^+$, as well as their reactions with Lewis bases.



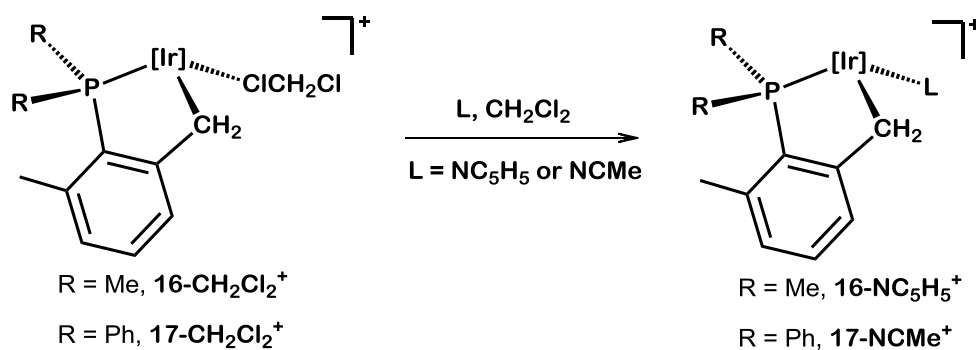
Scheme 54. Reaction of halide complexes (**14-17**)-Cl with NaBARF.

Compounds **16-CH₂Cl₂⁺** and **17-CH₂Cl₂⁺** were characterized by ¹H, ¹³C{¹H} and ³¹P{¹H} NMR spectroscopy. In the ³¹P{¹H} NMR spectrum they feature a broad signal at 8.3 and 35.5 ppm, respectively, whereas their ¹H NMR data are similar to those of their neutral chloride precursors, except for the resonances due to the Ir–CH₂ unit. Thus, at room temperature the ¹H NMR spectrum of compound **17-CH₂Cl₂⁺** did not present any resonance due to the metalated methylene group, although cooling at -20 °C resulted in the appearance of two broad doublets at 3.82 and 3.42 ppm (²J_{HH} = 15.6 Hz). Contrary to these observations, a broad signal at 2.90 ppm due to the Ir–CH₂ protons appeared in the ¹H NMR spectrum of **16-CH₂Cl₂⁺** at 25 °C, but it was necessary to cool the sample down to -90 °C to cause splitting of the broad resonance into two peaks with δ 3.52 and 3.20 ppm. These observations are indicative of dynamic behavior in solution that may consist in rapid CH₂Cl₂ dissociation, accompanied by reversible α-H elimination (Scheme 55). It is worth mentioning in this regard that the color of solutions of both cationic dichloromethane adducts is temperature dependent. At low temperatures (below -20 °C) the solutions are yellow, as found for **16-Cl**, **17-Cl** and other cationic adducts described below. However, warming above 10 °C results in darkening of the mixture to the characteristic intense orange color typical of hydride-alkylidenes **14⁺** and **15⁺**, that will be discussed below.



Scheme 55. Proposed mechanism for the dynamic behavior of **16-CH₂Cl₂⁺** and **17-CH₂Cl₂⁺**.

Compounds **16-CH₂Cl₂⁺** and **17-CH₂Cl₂⁺** readily reacted with Lewis bases such as NCMe or pyridine, to give the corresponding cationic adducts (Scheme 56). ³¹P{¹H} NMR signals due to **16-NC₅H₅⁺** (-0.5 ppm) and **17-NCMe⁺** (28.4 ppm) are sharp and have chemical shifts close to those of neutral compounds **16-Cl** (3.3 ppm) and **17-Cl** (28.6 ppm). In contrast to the related cationic dichloromethane adducts, the ¹H resonances of the Ir-CH₂ units are sharp, as a result of the much stronger coordination of the NC₅H₅ and NCMe ligands in comparison with CH₂Cl₂. The rest of ¹H and ¹³C{¹H} NMR data are in full agreement with previous findings.



Scheme 56. Reaction of cationic adducts **16-CH₂Cl₂⁺** and **17-CH₂Cl₂⁺** with Lewis bases.

The molecular structures of two cationic adducts, **16-NC₅H₅⁺** and **17-NCMe⁺**, have been confirmed by X-ray diffraction studies. Bond distances and angles are comparable to their neutral precursor **16-Cl** and **17-Cl**, as well as to other molecular structures of iridium complexes characterized by X-ray diffraction and already discussed herein.

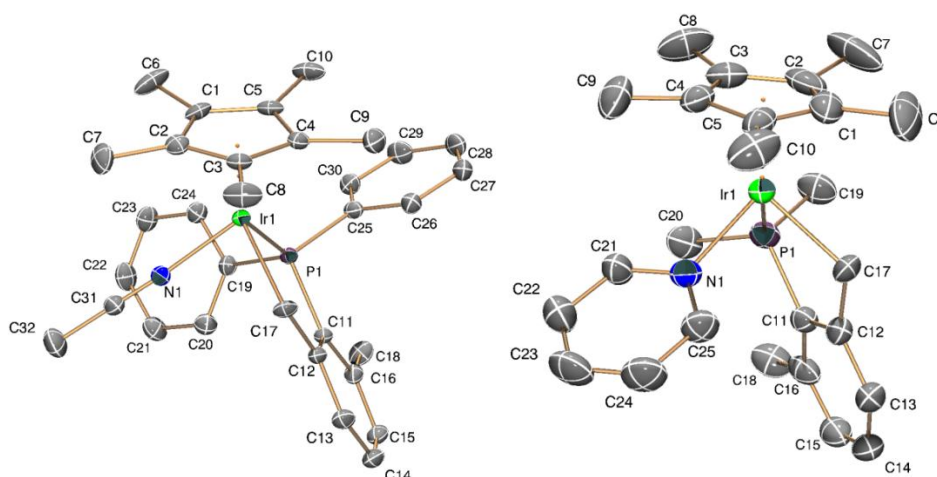
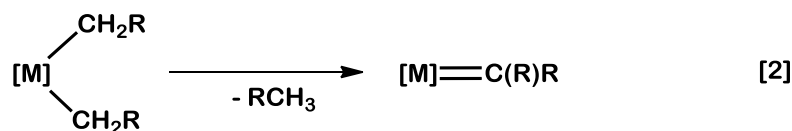


Figure 33. ORTEP diagram for compounds **16-NC₅H₅⁺** and **17-NCMe⁺**. Thermal ellipsoids are drawn at the 50 % probability and hydrogen atoms and counterions have been omitted for clarity.

It is well established since the early, pioneer work of Schrock and co-workers on Mo and W alkylidene complexes,⁶⁵ that the so-called α -H abstraction reaction, that eliminates a molecule of alkane RCH₃ from a dialkyl unit, [M](CH₂R)₂ (Eq. 2), becomes more facile upon increasing steric hindrance in the coordination sphere of the metal center.⁶⁵ As an illustrative example, α -H abstraction is favored in [M](CH₂CMe₃)₂ compounds over the [M](CH₂SiMe₃)₂ analogs, because of the steric pressure created in the proximity of M by the shorter C–C bond of the neopentyl group, in comparison with the C–Si bond of the trimethylsilylmethyl analog.

⁶⁵ (a) Schrock, R. R. *Acc. Chem. Res.* **1986**, *19*, 342. (b) Schrock, R. R. *Reactions of Coordinated Ligands*, **1986**, ed. P. R. Braterman, Plenum, New York. (c) Schrock, R. R. *J. Chem. Soc., Dalton Trans.* **2001**, 2541. (d) Fellmann, J. D.; Rupprecht, G. A.; Wood C. D.; Schrock, R. R. *J. Am. Chem. Soc.* **1978**, *100*, 5964.



With this knowledge in mind, we expected that the use of bulkier $\text{PR}_2(\text{Xyl})$ phosphines might allow to isolate the desired hydride alkylidenes, and indeed, under analogous conditions, reaction of NaBAr_F with the chloride derivatives of the cyclometalated $\text{P}^i\text{Pr}_2(\text{Xyl})$ (**14-Cl**) and $\text{PCy}_2(\text{Xyl})$ (**15-Cl**) derivatives gave the target compounds, **14**⁺ and **15**⁺, respectively, as the only reaction products (Scheme 54b).

The room-temperature ^1H NMR spectra of hydride-alkylidenes **14**⁺ and **15**⁺ are simpler than those of their halide precursors **14** and **15**, since the ^iPr and Cy substituents of the phosphine ligand appear as equivalent. Interestingly, ^1H NMR signals due to Ir-H and Ir=CH unit are not visible at room temperature. However, upon cooling to $-60\text{ }^\circ\text{C}$, ^1H NMR resonances at *ca.* 15.5 and -15.2 ppm due to Ir=CH and Ir-H protons of **14**⁺ (Figure 34) and **15**⁺ become discernible. The high-field peaks correspond to the hydride ligands and exhibit a two-bond coupling to the phosphorus nucleus of around 25 Hz, whereas signals due to the carbenic protons do not present any observable nuclear coupling. At these low temperatures ($< -60\text{ }^\circ\text{C}$), the phosphine ^iPr substituent become inequivalent and give rise to four somewhat broad, albeit clearly distinct, resonances.

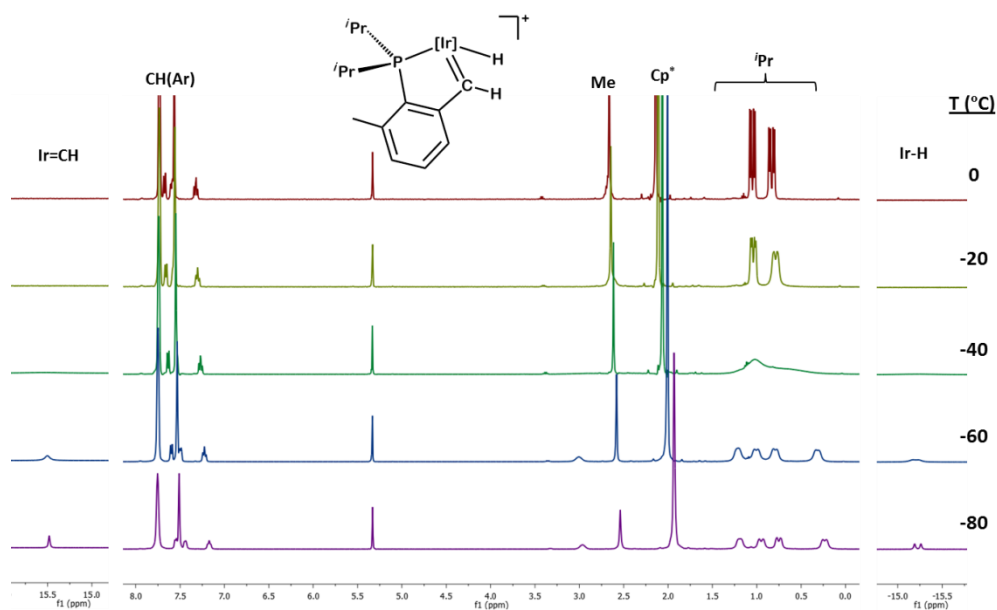


Figure 34. ^1H NMR (400 MHz, CD_2Cl_2) spectra of $\mathbf{14}^+$ at variable temperature (0 to -80°C).

This solution dynamic behavior results, most likely, from a rapid and reversible 1,2-H shift between Ir and the alkylidene carbon. We analyzed the exchange of these protons by 1D-EXSY studies. Rate constants of 14.7 and 45.5 s^{-1} were measured at -80°C for compounds $\mathbf{14}^+$ and $\mathbf{15}^+$, respectively. An Eyring analysis (Figure 35) in the temperature interval from -70 to -90°C yielded values of the activation parameters $\Delta H^\ddagger = 7.3 \pm 0.6\text{ kcal mol}^{-1}$ and $\Delta S^\ddagger = 12 \pm 1\text{ cal mol}^{-1}\text{K}^{-1}$, with $\Delta G^\ddagger_{298\text{K}} = 11 \pm 1\text{ kcal mol}^{-1}$ for compound $\mathbf{14}^+$ (and similar values for compound $\mathbf{15}^+$: $\Delta H^\ddagger = 9 \pm 2\text{ kcal mol}^{-1}$ and $\Delta S^\ddagger = 6 \pm 1\text{ cal mol}^{-1}\text{K}^{-1}$, with $\Delta G^\ddagger_{298\text{K}} = 11 \pm 2\text{ kcal mol}^{-1}$).

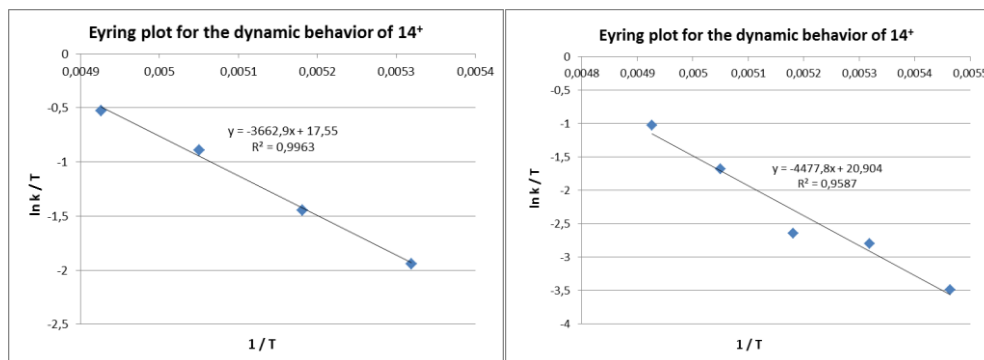


Figure 35. Eyring plots for the solution dynamic behavior of compounds (a) **14⁺** and (b) **15⁺** between -70 and -90 °C.

The molecular structure of compound **14⁺** was confirmed by X-ray diffraction studies. A characteristic Ir(1)–C(17) bond distance of 1.896(5) Å, considerably shorter than related Ir–CH₂ (*ca.* 2.1 Å) bond distances of complexes already discussed, is in accordance with the alkylidene formulation. Other geometrical parameters are in agreement with related structures already considered and do not need any further discussion.

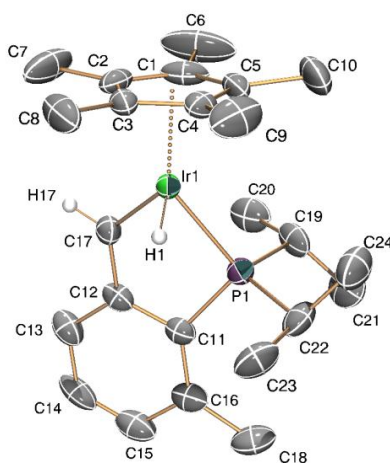
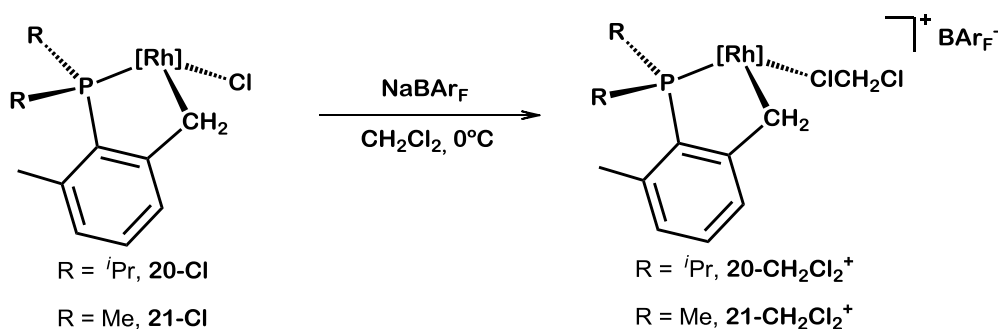


Figure 36. ORTEP diagram for compound **14⁺**. Thermal ellipsoids are drawn at the 50 % probability and hydrogen atoms and counterion have been omitted for clarity.

Considering now analogous Rh complexes, we chose two of these phosphines, namely $P^i\text{Pr}_2(\text{Xyl})$ and $\text{PMe}_2(\text{Xyl})$, for the synthesis of the related chloride derivatives **20-Cl** and **21-Cl**, respectively. In contrast with results already discussed for iridium, the two complexes reacted with NaBAR_F to generate the cationic adducts **20-CH₂Cl₂⁺** and **21-CH₂Cl₂⁺** (Scheme 57).



Scheme 57. Reaction of compounds **20-Cl** and **21-Cl** with NaBAR_F .

Slow diffusion of pentane into a concentrated dichloromethane solution of **20-CH₂Cl₂⁺** at -25°C gave suitable crystals for X-ray analysis (Figure 37). Only three previous examples of rhodium compounds with a dichloromethane molecule directly bound to the metal center have been reported to date,^{19,66} two of which are closely related to **20-CH₂Cl₂⁺**, namely $[(\eta^5\text{-C}_5\text{Me}_5)\text{Rh}(\text{PMe}_3)\text{Me}(\text{CH}_2\text{Cl}_2)]^+$ and $[(\eta^5\text{-C}_5\text{Me}_5)\text{Rh}(\text{PMe}_3)\text{Ph}(\text{CH}_2\text{Cl}_2)]^+$. These two complexes are air sensitive, and also thermally unstable and readily decompose at room temperature even under inert atmosphere. In contrast, **20-CH₂Cl₂⁺** is stable in solution for many days when stored under

⁶⁶ Cotton F. A., Murillo, C. A.; Stiriba, S.-E.; Wang, X.; Yu, R. *Inorg. Chem.* **2005**, *44*, 8223.

argon at room temperature, and remained unaltered after more than one year in the solid state. The related Ir adducts prepared in this work show similar stability. It is possible that the existence of an intramolecular CH– π interaction between the dichloromethane molecule and the metalated xylyl ring (Figure 37b) might account for the higher stability exhibited by our metalated compounds in comparison with previous examples.^{16,17,19} This intramolecular CH– π interaction is characterized by CH(25b)···C(12) and CH(25b)···C(13) bond distances of *ca.* 2.64 and 2.73 Å, whereas the C–H(25b)···Centr. angle has a value of *ca.* 157.6° (Centr. = metalated xylyl ring centroid).

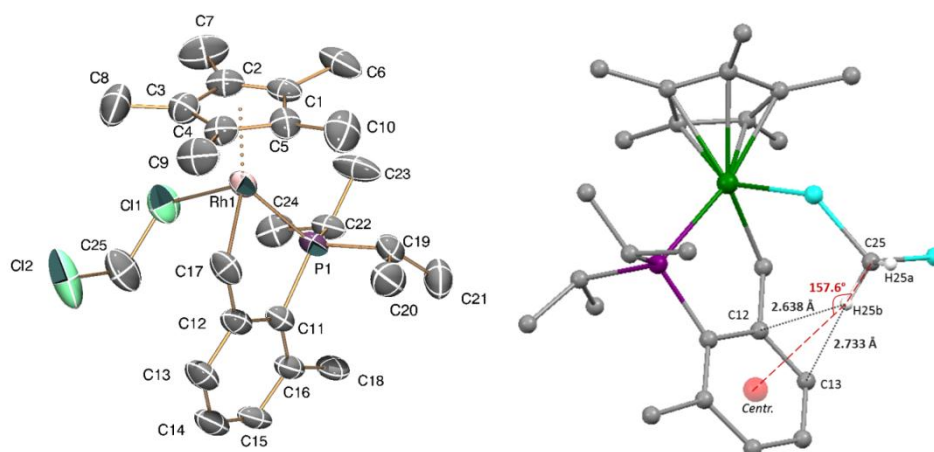


Figure 37. (a) ORTEP diagram for compound **20-CH₂Cl₂⁺**. Thermal ellipsoids are drawn at the 50 % probability and hydrogen atoms and counterion have been omitted for clarity. (b) Intramolecular CH– π contacts in **20-CH₂Cl₂⁺** (Centr. = xylyl ring centroid).

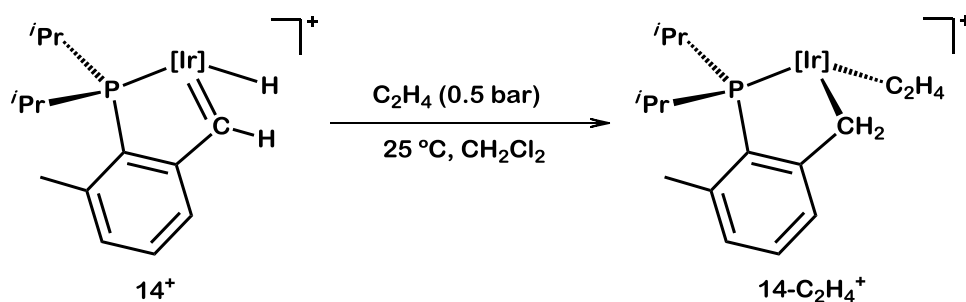
To conclude this section, it should be stated that for the iridium systems discussed in this Thesis α -H elimination that leads to the formation of

alkylidene functionalities is favored when the metal environment is sterically congested, as observed for compounds **14**⁺ and **15**⁺ with bulky phosphine ligands. On the other hand, reduced steric encumbrance around the metal favors coordination of a molecule of dichloromethane, to give the corresponding adducts (**16-CH₂Cl₂**⁺ and **17-CH₂Cl₂**⁺). Steric effects seem to be less significant in our rhodium compounds, where abstraction of the halide ligand led to the formation of the corresponding dichloromethane adduct in all cases.

2.B.3. Reactivity Studies of Hydride-Alkylidene **14**⁺

As already mentioned, iridium(III) alkylidenes are very rare.^{40b,42,43} Hence, the unusual stability of alkylidenes **14**⁺ and **15**⁺ is intriguing. We chose compound **14**⁺ to perform some reactivity studies whose results will be discussed herein. Treatment of a dichloromethane solution of **14**⁺ with C₂H₄ causes an immediate color change, from the characteristic intense red of the alkylidene to pale yellow, due to formation of the cationic ethylene adduct **14-C₂H₄**⁺ (Scheme 58). This compound is characterized by a typical ABX (X = ³¹P) spin system in the ¹H NMR spectrum due to the diastereotopic Ir-CH₂ protons, as already discussed for other cyclometalated iridium complexes. These signals appear at 3.67 (d, ²J_{HH} = 12.5 Hz) and 3.39 (dd, ²J_{HH} = 12.5, ³J_{HP} = 3.3 Hz). The ethylene group gives two broad signals (2 H each) at 2.77 and 2.29 ppm, with corresponding ¹³C{¹H} NMR broad resonances at 46.8

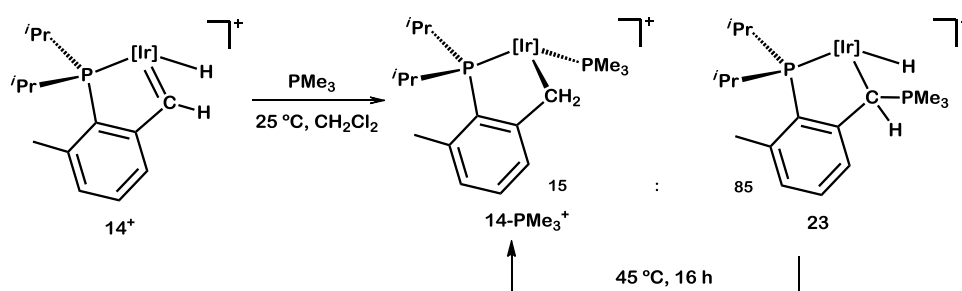
and 42.5 ppm. The $^{31}\text{P}\{^1\text{H}\}$ NMR resonance appears at 42.7 ppm, shielded with respect to the corresponding signal for compound **14**⁺ (73.1 ppm) and much closer to the corresponding resonance due to **14-Cl** (42.7 ppm).



Scheme 58. Reaction of **14**⁺ with C₂H₄.

Addition of nucleophiles to solutions of **14**⁺ confirmed the electrophilic character of its alkyldiene functionality. Reaction of **14**⁺ with PMe₃ (Scheme 59) resulted in an immediate color change, due to generation of the phosphonium ylid **23** as the major reaction product (85 %). The cationic adduct, **14-PMe}_3**⁺, was formed too, albeit in low yield (*ca.* 15 %). This result is in accordance with the electrophilic character of the alkyldiene moiety. Compound **14-PMe}_3**⁺ exhibit a $^{31}\text{P}\{^1\text{H}\}$ NMR signal at 48.1 ppm (very close to corresponding signals due to **14-Cl**, at 49.6 ppm, and **14-C}_2\text{H}_4**⁺, at 42.7 ppm), which appears as a doublet, due to coupling to the PMe₃ phosphorus nucleus. The latter also appears as a doublet (δ -47.3 ppm; $^2J_{\text{PP}} = 21$ Hz). In contrast, the $^{31}\text{P}\{^1\text{H}\}$ NMR signal due to the metalated phosphine of compound **23** appears at 59.3 ppm, and its phosphonium PMe₃ group yields a resonance at 33.1 ppm, highly deshielded with respect to the corresponding resonance in compound **14-PMe}_3**⁺ (-47.3 ppm), and without observable coupling to the phosphorus center of the cyclometalated phosphine. A

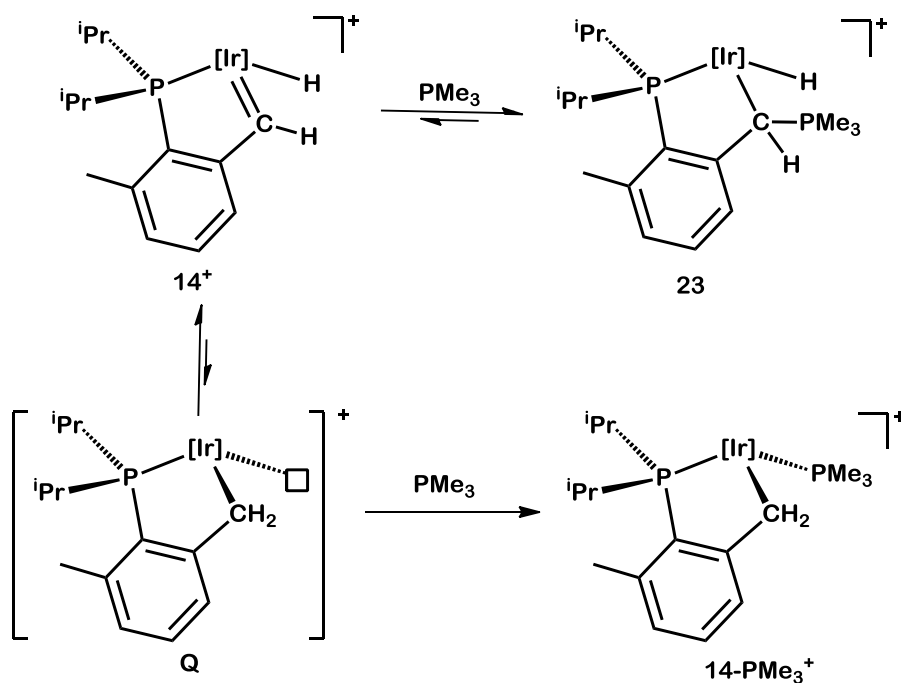
characteristic doublet due to the Ir–H unit appears in the ^1H NMR spectrum at -17.7 ppm (dd, $^2J_{\text{HP}} = 33.3$, $^3J_{\text{HP}} = 10.6$ Hz). In the $^{13}\text{C}\{^1\text{H}\}$ NMR spectrum, the signal due to the IrCHPMe₃ is observed at 6.3 ppm (d, $^1J_{\text{CP}} = 32$ Hz), widely shifted with respect to the resonance due to the carbenic carbon of **14**⁺ (263.8 ppm).



Scheme 59. Reaction of **14**⁺ with PMe₃.

Heating a mixture of **14-PMe₃**⁺ and **23** at 40 °C for 16 hours caused quantitative conversion of the ylide species **23** into the phosphine adduct **14-PMe₃**⁺. Monitoring the reaction by ^{31}P NMR spectroscopy provided a first-order kinetic rate constant of $3.39 \cdot 10^{-5} \text{ s}^{-1}$, which corresponds to a ΔG^\ddagger of $24.8 \pm 0.3 \text{ kcal} \cdot \text{mol}^{-1}$ at 40 °C (Figure 43 in the Experimental Section). The latter compound is thermally stable and does not revert to **23**, even after heating a $\text{ClCH}_2\text{CH}_2\text{Cl}$ solution of the compound over 80 °C for several hours. These results indicate that ylid **23** and adduct **14-PMe₃**⁺ are the kinetic and thermodynamic products of the reaction, respectively. Moreover, formation of the former is reversible, whereas the generation of the latter is an irreversible process. The already discussed solution dynamic behavior of **14**⁺ is in agreement with these findings. Thus, compound **14-PMe₃**⁺ must form by

attack of PMe_3 to intermediate **Q** in Scheme 60, whereas **23** would be the product of the direct reaction between hydride-alkylidene **14**⁺ and PMe_3 .



Scheme 60. Reaction products for the interaction of **14**⁺ with PMe_3 .

The molecular structure of compound **14-PMe}_3^+** was confirmed further by X-ray diffraction studies of crystals obtained from CH_2Cl_2 /pentane solutions of the complex (Figure 38a). The two Ir–P bond distances are identical within experimental error (*ca.* 2.28 Å), whereas the rest of geometrical parameters are similar to those already discussed for related compounds.

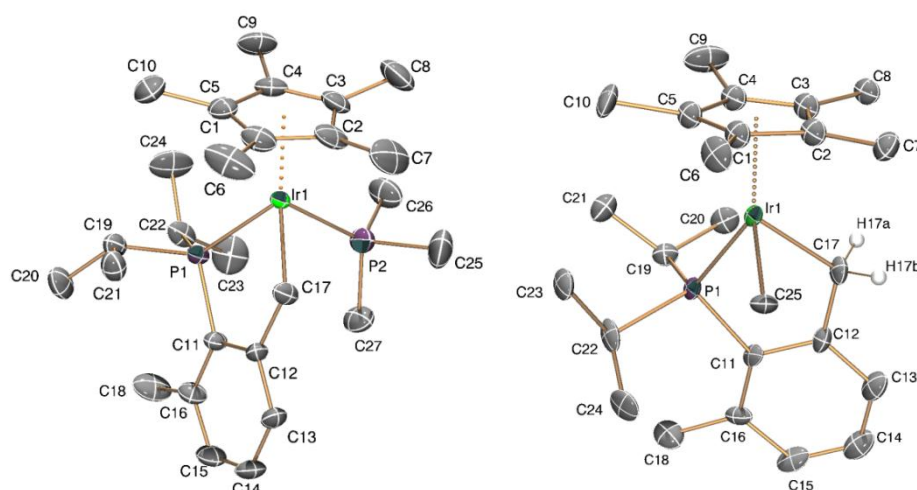
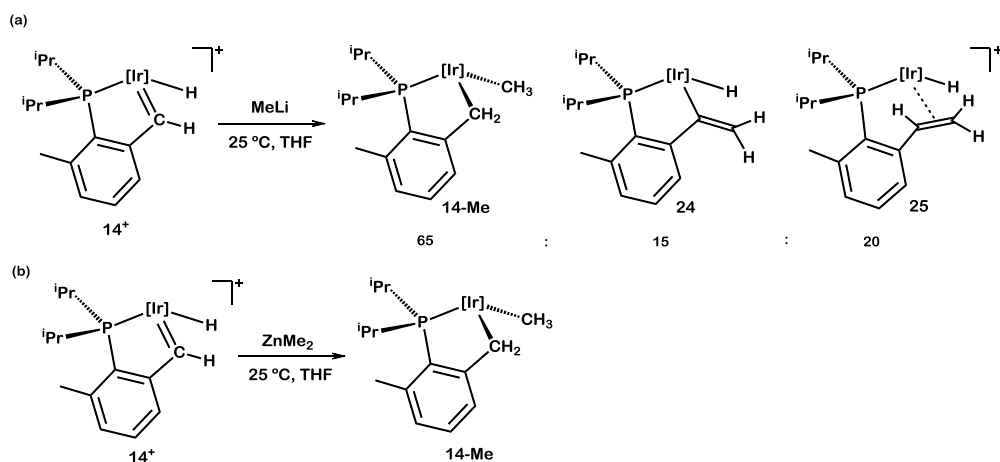


Figure 38. ORTEP diagram for compounds: (a) **14-PMe₃⁺** and (b) **14-Me**. Thermal ellipsoids are drawn at the 50 % probability and hydrogen atoms and the counterion of **14-PMe₃⁺** have been omitted for clarity.

The reaction of **14⁺** with LiMe led to the formation of neutral **14-Me** (Scheme 61a) as the major product (*ca.* 65 % yield), along with two other compounds, **24** (15 %) and **25** (20 %). Alkyl species **14-Me** features characteristic ¹H NMR signals due to diastereotopic Ir–CH₂ protons at 3.16 (d, ²*J*_{HH} = 14.2 Hz) and 2.05 (dd, ²*J*_{HH} = 14.2, ³*J*_{HP} = 3.4 Hz) ppm, as well as a shielded doublet at -0.20 ppm due to the Ir–Me unit, with a three-bond coupling to phosphorus of 3.4 Hz. The proposed formulation for this compound has been further demonstrated by reaction of the alkylidene **14⁺** with the milder alkylating reagent ZnMe₂, that led to quantitative formation of **14-Me** (Scheme 61b). Moreover, its molecular structure has been confirmed by X-ray diffraction studies (Figure 38b). The Ir(1)–C(17) and Ir(1)–C(25) bond distances are identical within the experimental error, with

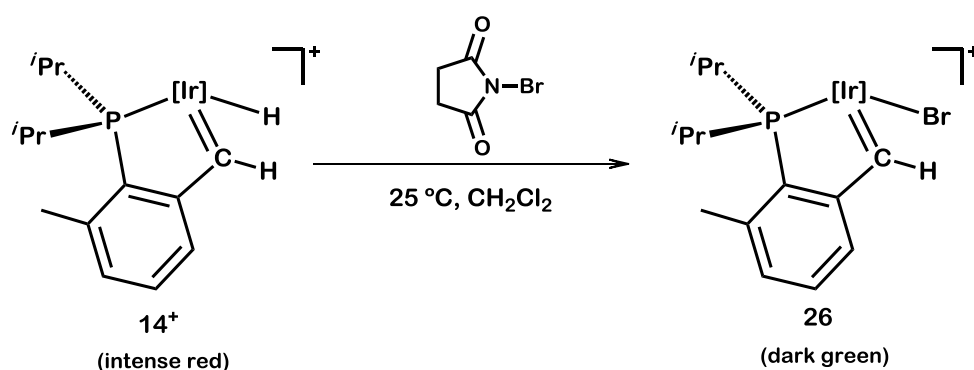
values of *ca.* 2.11 Å. Other bond angles and distances are in agreement with previously discussed molecular structures of related complexes.



Scheme 61. (a) Reaction of **14**⁺ with LiMe. (b) Reaction of **14**⁺ with ZnMe₂.

The formulation of compounds **24** and **25** was tentatively assigned on the basis of their solubility properties and spectroscopic data. Similarly to **14-Me**, compound **24** is soluble in pentane, while **25** can only be dissolved in polar solvents, like chlorinated solvents, tetrahydrofuran, etc. This indicates neutral formulation of the latter and ionic of the former. The two contain a hydride ligand (**24**, δ -18.7, $^2J_{\text{HP}}$ = 17.2 Hz; **25**, δ -16.6, $^2J_{\text{HP}}$ = 28.2 Hz) and while for **24** only a broad signal at δ 2.87 can be found for olefinic protons, three distinct resonances at 4.11 (dd, $^3J_{\text{HH}}$ = 10.3 Hz, $^3J_{\text{HH}}$ = 8.4 Hz), 2.26 (d, $^3J_{\text{HH}}$ = 8.4 Hz) and 2.18 (dt, $^3J_{\text{HH}}$ = 10.4, $^3J_{\text{HP}}$ = 2.5 Hz) are discerned for the olefinic protons of **25**. Corresponding $^{13}\text{C}\{^1\text{H}\}$ resonances appear at 60.1 and 33.9 ppm.

To characterize further the hydride alkylidene complex **14**⁺, it was converted into its bromide analog by reaction with *N*-bromosuccinimide (Scheme 62). The new alkylidene, **26**, features a dark green color and alkylidene NMR resonances at δ 16.1 (¹H) and 262.2 (¹³C) ppm, the latter with ¹*J*_{CH} = 152 Hz. Figure 39 shows an ORTEP view of the molecules of this compound, which exhibits an Ir–alkylidene bond length of 1.907(2) Å, similar to that found in related complexes prepared in this work.



Scheme 62. Reaction of **14**⁺ with *N*-bromosuccinimide.

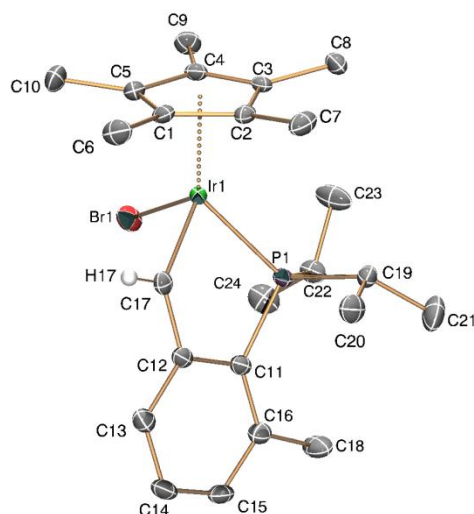
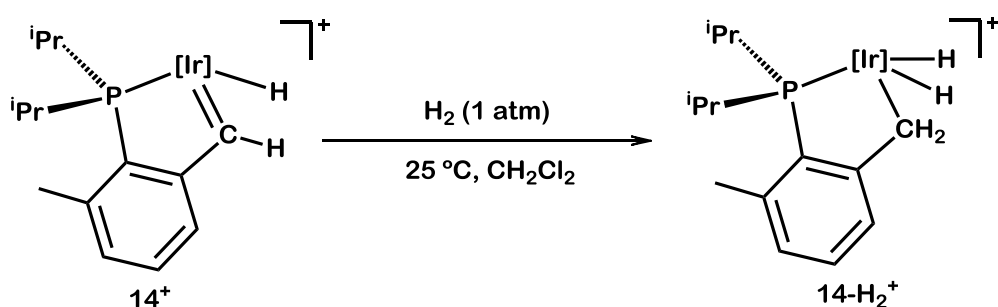


Figure 39. ORTEP diagram for compound **26**. Thermal ellipsoids are drawn at the 50 % probability and hydrogen atoms and the counterion have been omitted for clarity.

Finally, we also studied the reaction of **14**⁺ with H₂ (Scheme 63), which resulted in quantitative formation of the cationic alkyl-dihydride species **14-H₂**⁺. This reaction might proceed either from direct addition of H₂ to the Ir=CH unit or by dihydrogen-induced migratory insertion chemistry, that would involve coordination of H₂ to unsaturated species **Q** in Scheme 60, followed by oxidative cleavage. Interestingly, reaction of **14**⁺ with D₂ led to the formation of [**D**₅]-**14-D**₂⁺, in which the two benzylic positions of the xylyl ring became deuterated. H/D exchange at the non-metalated *o*-methyl group might proceed through formation of an intermediate alike **C** in Scheme 21.

Scheme 63. Reaction of 14^+ with H_2 .

Similarly to complex $1\text{-}H_2^+$ (see Figure 14), compound $14\text{-}H_2^+$ also exhibits dynamic behavior in solution, consisting in the exchange of the two hydride ligands and the two methylene protons. At room temperature, the 1H NMR spectrum does not contain any observable resonances due to these four protons. However, at $-20\text{ }^\circ\text{C}$, broad signals become visible at 2.45 and 2.93 ppm ($Ir\text{-}CH_2$), along with a broad resonance at -13.62 due to the hydride ligands. Coalescence is reached at *ca.* $-10\text{ }^\circ\text{C}$ and further cooling to $-40\text{ }^\circ\text{C}$ allowed identifying a two-bond coupling constant of 13.0 Hz between the diastereotopic methylene protons. At $-50\text{ }^\circ\text{C}$ the signal for the two hydride ligands splits into two different peaks. Heating the solution at $45\text{ }^\circ\text{C}$ resulted in the appearance of a broad signal due to four protons at -4.98 ppm (not shown in Figure 40). Lineshape analysis of the corresponding resonances at various temperatures in conjunction with Eyring analysis of the observed rate constants yields activation parameters for the overall process similar to those obtained for $1\text{-}H_2^+$: $\Delta H^\ddagger = 20.3 \pm 0.5\text{ kcal}\cdot\text{mol}^{-1}$, $\Delta S^\ddagger = 3 \pm 2\text{ cal}\cdot\text{mol}^{-1}\cdot\text{K}^{-1}$ and $\Delta G^\ddagger_{300\text{K}} = 12 \pm 2\text{ kcal}\cdot\text{mol}^{-1}$.

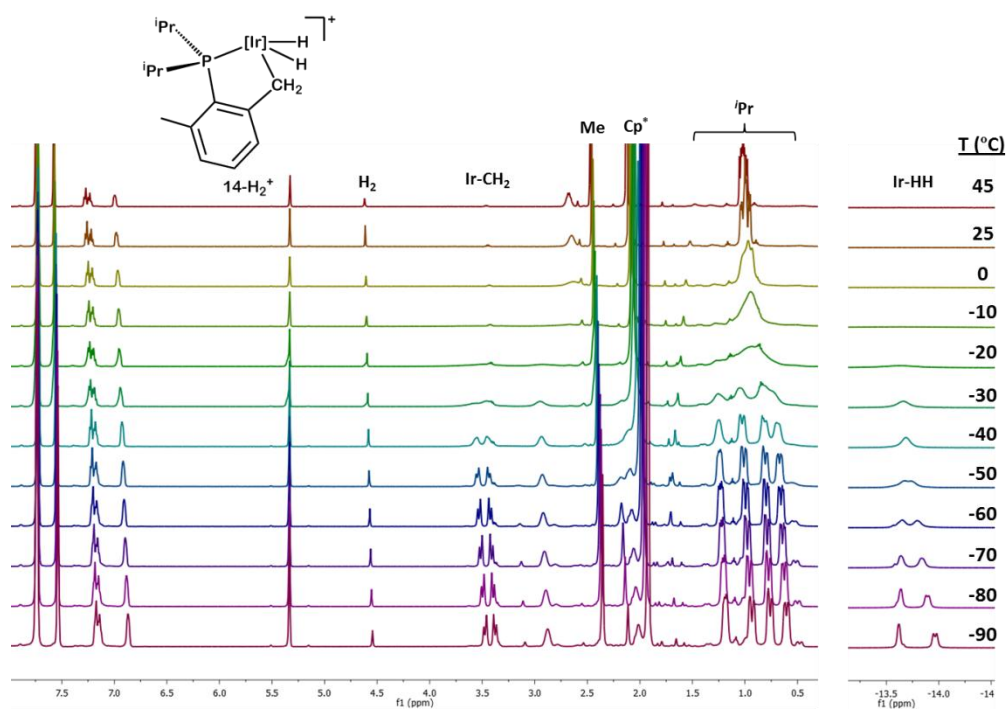


Figure 40. Solution dynamic behavior of 14-H_2^+ by ^1H NMR.

Summary and Conclusion

With the aim of isolating stable, cationic Ir(III) hydride alkylidene structures, we prepared cyclometalated rhodium and iridium chloride complexes derived from $PR_2(Xyl)$ phosphines, where $R = Me, Ph, ^iPr$ and Cy . In accordance with literature precedents, we found that the somewhat smaller $PMe_2(Xyl)$ and $PPh_2(Xyl)$ ligands afforded cationic $Ir(III)-CH_2Cl_2$ adducts, while the bulkier $P^iPr_2(Xyl)$ and $PCy_2(Xyl)$ yielded instead the desired alkylidenes, which undergo reversible migratory insertion/ α -H elimination reactivity. Analogous rhodium compounds provided only CH_2Cl_2 adducts. The electrophilic character of the new iridium alkylidenes was demonstrated by their reaction with Lewis bases, particularly with PMe_3 , which resulted in the formation of a trimethyl phosphonium ylide that subsequently rearranged into the thermodynamically more stable migratory insertion product.

II.3. EXPERIMENTAL SECTION

Part A:
**Study of (η^5 -C₅Me₅)Ir(PMe(Xyl)₂)-Derived
Compounds**

3.A. EXPERIMENTAL SECTION

3.A.1. Materials and Methods. General.

All operations were performed under an argon atmosphere using standard Schlenk techniques, employing dry solvents and glassware. HRMS data were obtained using a Jeol JMS-SX 102A mass spectrometer at the Analytical Services of the Universidad de Sevilla (CITIUS). Microanalyses were performed by the Microanalytical Service of the Instituto de Investigaciones Químicas (Sevilla, Spain). Infrared spectra were recorded on a Bruker Vector

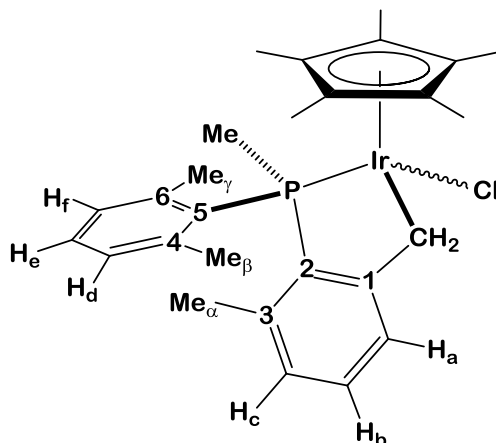
22 spectrometer. The NMR instruments were Bruker DRX-500, DRX-400 and DRX-300 spectrometers. Spectra were referenced to external SiMe₄ (δ 0 ppm) using the residual proton solvent peaks as internal standards (¹H NMR experiments), or the characteristic resonances of the solvent nuclei (¹³C NMR experiments), while ³¹P was referenced to external H₃PO₄. Spectral assignments were made by routine one- and two-dimensional NMR experiments where appropriate. The crystal structures were determined in a Bruker-Nonius, X8Kappa diffractometer. Dimer [(η^5 -C₅Me₅)IrCl₂]₂,⁶⁷ NaBAr_F⁶⁸ and [H(OEt)₂][BAr_F]⁶⁹ were prepared according to literature procedures. In the ¹H NMR spectra all aromatic couplings are of *ca.* 7.5 Hz. The ¹H and ¹³C{¹H} NMR spectral data for the BAr_F⁻ anion (BAr_F = B[3,5-(CF₃)₂C₆H₃]) in CD₂Cl₂ are identical for all complexes and therefore are not repeated below. BAr_F⁻: ¹H RMN: δ 7.75 (s, 8 H, *o*-Ar), 7.58 (s, 4 H, *p*-Ar). ¹³C{¹H} RMN: δ 162.1 (q, 37 Hz, *ipso*-Ar), 135.3 (*o*-Ar), 129.2 (q, 31 Hz, *m*-Ar), 124.9 (q, 273 Hz, CF₃), 117.8 (*p*-Ar). ¹H NMR simulations were performed employing the P.H.M. Budzelaar gNMR V4.01 package, Cherwell Scientific Publishing, Oxford, U.K.

⁶⁷ White, C.; Yates, A.; Maitlis, P. M.; Heinekey, D. M. *Inorg. Synth.* **1992**, 29, 228.

⁶⁸ Yakelis, N. A.; Bergman, R. G. *Organometallics*, **2005**, 24, 3579.

⁶⁹ Brookhart, M.; Grant, B.; Volpe, Jr. A. F. *Organometallics*, **1992**, 11, 3920.

3.A.2. Synthesis of iridium organometallic complexes



$[\text{Cp}^*\text{IrCl}_2]_2$ (1.53 g, *ca.* 1.92 mmol) was dissolved in dry CH_2Cl_2 (40 mL) in a Schlenk flask with a stir bar. The dark solution was cooled to 0°C and PXyl_2Me (1.00 g, 3.89 mmol) dissolved in CH_2Cl_2 (10 mL) was added, followed by the addition of 2,2,6,6-tetramethyl piperidine (660 μL , 3.89 mmol). The reaction mixture was allowed to warm to room temperature and additionally stirred for 2 h. The solvent was removed in vacuo and the product extracted with toluene in air. The solution was evaporated to dryness providing a bright yellow powder, which was washed with pentane to yield compound **1** as a mixture of two isomers (*ca.* 7:3 ratio; 2.16g, 3.50 mmol, 90%). Heating this mixture to 40°C in $\text{CH}_2\text{Cl}_2/\text{MeOH}$ (1:1) for 2 h provides exclusively the major stereomer for which characterization data are given below. Crystallization from $\text{CH}_2\text{Cl}_2/\text{pentane}$ provides analytically pure samples of the desired product.

Analytical and spectroscopic data

Anal. Calcd. for $C_{27}H_{35}ClIrP$: C, 52.46; H, 5.71. **Found:** C, 52.0; H, 6.1.

1H NMR (500 MHz, C_6D_6 , 25 °C) δ : 7.54 (d, 1 H, H_a), 7.04 (td, 1 H, $^5J_{HP}$ = 1.6 Hz, H_b), 6.89 (td, 1 H, $^3J_{HP}$ = 1.0 Hz, H_e), 6.84, 6.62 (dd, 1 H each, $^4J_{HP}$ = 2.3 Hz, H_d , H_f), 6.69 (dd, 1 H, $^4J_{HP}$ = 2.7 Hz, H_c), 4.15 (dd, 1 H, $^2J_{HH}$ = 14.5, $^3J_{HP}$ = 3.8 Hz, IrCHH), 3.87 (d, 1 H, $^2J_{HH}$ = 14.5 Hz, IrCHH), 2.35, 1.47 (s, 3 H each, Me_β , Me_γ), 2.28 (d, 3 H, $^2J_{HP}$ = 10.4 Hz, PMe), 1.78 (s, 3 H, Me_α), 1.32 (d, 15 H, $^4J_{HP}$ = 1.9 Hz, C_5Me_5). All aromatic couplings are of *ca.* 7.5 Hz.

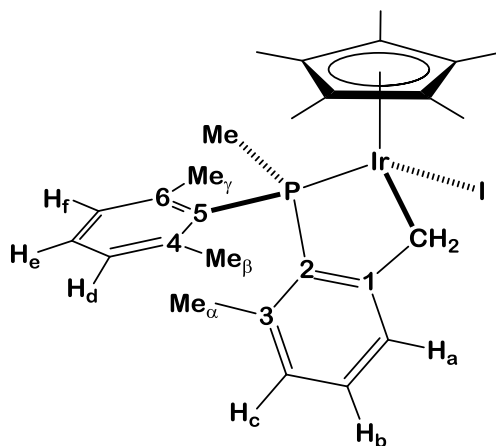
$^{13}C\{^1H\}$ NMR (125 MHz, C_6D_6 , 25 °C) δ : 158.3 (d, $^2J_{CP}$ = 32 Hz, C_1), 140.8 (d, $^1J_{CP}$ = 61 Hz, C_2), 141.5, 139.9 (d, $^2J_{CP}$ = 8 Hz, C_4 , C_6), 139.2 (C_3), 131.7 (d, $^1J_{CP}$ = 44 Hz, C_5), 129.4, 129.3 (CH_d , CH_f), 129.8 (CH_b), 128.9 (CH_e), 128.0 (CH_a), 127.1 (d, $^3J_{CP}$ = 6 Hz, CH_c), 91.7 (d, $^2J_{CP}$ = 2 Hz, C_5Me_5), 25.0, 22.7 (d, $^3J_{CP}$ = 4 Hz, 8Hz, Me_β , Me_γ), 20.8 (Me_α), 20.3 (IrCH₂), 18.0 (d, $^1J_{CP}$ = 40 Hz, PMe), 7.8 (C_5Me_5).

$^{31}P\{^1H\}$ NMR (200 MHz, C_6D_6 , 25 °C) δ : 11.3.

The minor diastereomer of compound **1-Cl** is characterized by 1H NMR multiplets with δ 4.70 and 3.59 ppm, due to the IrCH₂ protons and by a doublet at 1.47 ppm associated with the C_5Me_5 ligand. In the $^{31}P\{^1H\}$ NMR spectrum a singlet is recorded with δ 7.8 ppm.

General synthesis of halide and pseudohalide compounds 1-X

A mixture of **1-Cl** (100 mg, 0.16 mmol), with a *ca.* ten- or twenty-fold excess of LiBr, MgI₂ or NH₄SCN, was suspended in THF (10 mL) under argon, and heated at 60-70 °C for 12 hours (for **1-Br** the reaction mixture was refluxed for three days). The solvent was then evaporated under reduced pressure and the resulting residue extracted with CH₂Cl₂ (**1-Br**) or with toluene (3 x 10 mL for **1-I** and **1-SCN**). Filtration of the solution and removal of the solvent under vacuum yielded the desired complexes in the form of orange (**1-Br**; 98 mg, 0.15 mmol, 92% yield) or yellow powders (**1-I**; 91 mg, 0.13 mmol, 80%; **1-SCN**, 85 mg, 0.13 mmol, 83%). Crystalline, analytically pure samples of the compounds were obtained by crystallization from CH₂Cl₂/pentane solvent mixtures. The thiocyanate complex forms as a *ca.* 85:15 mixture of stereomers. Analytical and spectroscopic data for these compounds are given below.

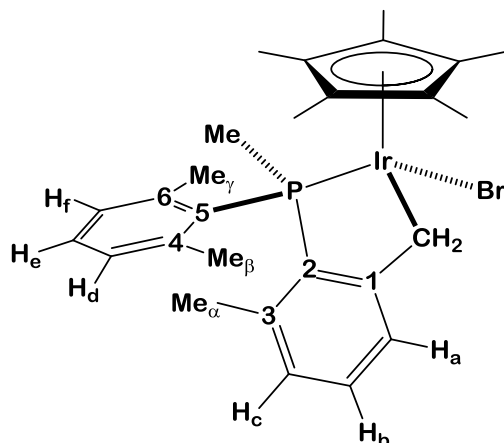
Compound 1-I**Analytical and spectroscopic data**

Anal. Calcd. for $C_{27}H_{35}IrP$: C, 45.70; H, 4.97. **Found:** C, 45.5; H, 4.6.

1H NMR (400 MHz, CD_2Cl_2 , 25 °C) δ : 7.30 (d, 1 H, H_a), 7.18, 6.91 (m, 2 H and 1 H, H_d , H_e , H_f), 7.10 (td, 1 H, $^5J_{HP} = 1.8$ Hz, H_b), 6.83 (dd, 1 H, $^4J_{HP} = 2.9$ Hz, H_c), 4.04 (dd, 1 H, $^2J_{HH} = 14.8$ Hz, $^3J_{HP} = 4.7$ Hz, IrCHH), 3.76 (d, 1 H, $^2J_{HH} = 14.8$ Hz, IrCHH), 2.70 (d, 3 H, $^2J_{HP} = 10.0$ Hz, PMe), 2.60, 1.44 (s, 3 H each, Me_β , Me_γ), 1.98 (s, 3 H, Me_α), 1.60 (d, 15 H, $^4J_{HP} = 1.7$ Hz, C_5Me_5). All aromatic couplings are of *ca.* 7.5 Hz.

$^{13}C\{^1H\}$ NMR (100 MHz, CD_2Cl_2 , 25 °C) δ : 159.1 (d, $^2J_{CP} = 30$ Hz, C_1), 141.6, 140.5 (C_4 , C_6), 141.3 ($^1J_{CP} = 60$ Hz, C_2), 140.2 (C_3), 132.1 (d, $^1J_{CP} = 44$ Hz, C_5), 130.4, 129.9 (d, $^3J_{CP} = 8$ Hz, CH_d , CH_f), 129.8 (CH_e), 129.5 (CH_b), 127.70 (d, $^4J_{CP} = 7$ Hz, CH_c), 127.3 (d, $^4J_{CP} = 14$ Hz, CH_a), 93.0 (C_5Me_5), 28.2 (d, $^1J_{CP} = 43$ Hz, PMe), 26.1, 22.9 (d, $^3J_{CP} = 5, 7$ Hz, Me_β , Me_γ), 20.8 (Me_α), 14.8 (IrCH₂), 8.9 (C_5Me_5).

$^{31}P\{^1H\}$ NMR (160 MHz, CD_2Cl_2 , 25 °C) δ : 3.2.

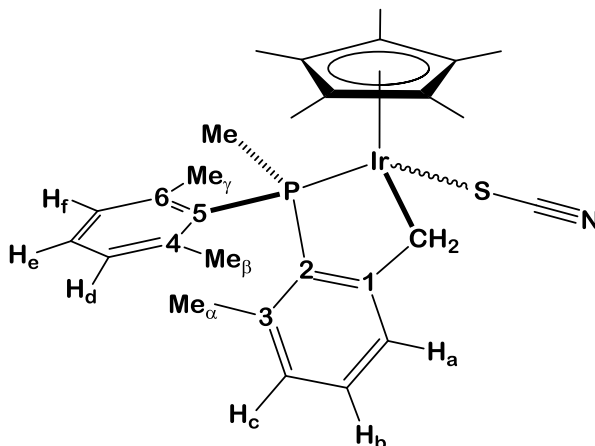
Compound 1-Br**Analytical and spectroscopic data**

Anal. Calcd. for $C_{27}H_{35}BrIrP$: C, 48.94; H, 5.32. **Found:** C, 48.7; H, 5.3.

1H NMR (400 MHz, $CDCl_3$, 25 °C) δ : 7.32 (d, 1 H, H_a), 7.12, 6.86 (m 2 H and 1 H, H_d , H_e , H_f), 7.04 (td, 1 H, $^5J_{HP} = 1.8$ Hz, H_b), 6.75 (dd, 1 H, $^4J_{HP} = 3.0$ Hz, H_c), 3.82 (dd, 1 H, $^2J_{HH} = 14.9$ Hz, $^3J_{HP} = 3.9$ Hz, IrCHH), 3.74 (d, 1 H, $^2J_{HH} = 14.9$ Hz, IrCHH), 2.61, 1.45 (s, 3H each, Me_β , Me_γ), 2.42 (d, 3 H, $^2J_{HP} = 10.2$ Hz, PMe), 1.96 (s, 3 H, Me_α), 1.49 (d, 15 H, $^4J_{HP} = 1.7$ Hz, C_5Me_5). All aromatic couplings are of *ca.* 7.5 Hz.

$^{13}C\{^1H\}$ NMR (100 MHz, $CDCl_3$, 25 °C) δ : 157.9 (d, $^2J_{CP} = 31$ Hz, C_1), 141.4, 139.9 (d, $^2J_{CP} = 8$ Hz, C_4 , C_6), 140.1 (d, $^1J_{CP} = 62$ Hz, C_2), 139.3 (C_3), 131.4 (d, $^1J_{CP} = 45$ Hz, C_5), 129.9, 129.5 (d, $J = 8$ Hz, CH_d , CH_f), 129.6 (CH_b), 129.1 (CH_e), 127.4 (d, $^3J_{CP} = 14$ Hz, CH_a), 127.1 (d, $^3J_{CP} = 7$ Hz, CH_c), 92.1 (d, $^2J_{CP} = 3$ Hz, C_5Me_5), 25.5, 22.7 (d, $^3J_{CP} = 5$ Hz, 7 Hz, Me_β , Me_γ), 21.3 (d, $^1J_{CP} = 41$ Hz, PMe), 20.5 (Me_α), 18.6 (IrCH₂), 8.2 (C_5Me_5).

$^{31}P\{^1H\}$ NMR (160 MHz, $CDCl_3$, 25 °C) δ : 7.9.

Compound 1-SCN**Analytical and spectroscopic data**

Anal. Calcd. for $C_{28}H_{35}IrNPS$: C, 52.48; H, 5.50; N, 2.19; S, 5.00.

Found: C, 52.5; H, 5.6; N, 2.2; S, 4.8.

IR (Nujol): Major diastereomer: $\nu(CN)$ 2100, $\nu(CS)$ 795 cm^{-1} ; minor diastereomer: $\nu(CS)$ 2123 cm^{-1} .

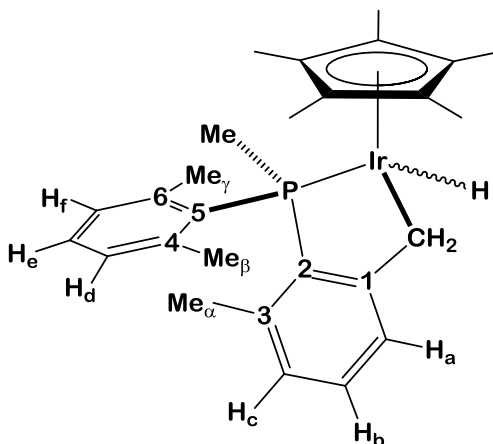
1H NMR (400 MHz, CD_2Cl_2 , 25 $^{\circ}C$) δ : 7.35 (d, 1 H, H_a), 7.20 (m, 2 H, $H_{d/f}$, H_e), 7.13 (t, 1 H, H_b), 6.93 (m, 1 H, $H_{d/f}$), 6.86 (dd, 1 H, $^4J_{CP} = 7.2$, 2.9 Hz, H_c), 3.55 (d, 1 H, $^2J_{HH} = 15.2$ Hz, IrCHH), 2.87 (dd, 1 H, $^2J_{HH} = 15.2$ Hz, $^3J_{HP} = 4.1$ Hz, IrCHH), 2.59, 1.47 (s, 3 H each, Me_{β} , Me_{γ}), 2.30 (d, 3 H, $^1J_{CP} = 9.8$ Hz, PMe), 2.01 (s, 3 H, Me_{α}), 1.52 (d, 15 H, $^4J_{HP} = 1.7$ Hz, C_5Me_5). All aromatic couplings are of *ca.* 7.5 Hz.

$^{13}C\{^1H\}$ NMR (100 MHz, CD_2Cl_2 , 25 $^{\circ}C$) δ : 157.3 (d, $^2J_{CP} = 30$ Hz, C_1), 141.8, 140.8 (d, $^2J_{CP} = 8$ Hz, C_4 , C_6), 140.2 (d, $^2J_{CP} = 2$ Hz, C_3), 140.1 (d, $^1J_{CP} = 60$ Hz, C_2), 130.6 (d, $^1J_{CP} = 46$ Hz, C_5), 130.4, 130.0 (d, $^3J_{CP} = 8$ Hz, CH_d , CH_f), 130.3, 129.9 (d, $^4J_{CP} = 2$ Hz, CH_b , CH_e), 128.1 (d, $^3J_{CP} = 7$ Hz, CH_c),

127.5 (d, $^3J_{\text{CP}} = 14$ Hz, CH_a), 121.2 (d, $^3J_{\text{CP}} = 4$ Hz, SCN) 94.4 (d, $^2J_{\text{CP}} = 3$ Hz, C_5Me_5), 25.5, 22.9 (d, $^3J_{\text{CP}} = 6$ Hz, 8 Hz, Me_β , Me_γ), 20.7 (Me_α), 18.5 (d, $^1J_{\text{CP}} = 41$ Hz, PMe), 17.0 (IrCH_2), 7.8 (C_5Me_5).

$^{31}\text{P}\{^1\text{H}\}$ NMR (160 MHz, CD_2Cl_2 , 25 °C) δ : 7.70.

The minor isomer of compound **1-SCN** is characterized by ^1H NMR multiplets with δ 3.49 and 3.36 ppm, due to the IrCH_2 protons and by a doublet at 2.20 ppm associated with the *PMe* methyl group. The signal corresponding to the C_5Me_5 ligand appears overlapped with the same signal for the major diastereomer. In the $^{31}\text{P}\{^1\text{H}\}$ NMR spectrum a singlet is recorded with δ 12.7 ppm.



Compound **1-Cl** (100 mg, 0.162 mmol) was dissolved in THF (5 mL) and heated at 45 °C under argon atmosphere. A solution of LiAlH_4 in THF (1M, 0.49 mL) was added via syringe. The reaction was heated at 45 °C for 2 h and then quenched with H_2O (10 μL). The solvent was removed under vacuum and the residue extracted with pentane, then evaporated to dryness to provide the product as a pale yellow powder (88 mg, 0.151 mmol, 93 %). For further purification, recrystallization from pentane yielded the product as colorless crystals (69 mg, 0.123 mmol) in 73% yield.

The same procedure was followed using LiAlD_4 (1M) in THF for the preparation of the deuterated material with similar yield.

A second procedure for the preparation of compound **1-H** was developed. A solution of **1-Cl** (40 mg, 0.065 mmol) in THF (2 mL) was cooled to -40 °C and a solution of Li^tBu in pentane (1.7 M, 50 μL) was added dropwise. The reaction mixture was allowed to warm gradually to room temperature and stirred for 4 h. The solvent was removed in vacuo and the product extracted

with pentane, then evaporated to dryness to provide the hydride as a yellow powder in 85% crude yield (32 mg, 0.055 mmol).

Analytical and spectroscopic data

Anal. Calcd. for $C_{27}H_{36}IrP$: C, 55.55; H, 6.22. **Found:** C, 56.0 ; H, 6.7.

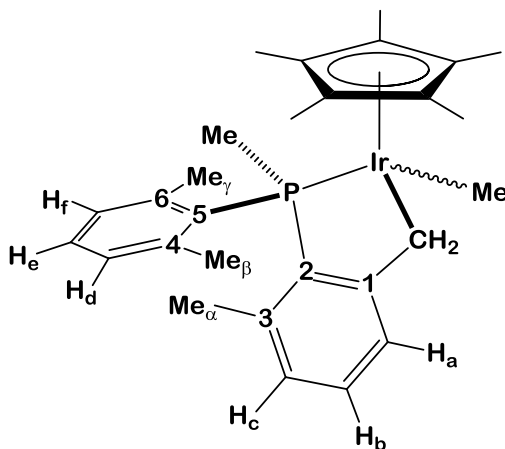
IR (Nujol): $\nu(\text{Ir-H})$ 2100 cm^{-1} .

^1H NMR (400 MHz, C_6D_6 , 25 $^\circ\text{C}$) δ : 7.54 (d, 1 H, H_a), 7.04 (dt, 1 H, $^5J_{\text{HP}} = 1.6$ Hz, H_b), 6.91, 6.70 (m, 2 H each, H_c , H_d , H_e , H_f), 3.98 (d, 1 H, $^2J_{\text{HH}} = 14.9$ Hz, IrCHH), 3.20 (d, 1 H, $^2J_{\text{HH}} = 14.9$, IrCHH), 2.41, 1.60 (s, 3 H each, Me_β , Me_γ), 2.21 (d, 3 H, $^2J_{\text{HP}} = 10.8$ Hz, PMe), 1.92 (s, 3 H, Me_α), 1.69 (d, 15 H, $^4J_{\text{HP}} = 1.5$ Hz, $C_5\text{Me}_5$), -17.24 (d, 1 H, $^2J_{\text{HP}} = 35.2$ Hz, Ir-H). All aromatic couplings are of *ca.* 7.5 Hz.

$^{13}\text{C}\{^1\text{H}\}$ NMR (100 MHz, C_6D_6 , 25 $^\circ\text{C}$) δ : 160.1 (d, $^2J_{\text{CP}} = 31$ Hz, C_1), 143.9 (d, $^1J_{\text{CP}} = 60$ Hz, C_2), 141.8, 139.1 (d, $^2J_{\text{CP}} = 8$ Hz, C_4 , C_6), 139.3 (C_3), 133.0 (d, $^1J_{\text{CP}} = 40$ Hz, C_5), 129.9, 129.7 (d, $^3J_{\text{CP}} = 7$ Hz, CH_d , CH_f), 129.5 (CH_b), 128.6 (CH_e), 127.6 (d, $^3J_{\text{CP}} = 14$ Hz, CH_a), 127.1 (d, $^3J_{\text{CP}} = 6$ Hz, CH_c), 91.9 (d, $^2J_{\text{CP}} = 3$ Hz, $C_5\text{Me}_5$), 31.0 (d, $^1J_{\text{CP}} = 44$ Hz, PMe), 25.1, 20.9 (d, $^3J_{\text{CP}} = 4$ Hz, Me_β , Me_γ), 21.9 (d, $^3J_{\text{CP}} = 9$ Hz, Me_α), 8.7 ($C_5\text{Me}_5$), 4.3 (IrCH_2).

$^{31}\text{P}\{^1\text{H}\}$ NMR (160 MHz, C_6D_6 , 25 $^\circ\text{C}$) δ : 8.3.

Only very small amounts of a minor isomer are present in solutions of compound **1-H**. This is characterized by a hydride signal with δ -17.57 ppm in the ^1H NMR spectrum and by a $^{31}\text{P}\{^1\text{H}\}$ resonance at 7.70 ppm.



A solution of **1-Cl** (100 mg, 0.162 mmol) in CH_2Cl_2 (4 mL) was cooled to 0°C and a solution of ZnMe_2 in toluene (2M, 120 μL) was added dropwise. The yellow solution rapidly cleared up to become nearly colorless. The mixture was stirred at 20°C for 1h, quenched with H_2O (10 μL) and the solvent removed in vacuo to provide crude compound **1-Me** as a pale yellow solid. The product was extracted with pentane, concentrated and cooled to -25°C . Yellow crystals of complex **1-Me** were isolated in 63% yield (62 mg, 0.104 mmol).

Compound **1-CD₃** was best synthesized by addition of a diethyl solution of $(\text{CD}_3)\text{MgI}$ (1M, 50 μL) to a CH_2Cl_2 solution of **1⁺** (50 mg, 0.035 mmol). The reaction mixture was stirred at room temperature for 15 min, then the volatiles were removed under vacuum and the residue extracted with pentane. The solvent was evaporated to dryness to give compound **1-CD₃** as a pale yellow powder (13 mg, 62 %).

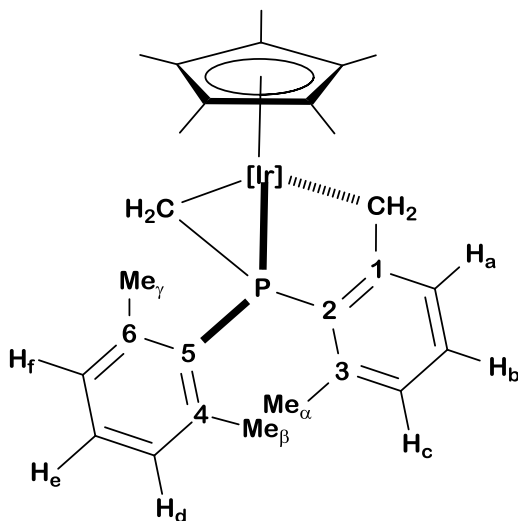
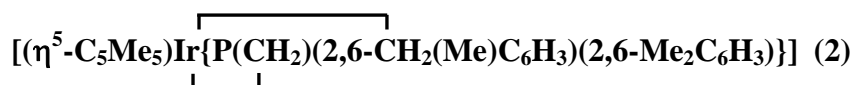
Analytical and spectroscopic data

Anal. Calcd. for $C_{28}H_{38}IrP$: C, 56.26; H, 6.41. **Found:** C, 56.2; H, 6.6.

1H NMR (400 MHz, C_6D_6 , 25 °C) δ : 7.56 (d, 1 H, H_a), 7.04 (td, 1 H, $^5J_{HP}$ = 1.8 Hz, H_b), 6.91, 6.70 (m, 2 H each, H_c , H_d , H_e , H_f), 3.50 (d, 1 H, $^2J_{HH}$ = 15.0 Hz, IrCHH), 2.89 (dd, 1 H, $^2J_{HH}$ = 15.0, $^3J_{HP}$ = 3.2 Hz, IrCHH), 2.32, 1.58 (s, 3 H each, Me_β , Me_γ), 1.91 (s, 3 H, Me_α), 1.83 (d, 3 H, $^2J_{HP}$ = 9.4 Hz, PMe), 1.43 (d, 15 H, $^4J_{HP}$ = 1.5 Hz, C_5Me_5), 0.35 (d, 3 H, $^3J_{HP}$ = 5.2 Hz, Ir-Me). All aromatic couplings are of *ca.* 7.5 Hz.

$^{13}C\{^1H\}$ NMR (100 MHz, C_6D_6 , 25 °C) δ : 159.2 (d, $^2J_{CP}$ = 31 Hz, C_1), 142.4 (d, $^1J_{CP}$ = 57 Hz, C_2), 141.8, 139.2 (d, $^2J_{CP}$ = 8 Hz, C_4 , C_6), 139.6 (C_3), 133.6 (d, $^1J_{CP}$ = 42 Hz, C_5), 129.9, 129.8 (d, $^3J_{CP}$ = 7 Hz, CH_d , CH_f), 129.5 (CH_b), 128.6 (CH_e), 128.5 (d, $^3J_{CP}$ = 6 Hz, CH_a), 127.3 (d, $^3J_{CP}$ = 6 Hz, CH_c), 91.7 (d, $^2J_{CP}$ = 4 Hz, C_5Me_5), 25.3, 22.3 (d, $^3J_{CP}$ = 7 Hz, Me_β , Me_γ), 21.0 (d, $^3J_{CP}$ = 9 Hz, Me_α), 16.9 (IrCH₂), 16.4 (d, $^1J_{CP}$ = 38 Hz, PMe), 8.2 (C_5Me_5), -22.9 (d, $^2J_{CP}$ = 8 Hz, Ir-Me).

$^{31}P\{^1H\}$ NMR (160 MHz, C_6D_6 , 25 °C) δ : 8.4.



The addition of a solution of $n\text{BuLi}$ in hexane (1.6M, 120 μL) to a solution of compound **1-Cl** (100 mg, 0.162 mmol) in THF (5 mL), previously cooled to 0 $^{\circ}\text{C}$, resulted in the rapid darkening of the reaction mixture. After 1 h of stirring at room temperature, addition of H_2O (10 μL) was carried out to quench the reaction and then the solvent was removed in vacuo. The product was extracted with pentane, concentrated and recrystallized qt -25 $^{\circ}\text{C}$ to yield **2** as yellow crystals in 78 % (74 mg, 0.127 mmol).

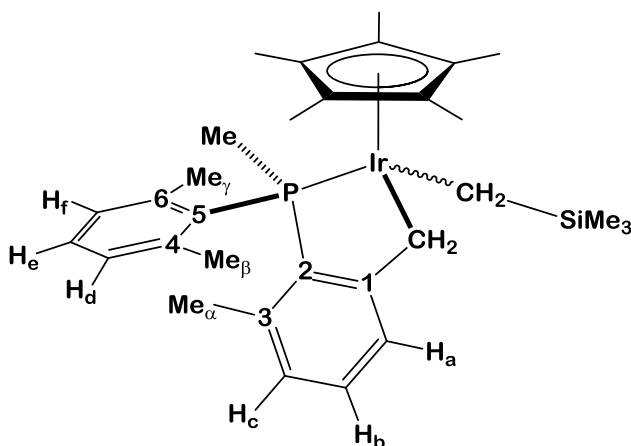
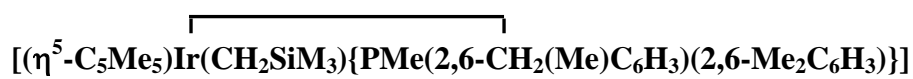
Analytical and spectroscopic data

Anal. Calcd. for $C_{27}H_{34}IrP$: C, 55.74; H, 5.89. **Found:** C, 56.2; H, 5.6.

1H NMR (400 MHz, C_6D_6 , 25 °C) δ : 7.50 (d, 1 H, H_a), 7.00 (td, 1 H, $^5J_{HP}$ = 1.7 Hz, H_b), 6.90 (m, 2 H, $H_{d/f}$, H_e), 6.66 (m, 2 H, H_c , $H_{d/f}$), 3.47 (m, 2 H, $IrCH_2$), 2.34, 1.47 (s, 3 H each, Me_β , Me_γ), 1.95 (d, 3H, $^2J_{HP}$ = 9.4 Hz, PMe), 1.91 (s, 3 H, Me_α), 1.37 (d, 15 H, $^4J_{HP}$ = 1.7 Hz, C_5Me_5), 0.30 – 0.19 (m, 2 H, $IrCH_2Si$, AB part of ABX system ($X = ^{31}P$)), 0.18 (s, 9 H, $SiMe_3$). The multiplet signal at 0.30 – 0.19 ppm, which may be described as the AB part of an ABX system ($X = ^{31}P$), has been simulated using *gnmr* software. The peak distribution within this region is in agreement with $\delta_A = 0.28$ and $\delta_B = 0.23$ ppm, and coupling constants $^2J_{AB} = 13.0$, $^3J_{AX} = 8.9$ and $^3J_{BX} = 3.5$ Hz. All aromatic couplings are of *ca.* 7.5 Hz.

$^{13}C\{^1H\}$ NMR (100 MHz, C_6D_6 , 25 °C) δ : 159.7 (d, $^2J_{CP} = 32$ Hz, C_1), 143.1 (d, $^1J_{CP} = 59$ Hz, C_2), 141.5, 140.0 (d, $^2J_{CP} = 8$ Hz, C_4 , C_6), 139.4 (C_3), 134.0 (d, $^1J_{CP} = 44$ Hz, C_5), 129.9, 129.6 (d, $^3J_{CP} = 8$ Hz, CH_d , CH_f), 129.5, 128.7 (CH_b , CH_e), 128.1 (CH_a , overlapped with C_6D_6), 127.4 (d, $^3J_{CP} = 6$ Hz, CH_c), 92.6 (d, $^2J_{CP} = 4$ Hz, C_5Me_5), 26.1, 23.0 (d, $^3J_{CP} = 7$ Hz, Me_β , Me_γ), 21.1 (Me_α), 17.9 (d, $^1J_{CP} = 39$ Hz, PMe), 12.2 ($IrCH_2$), 8.4 (C_5Me_5), 4.2 ($SiMe_3$), -29.6 (d, $^2J_{CP} = 7$ Hz, $IrCH_2Si$).

$^{31}P\{^1H\}$ NMR (160 MHz, C_6D_6 , 25 °C) δ : -41.6.



Compound **1-Cl** (100 mg, 0.16 mmol) was placed in a Schlenk flask and dissolved in THF (10 mL) under argon. A solution of $\text{LiCH}_2\text{SiMe}_3$ (1.78 mL, 0.1 M in pentane) was added at 0 °C and the mixture was allowed to warm slowly to room temperature, and then stirred for two hours. The solvent was evaporated under vacuum and the residue extracted with pentane and filtered under argon through a pad of silica. The bright yellow filtrate was evaporated to dryness to yield the product as a fine yellow powder (69 mg, 0.10 mmol, 64 %).

Analytical and spectroscopic data

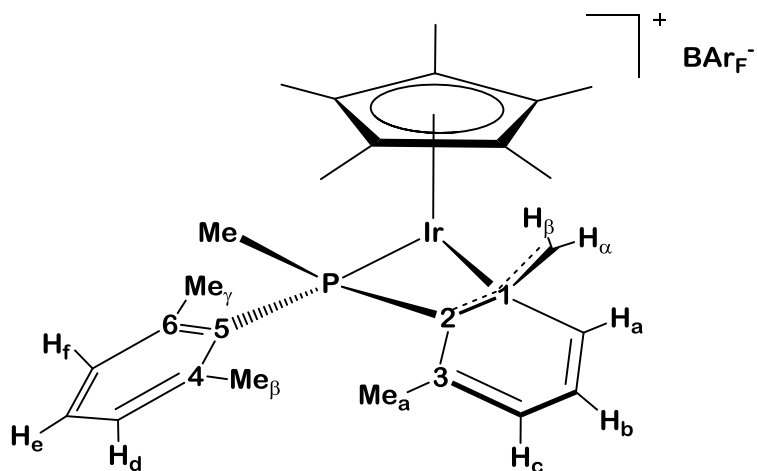
Anal. Calcd. for $C_{31}H_{46}IrPSi$: C, 55.57; H, 6.92. **Found:** C, 55.6; H, 6.7.

1H NMR (400 MHz, C_6D_6 , 25 °C) δ : 7.50 (d, 1 H, H_a), 7.00 (td, 1 H, $^5J_{HP}$ = 1.7 Hz, H_b), 6.90 (m, 2 H, $H_{d/f}$, H_e), 6.66 (m, 2 H, H_c , $H_{d/f}$), 3.47 (m, 2 H, $IrCH_2$), 2.34, 1.47 (s, 3 H each, Me_β , Me_γ), 1.95 (d, 3H, $^2J_{HP}$ = 9.4 Hz, PMe), 1.91 (s, 3 H, Me_α), 1.37 (d, 15 H, $^4J_{HP}$ = 1.7 Hz, C_5Me_5), 0.30 – 0.19 (m, 2 H, $IrCH_2Si$, AB part of ABX system ($X = ^{31}P$)), 0.18 (s, 9 H, $SiMe_3$). The multiplet signal at 0.30 – 0.19 ppm, which may be described as the AB part of an ABX system ($X = ^{31}P$), has been simulated using *gnmr* software. The peak distribution within this region is in agreement with $\delta_A = 0.28$ and $\delta_B = 0.23$ ppm, and coupling constants $^2J_{AB} = 13.0$, $^3J_{AX} = 8.9$ and $^3J_{BX} = 3.5$ Hz. All aromatic couplings are of *ca.* 7.5 Hz.

^{13}C NMR (100 MHz, C_6D_6 , 25 °C) δ : 159.7 (d, $^2J_{CP} = 32$ Hz, C_1), 143.1 (d, $^1J_{CP} = 59$ Hz, C_2), 141.5, 140.0 (d, $^2J_{CP} = 8$ Hz, C_4 , C_6), 139.4 (C_3), 134.0 (d, $^1J_{CP} = 44$ Hz, C_5), 129.9, 129.6 (d, $^3J_{CP} = 8$ Hz, CH_d , CH_f), 129.5, 128.7 (CH_b , CH_e), 128.1 (CH_a , overlapped with C_6D_6), 127.4 (d, $^3J_{CP} = 6$ Hz, CH_c), 92.6 (d, $^2J_{CP} = 4$ Hz, C_5Me_5), 26.1, 23.0 (d, $^3J_{CP} = 7$ Hz, Me_β , Me_γ), 21.1 (Me_α), 17.9 (d, $^1J_{CP} = 39$ Hz, PMe), 12.2 ($IrCH_2$), 8.4 (C_5Me_5), 4.2 ($SiMe_3$), -29.6 (d, $^2J_{CP} = 7$ Hz, $IrCH_2Si$).

$^{31}P\{^1H\}$ NMR (160 MHz, C_6D_6 , 25 °C) δ : 6.41

Synthesis of $[(\eta^5\text{-C}_5\text{Me}_5)\text{Ir}\{\text{PMe}(2,6\text{-CH}_2(\text{Me})\text{C}_6\text{H}_3)(2,6\text{-Me}_2\text{C}_6\text{H}_3)\}]^+\text{BAr}_\text{F}^-$ (**1**⁺)



To a solid mixture of **1-Cl** (100 mg, 0.16 mmol) and NaBAr_F (143 mg, 0.16 mmol) was added 5 mL of CH₂Cl₂ under argon. The reaction mixture was stirred for 10 min at room temperature, after which the solution turned from orange to yellow. The mixture was filtered and the solvent evaporated under reduced pressure to obtain a yellow solid (220 mg, 95%). For further purification, the complex can be crystallized from a 1:2 mixture of CH₂Cl₂:pentane.

Analytical and spectroscopic data

Anal. Calcd. for $C_{59}H_{47}BF_{24}IrP$: C, 49.01; H, 3.28. **Found:** C, 49.1; H, 3.7.

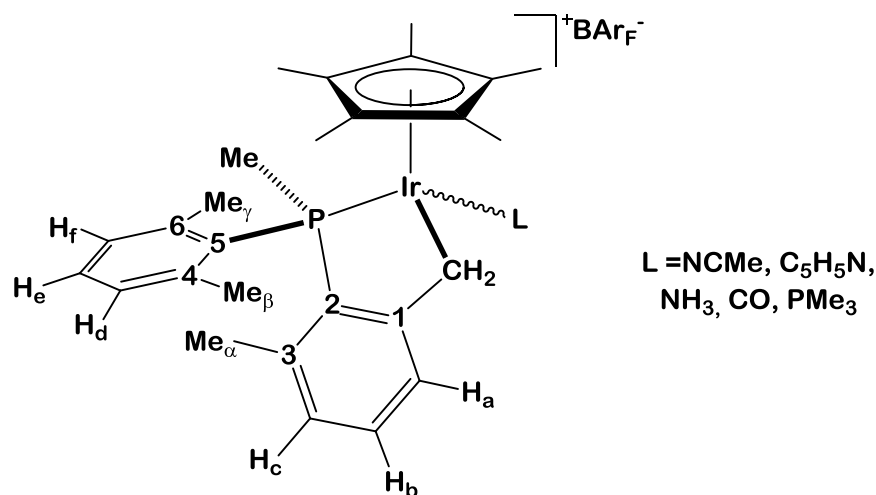
1H RMN (500 MHz, CD_2Cl_2 , $-60\text{ }^\circ C$) δ : 7.36 (m, 1 H, H_c), 7.28 (t, 1 H, H_b), 7.24 (t, 1 H, H_e), 7.04, 6.94 (m, 1 H each, H_d , H_f), 6.73 (dd, 1 H, $^4J_{HP} = 3.7$ Hz, H_a), 2.98 (t, 1 H, $^2J_{HH} = ^3J_{HP} = 4.8$ Hz, $IrCH_a$), 2.50 (s, 3 H, Me_γ), 2.44 (s, 3 H, Me_α), 2.20 (d, 3 H, $^2J_{HP} = 12.8$ Hz, PMe), 2.09 (s, 3 H, Me_β), 1.63 (s, 15 H, C_5Me_5), 1.15 (dd, 1 H, $^2J_{HH} = 4.8$, $^3J_{HP} = 15.6$ Hz, $IrCH_\beta$). All aromatic couplings are of *ca.* 7.5 Hz.

1H RMN (300 MHz, CD_2Cl_2 , $25\text{ }^\circ C$) δ : 7.36, (m, 2 H, $H_{a/b/c/d/e/f}$), 7.12 (br. s, 4 H, $H_{a/b/c/d/e/f}$), 2.44 (br. s, 11 H, Me_α , Me_β , Me_γ , $IrCH_2$), 2.28 (d, 3 H, $^2J_{HP} = 12.8$ Hz, PMe), 1.63 (d, 15 H, $^4J_{HP} = 1.8$ Hz, C_5Me_5).

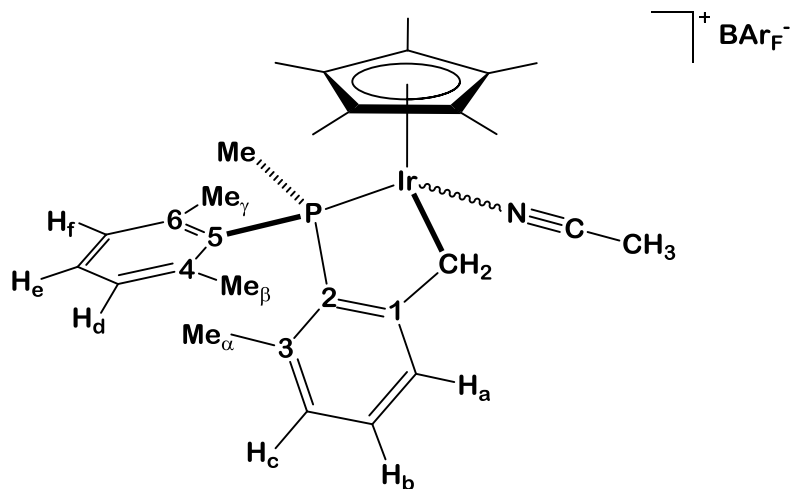
$^{13}C\{^1H\}$ RMN (125 MHz, CD_2Cl_2 , $-60\text{ }^\circ C$) δ : 142.2, 141.4 (s, d, $^2J_{CP} = 16$ Hz, C_4 , C_6), 136.7 (C_3), 132.7 (CH_b), 132.1 (CH_e), 131.2 (d, $^3J_{CP} = 4$ Hz, CH_c), 129.2, 128.7 (d, $^3J_{CP} = 10$ Hz, CH_d , CH_f), 126.8 (d, $^3J_{CP} = 6$ Hz, CH_a), 116.8 (d, $^1J_{CP} = 65$ Hz, C_5), 95.6 (d, $^2J_{CP} = 15$ Hz, C_1), 92.7 (C_5Me_5), 67.5 (d, $^1J_{CP} = 28$ Hz, C_2), 27.0 ($IrCH_2$), 22.7 (Me_α), 22.1, 21.9 (d, s, $^3J_{CP} = 16$ Hz, 7Hz, Me_β , Me_γ), 12.8 (d, $^1J_{CP} = 41$ Hz, PMe), 8.5 (C_5Me_5).

$^{31}P\{^1H\}$ NMR (200 MHz, CD_2Cl_2 , $-60\text{ }^\circ C$) δ : -44.9.

General synthesis of cationic adducts 1-L^+ ($\text{L} = \text{NCMe}$, $\text{C}_5\text{H}_5\text{N}$, NH_3 , CO , PMe_3)



To a solid mixture of **1-Cl** (50 mg, 0.08 mmol) and NaBAr_F (72 mg, 0.08 mmol) placed in a Schlenk flask were added 5 mL of CH_2Cl_2 . The reaction mixture was stirred for 5 min at room temperature under 1.5 bar of CO or NH_3 (a thick-wall vessel instead of a conventional Schlenk flask was employed in these cases), or alternatively treated with 100 μL of NCMe or pyridine (for corresponding NCMe or pyridine adducts, respectively), or with a toluene solution of PMe_3 (0.4 mL, 1M) (for corresponding cationic PMe_3 complex). The solution was filtered and the solvent was then evaporated under reduced pressure to obtain pale white (**1-NCMe** $^+$, **1-PMe** $_3^+$, **1-CO** $^+$) or yellow powders (**1-NC** $_5\text{H}_5^+$, **1-NH** $_3^+$) in *ca.* 95% yield. Complexes **1-NCMe** $^+$ and **1-NH** $_3^+$ were obtained as mixtures of diastereomers (88:12, $\text{L} = \text{NCMe}$; 94:6, $\text{L} = \text{NH}_3$). These complexes can be recrystallized from a 1:2 mixture of CH_2Cl_2 :pentane. Analytical and spectroscopic data for compounds **1-L** $^+$ are detailed below.

Compound 1-NCMe⁺**Analytical and spectroscopic data**

Anal. Calcd. for C₆₁H₅₀BF₂₄IrNP: C, 49.27; H, 3.39; N, 0.94. **Found:** C, 49.4; H, 3.6; N, 1.4.

IR (Nujol): $\nu(\text{CN})$ 2285 cm⁻¹.

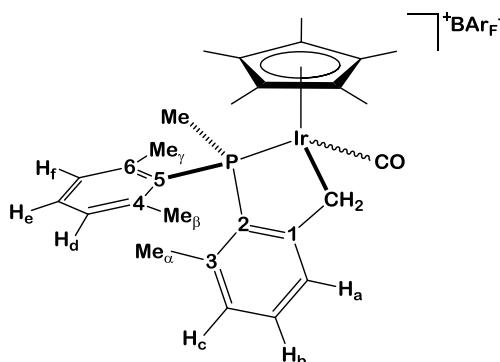
¹H NMR (400 MHz, CD₂Cl₂, 25 °C) δ : 7.44 (d, 1 H, H_a), 7.26, (m, 3 H each, H_b, H_{d/f}, H_e), 6.98 (m, 1 H, H_{d/f}), 6.94 (dd, 1 H, ⁴J_{HP} = 3.5 Hz, H_c) 3.52 (d, 1 H, ²J_{HH} = 15.0 Hz, IrCHH), 3.32 (dd, 1 H, ²J_{HH} = 15.0, ²J_{HP} = 3.5 Hz, IrCHH), 2.65, 1.44 (s, 3 H each, Me_β, Me_γ), 2.55 (s, 3H, NCMe), 2.26 (d, 3 H, ²J_{HP} = 9.9 Hz, PMe), 2.03 (s, 3H, Me_α), 1.55 (d, 15 H, ⁴J_{HP} = 1.8 Hz, C₅Me₅). All aromatic couplings are of *ca.* 7.5 Hz.

¹³C{¹H} NMR (100 MHz, CD₂Cl₂, 25 °C) δ : 155.9 (d, ²J_{CP} = 30 Hz, C₁), 142.0, 140.9 (d, ²J_{CP} = 8 Hz, C₄, C₆), 140.8 (C₃), 139.4 (d, ¹J_{CP} = 63 Hz, C₂), 131.0, 130.3 (CH_b, CH_e), 130.9, 130.5 (d, ³J_{CP} = 9 Hz, CH_d, CH_f), 127.4 (d, ¹J_{CP} = 51 Hz, C₅), 128.6 (d, ³J_{CP} = 7 Hz, CH_c), 126.8 (d, ³J_{CP} = 15 Hz, CH_a),

118.6 (NCMe), 95.0 (d, $^2J_{\text{CP}} = 2$ Hz, C_5Me_5), 25.6, 23.2 (d, $^3J_{\text{CP}} = 6$ Hz, $^3J_{\text{CP}} = 8$ Hz, resp., Me_β , Me_γ), 20.5 (d, $^3J_{\text{CP}} = 3$ Hz, Me_α), 19.4 (d, $^1J_{\text{CP}} = 39$ Hz, PMe), 17.3 (IrCH₂), 8.2 (C_5Me_5), 4.4 (NCMe).

$^{31}\text{P}\{^1\text{H}\}$ NMR (160 MHz, CD_2Cl_2 , 25 °C) δ : 8.9.

The minor diastereomer of compound **Ir-NCMe⁺** is characterized by ^1H NMR multiplets with δ 3.55 and 3.29 ppm, due to the IrCH₂ protons, which are partly overlapped with the signals corresponding to the IrCH₂ group of the major diastereomer. A doublet at 1.76 ppm is associated with the C_5Me_5 ligand. In the $^{31}\text{P}\{^1\text{H}\}$ NMR spectrum a singlet is recorded with δ 5.8 ppm.

Compound 1-CO⁺**Analytical and spectroscopic data**

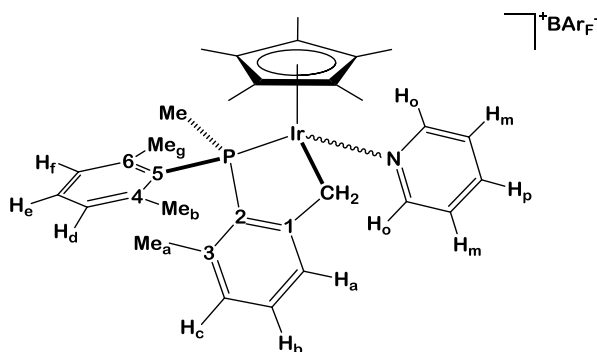
Anal. Calcd. for C₆₀H₄₈BF₂₄IrOP: C, 48.86; H, 3.28. **Found:** C, 48.6; H, 3.3.

IR (Nujol): ν(CO) 2025 cm⁻¹.

¹H NMR (400 MHz, CD₂Cl₂, 25 °C) δ: 7.37 (d, 1 H, H_a), 7.32 (t, 1 H, H_c), 7.24 (m, 2 H, H_b, H_{d/f}), 7.00 (m, 1 H, H_{d/f}), 6.95 (m, 1 H, H_c), 3.65 (dd, 1 H, ²J_{HH} = 14.2 Hz, ³J_{HP} = 2.5 Hz, IrCHH), 3.09 (d, 1 H, ²J_{HH} = 14.2 Hz, IrCHH), 2.59 (d, 2H, ²J_{HP} = 9.5 Hz, PMe), 2.58, 1.41 (s, 3 H each, Me_β, Me_γ) 2.01 (s, 3 H, Me_α), 1.79 (d, 15 H, ⁴J_{HP} = 1.8 Hz, C₅Me₅). All aromatic couplings are of ca. 7.5 Hz.

¹³C NMR (100 MHz, CD₂Cl₂, 25 °C) δ: 167.0 (d, ²J_{CP} = 11 Hz, CO), 153.3 (d, ²J_{CP} = 27 Hz, C₁), 141.6, 140.8 (d, ²J_{CP} = 10 Hz, 8 Hz, C₄, C₆), 140.1 (d, ²J_{CP} = 3 Hz, C₃), 137.0 (d, ¹J_{CP} = 66 Hz, C₂), 132.0 (m, CH_b, CH_e), 131.1, 120.5 (d, ³J_{CP} = 9 Hz, CH_d, CH_f), 129.6 (d, ³J_{CP} = 8 Hz, CH_c), 126.8 (d, ³J_{CP} = 15 Hz, CH_a), 124.4 (d, ¹J_{CP} = 53 Hz, C₅), 102.6 (C₅Me₅), 25.4, 23.1 (d, ³J_{CP} = 8 Hz, 5 Hz, Me_β, Me_γ), 24.9 (d, ¹J_{CP} = 46 Hz, PMe), 20.4 (d, ³J_{CP} = 4 Hz, Me_α), 10.2 (IrCH₂), 8.4 (C₅Me₅).

³¹P{¹H} NMR (160 MHz, CD₂Cl₂, 25 °C) δ: 1.0.

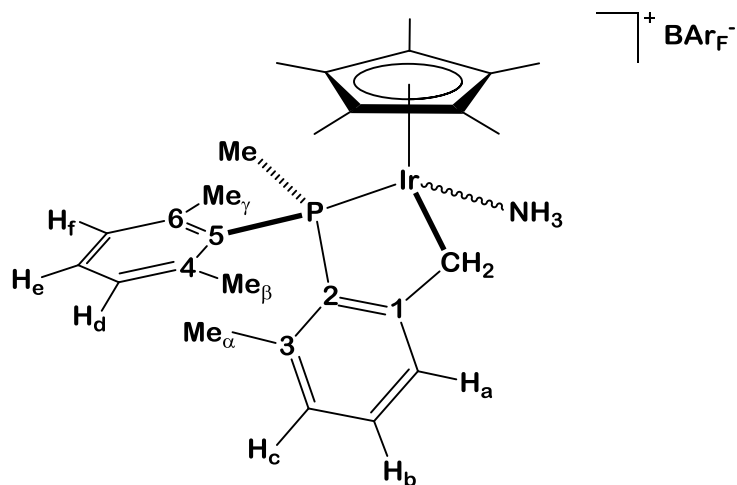
Compound 1-NC₅H₅⁺**Analytical and spectroscopic data**

Anal. Calcd. for C₆₄H₅₂BF₂₄IrNP: C, 50.40; H, 3.44; N, 0.92. **Found:** C, 50.7; H, 3.6; N, 1.3.

¹H NMR (400 MHz, CD₂Cl₂, 25 °C) δ : 8.47 (d, 2H, ³*J*_{HH} = 5.5 Hz, H_o), 7.78 (t, 1 H, ³*J*_{HH} = 7.5 Hz, H_p), 7.53 (d, 1 H, H_a), 7.30 – 7.19 (m, 5 H, H_m, H_b, H_{d/f}, H_e), 7.00 (dd, 1 H, ⁴*J*_{HP} = 3.7 Hz, H_{d/f}), 6.91 (dd, 1 H, ⁴*J*_{HP} = 3.3 Hz, H_c), 3.91 (d, 1 H, ²*J*_{HH} = 15.8 Hz, IrCHH), 2.91 (dd, 1 H, ²*J*_{HH} = 15.8, ³*J*_{HP} = 4.9 Hz, IrCHH), 2.61, 1.52 (s, 3 H each, Me_β, Me_γ), 1.96 (s, 3 H, Me_α), 1.46 (d, 3H, ²*J*_{HP} = 9.3 Hz, PMe), 1.35 (d, 15 H, ⁴*J*_{HP} = 1.7 Hz, C₅Me₅).

¹³C NMR (100 MHz, CD₂Cl₂, 25 °C) δ : 154.4 (CH_o), 153.3 (C₁, overlapped with CH_o), 138.6 (CH_p), 141.4, 140.1 (d, ²*J*_{CP} = 9 Hz, 8 Hz, C₄, C₆), 140.3 (Hz, C₃), 137.9 (d, ¹*J*_{CP} = 62 Hz, C₂), 131.0 (CH_b), 130.6 (CH_e), 130.3, 130.1 (d, ³*J*_{CP} = 8 Hz, CH_d, CH_f), 129.2 (d, ³*J*_{CP} = 7 Hz, CH_c), 127.3 (d, ³*J*_{CP} = 14 Hz, CH_a), 126.9 (CH_m), 127.4 (d, ¹*J*_{CP} = 51 Hz, C₅), 94.06 (C₅Me₅), 25.1, 22.8 (d, ³*J*_{CP} = 6 Hz, 7 Hz, Me_β, Me_γ), 22.2 (IrCH₂), 20.06 (Me_α), 15.8 (d, ¹*J*_{CP} = 38 Hz, PMe), 7.5 (C₅Me₅).

³¹P{¹H} NMR (160 MHz, CD₂Cl₂, 25 °C) δ : 11.4.

Compound 1-NH₃⁺**Analytical and spectroscopic data**

Anal. Calcd. for C₅₉H₄₉BF₂₄IrNP: C, 48.47; H, 3.38. **Found:** C, 48.6; H, 3.2.

IR (Nujol): ν(N-H) br. 3365 cm⁻¹.

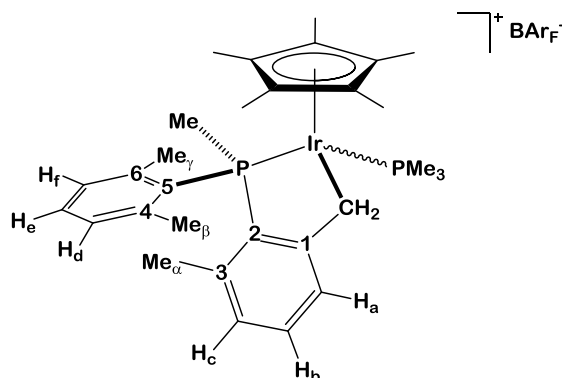
¹H NMR (400 MHz, CD₂Cl₂, 25 °C) δ: 7.39 (d, 1 H, H_a), 7.30 – 7.16 (m, 3 H, H_b, H_{d/f}, H_e), 6.98 (m, 1 H, H_{d/f}), 6.94 (dd, 1 H, ⁴J_{HP} = 3.2 Hz, H_c), 3.77 (d, 1 H, ²J_{HH} = 15.7 Hz, IrCHH), 2.89 (br. s, 3 H, NH₃), 2.78 (dd, 1 H, ²J_{HH} = 15.8, ³J_{HP} = 4.2 Hz, IrCHH), 2.63, 1.46 (s, 3 H each, Me_β, Me_γ), 2.10 (d, 3H, ²J_{HP} = 9.1 Hz, PMe), 2.01 (s, 3 H, Me_α), 1.49 (d, 15 H, ⁴J_{HP} = 1.9 Hz, C₅Me₅).

¹³C NMR (100 MHz, CD₂Cl₂, 25 °C) δ: 154.5 (d, ²J_{CP} = 32 Hz, C₁), 142.1, 140.2 (d, ²J_{CP} = 7 Hz, C₄, C₆), 140.7 (C₃), 139.2 (d, ¹J_{CP} = 60 Hz, C₂), 131.6 (CH_b), 131.2 (CH_e), 131.0, 130.7 (d, ³J_{CP} = 8 Hz, CH_d, CH_f), 129.6 (d, ³J_{CP} = 7 Hz, CH_c), 128.6 (d, ³J_{CP} = 15 Hz, CH_a), 127.3 (d, ¹J_{CP} = 52 Hz, C₅), 93.1 (d,

$^2J_{\text{CP}} = 3$ Hz, C_5Me_5), 25.7, 22.8 (d, $^3J_{\text{CP}} = 6$ Hz, 9 Hz, Me_β , Me_γ), 20.5 (Me_α), 19.9 (IrCH_2), 17.7 (d, $^1J_{\text{CP}} = 36$ Hz, PMe), 8.2 (C_5Me_5).

$^{31}\text{P}\{^1\text{H}\}$ NMR (160 MHz, CD_2Cl_2 , 25 °C) δ : 8.5.

The minor diastereomer of compound **1-NH₃⁺** is characterized by ^1H NMR multiplets with δ 3.50 and 2.81, due to the IrCH_2 protons and by a doublet at 1.69 associated with the C_5Me_5 ligand. In the $^{31}\text{P}\{^1\text{H}\}$ NMR spectrum a singlet is recorded with δ 7.5 ppm

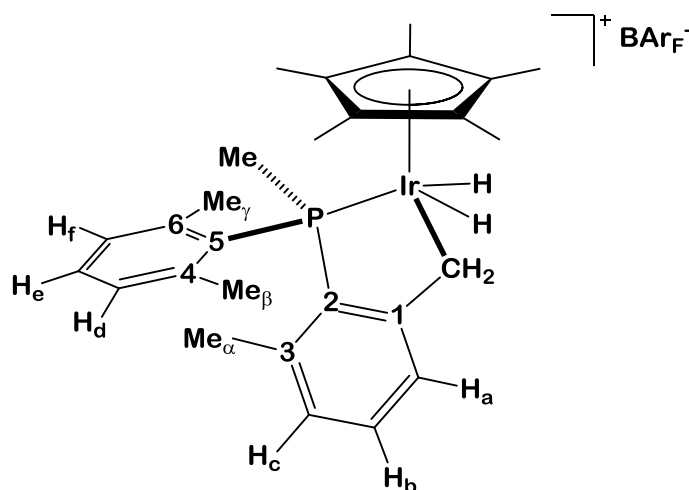
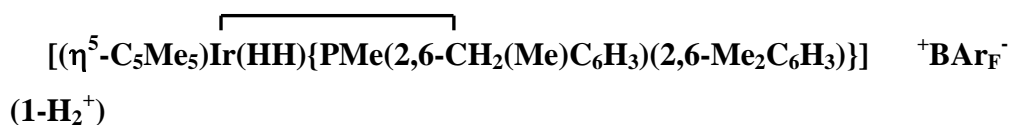
Compound 1- PMe_3^+ **Analytical and spectroscopic data**

Anal. Calcd. for $\text{C}_{61}\text{H}_{54}\text{BF}_{24}\text{IrP}_2$: C, 48.58; H, 3.61. **Found:** C, 49.0; H, 3.8.

^1H NMR (500 MHz, CD_2Cl_2 , 25 °C) δ : 7.34 (d, 1 H, H_a), 7.29 – 7.18 (m, 3 H, H_b , $\text{H}_{d/f}$, H_e), 6.95 (m, 2 H, H_c , $\text{H}_{d/f}$), 3.18 (dd, 1 H, $^2J_{\text{HH}} = 15.5$, $^3J_{\text{HP}} = 4.0$ Hz, IrCHH), 2.83 (m, 1 H, IrCHH), 2.55, 1.33 (s, 3 H each, Me_β , Me_γ), 2.32 (d, 3H, $^2J_{\text{HP}} = 9.2$ Hz, PMe), 1.97 (s, 3 H, Me_α), 1.55 (d, 15 H, $^4J_{\text{HP}} = 1.6$ Hz, C_5Me_5), 1.42 (d, 9 H, $^2J_{\text{HP}} = 9.9$ Hz, PMe_3). All aromatic couplings are of *ca.* 7.5 Hz.

^{13}C NMR (125 MHz, CD_2Cl_2 , 25 °C) δ : 156.8 (d, $^2J_{\text{CP}} = 29$ Hz, C_1), 141.6, 140.4 (d, $^2J_{\text{CP}} = 9$ Hz, C_4 , C_6), 140.7 (C_3), 137.7 (d, $^1J_{\text{CP}} = 61$ Hz, C_2), 131.6, 130.5 (d, $^4J_{\text{CP}} = 2$ Hz, CH_b , CH_e), 130.7, 130.1 (d, $^3J_{\text{CP}} = 8$ Hz, CH_d , CH_f), 129.4 (d, $^3J_{\text{CP}} = 7$ Hz, CH_c), 126.7 (d, $^3J_{\text{CP}} = 14$ Hz, CH_a), 98.6 (C_5Me_5), 25.9, 22.7 (d, $^3J_{\text{CP}} = 6$ Hz, 7 Hz, Me_β , Me_γ), 23.5 (dd, $^1J_{\text{CP}} = 40$, $^3J_{\text{CP}} = 5$ Hz, PMe), 20.6 (Me_α), 16.9 (d, $^1J_{\text{CP}} = 39$ Hz, PMe_3), 9.8 (d, $^2J_{\text{CP}} = 8$ Hz, IrCH_2), 8.5 (C_5Me_5).

$^{31}\text{P}\{^1\text{H}\}$ NMR (200 MHz, CD_2Cl_2 , 25 °C) δ : 1.0 (d, $^2J_{\text{PP}} = 22$ Hz, PMeXyl_2), -41.3 (d, $^2J_{\text{PP}} = 22$ Hz, PMe_3).



To a solid mixture of **1-Cl** (100 mg, 0.16 mmol) and NaBAr_F (143 mg, 0.16 mmol) placed in a thick-wall vessel were added 3 mL of CH₂Cl₂. The reaction mixture was stirred for 30 min at room temperature under 1 bar of H₂, after which the original solution with intense yellow color became almost colorless. Addition of pentane under hydrogen atmosphere caused precipitation of complex **1**·H₂⁺ as a fine, pale yellow powder in quantitative yield. Work-up of the complex in the absence of hydrogen led to release of H₂ and formation of **1**⁺.

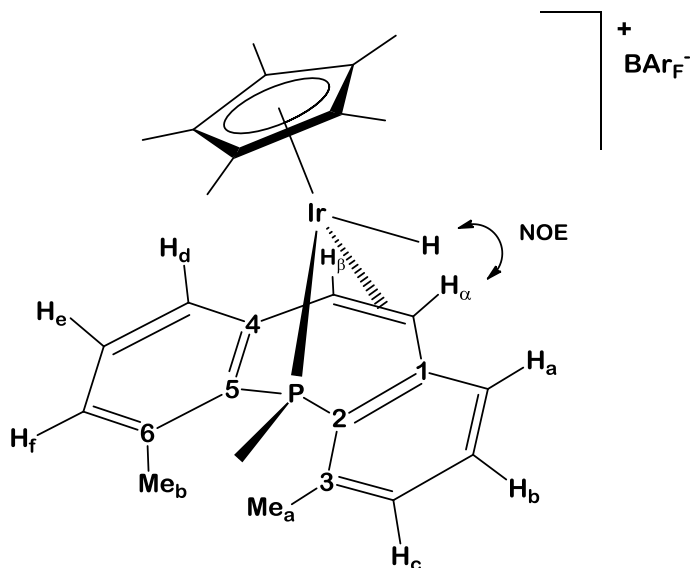
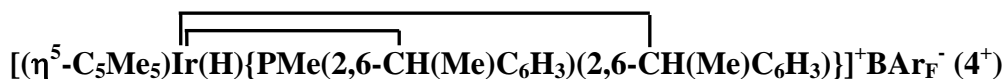
Spectroscopic Data

^1H NMR (500 MHz, CD_2Cl_2 , 25 °C, H_2 atmosphere) δ : 7.39 (d, 1 H, H_a), 7.33 – 7.25 (m, 3 H, H_b , $\text{H}_{d/f}$, H_e), 7.05 (dd, 1 H, $^4J_{\text{HP}} = 3.8$ Hz, $\text{H}_{d/f}$), 6.98 (dd, 1 H, $^4J_{\text{HP}} = 4.7$ Hz, H_c), 2.59, 1.50 (s, 3 H each, Me_β , Me_γ), 2.55 (d, 3H, $^2J_{\text{HP}} = 10.5$ Hz, PMe), 2.00 (s, 3 H, Me_a), 1.79 (d, 15 H, $^4J_{\text{HP}} = 1.1$ Hz, C_5Me_5), -4.63 (br. s, 4 H, IrCH_2 , Ir-H_2).

^1H NMR (400 MHz, CD_2Cl_2 , -80 °C, H_2 atmosphere) δ : 7.31 (d, 1 H, H_a), 7.22 – 7.10 (m, 3 H, H_b , $\text{H}_{d/f}$, H_e), 6.88 (m, 2 H, H_c , $\text{H}_{d/f}$), 3.93 (d, 1 H, $^2J_{\text{HH}} = 14.2$ Hz, IrCHH), 3.38 (d, 1 H, $^2J_{\text{HH}} = 14.2$, IrCHH), 2.45 (m, 6 H, $\text{Me}_{\beta/\gamma}$, PMe), 1.92 (s, 3 H, Me_a), 1.60 (s, 15 H, C_5Me_5), 1.31 (s, $\text{Me}_{\beta/\gamma}$), -12.79 (s, 1 H, IrHH), -13.37 (d, 1 H, $^2J_{\text{HP}} = 17.5$ Hz, IrHH).

^{13}C $\{^1\text{H}\}$ NMR (125 MHz, CD_2Cl_2 , 25 °C, H_2 atmosphere) δ : 152.4 (d, $^2J_{\text{CP}} = 29$ Hz, C_1), 141.6, 140.4 (d, $^2J_{\text{CP}} = 9$ Hz, 8 Hz, C_4 , C_6), 140.1 (d, $^2J_{\text{CP}} = 3$ Hz, C_3), 136.4 (d, $^1J_{\text{CP}} = 62$ Hz, C_2), 132.4, 132.1 (CH_b , CH_e), 131.3, 130.8 (d, $^3J_{\text{CP}} = 9$ Hz, CH_d , CH_f), 129.9 (d, $^3J_{\text{CP}} = 8$ Hz, CH_c), 126.4 (d, $^3J_{\text{CP}} = 17$ Hz, CH_a), 124.9 (br. s, C_5), 104.2 (C_5Me_5), 29.6 (br. d, $^1J_{\text{CP}} = 57$ Hz, PMe), 24.9, 23.4 (d, $^3J_{\text{CP}} = 5$ Hz, 8 Hz, Me_β , Me_γ), 20.3 (Me_a), 11.7 (br. s, IrCH_2), 8.8 (C_5Me_5).

$^{31}\text{P}\{^1\text{H}\}$ NMR (200 MHz, CD_2Cl_2 , 25 °C, H_2 atmosphere) δ : 3.7 (br. s).



A solid mixture of **1-Cl** (100 mg, 0.16 mmol) and NaBAr_F (145 mg, 0.16 mmol) placed in a Schlenk flask was suspended in CH₂Cl₂ (5 mL) under argon. A saturated aqueous solution of NaHCO₃ (5 μL) was added to the reaction mixture, which was stirred for 16 hours with intermittent vacuum-argon cycles to pump out the produced molecular hydrogen. The yellow solution was filtered and the solvent evaporated under reduced pressure to obtain a pale yellow solid, which was washed with pentane to yield compound **4**⁺ (210 mg, 90 %). For further purification **4**⁺ can be recrystallized from a 1:1 mixture of CH₂Cl₂:pentane.

Analytical and spectroscopic data

Anal. Calcd. for $C_{59}H_{45}BF_{24}IrP$: C, 49.08; H, 3.14. **Found:** C, 48.7; H, 3.1.

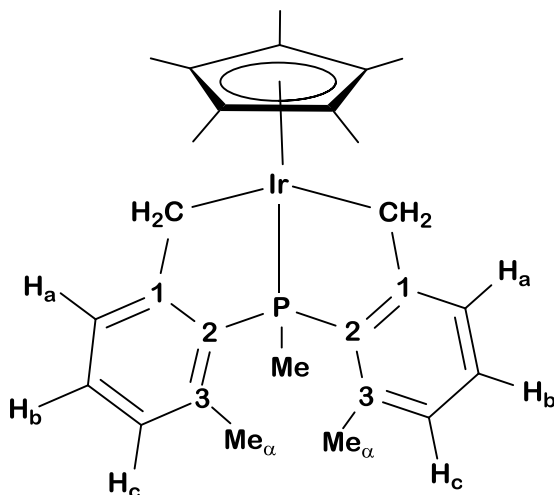
IR (Nujol): $\nu(\text{Ir-H})$ 2135 cm^{-1} .

EM (ES) m/z Calcd. for M^+ : 581.19. **Expt.:** 581.2.

^1H NMR (500 MHz, CD_2Cl_2 , 25 °C) δ : 7.34 (m, 2 H, H_a , H_d), 7.16 (m, 2 H, H_b , H_e), 6.95, 6.92 (dd, 1H, $^4J_{\text{HP}} = 3.9$ Hz H_c , H_f), 4.97 (dd, 1 H, $^3J_{\text{HH}} = 8.6$, $^4J_{\text{HP}} = 2.8$ Hz, CH_a), 4.51 (d, 1 H, $^3J_{\text{HH}} = 8.6$ Hz, CH_β), 2.58 (d, 3 H, $^2J_{\text{HP}} = 13.2$ Hz, PMe), 2.52, 2.50 (s, 3 H each, Me_a , Me_β), 1.97 (d, 15 H, $^4J_{\text{HP}} = 1.0$ Hz, C_5Me_5), -13.03 (d, 1 H, $^2J_{\text{HP}} = 28.5$ Hz, IrH).

$^{13}\text{C}\{^1\text{H}\}$ NMR (100 MHz, CD_2Cl_2 , 25 °C) δ : 148.2 (d, $^2J_{\text{CP}} = 17$ Hz, C_4), 143.6 (d, $^2J_{\text{CP}} = 23$ Hz, C_1), 139.2, 138.8, 137.1, 136.0 (C_2 , C_3 , C_5 , C_6), 131.3, 131.2, 131.1, 130.5 (CH_b , CH_c , CH_e , CH_f), 126.6, 124.8 (d, $^3J_{\text{CP}} = 15$, 10 Hz, CH_a , CH_d), 100.2 (s, C_5Me_5), 63.3 (d, $^2J_{\text{CP}} = 4$, CH_β), 56.1 (d, $^2J_{\text{CP}} = 8$ Hz, CH_a), 22.1, 21.6 (d, $^3J_{\text{CP}} = 3$ Hz, Me_a , Me_β), 12.6 (d, $^1J_{\text{CP}} = 36$ Hz, PMe), 8.9 (s, C_5Me_5).

$^{31}\text{P}\{^1\text{H}\}$ NMR (160 MHz, CD_2Cl_2 , 25 °C) δ : 8.9.



A solution of NaOH in MeOH (6 mL, 0.5M) was added to a solution of **1-Cl** (100 mg, 0.16 mmol) in CHCl₃ (6 mL) under nitrogen. The reaction mixture was stirred at room temperature for 15 hours, after which the suspension turned bright yellow. The solution was filtered and the solvent removed under vacuum. The residue was extracted with Et₂O, filtered through a pad of celite and the solution evaporated to dryness. Complex **5** was obtained as a fine yellow powder (78 mg, 0.13 mmol, 84%).

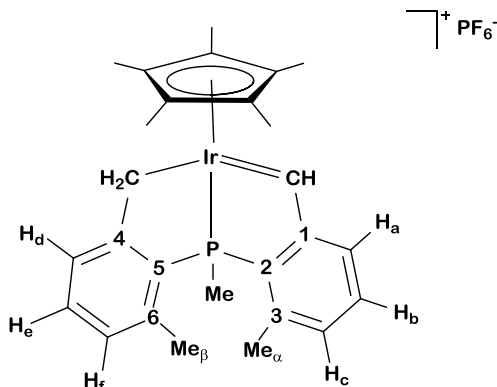
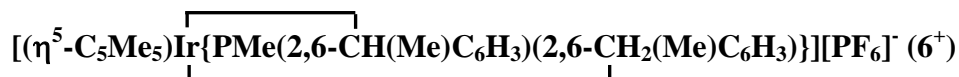
Analytical and spectroscopic data

Anal. Calcd. for $C_{27}H_{34}IrP$: C, 55.74; H, 5.89. **Found:** C, 55.3; H, 5.4.

1H NMR (400 MHz, C_6D_6 , 25 °C) δ : 7.29 (d, 2 H, H_a), 6.90 (td, 2 H, $^5J_{HP}$ = 1.4 Hz, H_b), 6.61 (dd, 2 H, $^4J_{HP}$ = 2.4 Hz, H_c), 3.19 (d, 2 H, $^2J_{HH}$ = 14.6 Hz, IrCHH), 2.79 (d, 2 H, $^2J_{HH}$ = 14.6, IrCHH), 2.35 (s, 6 H, Me_a), 1.94 (d, 3 H, $^2J_{HP}$ = 10.9 Hz, PMe), 1.67 (d, 15 H, $^4J_{HP}$ = 1.3 Hz, C_5Me_5).

$^{13}C \{^1H\}$ NMR (100 MHz, C_6D_6 , 25 °C) δ : 162.1 (d, $^2J_{CP}$ = 32 Hz, C_1), 140.1 (d, $^1J_{CP}$ = 54 Hz, C_2), 137.7 (d, $^2J_{CP}$ = 3 Hz, C_3), 128.9 (d, $^4J_{CP}$ = 2.2 Hz, CH_b), 126.8 (d, $^3J_{CP}$ = 6 Hz, CH_c), 126.7 (d, $^3J_{CP}$ = 14 Hz, CH_a), 90.5 (C_5Me_5), 21.4 (d, $^3J_{CP}$ = 2.4 Hz, Me_a), 14.0 (d, $^1J_{CP}$ = 29 Hz, PMe), 11.7 (d, $^2J_{CP}$ = 1.8 Hz, IrCH₂), 8.7 (C_5Me_5).

$^{31}P\{^1H\}$ NMR (160 MHz, C_6D_6 , 25 °C) δ : 34.5.



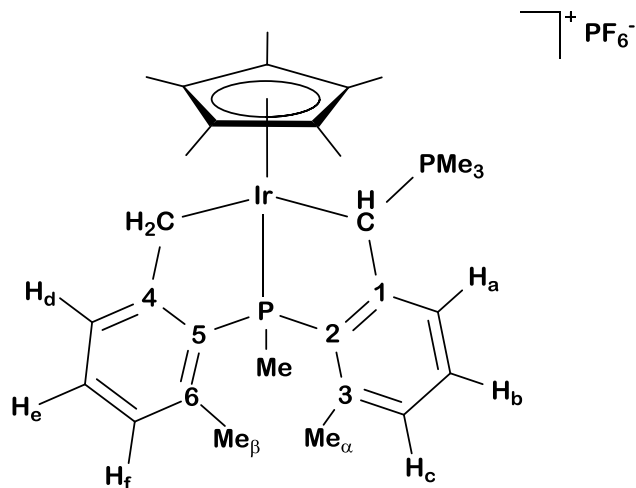
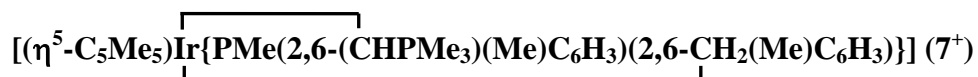
To a solid mixture of **1-Cl** (30 mg, 0.05 mmol) and $[\text{Ph}_3\text{C}]^+[\text{PF}_6]^-$ (18 mg, 0.05 mmol) placed in a screw-cap NMR tube were added 0.6 mL of CD_2Cl_2 at -60°C under argon. The tube was rapidly shaken and the resulting orange solution analyzed by ^1H , ^{31}P and ^{13}C NMR spectroscopy at -60°C

Spectroscopic data

^1H NMR (400 MHz, CD_2Cl_2 , -60°C) δ : 15.91 (s, 1 H, Ir=CH-), 7.82 (d, 1 H, H_a), 7.61 (m, 1 H, H_c), 7.41 (t, 1 H, H_b), 7.30 (m, 1 H, $\text{H}_{d/e/f}$, overlapped with Ph_3CH), 6.94 (m, 2 H, $\text{H}_{d/e/f}$), 3.70 (d, 1 H, $^2J_{\text{HH}} = 14.2$ Hz, IrCHH), 2.70 (d, 1 H, $^2J_{\text{HH}} = 14.2$, IrCHH), 2.61 (s, 3 H, Me_α), 2.55 (s, 3 H, Me_β), 2.24 (d, 3 H, $^2J_{\text{HP}} = 11.7$ Hz, PMe), 1.87 (s, 15 H, C_5Me_5).

^{13}C $\{^1\text{H}\}$ NMR (100 MHz, CD_2Cl_2 , -60°C) δ : 258.3 (Ir=CH-), 162.5 (d, $^2J_{\text{CP}} = 29$ Hz, C_1), 157.0 (d, $^2J_{\text{CP}} = 27$ Hz, C_4), 144.5 (C_3), 144.0 (C_5), 140.8 (C_2), 140.5 (C_6), 135.2, 135.1 (CH_b , CH_c), 130.4, 126.2, 128.1 (CH_d , CH_e , CH_f), 128.5 (CH_a), 104.2 (C_5Me_5), 22.5 (Me_α), 20.5 (Me_β), 11.3 (IrCH₂), 10.8 (d, $^1J_{\text{CP}} = 39$ Hz, PMe), 9.3 (C_5Me_5).

$^{31}\text{P}\{^1\text{H}\}$ NMR (160 MHz, CD_2Cl_2 , -60°C) δ : 47.3.



To a solid mixture of **5** (50 mg, 0.09 mmol) and $[\text{Ph}_3\text{C}]^+[\text{PF}_6]^-$ (33 mg, 0.09 mmol) placed in a Schlenk flask were added 5 mL of CH_2Cl_2 at $-80\text{ }^\circ\text{C}$ to give a dark orange solution. The reaction mixture was allowed to warm to $-60\text{ }^\circ\text{C}$ and additionally stirred for 15 minutes at this temperature. Then PMe_3 (1M in toluene, 140 μL , 0.14 mmol) was added at the same temperature and the solution turned pale yellow in a few seconds. The solvent was removed under vacuum and the crude washed with Et_2O to yield complex **7**⁺ as a yellow solid (61 mg, 88 %).

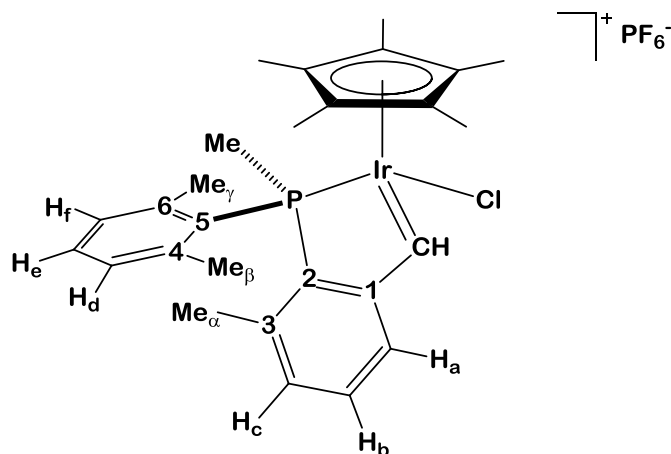
Analytical and spectroscopic data

Anal. Calcd. for $C_{30}H_{42}F_6IrP$: C, 44.94; H, 5.28. **Found:** C, 44.8; H, 5.3.

1H NMR (500 MHz, CD_2Cl_2 , 25 °C) δ : 7.38 (d, 1 H, H_d), 7.17 - 7.07 (m, 3 H, H_a , H_b , H_e), 7.01 (m, 1 H, H_c), 6.87 (dd, $^4J_{HP} = 2.8$ Hz, 1 H, H_f), 3.72 (d, 1 H, $^2J_{HP} = 21$ Hz, IrCHP), 3.54 (d, 1 H, $^2J_{HH} = 16.0$ Hz, IrCHH), 2.88 (dd, 1 H, $^2J_{HH} = 16.0$, $^3J_{HP} = 4.2$ Hz, IrCHH), 2.72 (s, 3 H, Me_a), 2.50 (s, 3 H, Me_β), 2.22 (d, 3 H, $^2J_{HP} = 11.2$ Hz, PMe), 1.71 (d, 15 H, $^4J_{HP} = 1.7$ Hz, C_5Me_5), 1.13 (d, 9 H, $^2J_{HP} = 12.6$ Hz, PMe_3).

$^{13}C \{^1H\}$ NMR (125 MHz, CD_2Cl_2 , 25 °C) δ : 160.6 (d, $^2J_{CP} = 30$ Hz, C_4), 152.3 (d, $^2J_{CP} = 31$ Hz, C_1), 144.0 (C_3), 142.2 (dd, $^1J_{CP} = 52$, $^3J_{CP} = 6$ Hz, C_2), 141.3 (d, $^1J_{CP} = 57$ Hz, C_5), 140.3 (C_6), 131.3 (CH_c), 131.0, 130.0 (CH_b , CH_e), 128.1 (d, $^3J_{CP} = 7$ Hz, CH_f), 127.6 (d, $^3J_{CP} = 14$ Hz, CH_d), 127.3 (dd, $^3J_{CP} = 13$, $^3J_{CP} = 5$ Hz, CH_a), 92.6 (C_5Me_5), 22.7 (Me_a), 21.1 (Me_β), 14.4 (d, $^1J_{CP} = 33$ Hz, PMe), 11.4 (d, $^1J_{CP} = 53$ Hz, PMe_3), 8.4 (C_5Me_5), 7.0 (IrCH₂), 2.5 (d, $^1J_{CP} = 26$ Hz, IrCHPMe₃).

$^{31}P\{^1H\}$ NMR (200 MHz, CD_2Cl_2 , 25 °C) δ : 33.3 (d, $^3J_{PP} = 3$ Hz, IrP), 26.8 (d, $^3J_{PP} = 3$ Hz, PMe_3).



A solid mixture of **1-Cl** (50 mg, 0.08 mmol) and [Ph₃C]⁺[PF₆]⁻ (32 mg, 0.08 mmol) was dissolved in CH₂Cl₂ (3 mL) at -20 °C and stirred at room temperature for 5 minutes, resulting in a dark green solution. Addition of pentane (10 mL) led to the precipitation of a green solid which was washed with diethyl ether to yield complex **8**⁺ as a dark green powder (54 mg, 87 %). Suitable crystals for X-ray analysis were obtained by slow diffusion of pentane into a dichloromethane solution of the compound.

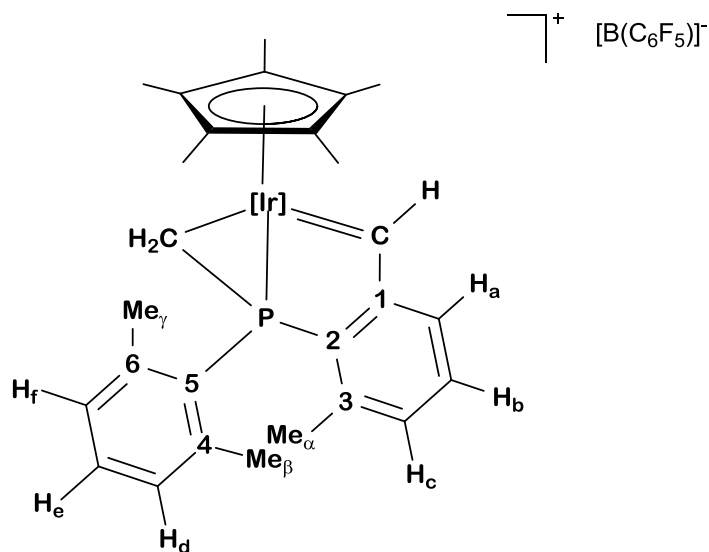
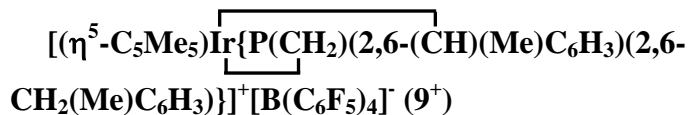
Analytical and spectroscopic data

Anal. Calcd. for $C_{27}H_{39}ClF_6IrP_2$: C, 42.27; H, 5.12. **Found:** C, 42.3; H, 4.8.

1H NMR (400 MHz, CD_2Cl_2 , 25 °C) δ : 16.61 (d, 1 H, $^3J_{HP} = 0.9$ Hz, Ir=CH), 8.18 (d, 1 H, H_a), 7.87 (dd, 1 H, $^4J_{HP} = 3.4$ Hz, H_c), 7.61 (td, 1 H, $^5J_{HP} = 2.4$ Hz, H_b), 7.40 (td, 1 H, $^5J_{HP} = 2.1$ Hz, H_e), 7.33, 7.06 (m, 1 H each, H_d , H_f), 2.56 (d, 3 H, $^2J_{HP} = 11.0$ Hz, PMe), 2.55, 1.32 (s, 3 H each, Me_β , Me_γ), 2.44 (s, 3 H, Me_α), 1.66 (d, 15 H, $^4J_{HP} = 1.8$ Hz, C_5Me_5). All aromatic couplings are of *ca.* 7.5 Hz.

^{13}C NMR (100 MHz, CD_2Cl_2 , 25 °C) δ : 262.4 ($^1J_{CH} = 153$ Hz, Ir=CH), 165.2 (d, $^2J_{CP} = 29$ Hz, C_1), 145.6 (C_3), 143.8 (d, $^1J_{CP} = 61$ Hz, C_2), 142.4 (d, $^2J_{CP} = 11$ Hz, $C_{4/6}$), 140.9 (d, $^2J_{CP} = 8$ Hz, $C_{4/6}$), 139.1 (d, $^3J_{CP} = 8$ Hz, CH_c), 135.2 (CH_b), 132.5 (d, $^4J_{CP} = 2$ Hz, CH_e), 131.9, 131.0 (d, $^3J_{CP} = 10$ Hz, CH_d , CH_f), 131.4 (d, $^3J_{CP} = 13$ Hz, CH_a), 121.0 (d, $^1J_{CP} = 54$ Hz, C_5), 108.7 (C_5Me_5), 25.6, 24.0 (d, $^3J_{CP} = 6$ Hz, Me_β , Me_γ), 20.4 (d, $^3J_{CP} = 2$ Hz, Me_α), 14.5 (d, $^1J_{CP} = 42$ Hz, PMe), 8.8 (C_5Me_5).

$^{31}P\{^1H\}$ NMR (160 MHz, CD_2Cl_2 , 25 °C) δ : 20.8.



A solution of $[\text{Ph}_3\text{C}]^+[\text{B}(\text{C}_6\text{F}_5)_4]^-$ (40 mg, 0.04) in dichloromethane (0.5 mL) was added under argon over a solution of **2** (25 mg, 0.04) in the same solvent at $-60\text{ }^\circ\text{C}$. The solution turned dark-red immediately and, after addition of pentane, compound $\mathbf{9}^+$ precipitated as a red powder. Washing with pentane and drying under vacuum gave alkylidene $\mathbf{9}^+$ in 60 % yield (31 mg). To avoid decomposition of the alkylidene, spectroscopic analyses were carried out at $-60\text{ }^\circ\text{C}$ with $\mathbf{9}^+$ prepared *in situ* into the NMR tube, without further purification. Crystals suitable for X-ray analysis were obtained by slow diffusion of pentane into a concentrated dichloromethane solution of the complex.

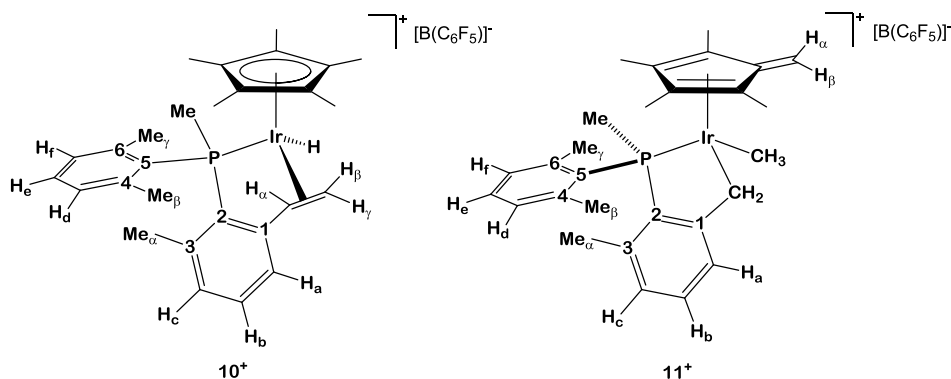
Spectroscopic data

Due to its instability toward moisture and oxygen, reliable microanalytical data could not be obtained.

^1H NMR (400 MHz, CD_2Cl_2 , 25 °C) δ : 14.9 (s, 1 H, Ir=CH), 7.76 (d, 1 H, H_a), 7.55 (m, 2 H, H_c , H_e), 7.40, 7.25 (m, 1 H each, H_d , H_f), 7.35 (m, 1 H, H_b), 3.40 (d, 1 H, $^2J_{\text{HH}} = 8.6$ Hz, IrCHH), 3.33 (d, 1 H, $^2J_{\text{HH}} = 8.6$ Hz, IrCHH), 2.91, 2.16 (s, 3 H each, Me_β , Me_γ), 2.27 (s, 3 H, Me_α), 1.96 (d, 15 H, $^4J_{\text{HP}} = 1.8$ Hz, C_5Me_5). All aromatic couplings are of *ca.* 7.5 Hz.

^{13}C NMR (125 MHz, CD_2Cl_2 , -60 °C) δ : 243.7 (d, $^2J_{\text{CP}} = 28$ Hz, Ir=CH), 162.4 (d, $^2J_{\text{CP}} = 27$ Hz, C_1), 144.8 (d, $^2J_{\text{CP}} = 4$ Hz, C_3), 143.9 (d, $^2J_{\text{CP}} = 16$ Hz, $\text{C}_{4/6}$), 141.5 (d, $^2J_{\text{CP}} = 6$ Hz, $\text{C}_{4/6}$), 134.4 (CH_b , overlapped with BAr_4^-), 133.3 (d, $^3J_{\text{CP}} = 10$ Hz, CH_c), 129.8 (CH_e), 129.1, 128.4 (d, $^3J_{\text{CP}} = 11$ Hz, CH_d , CH_f), 127.2 (d, $^3J_{\text{CP}} = 17$ Hz, CH_a), 111.1 (d, $^1J_{\text{CP}} = 69$ Hz, C_5), 101.9 (C_5Me_5), 24.4, 19.2 (d, $^3J_{\text{CP}} = 6, 14$ Hz, Me_β , Me_γ), 19.0 (d, $^3J_{\text{CP}} = 5$ Hz, Me_α), 13.7 (d, $^1J_{\text{CP}} = 45$ Hz, IrCH₂), 8.5 (C_5Me_5). Signal corresponding to C_2 was not identified.

$^{31}\text{P}\{^1\text{H}\}$ NMR (160 MHz, CD_2Cl_2 , 25 °C) δ : -13.1.

Reaction of **1-Me** with $[\text{Ph}_3\text{C}]^+[\text{B}(\text{C}_6\text{F}_5)_4]^-$ 

A solution of $[\text{Ph}_3\text{C}]^+[\text{B}(\text{C}_6\text{F}_5)_4]^-$ (92 mg, 0.10 mmol) in CH_2Cl_2 (1 mL) was added at 0 °C under argon over a CH_2Cl_2 solution of **1-Me** (60 mg, 0.10 mmol) placed in a Schlenk flask. The reaction mixture was stirred at room temperature for 30 min and analyzed by $^{31}\text{P}\{^1\text{H}\}$ NMR, which showed complete conversion of the methyl complex **1-Me** into a *ca.* 6:1:3 mixture of compounds **k-10⁺** : **t-10⁺** : **11⁺**. Heating the solution at 50 °C for 12 hours resulted in complete isomerization of **k-10⁺** into **t-10⁺**, while **11⁺** remained unaltered. The solvent was removed under vacuum and the residue washed with diethyl ether. Compounds **10⁺** and **11⁺** were purified by crystallization from CH_2Cl_2 /pentane to obtain a mixture of both isomers in 56 % overall yield (72 mg); however all attempts to isolate the individual complexes in a pure state were unsuccessful. Spectroscopic data obtained from mixtures of these isomers, are detailed below.

Analytical and spectroscopic data

Anal. Calcd. for $C_{52}H_{42}BF_{20}IrP$: C, 48.76; H, 3.31. **Found:** C, 48.9; H, 3.5.

Compound $t\text{-}10^+$ (thermodynamic isomer of 10^+)

1H NMR (500 MHz, CD_2Cl_2 , 25 °C) δ : 7.47 (d, 1 H, H_a), 7.36 – 7.23 (m, 3 H, CH_{Xyl}), 7.07 – 6.98 (m, 2 H, CH_{Xyl}), 4.27 (dd, 1 H, $^3J_{HH} = 10.5$, $^3J_{HH} = 8.6$ Hz, H_a), 2.83 (dt, 1 H, $^3J_{HH} = 10.5$, $^2J_{HH} = ^3J_{HP} = 2.4$ Hz, H_γ), 2.64 (dd, 1 H, $^3J_{HH} = 8.6$, $^2J_{HH} = 2.4$ Hz, H_β), 2.59, 1.45 (s, 3 H each, Me_β , Me_γ), 2.46 (d, 3 H, $^2J_{HP} = 9.0$ Hz, PMe), 1.91 (s, 3 H, Me_a), 1.73 (d, 15 H, $^4J_{HP} = 1.7$ Hz, C_5Me_5), -15.77 (d, 1 H, $^2J_{HP} = 30.1$ Hz, IrH). All aromatic couplings are of *ca.* 7.5 Hz.

^{13}C NMR (125 MHz, CD_2Cl_2 , 25 °C) δ : 146.9 (d, $^2J_{CP} = 23$ Hz, C_1), 141.8 (C_3), 141.6, 140.2 (d, $^2J_{CP} = 9$ Hz, C_4 , C_6), 136.8 (d, $^1J_{CP} = 61$ Hz, C_2), 131.8, 131.5 (CH_b , CH_e), 131.1, 130.3 (d, $^3J_{CP} = 8$ Hz, CH_d , CH_f), 130.7 (d, $^3J_{CP} = 8$ Hz, CH_c), 127.0 (d, $^3J_{CP} = 16$ Hz, CH_a), 123.4 (d, $^1J_{CP} = 52$ Hz, C_5), 101.0 (C_5Me_5), 62.7 (d, $^2J_{CP} = 4$ Hz, CH_a), 34.1 ($CH_\beta H_\gamma$), 28.0 (d, $^1J_{CP} = 50$ Hz, PMe), 24.7, 22.8 (d, $^3J_{CP} = 7$ Hz, Me_β , Me_γ), 19.9 (d, $^3J_{CP} = 18$ Hz, Me_a), 8.4 (C_5Me_5).

$^{31}P\{^1H\}$ NMR (200 MHz, CD_2Cl_2 , 25 °C) δ : -0.1.

Compound *k*-10⁺ (kinetic isomer of 10⁺)

¹H NMR (500 MHz, CD₂Cl₂, 25 °C) δ: 7.40 (m, 1 H, H_a), 7.35 – 7.19 (m, 3 H, CH_{Xyl}), 7.08 – 6.96 (m, 2 H, CH_{Xyl}), 4.41 (t, 1 H, ³J_{HH}, ³J_{HH} = 9.1 Hz, H_a), 2.67 (m, overlapped, H_γ), 2.65, 1.72 (s, 3 H each, Me_β, Me_β), 2.24 (d, 3 H, ²J_{HP} = 10.2 Hz, PMe), 2.12 (t, 1 H, ³J_{HH} = ²J_{HH} = 9.1 Hz, H_γ), 1.93 (d, 15 H, ⁴J_{HP} = 1.8 Hz, C₅Me₅), 1.89 (s, 3 H, Me_α), -14.31 (d, 1 H, ²J_{HP} = 28.5 Hz, IrH).

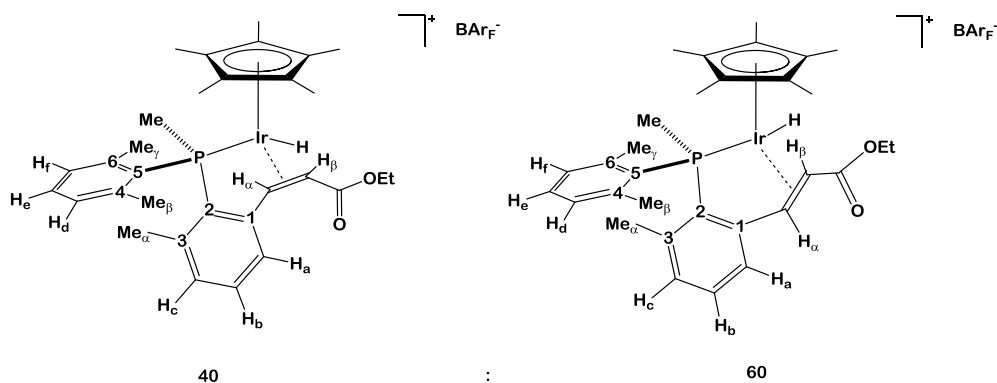
³¹P{¹H} NMR (200 MHz, CD₂Cl₂, 25 °C) δ: -9.8.

Compound 11⁺

¹H NMR (500 MHz, CD₂Cl₂, 25 °C) δ: 7.36 – 7.23 (m, 4 H, CH_{Xyl}), 7.07 – 6.98 (m, 2 H, CH_{Xyl}), 5.30 (d, 1 H, ⁴J_{HP} = 4.2 Hz, H_{αβ}), 4.54 (s, 1 H, H_{αβ}), 3.71 (d, 1 H, ²J_{HH} = 13.9 Hz, IrCHH), 2.99 (d, 1 H, ²J_{HH} = 13.9 Hz, IrCHH), 2.69, 1.45 (s, 3 H each, Me_β, Me_γ), 2.43 (d, 3 H, ²J_{HP} = 9.6 Hz, PMe), 2.01 (s, 3 H, Me_α), 1.80, 1.75 (d, 3 H each, ⁴J_{HP} = 2.8 Hz, 2 Cp-Me), 1.57 (s, 3 H, Cp-Me), 0.85 (d, 3 H, ³J_{HP} = 2.7 Hz, IrCH₃), 0.76 (d, 3 H, ⁴J_{HP} = 1.4 Hz, Cp-Me).

¹³C NMR (125 MHz, CD₂Cl₂, 25 °C) δ: 152.7 (d, ²J_{CP} = 27 Hz, C₁), 141.5, 140.1 (C_{4/6}), 140.2 (C₃), 134.8 (d, ¹J_{CP} = 65 Hz, C₂), 129.4 (d, ³J_{CP} = 9 Hz, CH_c), 132.1 (CH_b, CH_e), 131.2, 131.0 (d, ³J_{CP} = 9 Hz, CH_d, CH_f), 127.5 (d, ³J_{CP} = 16 Hz, CH_a), 124.8 (d, ¹J_{CP} = 53 Hz, C₅), 114.2, 111.8, 110.1, 109.4, 109.3 (C₅Me₄CH_αH_β), 68.6 (CH_αH_β), 29.6 (IrCH₂), 25.3, 24.7 (d, ³J_{CP} = 6 Hz, Me_β, Me γ), 21.0 (d, ¹J_{CP} = 44 Hz, PMe), 20.1 (d, ³J_{CP} = 16 Hz, Me_α), 8.2, 7.8, 6.8, 4.7 (C₅Me₄CH_αH_β), -10.9 (d, ²J_{CP} = 3 Hz, IrCH₃).

³¹P{¹H} NMR (200 MHz, CD₂Cl₂, 25 °C) δ: 12.2.

Synthesis of compounds 12^+ 

To a solid mixture of **1-Cl** (50 mg, 0.08 mmol) and NaBAr_F (72 mg, 0.08 mmol) placed in a Schlenk flask were added 5 mL of CH₂Cl₂. The reaction mixture was stirred for 5 min at room temperature and ethyldiazoacetate (10 μ L, 0.096 mmol) was added. The solution was filtered and the volatiles were evaporated under reduced pressure to obtain **12⁺** (102 mg, 86 %) as a pale yellow powder mixture of isomers in a *ca.* ratio of 60:40. It can be recrystallized from a 1:2 mixture of CH₂Cl₂:pentane.

Analytical and spectroscopic data

Anal. Calcd. for C₆₃H₅₃BF₂₄IrO₂P: C, 49.39; H, 3.49. **Found:** C, 49.0; H, 3.0.

Final composition of isomers: 60:40 (*trans* : *cis*). Isomer assignment for each set of signals is based on 2D-NOESY analysis, since NOE cross-peaks can be found between H _{α} and H _{β} only for the *cis* isomer, whereas the *trans* isomer presents a NOE cross-peak between H _{α} and H_a, which cannot be detected in the former case.

Major Isomer (*trans*, 60 %):

IR (Nujol): $\nu(\text{IrH})$ 2175, $\nu(\text{CO})$ 1710 cm^{-1} .

^1H NMR (400 MHz, CD_2Cl_2 , 25 $^\circ\text{C}$) δ : 7.57 (d, 1 H, H_a), 7.37, 7.30, 7.08 (m, H_{b-f} , overlapped with analogous signals of the minor isomer), 4.73 (d, 1 H, $^3J_{\text{HH}} = 9.3$ Hz, CH_a), 4.29 (m, 1 H, OCHHCH_3), 4.14 (m, 1 H, OCHHCH_3), 3.72 (d, 1 H, $^3J_{\text{HH}} = 9.3$ Hz, CH_β), 2.61, 1.46 (s, 3 H each, Me_β , Me_γ), 2.56 (d, 3 H, $^2J_{\text{HP}} = 10.0$ Hz, PMe), 1.95 (s, 3 H, Me_a), 1.73 (d, 15 H, $^4J_{\text{HP}} = 1.7$ Hz, C_5Me_5), 1.32 (t, 3 H, $^3J_{\text{HH}} = 7.1$ Hz, OCH_2CH_3), -15.35 (d, 1 H, $^2J_{\text{HP}} = 27.8$ Hz, IrH). All aromatic couplings are of *ca.* 7.5 Hz.

^{13}C NMR (100 MHz, CD_2Cl_2 , 25 $^\circ\text{C}$) δ : 170.0 (CO), 147.6 (d, $^2J_{\text{CP}} = 26$ Hz, C_1), 142.3, 141.7, 141.5, 141.1 (C_2 , C_3 , C_4 , C_6), 132.7 (CH_b), 132.2 (d, $^4J_{\text{CP}} = 2$ Hz, CH_e), 131.5 ($\text{CH}_{d/f}$), 131.4 (CH_c), 131.0 (d, $^3J_{\text{CP}} = 6$ Hz, $\text{CH}_{d/f}$), 127.1 (d, $^3J_{\text{CP}} = 16$ Hz, CH_a), 122.7 (d, $^1J_{\text{CP}} = 56$ Hz, C_5), 103.1 (C_5Me_5), 61.7 (OCH_2CH_3), 59.5 (d, $^2J_{\text{CP}} = 4$ Hz, CH_a), 40.9 (CH_β), 26.5 (d, $^1J_{\text{CP}} = 47$ Hz, PMe), 25.0, 23.7 (d, $^3J_{\text{CP}} = 6$ Hz, Me_β , Me_γ), 20.3 (d, $^3J_{\text{CP}} = 6$ Hz, Me_a), 14.5 (OCH_2CH_3), 8.8 (C_5Me_5).

$^{31}\text{P}\{^1\text{H}\}$ NMR (160 MHz, CD_2Cl_2 , 25 $^\circ\text{C}$) δ : 1.0.

Minor isomer (*cis*, 40 %):

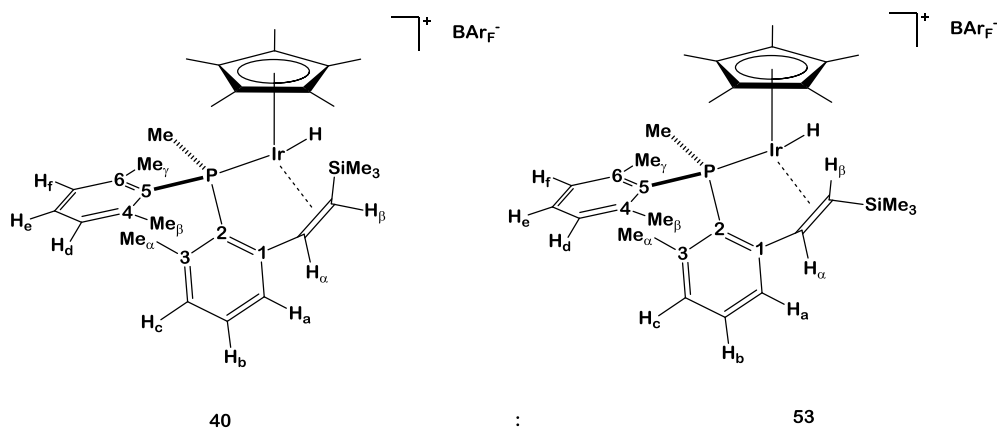
IR (Nujol): $\nu(\text{IrH})$ 2150, $\nu(\text{CO})$ 1650 cm^{-1} .

^1H NMR (400 MHz, CD_2Cl_2 , 25 $^\circ\text{C}$) δ : 7.46 (d, 1 H, H_a), 7.37, 7.30, 7.08 (m, H_{b-f} , overlapped with analogous signals of the major isomer), 4.67 (d, 1 H, $^3J_{\text{HH}} = 9.1$ Hz, CH_a), 4.02 (m, 1 H, OCHHCH_3), 3.96 (m, 1 H, OCHHCH_3), 3.49 (d, 1 H, $^3J_{\text{HH}} = 9.1$ Hz, CH_β), 2.61, 1.53 (s, 3 H each, Me_β , Me_γ), 2.56 (d, 3 H, $^2J_{\text{HP}} = 10.0$ Hz, PMe), 1.95 (s, 3 H, Me_a), 1.73 (d, 15 H, $^4J_{\text{HP}} = 1.7$ Hz, C_5Me_5), 1.32 (t, 3 H, $^3J_{\text{HH}} = 7.1$ Hz, OCH_2CH_3), -15.35 (d, 1 H, $^2J_{\text{HP}} = 27.8$ Hz, IrH). All aromatic couplings are of *ca.* 7.5 Hz.

Me_γ), 2.50 (d, 3 H, $^2J_{\text{HP}} = 11.1$ Hz, PMe), 1.92 (s, 3 H, Me_α), 1.75 (d, 15 H, $^4J_{\text{HP}} = 1.6$ Hz, C₅Me₅), 1.16 (t, 3 H, $^3J_{\text{HH}} = 7.1$ Hz, OCH₂CH₃), -16.39 (d, 1 H, $^2J_{\text{HP}} = 27.8$ Hz, IrH). All aromatic couplings are of *ca.* 7.5 Hz.

¹³C NMR (100 MHz, CD₂Cl₂, 25 °C) δ: 172.5 (CO), 146.4 (d, $^2J_{\text{CP}} = 23$ Hz, C₁), 142.2, 141.5, 141.4, 141.0 (C₂, C₃, C₄, C₆), 132.4 (d, $^4J_{\text{CP}} = 2$ Hz, CH_e), 132.0 (CH_b), 131.6 (CH_{d/f}), 131.3 (CH_c), 130.9 (d, $^3J_{\text{CP}} = 6$ Hz, CH_{d/f}), 126.8 (d, $^3J_{\text{CP}} = 17$ Hz, CH_a), 124.7 (C₅), 103.1 (C₅Me₅), 63.9 (d, $^2J_{\text{CP}} = 3$ Hz, CH_α), 61.4 (OCH₂CH₃), 40.3 (CH_β), 25.7 (d, $^1J_{\text{CP}} = 47$ Hz, PMe), 25.6, 23.4 (d, $^3J_{\text{CP}} = 5$ Hz, 8 Hz, Me_β, Me_γ), 20.1 (d, $^3J_{\text{CP}} = 6$ Hz, Me_α), 14.0 (OCH₂CH₃), 8.8 (C₅Me₅).

³¹P{¹H} NMR (160 MHz, CD₂Cl₂, 25 °C) δ: 3.1.

Synthesis of compounds **13**⁺

To a solid mixture of **1-Cl** (50 mg, 0.081 mmol) and NaBAR_F (72 mg, 0.081 mmol) placed in a Schlenk flask 3 mL of CH₂Cl₂ were added at -20 °C. After stirring for 10 min, a solution of N₂CHSiMe₃ (2M in hexanes, 50 μL) was added at this temperature and the reaction allowed to warm up to 25 °C and additionally stirred for 1 hour. The solution was filtered and the volatiles were removed under vacuum to give a pale yellow foam which was washed with pentane. ¹H and ³¹P{¹H} NMR spectroscopic analysis of the crude showed four different products in a ratio of *ca.* 53:40:4:3, all of which exhibited characteristic Ir–H resonances in the ¹H NMR spectrum. The two major species were identified as the *trans* (53 %) and *cis* (40 %) isomers. However, only *cis*-**12**⁺ was isolated as a single species by crystallization from Et₂O/pentane (1:1) in 30 % yield (38 mg).

Analytical and spectroscopic data for *cis*-13⁺

IR (Nujol): $\nu(\text{IrH})$ 2160 cm^{-1} .

Anal. Calcd. for $\text{C}_{63}\text{H}_{57}\text{BF}_{24}\text{IrPSi}$: C, 49.39; H, 3.75. **Found:** C, 49.3; H, 3.6.

¹H NMR (500 MHz, CD_2Cl_2 , 25 °C) δ : 7.41 (d, 1 H, H_a), 7.34 (m, 2 H, H_b , H_e), 7.26, 7.01 (dd, 1 H each, $^4J_{\text{HP}} = 4.2$ Hz, H_d , H_f), 7.05 (dd, 1 H, $^4J_{\text{HP}} = 4.1$ Hz, H_c), 4.85 (d, 1 H, $^3J_{\text{HH}} = 11.7$ Hz, CH_a), 2.62, 1.53 (s, 3 H each, Me_β , Me_γ), 2.52 (d, 3 H, $^2J_{\text{HP}} = 10.5$ Hz, PMe), 2.38 (d, 1 H, $^3J_{\text{HH}} = 11.7$ Hz, CH_β), 1.89 (s, 3 H, Me_a), 1.70 (d, 15 H, $^4J_{\text{HP}} = 1.6$ Hz, C_5Me_5), 0.13 (s, 9 H, SiMe_3), -15.85 (d, 1 H, $^2J_{\text{HP}} = 30.7$ Hz, IrH). All aromatic couplings are of *ca.* 7.5 Hz.

¹³C NMR (125 MHz, CD_2Cl_2 , 25 °C) δ : 147.2 (d, $^2J_{\text{CP}} = 27$ Hz, C_1), 142.2, 140.5 (d, $^2J_{\text{CP}} = 10$, 8 Hz, C_4 , C_6), 141.6 (C_3), 132.3, 131.6 (CH_b , CH_e), 131.3 (d, $^3J_{\text{CP}} = 10$ Hz, $\text{CH}_{d/f}$), 130.9 (m, CH_c , $\text{CH}_{d/f}$), 128.8 (C_2 , overlapped with BAr_F), 127.3 (d, $^3J_{\text{CP}} = 17$ Hz, CH_a), 124.4 (d, $^1J_{\text{CP}} = 49$ Hz, C_5), 101.0 (C_5Me_5), 71.6 (d, $^2J_{\text{CP}} = 4$ Hz, CH_a), 44.4 (CH_β), 28.4 (d, $^1J_{\text{CP}} = 48$ Hz, PMe), 25.8, 22.5 (d, $^3J_{\text{CP}} = 5$, 8 Hz, Me_β , Me_γ), 19.8 (d, $^3J_{\text{CP}} = 4$ Hz, Me_a), 8.6 (C_5Me_5), 0.0 (SiMe_3).

³¹P{¹H} NMR (200 MHz, CD_2Cl_2 , 25 °C) δ : -7.6.

The major isomer of compounds **13⁺** (*trans* isomer, *ca.* 53 % of the crude) is characterized by a ¹H NMR doublet at 4.36 ($^3J_{\text{HH}} = 12.7$ Hz) corresponding to CH_a , as well as a doublet with δ 2.27 associated with the PMe group,

which overlaps the signal due to CH_β . A doublet at 1.94 ppm is due to the C_5Me_5 ligand, and the SiMe_3 fragment gives a singlet at 0.26 ppm and the hydride exhibits a doublet at -16.84 (d, $^2J_{\text{CP}} = 30.7$ Hz) ppm. In the $^{31}\text{P}\{^1\text{H}\}$ NMR spectrum a signal is recorded with δ 0.9 ppm. Other two minor isomers (*ca.* 5 % of the overall reaction mixture) present characteristic hydridic signals at -14.31 (d, $^2J_{\text{CP}} = 28.9$ Hz) and -15.01 (d, $^2J_{\text{CP}} = 32.9$ Hz) ppm. The corresponding $^{31}\text{P}\{^1\text{H}\}$ NMR peaks appear at -9.9 and -12.8 ppm, respectively.

3.A.3. Hydrogen/Deuterium Exchange Reactions.

H/D exchange of complexes 1-X (X = Cl, Br, I, SCN). Following by ^1H NMR spectroscopy the reaction of compounds **1-X** with a 1:1 mixture of CD_2Cl_2 and CD_3OD , under argon, a progressive decline in the intensity of the resonances due to the methylene and methyl protons of the metalated ligand, and a concomitant increase of the CD_3OH signal was apparent. In a typical experiment, a solution of **1-X** (0.01 mmol) in 0.5 mL of a 1:1 mixture of CD_2Cl_2 : CD_3OD was heated in an oil bath at 45 °C (bath temperature). From these experiments a $t_{1/2}$ value of 490 min was determined for **1-Cl**. After *ca.* 24 h the deuteration was essentially complete. The velocity of deuteration was proved to be highly dependent upon the concentration of CD_3OD (see Table 3). The rate of deuteration of **1-Br** under the same conditions is similar to that observed for **1-Cl**, whereas no exchange was observed either for **1-I** or for **1-SCN**, even by heating at 80 °C.

H/D exchange of complex 1-H. Deuteration experiments with **1-H** were performed as described above for **1-X** although in this case a *ca.* 10:1 mixture of CD_2Cl_2 : CD_3OD was utilized. Deuteration occurred at room temperature with a half-life of $t_{1/2} = 130$ min. For comparative purposes $t_{1/2}$ for the H/D exchange in **1-Cl** measured also at 25 °C is *ca.* 10 days.

3.A.4. Kinetic studies.

Dehydrogenative C–C bond formation from 1^+ . Kinetic measurements were made by preparing a solution of 1^+ (23 mg, 0.016 mmol) in CD_2Cl_2 (0.6 mL) in a screw-capped NMR tube at 0 °C. A CD_2Cl_2 solution of 2,2,6,6-tetramethylpiperidine (25 μL , 0.032 M) was then added under argon and the reaction mixture was monitored by ^1H and $^{31}\text{P}\{^1\text{H}\}$ NMR at 25 °C over a period of *ca.* 3.3 hours. The concentration of 1^+ , which exhibits broad NMR signals at this temperature, was estimated from the concentrations of 1-H_2^+ and 4^+ . The first-order kinetic plot for the consumption of 4^+ is depicted in Figure 41 and the corresponding k value was calculated to be $(2.5 \pm 0.2) \cdot 10^{-4} \text{ s}^{-1}$. The experiment was performed in duplicate.

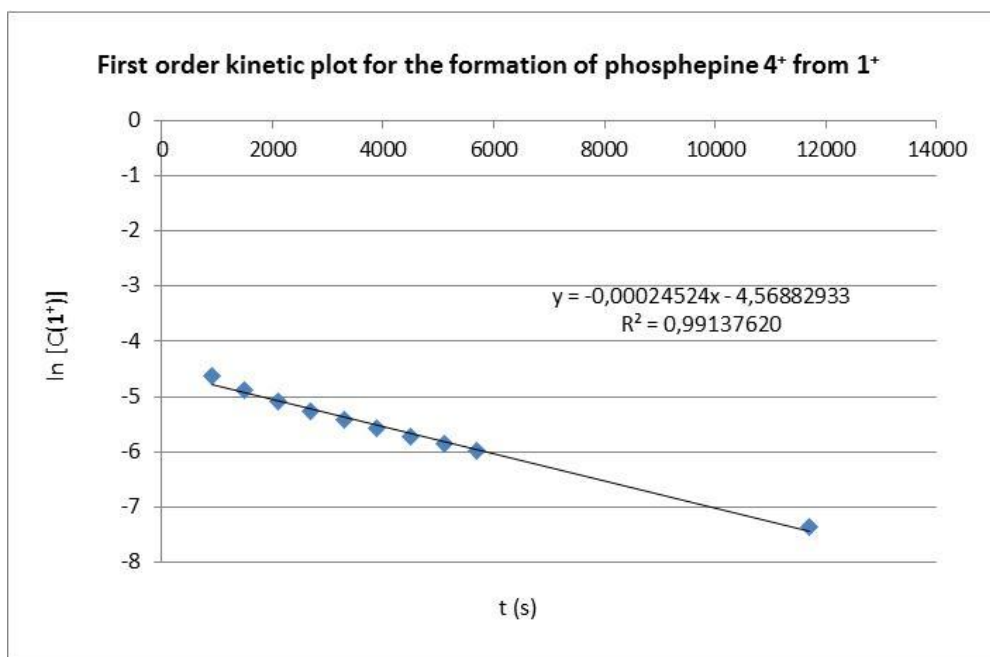


Figure 41. First order kinetic plot for the base-catalyzed formation of phosphepine complex 4^+ from 1^+ at 25 °C.

Direct C–C bond coupling from alkylidene 6^+ . A screw-capped NMR tube was charged with **5** (10 mg, 0.017 mmol) and $[\text{Ph}_3\text{C}][\text{B}(\text{C}_6\text{F}_5)_4]$ (16 mg, 0.017 mmol) inside a glovebox and then CD_2Cl_2 (0.6 mL) was added at -60°C . The NMR tube was rapidly shaken to give a dark red solution which was placed in the pre-cooled NMR probe at 0°C . The conversion of 6^+ to 4^+ was monitored by $^{31}\text{P}\{^1\text{H}\}$ NMR spectroscopy and exhibited a first order kinetic dependence on the concentration of 6^+ . From the corresponding plot depicted in Figure 42 a k value of $(2.22 \pm 0.06) \cdot 10^{-4} \text{ s}^{-1}$ was obtained. This measurement was repeated twice with similar results.

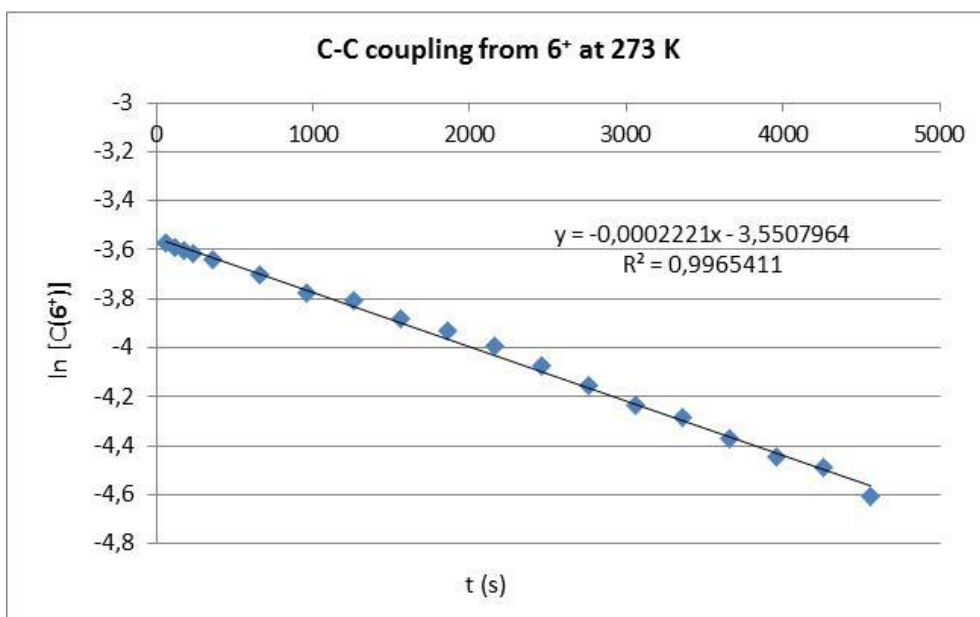


Figure 42. First order kinetic plot for the formation of phosphepine compound 4^+ from 6^+ at 0°C .

Part B: Studies on $(\eta^5\text{-C}_5\text{Me}_5)\text{Ir}(\text{PR}_2(\text{Xyl}))$ Units

3.B. EXPERIMENTAL SECTION

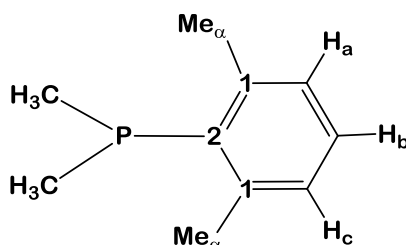
3.B.1. Materials and Methods. General.

All operations were performed under an argon atmosphere using standard Schlenk techniques, employing dry solvents and glassware. HRMS data were obtained using a Jeol JMS-SX 102A mass spectrometer at the Analytical Services of the Universidad de Sevilla (CITIUS). Microanalyses were performed by the Microanalytical Service of the Instituto de Investigaciones Químicas (Sevilla, Spain). Infrared spectra were recorded on a Bruker Vector 22 spectrometer. The NMR instruments were Bruker DRX-500, DRX-400 and DRX-300 spectrometers. Spectra were referenced to external SiMe_4 (δ 0

ppm) using the residual proton solvent peaks as internal standards (^1H NMR experiments), or the characteristic resonances of the solvent nuclei (^{13}C NMR experiments), while ^{31}P was referenced to external H_3PO_4 . Spectral assignments were made by routine one- and two-dimensional NMR experiments where appropriate. The crystal structures were determined in a Bruker-Nonius, X8Kappa diffractometer. Dimer $[(\eta^5\text{-C}_5\text{Me}_5)\text{IrCl}_2]_2$ ⁷⁰ and NaBAr_F ⁷¹ were prepared according to literature procedures. In the ^1H NMR spectra all aromatic couplings are of *ca.* 7.5 Hz. The ^1H and $^{13}\text{C}\{^1\text{H}\}$ NMR spectral data for the BAr_F^- anion ($\text{BAr}_\text{F} = \text{B}[3,5\text{-(CF}_3)_2\text{C}_6\text{H}_3]$) in CD_2Cl_2 are identical for all complexes and therefore are not repeated below. BAr_F^- : ^1H RMN: δ 7.75 (s, 8 H, *o*-Ar), 7.58 (s, 4 H, *p*-Ar). $^{13}\text{C}\{^1\text{H}\}$ RMN: δ 162.1 (q, 37 Hz, *ipso*-Ar), 135.3 (*o*-Ar), 129.2 (q, 31 Hz, *m*-Ar), 124.9 (q, 273 Hz, CF_3), 117.8 (*p*-Ar).

⁷⁰ White, C.; Yates, A.; Maitlis, P. M.; Heinekey, D. M. *Inorg. Synth.* **1992**, 29, 228.

⁷¹ Yakelis, N. A.; Bergman, R. G. *Organometallics*, **2005**, 24, 3579.

3.B.2. Synthesis of phosphines.**PMe₂(Xyl)**Preparation of PXX'(Xyl), X, X' = Cl, Br

A solution of PCl₃ (1 mL, 11.5 mmol) in THF (20 mL) placed in a three-neck round-bottom flask was cooled down to -78 °C. Using a dropping funnel a THF solution of (2,6-C₆H₃)MgBr (15.5 mL, 0.71 M, 11.0 mmol) (prepared as detailed for the synthesis of PMe(Xyl)₂; see Experimental Section of Chapter 1) was added to the former solution at this temperature, resulting in the formation of a white precipitate. The reaction mixture was allowed to warm to room temperature and additionally stirred for 12 h. The solvent was removed under reduced pressure and the crude product extracted with pentane (4 x 30 mL). The volatiles were evaporated under vacuum to give a mixture of PCl₂(Xyl), PBrCl(Xyl) and PBr₂(Xyl) in a *ca.* ratio of 40:45:15.

PCl₂(Xyl): ³¹P{¹H} RMN (162 MHz, C₆D₆, 25 °C) δ: 166.1.

PBrCl(Xyl): ³¹P{¹H} RMN (162 MHz, C₆D₆, 25 °C) δ: 159.8.

PBr₂(Xyl): ³¹P{¹H} RMN (162 MHz, C₆D₆, 25 °C) δ: 151.4.

Preparation of PMe₂(Xyl)

The above mixture of halophosphines PCl₂(Xyl), PBrCl(Xyl) and PBr₂(Xyl) (*ca.* 40:45:15; 800 mg, *ca.* 2.70 mmol) was placed in a three-necked round-bottom flask and dissolved in diethyl ether (30 mL). MeMgBr (2.7 mL, 3 M in Et₂O, 8 mmol) was added dropwise at -78 °C using a dropping funnel, then the reaction mixture was slowly warmed up to 25 °C and additionally stirred for 12 h. The solvent was removed at 0 °C under vacuum and the residue extracted with pentane. The volatiles was evaporated at 0 °C under reduced pressure to yield PMe(Xyl)₂ as a colourless oil (290 mg, *ca.* 65 %).

Spectroscopic data

¹H NMR (400 MHz, C₆D₆, 25 °C) δ: 7.00 (t, 1 H, H_b), 6.83 (dd, 2 H, ⁴J_{HP} = 2.2 Hz, H_a), 2.50 (s, 6 H, Me_a), 1.24 (d, 6 H, ²J_{HP} = 5.3 Hz, PMe). All aromatic couplings are of *ca.* 7.5 Hz.

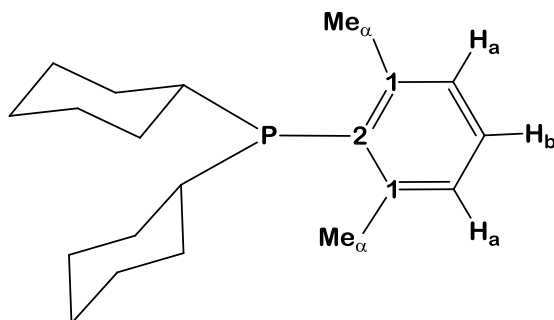
¹³C{¹H} NMR (100 MHz, C₆D₆, 25 °C) δ: 144.2 (d, ²J_{CP} = 15 Hz, C₁), 136.5 (d, ¹J_{CP} = 24 Hz, C₂), 129.4 (d, ³J_{CP} = 4 Hz, CH_a), 129.3 (CH_b), 23.4 (d, ³J_{CP} = 20 Hz, Me_a), 12.4 (d, ¹J_{CP} = 15 Hz, PMe).

³¹P{¹H} NMR (160 MHz, C₆D₆, 25 °C) δ: -54.0.

General procedure for the synthesis of $\text{PR}_2(\text{Xyl})$ ($\text{R} = \text{Ph}, ^i\text{Pr}, \text{Cy}$).

A freshly prepared THF solution of 2,6-dimethylphenylmagnesium bromide (prepared as detailed for the synthesis of $\text{PMe}(\text{Xyl})_2$, see Experimental Section of Chapter 1) was added dropwise to a stirred solution of an equimolar amount of the corresponding chlorophosphine (PClR_2) (13.5 mmol) in 20 mL THF at $-78\text{ }^\circ\text{C}$. After addition was completed, the reaction mixture was allowed to reach room temperature and stirred overnight. All the volatiles were then removed under reduced pressure and the pale yellow solid residue was extracted with pentane ($3 \times 20\text{ mL}$). Evaporation of the organic solvent *in vacuo* afforded a yellow oil ($\text{PPh}_2(\text{Xyl})$)⁷² and $\text{P}(^i\text{Pr})_2(\text{Xyl})$ or a white solid ($\text{P}(\text{Cy})_2\text{Xyl}$), which was characterized as the corresponding phosphine. For $\text{P}(^i\text{Pr})_2\text{Xyl}$ all evaporation steps were carried out at $0\text{ }^\circ\text{C}$ in order to avoid partial evaporation of the phosphine.

⁷² Baratta, W.; Mealli, C.; Herdtweck, E.; Ienco, A.; Mason, S. A.; Rigo, P. *J. Am. Chem. Soc.* **2004**, *126*, 5549.

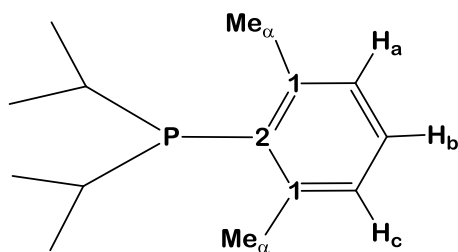
P(Cy)₂(Xyl)

¹H NMR (400 MHz, CD₂Cl₂, 25 °C) δ : 7.10 (t, 1 H, H_b), 6.99 (br. d, 2 H, H_a), 2.58, 2.47 (br. s, 3 H each, Me _{α}), 2.23 (m, 2 H, 2 PCH), 1.97 (m, 2 H, CH₂(Cy)), 1.78 (m, 2 H, CH₂(Cy)), 1.62 (m, 4 H, CH₂(Cy)), 1.34 (m, 4 H, CH₂(Cy)), 1.23 (m, 6 H, CH₂(Cy)), 0.95 (m, 2 H, CH₂(Cy)). All aromatic couplings are of *ca.* 7.5 Hz.

¹³C{¹H} NMR (100 MHz, CD₂Cl₂, 25 °C) δ : 128.9 (CH_b), 128.3 (br. s, CH_a), 35.5 (d, ¹J_{CP} = 14 Hz, PCH), 34.0 (CH₂(Cy)), 33.8 (CH₂(Cy)), 30.9 (d, J_{CP} = 10 Hz, CH₂(Cy)), 27.5 (d, J_{CP} = 8 Hz, CH₂(Cy)), 27.2 (d, J_{CP} = 14 Hz, CH₂(Cy)), 26.7 (CH₂(Cy)), 24.8, 23.3 (br. s, Me _{α}). Signals due to C₁ and C₂ were not located due to their broadening.

³¹P{¹H} NMR (160 MHz, CD₂Cl₂, 25 °C) δ : -5.6.

P(^{*i*}Pr)₂(Xyl)



^1H NMR (500 MHz, CDCl_3 , 60 $^\circ\text{C}$) δ : 7.09 (t, 1 H, H_b), 7.00 (d, 2 H, H_a), 2.58 (br s, 6 H, Me_α), 2.46 (sept, 2 H, $^3J_{\text{HH}} = 7.0$ Hz, $\text{CH}(\textit{i}\text{Pr})$), 1.23 (dd, 6 H, $^3J_{\text{HH}} = 7.0$, $^3J_{\text{HP}} = 16.7$ Hz, $\text{Me}(\textit{i}\text{Pr})$), 0.85 (dd, 6 H, $^3J_{\text{HH}} = 7.0$, $^3J_{\text{HP}} = 13.2$ Hz, $\text{Me}(\textit{i}\text{Pr})$). All aromatic couplings are of *ca.* 7.5 Hz.

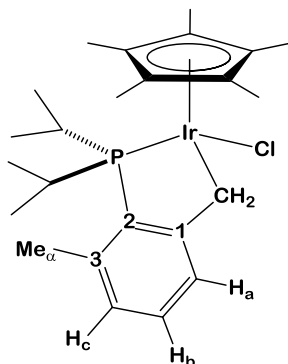
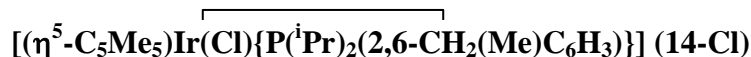
$^{13}\text{C}\{^1\text{H}\}$ NMR (125 MHz, CDCl_3 , 60 $^\circ\text{C}$) δ : 144.9 (br s, C_1), 134.6 (d, $^1J_{\text{CP}} = 24$ Hz, C_2), 128.8 (CH_b), 128.5 (br s, CH_a), 24.9 (d, $^1J_{\text{CP}} = 14$ Hz, $\text{Me}(\textit{i}\text{Pr})$), 23.8 (br s, Me_α), 22.8 (d, $^2J_{\text{CP}} = 28$ Hz, $\text{Me}(\textit{i}\text{Pr})$), 21.2 (d, $^2J_{\text{CP}} = 14$ Hz, $\text{Me}(\textit{i}\text{Pr})$).

$^{31}\text{P}\{^1\text{H}\}$ NMR (200 MHz, CDCl_3 , 60 $^\circ\text{C}$) δ : 7.2.

3.B.3. Synthesis of Iridium Organometallic Complexes

General Synthesis of Iridium Chloride Compounds.

[Cp*IrCl₂]₂ (0.30 g, ca. 0.38 mmol) dissolved in dry CH₂Cl₂ (5 mL) and cooled at 0°C reacted with a dichloromethane solution of the phosphine (0.76 mmol), in the presence of 2,2,6,6-tetramethyl piperidine (TMPP, 130 µL, 0.76 mmol). The reaction mixture was allowed to warm to room temperature and additionally stirred for 2 h (16 hours at 45 °C in the case of PMe₂(Xyl) and 4 hours at this temperature when adding PPh₂(Xyl)). The solvent was removed under vacuum and the product extracted with toluene. The solution was evaporated to dryness providing a bright yellow powder, which was washed with pentane to yield the desired chloride complexes in yields *ca.* 90 %. Variable amounts of the non-metalated iridium bis(chloride) compounds (**18** and **19**) were identified when performing the reactions with PMe₂(Xyl) and PPh₂(Xyl) at room temperature.



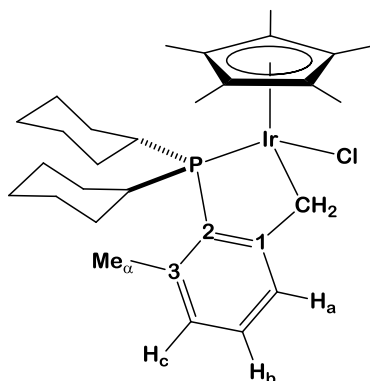
Analytical and spectroscopic data

Anal. Calcd. for $\text{C}_{24}\text{H}_{37}\text{ClIrP}$: C, 49.34; H, 6.38. **Found:** C, 49.3; H, 6.6.

^1H NMR (500 MHz, CD_2Cl_2 , 25 °C) δ : 7.22 (d, 1 H, H_a), 7.06 (td, 1 H, $^3J_{\text{HP}} = 1.6$ Hz, H_b), 6.85 (d, 1 H, H_c), 3.67 (d, 1 H, $^2J_{\text{HH}} = 13.9$ Hz, IrCHH), 3.24 (m, 1 H, CH(iPr)), 3.07 (dd, 1 H, $^2J_{\text{HH}} = 13.9$, $^3J_{\text{HP}} = 4.4$ Hz, IrCHH), 2.50 (s, 3 H, Me_a), 2.27 (m, 1 H, CH(iPr)), 1.71 (d, 15 H, $^4J_{\text{HP}} = 1.3$ Hz, C_5Me_5), 1.30 (dd, 3 H, $^3J_{\text{HP}} = 18.6$, $^3J_{\text{HH}} = 6.8$ Hz, $\text{Me}(\text{iPr})$), 1.24 (dd, 3 H, $^3J_{\text{HP}} = 12.8$, $^3J_{\text{HH}} = 7.2$ Hz, $\text{Me}(\text{iPr})$), 1.18 (dd, 3 H, $^3J_{\text{HP}} = 14.6$, $^3J_{\text{HH}} = 7.1$ Hz, $\text{Me}(\text{iPr})$), 0.73 (dd, 3 H, $^3J_{\text{HP}} = 15.7$, $^3J_{\text{HH}} = 7.1$ Hz, $\text{Me}(\text{iPr})$). All aromatic couplings are of *ca.* 7.5 Hz.

$^{13}\text{C}\{^1\text{H}\}$ NMR (125 MHz, CD_2Cl_2 , 25 °C) δ : 162.9 (d, $^2J_{\text{CP}} = 26$ Hz, C_1), 140.5 (C_3), 133.6 (d, $^1J_{\text{CP}} = 48$ Hz, C_2), 129.9 (CH_b), 128.0 (d, $^3J_{\text{CP}} = 7$ Hz, CH_c), 127.5 (d, $^3J_{\text{CP}} = 12$ Hz, CH_a), 91.9 (C_5Me_5), 30.9 (d, $^1J_{\text{CP}} = 30$ Hz, CH(iPr)), 27.4 (d, $^1J_{\text{CP}} = 29$ Hz, CH(iPr)), 22.8 (Me_a), 20.9 (d, $^2J_{\text{CP}} = 7$ Hz, $\text{Me}(\text{iPr})$), 20.2 ($\text{Me}(\text{iPr})$), 19.2 (d, $^2J_{\text{CP}} = 5$ Hz, $\text{Me}(\text{iPr})$), 18.5 ($\text{Me}(\text{iPr})$), 16.9 (d, $^2J_{\text{CP}} = 3$ Hz, IrCH₂), 9.0 (C_5Me_5).

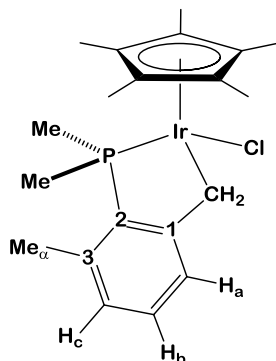
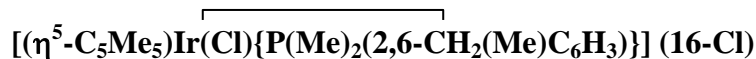
$^{31}\text{P}\{^1\text{H}\}$ NMR (202 MHz, CD_2Cl_2 , 25 °C) δ : 49.6.



Anal. Calcd. for C₃₀H₄₅ClIrP: C, 54.24; H, 6.83. **Found:** C, 54.3; H, 6.9.

$^{13}\text{C}\{\text{H}\}$ NMR (100 MHz, CD_2Cl_2 , 25 °C) δ : 163.0 (d, $^2J_{\text{CP}} = 26$ Hz, C_1), 140.6 (C_3), 133.4 (d, $^1J_{\text{CP}} = 48$ Hz, C_2), 129.8 (CH_b), 127.9 (d, $^3J_{\text{CP}} = 7$ Hz, CH_c), 127.5 (d, $^3J_{\text{CP}} = 12$ Hz, CH_a), 91.9 (C_5Me_5), 41.1 (d, $^1J_{\text{CP}} = 29$ Hz, PCHCH), 36.8 (d, $^1J_{\text{CP}} = 29$ Hz, PCHCH), 31.3 (d, $J_{\text{CP}} = 5$ Hz, $\text{CH}_2(\text{Cy})$), 29.8 (d, $J_{\text{CP}} = 6$ Hz, $\text{CH}_2(\text{Cy})$), 29.2 ($\text{CH}_2(\text{Cy})$), 28.1 ($\text{CH}_2(\text{Cy})$), 28.0 (d, $J_{\text{CP}} = 8$ Hz, $\text{CH}_2(\text{Cy})$), 27.7 (d, $J_{\text{CP}} = 10$ Hz, $\text{CH}_2(\text{Cy})$), 27.5 (d, $J_{\text{CP}} = 12$ Hz, $\text{CH}_2(\text{Cy})$), 27.2 (d, $J_{\text{CP}} = 14$ Hz, $\text{CH}_2(\text{Cy})$), 26.7 ($\text{CH}_2(\text{Cy})$), 26.6 ($\text{CH}_2(\text{Cy})$), 22.9 (Me_a), 17.2 (d, $^2J_{\text{CP}} = 4$ Hz, IrCH_2), 9.2 (C_5Me_5).

326



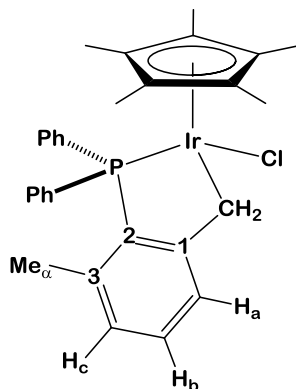
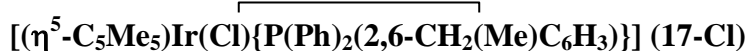
Analytical and spectroscopic data

Anal. Calcd. for $\text{C}_{20}\text{H}_{29}\text{ClIrP}$: C, 45.49; H, 5.54. **Found:** C, 45.3; H, 5.4.

^1H NMR (400 MHz, CDCl_3 , 25 °C) δ : 7.25 (d, 1 H, H_a), 7.04 (td, $^5J_{\text{HP}} = 1.6$ Hz, H_b), 6.78 (dd, 1 H, $^4J_{\text{HP}} = 1.9$ Hz, H_c), 3.50 (d, 1 H, $^2J_{\text{HH}} = 14.4$ Hz, IrCHH), 3.29 (dd, 1 H, $^2J_{\text{HH}} = 14.4$, $^3J_{\text{HP}} = 5.1$ Hz, IrCHH), 2.45 (s, 3 H, Me), 2.06 (d, 3 H, $^2J_{\text{HP}} = 11.1$ Hz, PMeMe), 1.79 (d, 3 H, $^2J_{\text{HP}} = 11.3$ Hz, PMeMe), 1.78 (d, 15 H, $^4J_{\text{HP}} = 1.9$ Hz, C_5Me_5). All aromatic couplings are of *ca.* 7.5 Hz.

$^{13}\text{C}\{^1\text{H}\}$ NMR (100 MHz, CDCl_3 , 25 °C) δ : 160.8 (d, $^2J_{\text{CP}} = 30$ Hz, C_1), 139.7 (C_3), 135.3 (d, $^1J_{\text{CP}} = 59$ Hz, C_2), 130.2 (CH_b), 127.5 (d, $^3J_{\text{CP}} = 7$ Hz, CH_c), 127.4 (d, $^3J_{\text{CP}} = 14$ Hz, CH_a), 91.1 (C_5Me_5), 20.8 (d, $^3J_{\text{CP}} = 3$ Hz, Me_a), 15.2 (d, $^1J_{\text{CP}} = 36$ Hz, PMeMe), 13.9 (d, $^1J_{\text{CP}} = 37$ Hz, PMeMe), 16.4 (d, $^2J_{\text{CP}} = 3$ Hz, IrCH_2), 8.8 (C_5Me_5).

$^{31}\text{P}\{^1\text{H}\}$ NMR (160 MHz, CDCl_3 , 25 °C) δ : 3.3.



Analytical and spectroscopic data

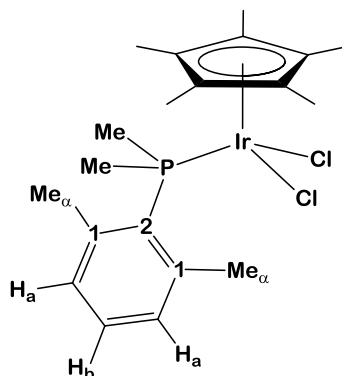
Anal. Calcd. for $\text{C}_{30}\text{H}_{32}\text{ClIrP}$: C, 55.33; H, 4.95. **Found:** C, 55.2; H, 5.1.

^1H NMR (500 MHz, CDCl_3 , 25 °C) δ : 7.52 – 7.44 (m, 3 H, H_a , PPh_2), 7.43 – 7.33 (m, 4 H, PPh_2), 7.33 – 7.28 (m, 4 H, PPh_2), 7.17 (td, 1 H, $^5J_{\text{HP}} = 1.9$ Hz, H_b), 6.83 (dd, 1 H, $^4J_{\text{HP}} = 3.2$ Hz, H_c), 3.86 (d, 1 H, $^2J_{\text{HH}} = 14.6$ Hz, IrCHH), 3.73 (dd, 1 H, $^2J_{\text{HH}} = 14.6$, $^3J_{\text{HP}} = 4.1$ Hz, IrCHH), 1.78 (s, 3 H, Me_a), 1.56 (d, 15 H, $^4J_{\text{HP}} = 2.0$ Hz, C_5Me_5). All aromatic couplings are of *ca.* 7.5 Hz.

$^{13}\text{C}\{^1\text{H}\}$ NMR (125 MHz, CDCl_3 , 25 °C) δ : 163.2 (d, $^2J_{\text{CP}} = 30$ Hz, C_1), 141.4 (C_3), 134.7 (d, $^1J_{\text{CP}} = 42$ Hz, *ipso*-Ph), 134.2 (d, $^1J_{\text{CP}} = 53$ Hz, C_2), 133.1, 133.0, 132.0, 131.9, 131.0 (PPh_2), 130.9 (d, $^4J_{\text{CP}} = 2$ Hz, CH_b), 130.7 (d, $^1J_{\text{CP}} = 57$ Hz, *ipso*-Ph), 129.5, 129.3 (d, $J_{\text{CP}} = 3$ Hz, PPh_2), 128.0, 127.9 (PPh_2), 127.6 (CH_c), 127.5 (d, $^3J_{\text{CP}} = 8$ Hz, CH_a), 127.2, 127.1 (PPh_2), 92.0 (C_5Me_5), 21.7 (d, $^3J_{\text{CP}} = 3$ Hz, Me_a), 16.7 (d, $^2J_{\text{CP}} = 3$ Hz, IrCH_2), 8.6 (C_5Me_5).

$^{31}\text{P}\{^1\text{H}\}$ NMR (200 MHz, CDCl_3 , 25 °C) δ : 28.6.

When the reaction was carried out at room temperature for 6 hours the final product was a mixture of the metalated chloride complex **17-Cl** and the non-metalated bis-chloride species **19** in a *ca.* ratio of 65:35. To achieve the complete metalation of the phosphine ligand the reaction must be carried out at 45 °C. The non-metalated compound **19** is characterized by ^1H NMR signals at 2.31 and 1.39 (d, $^4J_{\text{HP}} = 2.4$ Hz) ppm, due to the methyl groups of the xylyl ring and the Cp^* ligand, respectively. In the $^{31}\text{P}\{^1\text{H}\}$ NMR spectrum a broad singlet is recorded at -1.1 ppm.



$[\text{Cp}^*\text{IrCl}_2]_2$ (0.10 g, ca. 0.13 mmol) was dissolved in dry CH_2Cl_2 (5 mL) in a Schlenk flask. The dark solution was cooled to 0°C and a dichloromethane solution of the phosphine (43 mg, 0.26 mmol) was added. The reaction mixture was stirred for 30 min at 0°C and the solvent removed under reduced pressure. The crude was washed with pentane to afford compound **18** as a pale orange powder (160 mg, 88 %).

Analytical and spectroscopic data

Anal. Calcd. for $\text{C}_{20}\text{H}_{30}\text{Cl}_2\text{IrP}$: C, 42.6; H, 5.4. **Found:** C, 43.0; 5.2.

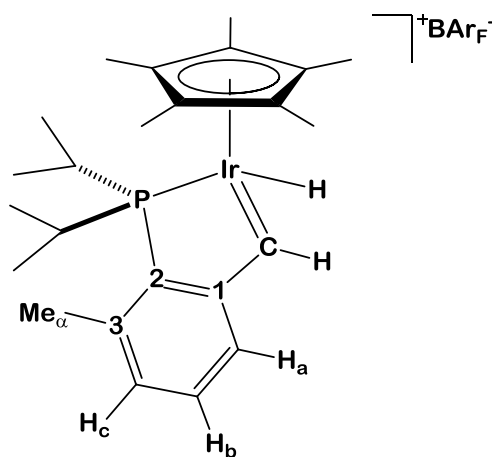
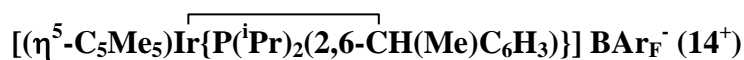
^1H NMR (400 MHz, CDCl_3 , 25°C) δ : 7.15 (td, $^5J_{\text{HP}} = 1.7$ Hz, H_b), 7.01 (dd, 2 H, $^4J_{\text{HP}} = 3.2$ Hz, H_a), 2.59 (s, 6 H, Me_α), 2.02 (d, 6 H, $^2J_{\text{HP}} = 10.4$ Hz, PMe_2), 1.39 (d, 15 H, $^4J_{\text{HP}} = 2.2$ Hz, C_5Me_5). All aromatic couplings are of ca. 7.5 Hz.

$^{13}\text{C}\{^1\text{H}\}$ NMR (100 MHz, CDCl_3 , 25°C) δ : 141.8 (d, $^2J_{\text{CP}} = 9$ Hz, C_1), 130.3 (d, $^3J_{\text{CP}} = 8$ Hz, CH_a), 129.9 (CH_b), 129.3 (d, $^1J_{\text{CP}} = 45$ Hz, C_2), 91.6 (d, $^2J_{\text{CP}} = 3$ Hz, C_5Me_5), 24.7 (d, $^3J_{\text{CP}} = 5$ Hz, Me_α), 16.8 (d, $^1J_{\text{CP}} = 40$ Hz, PMe_2), 8.3 (C_5Me_5).

$^{31}\text{P}\{^1\text{H}\}$ NMR (160 MHz, CDCl_3 , 25°C) δ : -20.2.

Synthesis of cationic hydride-alkylidenes 14^+ and 15^+

To a solid mixture of **14-Cl** or **15-Cl** (0.08 mmol) and NaBAr_F (72 mg, 0.08 mmol) placed in a Schlenk flask were added 5 mL of CH₂Cl₂. The resulting intense red solution was stirred for 15 min at room temperature, then filtered and the solvent removed under vacuum. The red solid was washed with pentane to give alkylidenes **14⁺** or **15⁺** in *ca.* 95 % yield. These complexes can be recrystallized from a 1:2 mixture of CH₂Cl₂:pentane.

**Analytical and spectroscopic data**

Anal. Calcd. for C₅₆H₄₈BF₂₄IrP: C, 47.67 ; H, 3.43. **Found:** C, 47.4; H, 3.5.

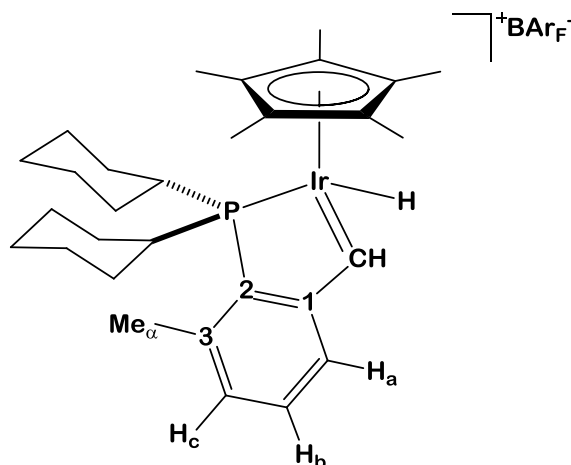
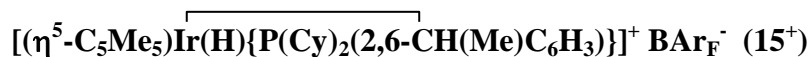
IR (Nujol): $\nu(\text{IrH})$ 2165 cm⁻¹.

^1H NMR (500 MHz, CD_2Cl_2 , 25 °C) δ : 7.69 (d, 1 H, H_a), 7.62 (dd, $^4J_{\text{HP}} = 2.6$ Hz, H_c), 7.34 (td, $^5J_{\text{HP}} = 2.2$ Hz, 1 H, H_b), 2.73 (m, 2 H, 2 $\text{CH}(\text{iPr})$), 2.69 (s, 3 H, Me), 2.17 (s, 15 H, C_5Me_5), 1.06, (dd, 6 H, $^3J_{\text{HP}} = 17.2$, $^3J_{\text{HH}} = 6.9$ Hz, $\text{Me}(\text{iPr})$), 0.89 (dd, 3 H, $^3J_{\text{HP}} = 18.5$, $^3J_{\text{HH}} = 6.9$ Hz, $\text{Me}(\text{iPr})$). All aromatic couplings are of *ca.* 7.5 Hz;

^1H NMR (500 MHz, CD_2Cl_2 , -80 °C) δ : 15.51 (s, 1 H, IrCH), -15.21 (d, 1 H, $^2J_{\text{HP}} = 24.7$ Hz, Ir-H). Hydride and carbene signals are only detectable at temperatures below -50°C.

$^{13}\text{C}\{^1\text{H}\}$ NMR (125 MHz, CD_2Cl_2 , 25 °C) δ : 263.8 (Ir=CH), 166.4 (d, $^2J_{\text{CP}} = 27$ Hz, C_1), 144.2 (C_3) 137.2 (d, $^3J_{\text{CP}} = 7$ Hz, CH_c), 135.2 (C_2 , overlapped with BAr_F), 134.1 (CH_b), 128.7 (d, $^3J_{\text{CP}} = 12$ Hz, CH_a), 104.5 (C_5Me_5), 25.5 (d, $^1J_{\text{CP}} = 32$ Hz, $\text{CH}(\text{iPr})$), 22.0 (Me), 18.7, 18.3 ($\text{Me}(\text{iPr})$), 10.3 (C_5Me_5).

$^{31}\text{P}\{^1\text{H}\}$ NMR (202 MHz, CD_2Cl_2 , 25 °C) δ : 73.1.



Analytical and spectroscopic data

Anal. Calcd. for $\text{C}_{62}\text{H}_{56}\text{BF}_{24}\text{IrP}$: C, 49.94; H, 3.79. **Found:** C, 50.1; H, 3.5.

IR (Nujol): $\nu(\text{IrH})$ 2150 cm^{-1} .

^1H NMR (400 MHz, CD_2Cl_2 , 25 $^\circ\text{C}$) δ : 7.68 (d, 1 H, H_a), 7.61 (dd, 1 H, $^4J_{\text{HP}} = 3.3$ Hz, H_c), 7.33 (td, 1 H, $^5J_{\text{HP}} = 2.4$ Hz, H_b), 2.69 (s, 3 H, Me_α), 2.41 (m, 2 H, $\text{P}(\text{CH})_2$), 2.17 (d, 15 H, $^4J_{\text{HP}} = 1.1$ Hz, C_5Me_5), 1.88 – 1.69 (m, 8 H, $\text{CH}_2(\text{Cy})$), 1.51 – 1.25 (m, 8 H, $\text{CH}_2(\text{Cy})$), 1.14 (m, 2 H, $\text{CH}_2(\text{Cy})$), 0.78 (m, 2 H, $\text{CH}_2(\text{Cy})$). All aromatic couplings are of *ca.* 7.5 Hz.

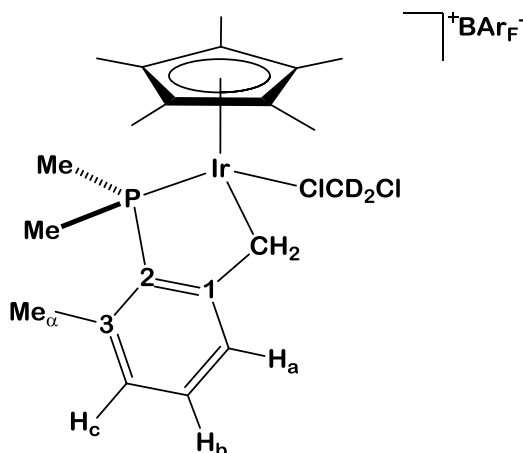
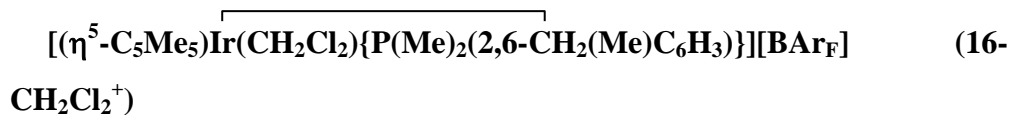
^1H NMR (500 MHz, CD_2Cl_2 , -80 $^\circ\text{C}$) δ : 15.50 (s, 1 H, IrCH), -15.14 (d, 1 H, $^2J_{\text{HP}} = 27.3$ Hz, Ir–H). Hydride and carbene signals are only detectable at temperatures below -50 $^\circ\text{C}$.

$^{13}\text{C}\{^1\text{H}\}$ NMR (100 MHz, CD_2Cl_2 , 25 °C) δ : 263.1 (Ir=CH), 166.6 (C_1), 144.0 (C_3), 137.1 (d, $^1J_{\text{CP}} = 54$ Hz, C_2), 137.0 (d, $^3J_{\text{CP}} = 8$ Hz, CH_c), 133.9 (CH_b), 128.6 (d, $^3J_{\text{CP}} = 12$ Hz, CH_a), 104.4 (C_5Me_5), 34.8 (d, $^1J_{\text{CP}} = 31$ Hz, $\text{P}(\text{CH})_2$), 29.0 ($\text{CH}_2(\text{Cy})$), 28.9 (d, $J_{\text{CP}} = 4$ Hz, $\text{CH}_2(\text{Cy})$), 26.7 (d, $J_{\text{CP}} = 14$ Hz, $\text{CH}_2(\text{Cy})$), 26.6 (d, $J_{\text{CP}} = 12$ Hz, $\text{CH}_2(\text{Cy})$), 26.2 ($\text{CH}_2(\text{Cy})$), 22.1 (Me_a), 10.3 (C_5Me_5).

$^{31}\text{P}\{^1\text{H}\}$ NMR (160 MHz, CD_2Cl_2 , 25 °C) δ : 62.1.

Synthesis of dichloromethane adducts **16-CH₂Cl₂⁺** and **17-CH₂Cl₂⁺**

To a solid mixture of **16-Cl** or **17-Cl** (0.08 mmol) and NaBAR_F (72 mg, 0.08 mmol) placed in a Schlenk flask were added 5 mL of CH_2Cl_2 at 0°C. The resulting orange solution was stirred for 15 min at the same temperature and then filtered. ^{31}P NMR monitoring of the reaction showed quantitative conversion of the chloride complex to the dichloromethane adduct. Spectroscopic analysis was undertaken with a sample of the complex directly prepared in CD_2Cl_2 without further purification. All attempts to obtain crystals suitable for X-ray analysis were unsuccessful due to the formation of dark orange oils.



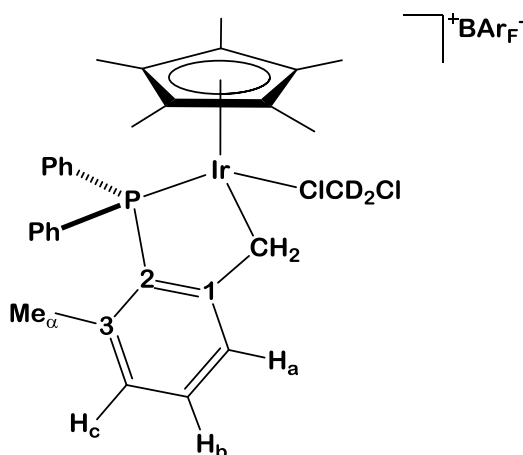
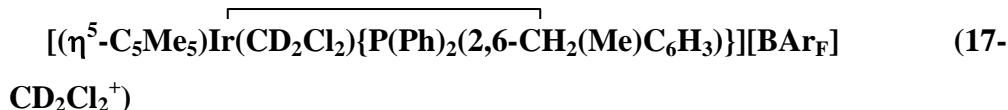
Spectroscopic data

^1H NMR (500 MHz, CD_2Cl_2 , 0 °C) δ : 7.37 (d, 1 H, H_a), 7.24 (t, 1 H, H_b), 7.08 (m, 1 H, H_c), 2.90 (br. s, 2 H, IrCH_2), 2.49 (s, 3 H, Me_α), 2.00 (d, 6 H, $^2J_{\text{HP}} = 10.8$ Hz, PMe_2), 1.88 (s, 15 H, C_5Me_5). All aromatic couplings are of *ca.* 7.5 Hz.

^1H NMR (500 MHz, CD_2Cl_2 , -90 °C) δ : 3.55 (br. s, 1 H, IrCHH), 3.17 (br. s, 1 H, IrCHH).

$^{13}\text{C}\{^1\text{H}\}$ NMR (100 MHz, CD_2Cl_2 , 0 °C) δ : 159.2 (d, $^2J_{\text{CP}} = 31$ Hz, C_1), 142.0 (C_3), 135.3 (C_2 , overlapped with BAr_F), 133.0 (CH_b), 131.0 (CH_c), 126.7 (d, $^3J_{\text{CP}} = 13$ Hz, CH_a), 96.6 (C_5Me_5), 20.7 (Me_α), 18.0 (br. s, IrCH_2), 14.4 (d, $^1J_{\text{CP}} = 38$ Hz, PMe_2), 8.8 (C_5Me_5).

$^{31}\text{P}\{^1\text{H}\}$ NMR (160 MHz, CD_2Cl_2 , 0 °C) δ : 8.3 (br. s).



Spectroscopic data

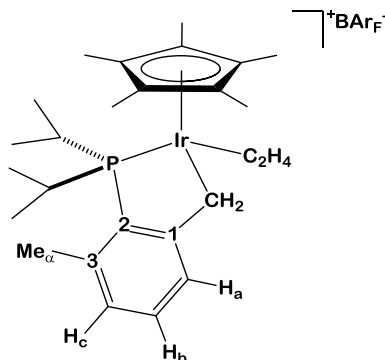
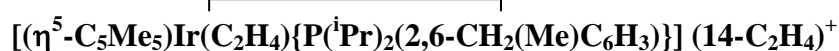
^1H NMR (500 MHz, CD_2Cl_2 , $-20\text{ }^\circ\text{C}$) δ : 7.53 – 7.19 (m, 12 H, H_a , H_b , PPh_2), 6.64 (m, 1 H, H_c), 3.82 (d, 1 H, $^2J_{\text{HH}} = 15.6\text{ Hz}$, IrCHH), 3.42 (d, 1 H, $^2J_{\text{HH}} = 15.6\text{ Hz}$, IrCHH), 1.75 (s, 3 H, Me_α), 1.00 (s, 15 H, C_5Me_5). All aromatic couplings are of *ca.* 7.5 Hz.

$^{13}\text{C}\{^1\text{H}\}$ NMR (100 MHz, CD_2Cl_2 , $-20\text{ }^\circ\text{C}$) δ : 163.5 (d, $^2J_{\text{CP}} = 34\text{ Hz}$, C_1), 141.7 (C_3), 133.9 (d, $^1J_{\text{CP}} = 61\text{ Hz}$, *ipso*-Ph), 132.3 (d, $^1J_{\text{CP}} = 56\text{ Hz}$, C_2), 131.7, 131.4, 129.9, 129.6, 129.1, 128.8, 128.6, 128.3, 127.6, 127.4, 127.0, 126.8 (CH_a , CH_b , CH_c , PPh_2), 94.1 (C_5Me_5), 22.1 (Me_α), 18.3 (IrCH_2), 8.2 (C_5Me_5).

$^{31}\text{P}\{^1\text{H}\}$ NMR (160 MHz, CD_2Cl_2 , $-20\text{ }^\circ\text{C}$) δ : 35.5.

General synthesis of cationic adducts (14-17)-L⁺ (L = NCMe, NC₅H₅, C₂H₄).

To a solid mixture of the iridium chloride complex (0.08 mmol) and NaBAr_F (72 mg, 0.08 mmol) placed in a Schlenk flask were added 5 mL of CH₂Cl₂. The reaction mixture was stirred for 5 min at room temperature under 1 bar C₂H₄ (a thick-wall vessel instead of a conventional Schlenk flask was employed in this case), or alternatively treated with 100 μL of NCMe or pyridine (for corresponding NCMe or pyridine adducts, respectively). The solution was filtered and the solvent was then evaporated under reduced pressure to obtain pale white (**Ir-NCMe⁺**, **Ir-C₂H₄⁺**) or a yellow powder (**Ir-NC₅H₅⁺**) in *ca.* 95% yield. These complexes can be recrystallized from a 1:2 mixture of CH₂Cl₂:pentane.



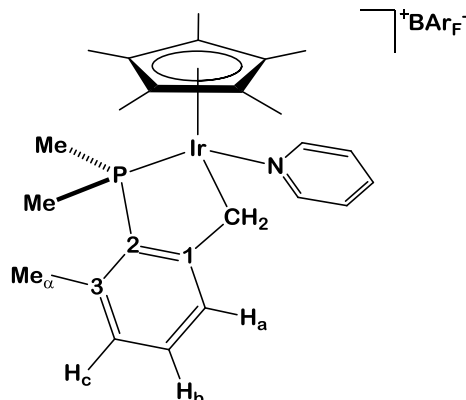
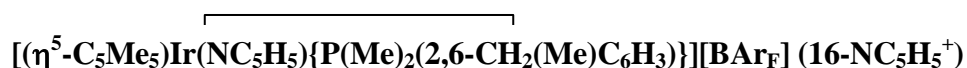
Analytical and spectroscopic data

Anal. Calcd. for $\text{C}_{58}\text{H}_{53}\text{BF}_{24}\text{IrP}$: C, 48.38; H, 3.71. **Found:** C, 48.3; H, 3.8.

^1H NMR (400 MHz, CD_2Cl_2 , 25 °C) δ : 7.29 (d, 1 H, H_a), 7.20 (td, 1 H, $^5J_{\text{HP}} = 2.4$ Hz, H_b), 6.99 (dd, 1 H, $^5J_{\text{HP}} = 3.5$ Hz, H_c), 3.67 (d, 1 H, $^2J_{\text{HH}} = 12.5$ Hz, IrCHH), 3.39 (dd, 1 H, $^2J_{\text{HH}} = 12.5$, $^3J_{\text{HP}} = 3.3$ Hz, IrCHH), 3.28 (dseptet, 1 H, $^2J_{\text{HP}} = 13.4$, $^3J_{\text{HH}} = 7.4$ Hz, 2 H, C_2H_4), 2.40 (s, 3 H, Me_a), 2.38 (m, 1 H, $\text{CH}(\text{iPr})$), 2.29 (m, 2 H, C_2H_4), 1.77 (d, 15 H, $^4J_{\text{HP}} = 1.5$ Hz, C_5Me_5), 1.31 (dd, 3 H, $^3J_{\text{HP}} = 13.7$, $^3J_{\text{HH}} = 7.3$ Hz, $\text{Me}(\text{iPr})$), 1.25 (dd, 3 H, $^3J_{\text{HP}} = 19.0$, $^3J_{\text{HH}} = 7.1$ Hz, $\text{Me}(\text{iPr})$), 1.17 (dd, 3 H, $^3J_{\text{HP}} = 13.9$, $^3J_{\text{HH}} = 7.2$ Hz, $\text{Me}(\text{iPr})$), 0.69 (dd, 3 H, $^3J_{\text{HP}} = 16.8$, $^3J_{\text{HH}} = 7.2$ Hz, $\text{Me}(\text{iPr})$). All aromatic couplings are of *ca.* 7.5 Hz.

$^{13}\text{C}\{^1\text{H}\}$ NMR (100 MHz, CD_2Cl_2 , 25 °C) δ : 157.6 (d, $^2J_{\text{CP}} = 26$ Hz, C_1), 141.4 (C_3), 129.5 (C_2 , overlapped with BArF), 131.9 (CH_b), 130.6 (d, $^3J_{\text{CP}} = 8$ Hz, CH_c), 126.8 (d, $^3J_{\text{CP}} = 14$ Hz, CH_a), 100.7 (C_5Me_5), 46.8 (br. s, C_2H_4), 42.5 (br. s, C_2H_4), 30.9 (d, $^1J_{\text{CP}} = 29$ Hz, $\text{CH}(\text{iPr})$), 27.4 (d, $^1J_{\text{CP}} = 30$ Hz, $\text{CH}(\text{iPr})$), 22.6 (Me_a), 20.5 ($\text{Me}(\text{iPr})$), 20.2 (d, $^2J_{\text{CP}} = 6$ Hz, $\text{Me}(\text{iPr})$), 19.8 ($\text{Me}(\text{iPr})$), 19.7 (d, $^2J_{\text{CP}} = 4$ Hz, $\text{Me}(\text{iPr})$), 11.9 (d, $^2J_{\text{CP}} = 2$ Hz, IrCH₂), 8.4 (C_5Me_5).

$^{31}\text{P}\{^1\text{H}\}$ NMR (160 MHz, CD_2Cl_2 , 25 °C) δ : 42.7.



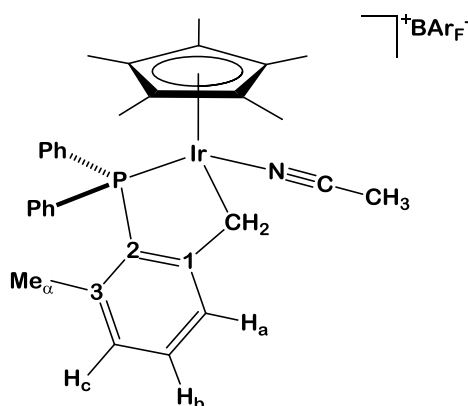
Analytical and spectroscopic data

Anal. Calcd. for $\text{C}_{57}\text{H}_{46}\text{BF}_{24}\text{IrNP}$: C, 47.71; H, 3.23. **Found:** C, 47.2; H, 3.3.

^1H NMR (400 MHz, CDCl_3 , 25 °C) δ : 8.36 (d, 2 H, *o*-py), 7.73 (1 H, *p*-py, overlapped with BAr_F), 7.25 (d, 1 H, H_a), 7.19 (t, 2 H, *m*-py), 7.07 (td, 1 H, $^5J_{\text{HP}} = 1.9$ Hz, H_b), 6.79 (dd, 1 H, $^4J_{\text{HP}} = 3.4$ Hz, H_c), 3.57 (d, 1 H, $^2J_{\text{HH}} = 14.3$ Hz, IrCHH), 2.70 (dd, 1 H, $^2J_{\text{HH}} = 14.3$, $^3J_{\text{HP}} = 5.8$ Hz, IrCHH), 2.32 (s, 3 H, Me_α), 2.90 (d, 3 H, $^2J_{\text{HP}} = 10.7$ Hz, PMeMe), 1.82 (d, 3 H, $^2J_{\text{HP}} = 10.4$ Hz, PMeMe), 1.63 (d, 15 H, $^4J_{\text{HP}} = 1.8$ Hz, C_5Me_5). All aromatic couplings are of *ca.* 7.5 Hz.

$^{13}\text{C}\{^1\text{H}\}$ NMR (100 MHz, CDCl_3 , 25 °C) δ : 157.5 (d, $^2J_{\text{CP}} = 28$ Hz, C_1), 155.2 (*o*-py), 140.5 (C_3), 139.0 (*p*-py), 133.2 (d, $^1J_{\text{CP}} = 51$ Hz, C_2), 131.8 (CH_b), 129.5 (d, $^3J_{\text{CP}} = 8$ Hz, CH_c), 127.2 (*m*-py), 126.8 (d, $^3J_{\text{CP}} = 13$ Hz, CH_a), 93.4 (C_5Me_5), 21.2 (Me_α), 18.0 (IrCH_2), 15.3 (d, $^1J_{\text{CP}} = 37$ Hz, PMeMe), 13.6 (d, $^1J_{\text{CP}} = 33$ Hz, PMeMe), 8.7 (C_5Me_5).

$^{31}\text{P}\{^1\text{H}\}$ NMR (160 MHz, CDCl_3 , 25 °C) δ : -0.5.



Analytical and spectroscopic data

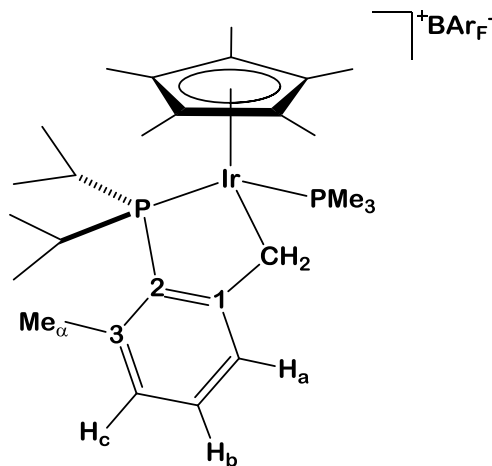
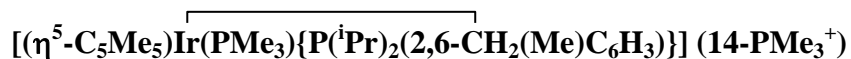
Anal. Calcd. for $\text{C}_{64}\text{H}_{47}\text{BF}_{24}\text{IrNP}$: C, 50.57; H, 3.12. **Found:** C, 50.6; H, 3.4.

IR (Nujol): $\nu(\text{CN})$ 2290 cm^{-1} .

^1H NMR (500 MHz, CD_2Cl_2 , 25 °C) δ : 7.55 – 7.40 (m, 9 H, H_a , PPh_2), 7.36 (m, 3 H, H_b , PPh_2), 7.02 (dd, 1 H, $^4J_{\text{HP}} = 3.6$ Hz, H_c), 3.61 (d, 1 H, $^2J_{\text{HH}} = 15.0$ Hz, IrCHH), 3.27 (dd, 1 H, $^2J_{\text{HH}} = 15.0$, $^3J_{\text{HP}} = 3.0$ Hz, IrCHH), 1.79 (s, 3 H, Me_α), 1.74 (d, 3 H, $^5J_{\text{HP}} = 1.1$ Hz, NCMe), 1.56 (d, 15 H, $^4J_{\text{HP}} = 1.9$ Hz, C_5Me_5). All aromatic couplings are of *ca.* 7.5 Hz.

$^{13}\text{C}\{^1\text{H}\}$ NMR (125 MHz, CD_2Cl_2 , 25 °C) δ : 160.9 (d, $^2J_{\text{CP}} = 31$ Hz, C_1), 142.5 (C_3), 132.3, 132.2, 132.1 (PPh_2), 131.7 (C_2 , overlapped with other aromatic signals), 131.5, 131.3, 130.7 (PPh_2), 129.5 (d, $^1J_{\text{CP}} = 39$ Hz, *ipso*-Ph), 129.1, 128.8, 128.7 (PPh_2), 128.1 (d, $^1J_{\text{CP}} = 45$ Hz, *ipso*-Ph), 129.0 (d, $^3J_{\text{CP}} = 6$ Hz, CH_c), 127.6 (d, $^3J_{\text{CP}} = 15$ Hz, CH_a), 115.0 (NCMe), 94.7 (C_5Me_5), 21.4 (Me_α), 15.7 (IrCH_2), 8.1 (C_5Me_5), 1.6 (NCMe).

$^{31}\text{P}\{^1\text{H}\}$ NMR (200 MHz, CD_2Cl_2 , 25 °C) δ : 28.4.



A solution of PMe_3 in toluene (33 μL , 1.1 M, 0.033 mmol) was added under argon over a CH_2Cl_2 (1 mL) solution of alkylidene **14**⁺ (40 mg, 0.028 mmol) placed in a Schlenk flask. The solution rapidly cleared up and then it was heated at 40 °C for 16 hours. The volatiles were removed under vacuum and the residue washed with pentane to give complex **14-PMe**₃⁺ as a pale orange powder (35 mg, 84 %). Crystals suitable for X-ray analysis were obtained by slow diffusion from CH_2Cl_2 /pentane.

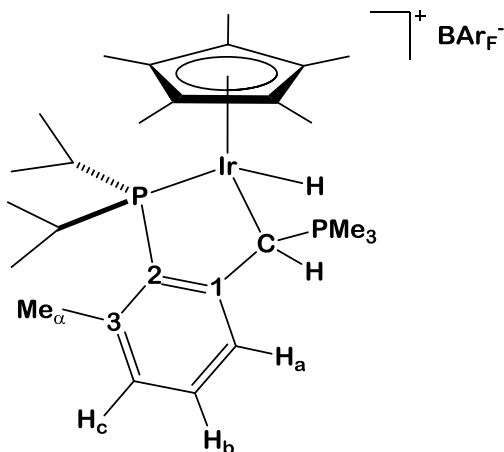
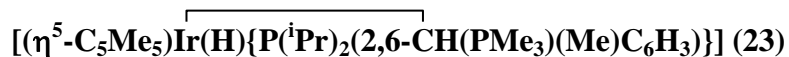
Analytical and spectroscopic data

Anal. Calcd. for $C_{59}H_{58}BF_{24}IrP_2$: C, 47.62; H, 3.93. **Found:** C, 47.9; H, 3.8.

1H NMR (400 MHz, CD_2Cl_2 , 25 °C) δ : 7.27 (d, 1 H, H_a), 7.20 (td, 1 H, $^5J_{HP} = 2.7$ Hz, H_b), 6.98 (dd, 1 H, $^5J_{HP} = 3.1$ Hz, H_c), 3.43 (m, 1 H, IrCHH), 3.29 (dd, 1 H, $^2J_{HH} = 7.6$, $^3J_{HP} = 3.1$ Hz, IrCHH), 3.28 (dseptet, 1 H, $^2J_{HP} = 10.9$, $^3J_{HH} = 7.1$ Hz, CH(i Pr)), 2.51 (s, 3 H, Me_a), 2.33 (m, 1 H, CH(i Pr)), 1.77 (t, 15 H, $^4J_{HP} = 1.9$ Hz, C_5Me_5), 1.28 (dd, 3 H, $^3J_{HP} = 13.2$, $^3J_{HH} = 7.2$ Hz, $Me(iPr)$), 1.24 (d, 9 H, $^2J_{HP} = 10.3$ Hz, PMe_3), 1.15 (dd, 3 H, $^3J_{HP} = 18.9$, $^3J_{HH} = 7.1$ Hz, $Me(iPr)$), 1.03 (dd, 3 H, $^3J_{HP} = 16.5$, $^3J_{HH} = 6.7$ Hz, $Me(iPr)$), 0.59 (dd, 3 H, $^3J_{HP} = 16.3$, $^3J_{HH} = 7.1$ Hz, $Me(iPr)$). All aromatic couplings are of *ca.* 7.5 Hz.

$^{13}C\{^1H\}$ NMR (100 MHz, CD_2Cl_2 , 25 °C) δ : 158.5 (d, $^2J_{CP} = 24$ Hz, C_1), 140.1 (C_3), 132.4 (d, $^1J_{CP} = 47$ Hz, C_2), 131.9 (d, $^4J_{CP} = 3$ Hz, CH_b), 130.4 (d, $^3J_{CP} = 7$ Hz, CH_c), 126.9 (d, $^3J_{CP} = 12$ Hz, CH_a), 98.5 (C_5Me_5), 31.2 (dd, $^1J_{CP} = 29$, $^3J_{CP} = 2$ Hz, CH(i Pr)), 26.3 (d, $^1J_{CP} = 30$ Hz, CH(i Pr)), 22.6 (Me_a), 20.7 ($Me(iPr)$), 20.4 (d, $^2J_{CP} = 5$ Hz, $Me(iPr)$), 20.0 (d, $^2J_{CP} = 6$ Hz, $Me(iPr)$), 18.6 ($Me(iPr)$), 18.4 (d, $^1J_{CP} = 39$ Hz, PMe_3), 9.8 (C_5Me_5), 6.4 (dd, $^2J_{CP} = 8$, $^2J_{CP} = 3$ Hz, IrCH₂).

$^{31}P\{^1H\}$ NMR (160 MHz, CD_2Cl_2 , 25 °C) δ : 48.1 (d, $^2J_{PP} = 21$ Hz, $P(iPr)_2Xyl$), -47.3 (d, $^2J_{PP} = 21$ Hz, PMe_3).



A screw-capped NMR tube was charged with **14**⁺ (30 mg, 0.021 mmol) and CD₂Cl₂ (0.6 mL). The tube was shaken, placed at -40 °C and PMe₃ (2.5 μL, 0.026 mmol) was added at this temperature. ³¹P{¹H} NMR monitoring of the reaction showed immediate conversion of the alkylidene to a mixture of the ylide **23** and the cationic adduct **14-PMe₃**⁺ in a *ca.* ratio of 97:3. Spectroscopic data were obtained at -40 °C without further purification in order to avoid isomerization to **14-PMe₃**⁺, which is slow at this temperature.

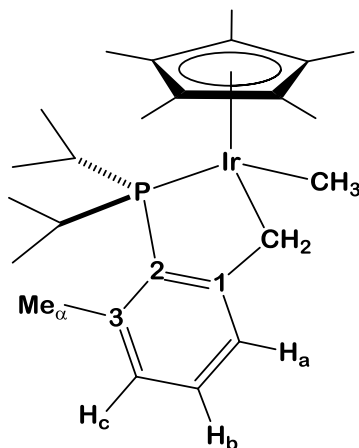
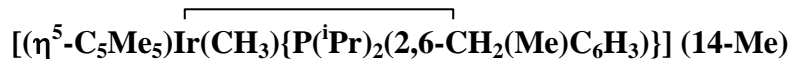
Analytical and Spectroscopic data

Anal. Calcd. for $C_{59}H_{58}BF_{24}IrP_2$: C, 47.62; H, 3.93. **Found:** C, 47.6; H, 3.8.

1H NMR (500 MHz, CD_2Cl_2 , 25 °C) δ : 7.19 (m, 2 H, H_a , H_b), 7.10 (m, 1 H, H_c), 3.60 (d, 1 H, $^2J_{HP} = 11.0$ Hz, $IrCHPMe_3$), 2.94 (m, 1 H, $CH(^iPr)$), 2.56 (s, 3 H, Me_a), 2.31 (m, 1 H, $CH(^iPr)$), 1.90 (t, 15 H, $^4J_{HP} = 1.8$ Hz, C_5Me_5), 1.33 (d, 9 H, $^2J_{HP} = 11.9$ Hz, PMe_3), 1.23 (dd, 3 H, $^3J_{HP} = 12.8$, $^3J_{HH} = 7.4$ Hz, $Me(^iPr)$), 1.13 (dd, 3 H, $^3J_{HP} = 18.3$, $^3J_{HH} = 6.8$ Hz, $Me(^iPr)$), 1.03 (dd, 3 H, $^3J_{HP} = 12.0$, $^3J_{HH} = 7.2$ Hz, $Me(^iPr)$), 0.16 (dd, 3 H, $^3J_{HP} = 16.0$, $^3J_{HH} = 7.1$ Hz, $Me(^iPr)$), -17.7 (dd, 1 H, $^2J_{HP} = 33.3$, $^3J_{HP} = 10.6$ Hz, IrH). All aromatic couplings are of *ca.* 7.5 Hz.

$^{13}C\{^1H\}$ NMR (125 MHz, CD_2Cl_2 , -40 °C) δ : 150.6 (d, $^2J_{CP} = 27$ Hz, C_1), 141.8 (C_3), 133.4 (C_2 , overlapped with BAr_F), 130.2 (CH_b), 129.3 (CH_c), 125.4 (CH_a), 92.1 (C_5Me_5), 27.6 (d, $^1J_{CP} = 28$ Hz, $CH(^iPr)$), 24.7 (d, $^1J_{CP} = 36$ Hz, $CH(^iPr)$), 22.0 (Me_a), 18.5 ($Me(^iPr)$), 18.3 ($Me(^iPr)$), 17.8 ($Me(^iPr)$), 16.5 ($Me(^iPr)$), 10.6 (d, $^1J_{CP} = 56$ Hz, PMe_3), 9.8 (C_5Me_5), 6.3 (dd, $^1J_{CP} = 32$ Hz, $IrCHPMe_3$).

$^{31}P\{^1H\}$ NMR (200 MHz, CD_2Cl_2 , 25 °C) δ : 59.3 ($P(^iPr)_2Xyl$), 33.1 (PMe_3).



A solution of **14-Cl** (50 mg, 0.086 mmol) in CH_2Cl_2 (5 mL) was cooled to 0°C and a solution of ZnMe_2 in toluene (2M, 80 μL) was added dropwise. The yellow solution rapidly cleared up to become nearly colourless. The mixture was stirred at 20°C for 3 h, quenched with H_2O (10 μL) and the solvent removed under reduced pressure to provide crude compound **14-Me** as a pale yellow solid. The product was extracted with pentane and the solvent removed under vacuum to yield complex **14-Me** as a pale yellow powder (38 mg, 79 %).

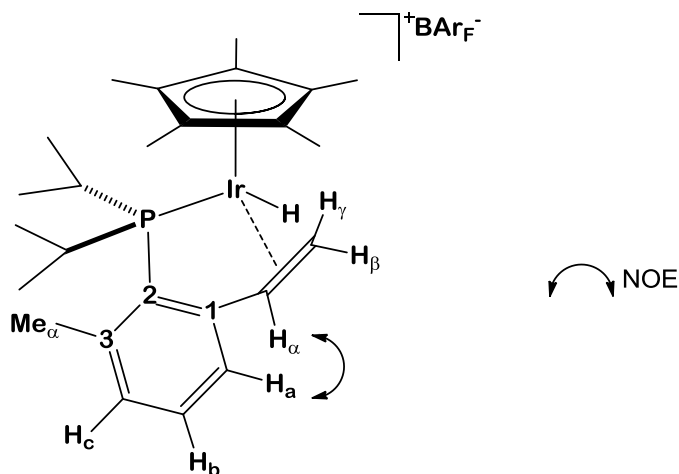
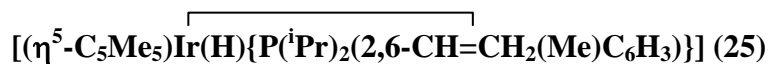
Analytical and spectroscopic data

Anal. Calcd. for $C_{25}H_{40}IrP$: C, 53.26; H, 7.15. **Found:** C, 53.2; H, 7.2.

1H NMR (500 MHz, CD_2Cl_2 , 25 °C) δ : 7.17 (d, 1 H, H_a), 6.98 (td, 1 H, $^5J_{HP} = 1.8$ Hz, H_b), 6.80 (d, 1 H, H_c), 3.16 (d, 1 H, $^2J_{HH} = 14.2$ Hz, IrCHH), 3.05 (dseptet, 1 H, $^2J_{HP} = 11.5$, $^3J_{HH} = 6.9$ Hz, $CH(iPr)$), 2.48 (s, 3 H, Me_w), 2.23 (octet, 1 H, $^2J_{HP} = ^3J_{HH} = 7.1$ Hz, $CH(iPr)$), 2.05 (dd, 1 H, $^2J_{HH} = 14.2$, $^3J_{HP} = 3.4$ Hz, IrCHH), 1.72 (d, 15 H, $^4J_{HP} = 1.5$ Hz, C_5Me_5), 1.11 (dd, 3 H, $^3J_{HP} = 17.7$, $^3J_{HH} = 6.8$ Hz, $Me(iPr)$), 1.03 (dd, 3 H, $^3J_{HP} = 13.4$, $^3J_{HH} = 7.1$ Hz, $Me(iPr)$), 0.91 (dd, 3 H, $^3J_{HP} = 13.8$, $^3J_{HH} = 7.1$ Hz, $Me(iPr)$), 0.81 (dd, 3 H, $^3J_{HP} = 15.3$, $^3J_{HH} = 7.1$ Hz, $Me(iPr)$), -0.20 (d, 3 H, $^3J_{HP} = 3.4$ Hz, IrCH₃). All aromatic couplings are of *ca.* 7.5 Hz.

$^{13}C\{^1H\}$ NMR (125 MHz, CD_2Cl_2 , 25 °C) δ : 162.6 (d, $^2J_{CP} = 26$ Hz, C_1), 140.3 (C_3), 134.7 (d, $^1J_{CP} = 45$ Hz, C_2), 128.5 (CH_b), 128.0 (d, $^3J_{CP} = 7$ Hz, CH_c), 127.5 (d, $^3J_{CP} = 12$ Hz, CH_a), 90.9 (C_5Me_5), 31.3 (d, $^1J_{CP} = 29$ Hz, $CH(iPr)$), 27.8 (d, $^1J_{CP} = 29$ Hz, $CH(iPr)$), 22.3 (Me_w), 20.4 (d, $^2J_{CP} = 7$ Hz, $Me(iPr)$), 19.6 ($Me(iPr)$), 18.8 ($Me(iPr)$), 18.1 ($Me(iPr)$), 13.1 (IrCH₂), 8.7 (C_5Me_5), -25.2 (d, $^2J_{CP} = 8$ Hz, IrCH₃).

$^{31}P\{^1H\}$ NMR (200 MHz, CD_2Cl_2 , 25 °C) δ : 52.8.



Complex **25** was isolated as a minor product (*ca.* 20 % conversion) of the reaction of alkylidene **14**⁺ with LiMe. A diethyl ether solution of LiMe (1.6 M, 32 μL) was added at -40 $^\circ\text{C}$ to a THF (5 mL) solution of **14**⁺ (60 mg, 0.042 mmol) under argon and the reaction mixture cleared up. The volatiles were removed under vacuum and the residue extracted with dichloromethane and passed through a pad of neutral alumina. The mixture was evaporated to dryness and the solid several times washed with pentane to give **25** as a pale yellow powder (8 mg, 13 %).

Analytical and spectroscopic data

Anal. Calcd. for $C_{57}H_{51}BF_{24}IrP$: C, 48.01; H, 3.60. **Found:** C, 48.1; H, 3.7.

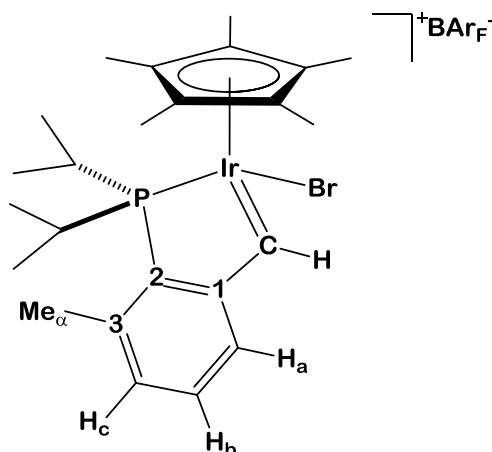
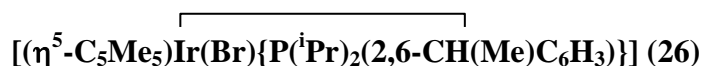
EM (ES) m/z Calcd. for M^+ : 563.24. **Expt.:** 563.3.

IR (Nujol): $\nu(\text{IrH})$ 2185 cm^{-1} .

^1H NMR (400 MHz, CD_2Cl_2 , 25 °C) δ : 7.38 (d, 1 H, H_a), 7.30 (td, 1 H, $^5J_{\text{HP}} = 2.6$ Hz, H_b), 7.13 (dd, 1 H, $^4J_{\text{HP}} = 3.7$ Hz, H_c), 4.11 (dd, 1 H, $^3J_{\text{HH}} = 10.3$, $^3J_{\text{HH}} = 8.4$ Hz, H_d), 2.90 (m, 1 H, $\text{CH}(\text{iPr})$), 2.46 (s, 3 H, Me_a), 2.29 (m, 1 H, $\text{CH}(\text{iPr})$), 2.26 (d, 1 H, $^3J_{\text{HH}} = 8.4$, H_e), 2.18 (dt, 1 H, $^3J_{\text{HH}} = 10.4$, $^2J_{\text{HH}} = ^3J_{\text{HP}} = 2.5$ Hz, H_f), 1.99 (d, 15 H, $^4J_{\text{HP}} = 1.3$ Hz, C_5Me_5), 1.32 (dd, 3 H, $^3J_{\text{HP}} = 14.7$, $^3J_{\text{HH}} = 7.2$ Hz, $\text{Me}(\text{iPr})$), 1.15 (dd, 3 H, $^3J_{\text{HP}} = 18.8$, $^3J_{\text{HH}} = 6.6$ Hz, $\text{Me}(\text{iPr})$), 0.85 (dd, 3 H, $^3J_{\text{HP}} = 18.2$, $^3J_{\text{HH}} = 6.7$ Hz, $\text{Me}(\text{iPr})$), 0.55 (dd, 3 H, $^3J_{\text{HP}} = 17.5$, $^3J_{\text{HH}} = 7.0$ Hz, $\text{Me}(\text{iPr})$), -16.6 (d, 1 H, $^3J_{\text{HP}} = 28.2$ Hz, IrH). All aromatic couplings are of *ca.* 7.5 Hz.

$^{13}\text{C}\{^1\text{H}\}$ NMR (100 MHz, CD_2Cl_2 , 25 °C) δ : 151.1 (d, $^2J_{\text{CP}} = 22$ Hz, C_1), 142.4 (C_3), 132.4 (d, $^4J_{\text{CP}} = 3$ Hz, CH_b), 132.0 (d, $^3J_{\text{CP}} = 8$ Hz, CH_c), 126.6 (d, $^3J_{\text{CP}} = 14$ Hz, CH_a), 125.6 (C_2), 101.1 (C_5Me_5), 60.1 (CH_d), 33.9 (CH_bH_f), 28.5 (d, $^1J_{\text{CP}} = 30$ Hz, $\text{CH}(\text{iPr})$), 25.4 (d, $^1J_{\text{CP}} = 37$ Hz, $\text{CH}(\text{iPr})$), 22.7 (Me_a), 19.4 (d, $^2J_{\text{CP}} = 2$ Hz, $\text{Me}(\text{iPr})$), 18.7 (d, $^2J_{\text{CP}} = 6$ Hz, $\text{Me}(\text{iPr})$), 18.1 ($\text{Me}(\text{iPr})$), 17.5 ($\text{Me}(\text{iPr})$), 9.7 (C_5Me_5).

$^{31}\text{P}\{^1\text{H}\}$ NMR (160 MHz, CD_2Cl_2 , 25 °C) δ : 60.4.



Chloride complex **14-Cl** (100 mg, 0.171 mmol) and NaBAr_F (152 mg, 0.171 mmol) were placed in a Schlenk and dissolved in CH₂Cl₂ (5 mL) under argon. After stirring at room temperature for 15 minutes the red solution was filtered over a Schlenk flask containing *N*-bromosuccinimide (30 mg, 0.171 mmol), with a change in color to dark green. The reaction mixture was stirred for 15 minutes and then the succinimide removed by extraction with deoxygenated water. Compound **26** was obtained as dark green crystals (215 mg, 84 %) by slow diffusion of pentane into a dichloromethane solution of the alkylidene.

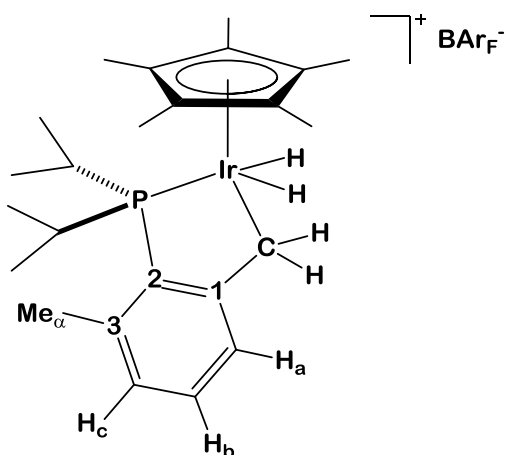
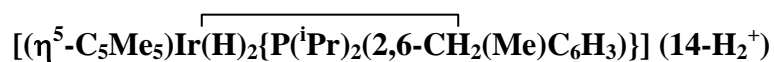
Analytical and spectroscopic data

Anal. Calcd. for $C_{56}H_{47}BBrF_{24}IrP$: C, 45.15; H, 3.18. **Found:** C, 45.1; H, 3.2.

1H NMR (500 MHz, CD_2Cl_2 , 25 °C) δ : 16.1 (s, 1 H, Ir=CH), 8.10 (d, 1 H, H_a), 6.98 (dd, 1 H, $^5J_{HP} = 2.9$ Hz, H_c), 7.56 (H_b , overlapped with NaBArF), 3.74 (dseptet, 1 H, $^2J_{HP} = 11.9$, $^3J_{HH} = 6.8$ Hz), 2.79 (s, 3 H, Me_a), 1.98 (m, 1 H, $CH(iPr)$), 1.94 (t, 15 H, $^4J_{HP} = 1.1$ Hz, C_5Me_5), 1.66 (dd, 3 H, $^3J_{HP} = 15.8$, $^3J_{HH} = 6.9$ Hz, $Me(iPr)$), 1.30 (m, 6 H, 2 $Me(iPr)$), 0.24 (dd, 3 H, $^3J_{HP} = 17.3$, $^3J_{HH} = 7.0$ Hz, $Me(iPr)$). All aromatic couplings are of *ca.* 7.5 Hz.

$^{13}C\{^1H\}$ NMR (125 MHz, CD_2Cl_2 , 25 °C) δ : 262.2 ($^1J_{CH} = 152$ Hz, Ir=CH), 167.2 (d, $^2J_{CP} = 25$ Hz, C_1), 145.5 (C_3), 139.9 (d, $^3J_{CP} = 8$ Hz, CH_a), 139.1 (d, $^1J_{CP} = 47$ Hz, C_2), 134.2 (CH_b), 131.1 (d, $^3J_{CP} = 12$ Hz, CH_c), 107.6 (C_5Me_5), 29.7 (Me_a), 28.1 (d, $^1J_{CP} = 28$ Hz, $CH(iPr)$), 27.2 (d, $^1J_{CP} = 31$ Hz, $CH(iPr)$), 22.4 ($Me(iPr)$), 19.5 (d, $^2J_{CP} = 4$ Hz, $Me(iPr)$), 18.6 (d, $^2J_{CP} = 6$ Hz, $Me(iPr)$), 18.5 ($Me(iPr)$), 9.4 (C_5Me_5).

$^{31}P\{^1H\}$ NMR (200 MHz, CD_2Cl_2 , 25 °C) δ : 60.3.



A *J. Young* NMR tube was charged with **14**⁺ (30 mg, 0.021 mmol) and CD₂Cl₂ (0.6 mL). The tube was charged with H₂ (1 bar) and shaken. The solution rapidly turned from red to yellow and ³¹P{¹H} NMR monitoring of the reaction showed clean and quantitative conversion to **14-H₂**⁺. Spectroscopic data were obtained without further purification.

Spectroscopic data

^1H NMR (400 MHz, CD_2Cl_2 , 25 °C) δ : 7.26 (d, 1 H, H_a), 7.21 (td, 1 H, $^5J_{\text{HP}} = 2.4$ Hz, H_b), 6.97 (dd, 1 H, $^5J_{\text{HP}} = 4.0$ Hz, H_c), 2.64 (br. s, 2 H, $\text{CH}(\text{iPr})$), 2.45 (s, 3 H, Me_a), 2.10 (d, 15 H, $^4J_{\text{HP}} = 1.3$ Hz, C_5Me_5), 1.02 (dd, 6 H, $^3J_{\text{HP}} = 18.1$, $^3J_{\text{HH}} = 6.8$ Hz, $\text{Me}(\text{iPr})$), 0.96 (dd, 3 H, $^3J_{\text{HP}} = 18.7$, $^3J_{\text{HH}} = 7.0$ Hz, $\text{Me}(\text{iPr})$). All aromatic couplings are of *ca.* 7.5 Hz. Hydride and methylene signals are only detectable at temperatures below -20°C.

^1H NMR (400 MHz, CD_2Cl_2 , -80 °C) δ : 7.16 (m, 2 H, H_a , H_b), 6.87 (br. s, 1 H, H_c), 3.47 (d, 1 H, $^2J_{\text{HH}} = 13.0$ Hz, IrCHH), 3.38 (d, 1 H, $^2J_{\text{HH}} = 13.0$ Hz, IrCHH), 2.87 (br. s, 1 H, $\text{CH}(\text{iPr})$), 2.35 (s, 3 H, Me_a), 2.02 (br. s, 1 H, $\text{CH}(\text{iPr})$), 1.92 (s, 15 H, C_5Me_5), 1.19 (dd, 3 H, $^3J_{\text{HP}} = 14.5$, $^3J_{\text{HH}} = 6.9$ Hz, $\text{Me}(\text{iPr})$), 0.93 (dd, 3 H, $^3J_{\text{HP}} = 19.0$, $^3J_{\text{HH}} = 6.3$ Hz, $\text{Me}(\text{iPr})$), 0.76 (dd, 3 H, $^3J_{\text{HP}} = 19.2$, $^3J_{\text{HH}} = 6.2$ Hz, $\text{Me}(\text{iPr})$), 0.61 (dd, 3 H, $^3J_{\text{HP}} = 17.8$, $^3J_{\text{HH}} = 6.7$ Hz, $\text{Me}(\text{iPr})$), -13.62 (s, 1 H, Ir-H), -13.97 (d, 1 H, $^2J_{\text{HP}} = 16.1$ Hz).

$^{13}\text{C}\{^1\text{H}\}$ NMR (100 MHz, CD_2Cl_2 , 25 °C) δ : 158.0 (d, $^2J_{\text{CP}} = 23$ Hz, C_1), 140.7 (d, $^2J_{\text{CP}} = 4$ Hz, C_3), 132.0 (CH_b), 130.6 (d, $^3J_{\text{CP}} = 9$ Hz, CH_c), 125.7 (d, $^3J_{\text{CP}} = 14$ Hz, CH_a), 125.6 (C_2), 103.3 (C_5Me_5), 27.6 (br. d, $^1J_{\text{CP}} = 32$ Hz, $\text{CH}(\text{iPr})$), 22.6 (Me_a), 18.6 ($\text{Me}(\text{iPr})$), 18.4 (d, $^2J_{\text{CP}} = 2$ Hz, $\text{Me}(\text{iPr})$), 9.8 (C_5Me_5), 9.5 (IrCH_2).

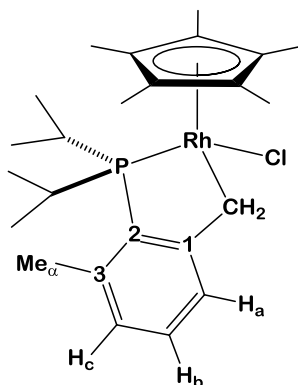
$^{31}\text{P}\{^1\text{H}\}$ NMR (160 MHz, CD_2Cl_2 , 25 °C) δ : 60.7.

3.B.4. Synthesis of rhodium organometallic complexes

Synthesis of rhodium chloride compounds.

A solution of the phosphine ($\text{P}(\text{}^i\text{Pr})_2(\text{Xyl})$): 111 mg, 0.5 mmol; $\text{PMe}_2(\text{Xyl})$: 83 mg, 0.5 mmol) in 2 mL of THF was added, at $-40\text{ }^\circ\text{C}$, to a solution of $[\text{RhCl}(\text{C}_2\text{H}_4)_2]_2$ (100 mg, 0.25 mmol) in 3 mL of THF. The reaction mixture was stirred for 3 h at this temperature. Then, a solution of ZnCp_2^* (84 mg, 0.25 mmol) in 1 mL of THF was added and the mixture stirred for 5 h, allowing to warm slowly to $-25\text{ }^\circ\text{C}$. The solvent was removed under vacuum and the residue extracted with diethyl ether, then evaporated to dryness. The solid was dissolved in 5 mL of CHCl_3 and stirred for 3 h at room temperature. The solvent was removed under vacuum and the crude product washed with pentane to yield chloride complexes **20-Cl** and **21-Cl** as orange solids, which were purified by column chromatography from Et_2O /pentane (**20-Cl**, 175 mg, 70 %; **21-Cl**, 110 mg, 83 %). Reaction with $\text{PMe}_2(\text{Xyl})$ gave a mixture of metalated (**21-Cl**) and non-metalated (**22**) complexes in a *ca.* ratio of 30:70. Both compounds were isolated by column chromatography from Et_2O /pentane to give pure samples of **21-Cl** (42 mg, 19 %) and **21** (130 mg, 55 %) as crystalline orange solids. In order to increase the amount of **21-Cl**, a THF solution of **22** (50 mg, 0.105 mmol) was reacted with a solution of Li^nBu (3 M in hexanes, 45 μL) at $-20\text{ }^\circ\text{C}$. After 30 min of stirring at this temperature, the reaction was quenched with MeOH (10 μL) and the volatiles removed under vacuum. The product was extracted with Et_2O , the solvent evaporated to dryness and the orange solid washed with pentane to give complex **21-Cl** in 62 % yield (29 mg).

(η^5 -C₅Me₅)Rh(Cl){P(ⁱPr)₂(2,6-CH₂(Me)C₆H₃)} (20-Cl)



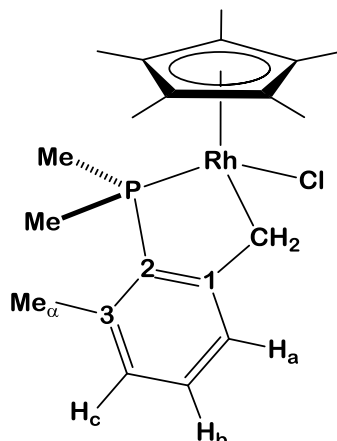
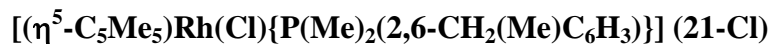
Analytical and spectroscopic data

Anal. Calcd. for C₂₄H₃₇ClIPRh: C, 58.25; H, 7.54. **Found:** C, 58.4; H, 7.4.

¹H NMR (500 MHz, CDCl₃, 25 °C) δ : 7.14 (d, 1 H, H_a), 7.01 (td, 1 H, ⁵J_{HP} = 2.2 Hz, H_b), 6.81 (dd, 1 H, ⁴J_{HP} = 2.4 Hz, H_c), 3.42 (br. d, 1 H, ²J_{HH} = 12.1 Hz, RhCHH), 3.24 (br. d, 1 H, ²J_{HH} = 12.1 Hz, RhCHH), 2.95 (septet, 2 H, ³J_{HH} = 7.0 Hz, CH(ⁱPr)), 2.42 (s, 3 H, Me_a), 2.29 (m, 2 H, CH(ⁱPr)), 1.63 (d, 15 H, ⁴J_{HP} = 2.4 Hz, C₅Me₅), 1.36 (dd, 6 H, ³J_{HP} = 19.1, ³J_{HH} = 6.8, Me(ⁱPr)), 1.24 (dd, 6 H, ³J_{HP} = 12.3, ³J_{HH} = 7.1, Me(ⁱPr)), 1.19 (dd, 6 H, ³J_{HP} = 14.5, ³J_{HH} = 7.1, Me(ⁱPr)), 0.80 (dd, 6 H, ³J_{HP} = 15.5, ³J_{HH} = 7.1, Me(ⁱPr)). All aromatic couplings are of *ca.* 7.5 Hz.

¹³C{¹H} NMR (160 MHz, CDCl₃, 25 °C) δ : 160.7 (d, ²J_{CP} = 28 Hz, C₁), 139.5 (C₃), 131.2 (d, ¹J_{CP} = 42 Hz, C₂), 129.6 (d, ⁴J_{CP} = 2 Hz, CH_b), 127.7 (d, ⁴J_{CP} = 6 Hz, CH_c), 126.6 (d, ⁴J_{CP} = 15 Hz, CH_a), 98.1 (t, ¹J_{CRh} = ²J_{CP} = 4 Hz, C₅Me₅), 30.5 (dd, ¹J_{CRh} = 23, ²J_{CP} = 8 Hz, RhCH₂), 30.1 (d, ¹J_{CP} = 21 Hz, CH(ⁱPr)), 27.5 (d, ¹J_{CP} = 22 Hz, CH(ⁱPr)), 22.8 (Me_a), 20.7 (d, ²J_{CP} = 8 Hz, Me(ⁱPr)), 20.2 (Me(ⁱPr)), 19.4 (d, ²J_{CP} = 5 Hz, Me(ⁱPr)), 19.1 (Me(ⁱPr)), 9.6 (C₅Me₅).

³¹P{¹H} NMR (200 MHz, CDCl₃, 25 °C) δ : 83.0 (d, ¹J_{RhP} = 159 Hz).



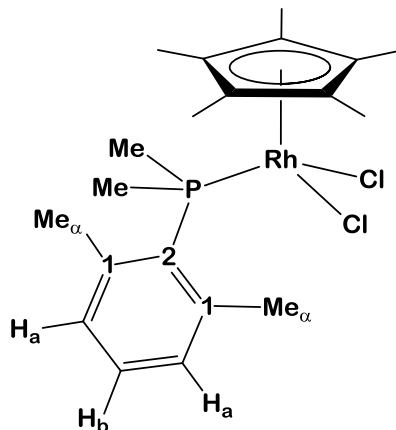
Analytical and spectroscopic data

Anal. Calcd. for $\text{C}_{20}\text{H}_{29}\text{ClPRh}$: C, 54.8; H, 6.7. **Found:** C, 54.8; H, 6.7.

^1H NMR (500 MHz, CD_2Cl_2 , 25 °C) δ : 7.15 (d, 1 H, H_a), 7.09 (td, 1 H, $^5J_{\text{HP}} = 2.2$ Hz, H_b), 6.87 (dd, 1 H, $^4J_{\text{HP}} = 2.9$ Hz, H_c), 3.21 (m, 2 H, RhCH_2), 2.46 (s, 3 H, Me_α), 1.98 (d, 3 H, $^2J_{\text{CP}} = 11.5$ Hz, PMeMe), 1.74 (d, 3 H, $^2J_{\text{CP}} = 10.4$ Hz, PMeMe), 1.72 (d, 15 H, $^4J_{\text{HP}} = 2.7$ Hz, C_5Me_5). All aromatic couplings are of *ca.* 7.5 Hz.

$^{13}\text{C}\{^1\text{H}\}$ NMR (125 MHz, CD_2Cl_2 , 25 °C) δ : 159.5 (d, $^2J_{\text{CP}} = 31$ Hz, C_1), 139.8 (C_3), 134.4 (d, $^1J_{\text{CP}} = 51$ Hz, C_2), 129.8 (CH_b), 127.3 (d, $^4J_{\text{CP}} = 7$ Hz, CH_c), 126.0 (d, $^4J_{\text{CP}} = 26$ Hz, CH_a), 97.3 (C_5Me_5), 28.9 (dd, $^1J_{\text{CRh}} = 24$, $^2J_{\text{CP}} = 9$ Hz, RhCH_2), 20.8 (Me_α), 14.8 (d, $^1J_{\text{CP}} = 30$ Hz, PMeMe), 14.5 (d, $^1J_{\text{CP}} = 27$ Hz, PMeMe), 8.9 (C_5Me_5).

$^{31}\text{P}\{^1\text{H}\}$ NMR (200 MHz, CD_2Cl_2 , 25 °C) δ : 41.2 (d, $^1J_{\text{RhP}} = 158$ Hz).



Analytical and spectroscopic data

Anal. Calcd. for $\text{C}_{20}\text{H}_{30}\text{Cl}_2\text{PRh}$: C, 50.55; H, 6.36. **Found:** C, 50.3; H, 6.5.

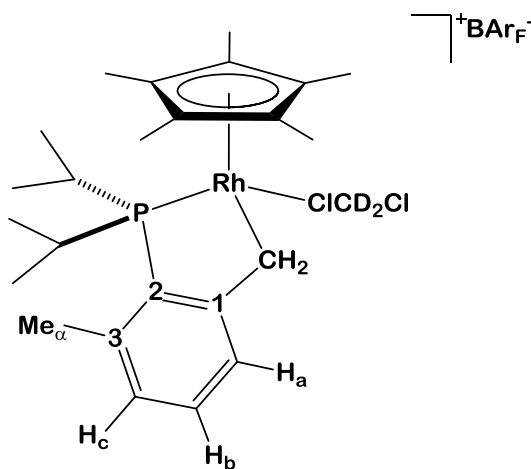
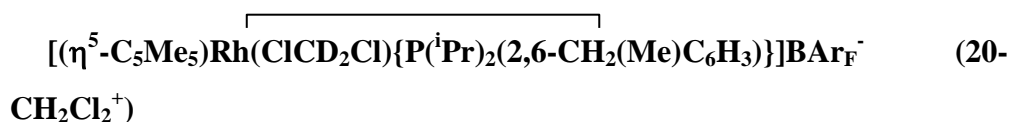
^1H NMR (500 MHz, CDCl_3 , 25 °C) δ : 7.20 (td, 1 H, $^5J_{\text{HP}} = 1.8$ Hz, H_b), 7.06 (dd, 2 H, $^4J_{\text{HP}} = 3.0$ Hz, H_a), 2.63 (s, 6 H, Me_α), 1.98 (d, 6 H, $^2J_{\text{CP}} = 10.7$ Hz, PMe_2), 1.42 (d, 15 H, $^4J_{\text{HP}} = 3.5$ Hz, C_5Me_5). All aromatic couplings are of *ca.* 7.5 Hz.

$^{13}\text{C}\{^1\text{H}\}$ NMR (125 MHz, CDCl_3 , 25 °C) δ : 142.7 (d, $^2J_{\text{CP}} = 8$ Hz, C_1), 130.8 (d, $^4J_{\text{CP}} = 8$ Hz, CH_a), 130.5 (d, $^1J_{\text{CP}} = 33$ Hz, C_2), 130.3 (d, $^4J_{\text{CP}} = 3$ Hz, CH_b), 98.6 (dd, $^1J_{\text{CRh}} = 7$, $^2J_{\text{CP}} = 3$ Hz, C_5Me_5), 25.5 (d, $^3J_{\text{CP}} = 6$ Hz, Me_α), 18.3 (d, $^1J_{\text{CP}} = 34$ Hz, PMe_2), 9.1 (C_5Me_5).

$^{31}\text{P}\{^1\text{H}\}$ NMR (200 MHz, CDCl_3 , 25 °C) δ : 12.0 (d, $^1J_{\text{RhP}} = 143$ Hz).

Synthesis of cationic rhodium dichloromethane adducts

A solid mixture of the rhodium chloride complex (**20-Cl**, 49 mg, 0.1 mmol; **21-Cl**, 44 mg, 0.1 mmol) and NaBAR_F (88 mg, 0.1 mmol) placed in a Schlenk flask was dissolved in CH₂Cl₂ (3 mL) at -20 °C. Monitoring of the reaction by ³¹P{¹H} NMR after 5 min showed quantitative conversion into the dichloromethane adduct. The solution was filtered and the cationic adducts isolated as red crystals (**20-CH₂Cl₂⁺**, 107 mg, 76 %; **21-CH₂Cl₂⁺**, 84 mg, 62 %) by slow diffusion of pentane into the dichloromethane solution at -25 °C.



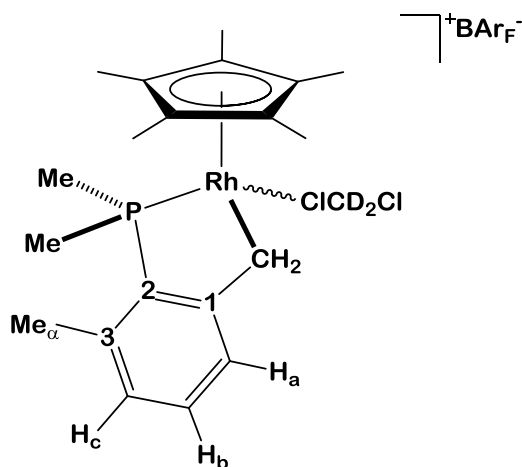
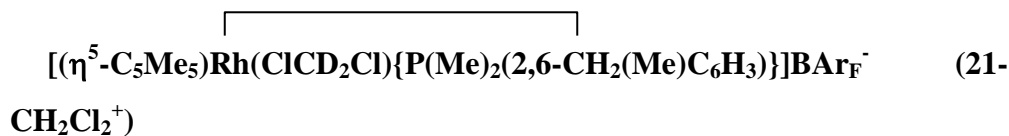
Analytical and spectroscopic data

Anal. Calcd. for $C_{57}H_{51}BCl_2F_{24}PRh$: C, 48.64; H, 3.65. **Found:** C, 48.8; H, 3.3.

1H NMR (400 MHz, CD_2Cl_2 , 25 °C) δ : 7.26 (m, 2 H, H_a , H_b), 7.12 (d, 1 H, H_c), 3.49 (m, 2 H, $RhCH_2$), 2.74 (m, 2 H, $CH(^iPr)$), 2.50 (s, 3 H, Me_a), 1.68 (d, 15 H, $^4J_{HP} = 2.0$ Hz, C_5Me_5), 1.20 (dd, 6 H, $^3J_{HH} = 7.1$, $Me(^iPr)$), 1.17 (d, 6 H, $^3J_{HH} = 7.0$, $Me(^iPr)$). All aromatic couplings are of *ca.* 7.5 Hz.

$^{13}C\{^1H\}$ NMR (100 MHz, CD_2Cl_2 , 25 °C) δ : 150.7 (br. d, $^2J_{CP} = 25$ Hz, C_1), 141.1 (C_3), 132.0 (CH_b), 130.6 (d, $^4J_{CP} = 7$ Hz, CH_c), 126.7 (d, $^4J_{CP} = 14$ Hz, CH_a), 124.5 (d, $^1J_{CP} = 43$ Hz, C_2), 101.2 (C_5Me_5), 33.9 (d, $^1J_{CRh} = 23$ Hz, $RhCH_2$), 27.4 (d, $^1J_{CP} = 22$ Hz, $CH(^iPr)$), 22.4 (Me_a), 19.2 ($Me(^iPr)$), 19.1 ($Me(^iPr)$), 9.6 (C_5Me_5).

$^{31}P\{^1H\}$ NMR (160 MHz, CD_2Cl_2 , 25 °C) δ : 77.3 (d, $^1J_{RhP} = 158$ Hz).



Spectroscopic data

^1H NMR (400 MHz, CD_2Cl_2 , 25 °C) δ : 7.25, 7.23 (d, 1 H each, H_a , H_b), 7.02 (m, 1 H, H_c), 3.40 (m, 2 H, RhCH_2), 2.46 (s, 3 H, Me_a), 1.91 (d, 6 H, $^2J_{\text{CP}} = 10.1$ Hz, $\text{P}(\text{Me})_2$), 1.72 (d, 15 H, $^4J_{\text{HP}} = 2.7$ Hz, C_5Me_5). All aromatic couplings are of *ca.* 7.5 Hz.

$^{13}\text{C}\{^1\text{H}\}$ NMR (100 MHz, CD_2Cl_2 , 25 °C) δ : 155.0 (C_1), 141.5 (C_3), 131.5 (C_2), 132.7 (d, $^5J_{\text{CP}} = 2$ Hz, CH_b), 130.0 (d, $^4J_{\text{CP}} = 8$ Hz, CH_c), 126.1 (d, $^4J_{\text{CP}} = 18$ Hz, CH_a), 101.1 (C_5Me_5), 31.1 (dd, $^1J_{\text{CRh}} = 24$, $^2J_{\text{CP}} = 6$ Hz, RhCH_2), 21.2 (d, $^3J_{\text{CP}} = 4$ Hz, Me_a), 14.6 (d, $^1J_{\text{CP}} = 29$ Hz, $\text{P}(\text{Me})_2$), 9.4 (C_5Me_5).

$^{31}\text{P}\{^1\text{H}\}$ NMR (160 MHz, CD_2Cl_2 , 25 °C) δ : 36.0 (d, $^1J_{\text{RhP}} = 161$ Hz).

3.B.5. Kinetic studies on the conversion of **23** into **14-PMe₃⁺**

A screw-capped NMR tube was charged with compound **14-BAr_F** (20 mg, 0.014 mmol) and CD₂Cl₂ (0.6 mL) under argon. Then PMe₃ (1.6 μL, 0.015 mmol) was added at -40 °C and the NMR tube rapidly shaken. The course of the reaction was monitored by ³¹P{¹H} NMR and a first-order kinetic dependence on the concentration of **23** was measured. Representation of ln[**23**] vs. time (Figure 43) allowed measuring a first-order kinetic rate of 3.4·10⁻⁵ s⁻¹, which corresponds to a ΔG[‡] = 24.8 ± 0.3 kcal·mol⁻¹.

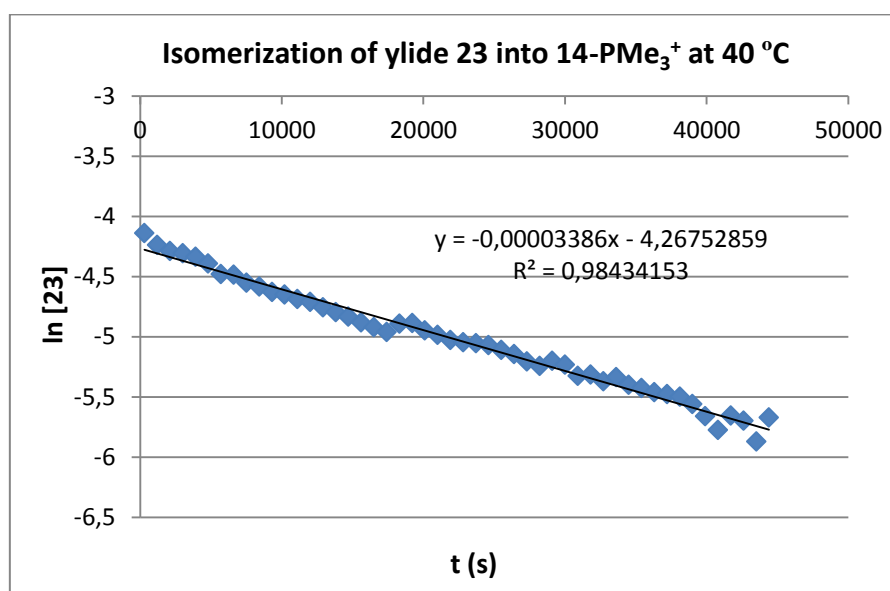


Figure 43. First-order representation of ln[**23**] vs. time for the isomerization of **23** into **14-PMe₃⁺**.

II.4.REFERENCES

4. REFERENCES

- ¹ For selected reviews on the topic: (a) Bergman, R. G. *Nature* **2007**, *446*, 391. (b) Crabtree, R. H. *Chem. Rev.* **2010**, *110*, 575. (c) Balcells, D.; Clot, E.; Eisenstein, O. *Chem. Rev.* **2010**, *110*, 749. (d) Labinger, J. A.; Bercaw, J. E. *Nature* **2002**, *417*, 507. (e) Crabtree, R. H. *J. Organomet. Chem.* **2004**, *689*, 4083. (f) Newhouse, T.; Baran, P. S. *Angew. Chem. Int. Ed.* **2011**, *15*, 3362. (g) Wencel-Delord, J.; Dröge, T.; Liu, F.; Glorius, F. *Chem. Soc. Rev.* **2011**, *40*, 4740. (h) Yang, L.; Huang, H. *Catal. Sci. Technol.* **2012**, *6*, 1099.
- ² Goldberg, K. I.; Goldman, A. S., Eds. *Activation and Functionalization of C-H Bonds*; ACS Symposium Series 885; American Chemical Society: Washington, DC, **2004**.
- ³ See: Hartwig, J. F. *Nature* **2008**, *455*, 314, and references cited therein.
- ⁴ See: Colby, D. A.; Bergman, R. G.; Ellman J. A. *Chem. Rev.* **2010**, *110*, 624, and references cited therein.
- ⁵ de Meijere, A.; Diederich, F. *Metal-Catalyzed Cross-Coupling Reactions* **2004**, Eds.; Wiley-VCH: Weinheim.
- ⁶ Chatt, J.; Watson, H. R. *J. Chem. Soc.*, **1962**, 2545.
- ⁷ (a) Hodges, R. J.; Garnett, J. L. *J. Phys. Chem.* **1969**, *73*, 1525. (b) Hodges, R. J.; Garnett, J. L. *J. Phys. Chem.* **1968**, *72*, 1673. (c) Hodges, R. J.; Garnett, J. L. *J. Catal.* **1969**, *13*, 83.

- ⁸ Goldshleger, N.F.; Shteinman, A.A.; Shilov, A.E. Eskova, V.V. *Zh. Fiz. Khim.* **1972**, *46*, 1353.
- ⁹ (a) Green, M. L. H.; Knowles, P. J. *J. Chem. Soc. Chem. Commun.* **1970**, 1677; (b) Foley, P.; Whitesides, G. M. *J. Am. Chem. Soc.* **1979**, *101*, 2732. (c) Bennett, M. A.; Milner, D. L. *J. Chem. Soc. Chem. Commun.* **1967**, 581. (d) Crabtree, R. H.; Mihelcic, J. M.; Quirk, J. M. *J. Am. Chem. Soc.* **1979**, *101*, 7738.
- ¹⁰ Janowicz, A. H.; Bergman, R. G. *J. Am. Chem. Soc.* **1982**, *104*, 352.
- ¹¹ Hoyano, J. K.; Graham, W. A. G. *J. Am. Chem. Soc.* **1982**, *104*, 3723.
- ¹² A review of that achievements can be found in: Shilov, A. E.; Shul'pin, G. B. *Activation and Catalytic Reactions of Saturated Hydrocarbons in the Presence of Metal Complexes*, **2000**, Kluwer Academic, Dordrecht.
- ¹³ Crabtree, R. H. *Angew. Chem. Int. Ed.* **1993**, *32*, 789.
- ¹⁴ Perutz, R. N.; Sabo-Etienne, S. *Angew. Chem. Int. Ed.* **2007**, *46*, 2578.
- ¹⁵ Buger, P.; Bergman, R. G. *J. Am. Chem. Soc.* **1993**, *115*, 10462.
- ¹⁶ Arndtsen, B. A.; Bergman, R. G. *Science* **1995**, *270*, 1970.
- ¹⁷ (a) Skaddan M. B.; Yung C. M.; Bergman, R. G.; *Org Lett* **2004**, *6*: 11. (b) Yung C. M.; Skaddan, M. B.; Bergman R. G. *J. Am. Chem. Soc.* **2004**, *126*, 13033. (c) Skaddan, M. B.; Bergman, R. G. *J. Label. Comp. Radiopharm.* **2006**, *49*, 623. (d) Klei, S. R.; Golden, J. T.; Tilley, T. D.; Bergman, R. G. *J. Am. Chem. Soc.* **2002**, *124*, 2092.
- ¹⁸ (a) Jones, W. D.; Feher, F. J. *J. Am. Chem. Soc.* **1982**, *104*, 4240. (b) Jones, W. D.; Feher, F. J. *Organometallics*, **1983**, *2*, 562.
- ¹⁹ (a) Taw, F. L.; Mellows, H.; White, P. S.; Hollander, F. J.; Bergman, R. G.; Brookhart, M.; Heinekey, D. M. *J. Am. Chem. Soc.* **2002**, *124*, 5100. (b) Corkey, B. K.; Felicia, F. L.; Bergman, R. G.; Brookhart, M. *Polyhedron*, **2004**, *23*, 2943.
- ²⁰ (a) Tellers, D. M.; Yung, C. M.; Arndtsen, B.; Adamson, D. R.; Bergman, R. G. *J. Am. Chem. Soc.* **2002**, *124*, 1400. (b) Meredith J. M.; Goldberg, K. I.; Kaminsky W.; Heinekey, D. M. *Organometallics* **2009**, *28*, 3546. (c) Meredith, J. M.; Robinson Jr., R.; Goldberg, K. I.; Kaminsky, W.; Heinekey, D. M. *Organometallics*, **2012**, *31*, 1879. (d) Tellers, D. M.; Bergman, R. G. *Organometallics* **2001**, *20*, 4819. (e) Hinderling, C.; Plattner, D. A.; Chen, P. *Angew. Chem. Int. Ed.* **1997**, *36*, 243. (f) Hinderling, C.; Feichtinger, D.; Plattner, D. A.; Chen, P. *J. Am. Chem. Soc.* **1997**, *119*, 848.
- ²¹ Luecke, H. F.; Bergman, R. G. *J. Am. Chem. Soc.* **1997**, *119*, 11538.
- ²² (a) Wu, X.; Xiao, J. *Chem. Commun.* **2007**, 2449. (b) Mashima, K.; Abe, T.; Tani, K. *Chem. Lett.* **1998**, *27*, 1201. (c) Fujita, K.; Tanino, N.; Yamaguchi, R. *Org. Lett.* **2007**, *9*, 109. (d) Tanabe, Y.; Hanasaka, F.; Fujita, K.; Yamaguchi, R. *Organometallics* **2007**, *26*, 4618.
- ²³ Daugulis, O.; Brookhart, M. *Organometallics* **2004**, *23*, 527.
- ²⁴ (a) Carmona, D.; Lamata, M. P.; Viguri, F.; Rodríguez, R.; Lahoz, F. J.; Dobrinovitch, I. T.; Oro, L. A. *Dalton Trans.* **2007**, 1911. (b) Carmona, D.; Lahoz, F. J.; Elipse, S.; Oro, L.

- A.; Lamata, M. P.; Viguri, F.; Sanchez, F.; Martinez, S.; Cativiela, C.; Lopez-Ram de Viu, M. P. *Organometallics*, **2002**, *21*, 5100.
- ²⁵ (a) Prades, A.; Corberán, R.; Poyatos, M.; Peris, E. *Chem. Eur. J.* **2008**, *14*, 11474. (b) Prades, A.; Corberán, R.; Poyatos, M.; Peris, E. *Chem. Eur. J.* **2009**, *15*, 4610.
- ²⁶ Liu, J.; Wu, X.; Iggo, J. A.; Xiao, J. *Coord. Chem. Rev.* **2008**, *252*, 782.
- ²⁷ Albrecht, M. *Chem. Rev.* **2010**, *110*, 576.
- ²⁸ (a) Göttker-Schnetmann, I.; White, P.; Brookhart, M. *J. Am. Chem. Soc.* **2004**, *126*, 1804. (b) Saidi, O.; Marafie, J.; Ledger, A. E. W.; Liu, P. M.; Mahon, M. F.; Kociok-Köhn, G.; Whittlesey, M. K.; Frost, C. G. *J. Am. Chem. Soc.* **2011**, *133*, 19298. (c) Feng, J.-J.; Chen, X.-F.; Shi, M.; Duan, W.-L. *J. Am. Chem. Soc.* **2010**, *132*, 5562. (d) Selander, N.; Szabó, K. J. *Dalton Trans.* **2009**, 6267. (e) Bedford, R. B. *Chem. Commun.* **2003**, 1787.
- ²⁹ (a) Severin, K.; Bergs, R.; Beck, W. *Angew. Chem. Int. Ed.* **1998**, *37*, 1634. (b) Dyson, P. J.; Sava, G. *Dalton Trans.* **2006**, 1929. (c) Ryabov, A. D.; Sukharev, V. S.; Alexandrova, L.; Lagadec, R. L.; Pfeffer, M. *Inorg. Chem.* **2001**, *40*, 6529.
- ³⁰ (a) Patoux, C.; Launay, J.-Pierre; Beley, M.; Chodorowski-kimmes, S.; Collin, J.-Paul; James, S.; Sauvage, J.-Pierre *J. Am. Chem. Soc.* **1998**, *120*, 3717. (b) Isozaki, K.; Takaya, H.; Naota, T. *Angew. Chem. Int. Ed.* **2007**, *119*, 2913. (c) Wadman, S. H.; Lutz, M.; Toohe, D. M.; Spek, A. L.; Havenith, R. W. A.; Klink, G. P. M. V.; Koten, G. V. *Inorg. Chem.* **2009**, *48*, 1887. (d) Wadman, S. H.; Kroon, J. M.; Bakker, K.; Lutz, M.; Spek, A. L.; van Klink, G. P. M.; van Koten, G. *Chem. Commun.* **2007**, 1907.
- ³¹ Denney, M. C.; Pons, V.; Hebden, T. J.; Heinekey, D. M.; Goldberg, K. I. *J. Am. Chem. Soc.*, **2006**, *28*, 12048.
- ³² Chou, P.-T.; Chi, Y. *Chem. Eur. J.* **2007**, *13*, 380
- ³³ (a) Bennett, M. A.; Longstaff, P. *J. Am. Chem. Soc.* **1969**, *91*, 6266. (b) Bennett, M. A.; Clark, P. W. *J. Organom. Chem.* **1976**, *110*, 367. (c) Bennett, M. A.; Clark, P. W.; Robertson, G. B.; Whimp, P. O. *J. Chem. Soc., Chem. Commun.* **1972**, 1011.
- ³⁴ (a) Baratta, W.; Herdtweck, E.; Martinuzzi, P.; Rigo, P. *Organometallics* **2001**, *20*, 305. (b) Baratta, W.; Ballico, M.; Del Zotto, A.; Zangrando, E.; Rigo, P. *Chem. Eur. J.* **2007**, *13*, 6701.
- ³⁵ (a) Shintani, R.; Duan, W.-L.; Nagano, T.; Okada, A.; Hayashi, T. *Angew. Chem. Int. Ed.* **2005**, *44*, 4611. (b) Maire, P.; Deblon, S.; Breher, F.; Geier, J.; Böhler, C.; Rügger, H.; Schönberg, H.; Grützmacher, H. *Chem. Eur. J.* **2004**, *10*, 4198. (c) Mora, G.; Van Zutphen, S.; Thoumazet, C.; Le Goff, X. F.; Ricard, L.; Grützmacher, H.; Le Floch, P. *Organometallics* **2006**, *25*, 5528. (d) Thoumazet, C.; Ricard, L.; Grützmacher, H.; Le Floch, P. *Chem. Commun.* **2005**, 1592. (e) Thoumazet, C.; Ricard, L.; Grützmacher, H.; Le Floch, P. *Chem. Commun.* **2005**, 1592. (f) Bettucci, L.; Bianchini, C.; Oberhauser, W.; Vogt, M.; Grützmacher, H. *Dalton Trans.* **2010**, *39*, 6509. (g) Bettucci, L.; Bianchini, C.; Oberhauser, W.; Vogt, M.; Grützmacher, H. *Dalton Trans.* **2010**, *39*, 6509. (h) Bettucci, L.; Bianchini, C.; Oberhauser, W.; Vogt, M.; Grützmacher, H. *Dalton Trans.* **2010**, *39*, 6509. (i) Christ, M. L.; Sabo-Etienne, S.; Chaudret, B. *Organometallics* **1995**, *14*, 1082. (j) Douglas, T. M.; Le Nôtre, J.; Brayshaw, S. K.; Frost, C. G.; Weller, A. S. *Chem. Commun.* **2006**, 3408. (k) Lewis, J. C.; Wu, J. Y.; Bergman, R. G.; Ellman, J. A. *Ang. Chem. Int. Ed.* **2006**, *45*, 1589. (l) Lewis, J. C.; Berman, A. M.; Bergman, R. G.; Ellman, J. A. *J. Am. Chem. Soc.* **2008**, *130*, 2493.

- ³⁶ Arduengo, A. J.; Bertrand, G. *Chem. Rev.* **2009**, *109*, 3209.
- ³⁷ Crabtree, R. H. *The Organometallic Chemistry of the Transition Metals* **2005**, Chap. 11, Ed. John Wiley & Sons, New Jersey.
- ³⁸ Cooper, N. J. *Pure Appl. Chem.* **56**, 25, 1984.
- ³⁹ (a) Elschenbroich, C. *Organometallics*, Chap 14, Ed. VCH, Weinheim. (b) Astruc, D. *Organometallic Chemistry and Catalysis* **2007**, Chap. 9, Ed. Springer Verlag.
- ⁴⁰ (a) Clark, G. R.; Hoskins, S. V.; Roper, W. R. *J. Organom. Chem.* **1982**, *234*, C9. (b) Alías, F. M.; Poveda, M. L.; Sellin, M.; Carmona, E. *J. Am. Chem. Soc.* **1998**, *120*, 5816. (c) Schwab, P.; France, M. B.; Ziller, J. W.; Grubbs R. H. *Angew. Chem. Int. Ed.* **1995**, *34*, 2039.
- ⁴¹ See for example: (a) Alías, F. M.; Poveda, M. L.; Sellin, M.; Carmona, E.; Gutiérrez, E.; Monge, A. *Organometallics* **1998**, *17*, 4124. (b) Lee, D.-H.; Chen, J.; Faller, J. W.; Crabtree, R. *Chem. Commun.* **2001**, 213-214 (c) Werner, H. *Ang. Chem. Int. Ed.* **2010**, *49*, 4714. (d) Poverenov, E.; Milstein, D. *Chem. Commun.* **2007**, 3189. (e) Fryzuk, M. D.; Macneil, P. A.; Rettig, S. J. *J. Am. Chem. Soc.* **1985**, *107*, 6708.
- ⁴² See for example: (a) Paneque, M.; Posadas, C. M.; Poveda, M. L.; Rendon, N.; Mereiter, K. *Organometallics* **2007**, *26*, 1900. (b) Luecke, H. F.; Bergman, R. G. *J. Am. Chem. Soc.* **1998**, *120*, 11008. (c) Besora, M.; Vyboishchikov, S. F.; Lledós, A.; Maseras, F.; Carmona, E.; Poveda, M. L. *Organometallics* **2010**, *29*, 2040. (d) Carmona, E.; Paneque, M.; Poveda, M. L. *Dalton Trans.* **2003**, 4022. (e) Thorn, D. L.; Tulip, T. H. *J. Am. Chem. Soc.* **1981**, *103*, 5984. (f) Thorn, D. L. *Organometallics* **1982**, *1*, 879. (g) Thorn, D. L.; Tulip, T. H. *Organometallics* **1982**, *1*, 1580. (h) Bell, T. W.; Haddleton, D. M.; McCamley, A.; Partridge, M. G.; Perutz, R. N.; Willner, H. *J. Am. Chem. Soc.* **1990**, *112*, 9212. (i) France, M. B.; Feldman, J.; Grubbs, R. H. *J. Chem. Soc., Chem. Commun.* **1994**, 1307. (j) Bleeke, J. R.; Behm, R. *J. Am. Chem. Soc.* **1997**, *119*, 8503.
- ⁴³ (a) Ortmann, D. A.; Weberndo, B.; Schoneboom, J.; Werner, H. *Organometallics* **1999**, *18*, 952. (b) Ortmann, D. A.; Weberndo, B.; Kerstin, I.; Laubender, M.; Schoneboom, J.; Werner, H. *Organometallics* **1999**, *18*, 952.
- ⁴⁴ (a) Pearson, R. G. *J. Am. Chem. Soc.* **1963**, *85*, 3533. (b) Schmidtke, H. H. *J. Am. Chem. Soc.* **1965**, *87*, 2522.
- ⁴⁵ Chisholm, M. A.; Rothwell, I. P., *Compreh. Coord. Chem.*, **1987**, Chapter 3.4. Wilkinson, G. W.; Guillard, R. D.; McCleverty, J. A. Eds. Pergamon Press, Oxford.
- ⁴⁶ Norbury, A. H. *Adv. Inorg. Chem. Radiochem.* **1975**, *17*, 231.
- ⁴⁷ Müller, P.; Herbst-Irmer, R.; Spek, A. L.; Schneider, T. R.; Sawaya, M. R. *Crystal Structure Refinement* **2006**, Chapter 4, Ed. Oxford Univ. Press, New York.
- ⁴⁸ Data collected from The Cambridge Structural Database (CSD). Cambridge Crystallographic Data Centre, 12 Union Road, Cambridge, England.
- ⁴⁹ See for example: (a) Comba, P.; Jurisic, P.; Lampeka, Y. D.; Peters, A.; Prikhod'ko, A. I.; Pritzkow, H. *Inorg. Chim. Acta* **2001**, *324*, 99. (b) Bernhardt, P. V.; Dyahningtyas, T. E.; Han, S. C.; Harrowfield, J. M.; Kim, I.C.; Kim, Y.; Koutsantonis, G. A.; Rukmini, E.; Thuéry, P. *Polyhedron* **2004**, *23*, 869. (c) Majumdar, A.; Pal, K.; Sarkar, S. *Dalton Trans.* **2009**, 1927.

- ⁵⁰ Data collected from The Cambridge Structural Database (CSD) and analyzed with VISTA software. CCDC (1994). Vista - A Program for the Analysis and Display of Data Retrieved from the CSD. Cambridge Crystallographic Data Centre, 12 Union Road, Cambridge, England.
- ⁵¹ (a) Hinderling, C.; Feichtinger, D.; Plattner, D. A.; Chen, P. *J. Am. Chem. Soc.* **1997**, *119*, 10793. (b) Casalnuovo, A. L.; Calabrese, J. C.; Milstein, D. *J. Am. Chem. Soc.* **1988**, *110*, 6738.
- ⁵² (a) Wenzel, T. T.; Bergman R. G. *J. Am. Chem. Soc.* **1996**, *108*, 4856. (b) Bergman, R. G.; Seidler, P. F.; Wenzel, T. T. *J. Am. Chem. Soc.* **1985**, *107*, 4358.
- ⁵³ Shinomoto, R. S.; Desrosiers, P. J.; Harper, G. P.; Flood, T. C. *J. Am. Chem. Soc.* **1990**, *112*, 704.
- ⁵⁴ (a) Rybtchinski, B. Cohen, R. Ben-David, Y. Martin, J. M. L. Milstein, D. *J. Am. Chem. Soc.* **2003**, *125*, 11041. (b) Corberán, R. Sanaú, M Peris, E. *J. Am. Chem. Soc.* **2006**, *128*, 3974. (c) Kloek, S. M. Heinekey, D. M. Goldberg, K. I. *Angew. Chem. Int. Ed.* **2007**, *46*, 4736. (d) Bercaw, J. E. Hazari, N. Labinger, J. A. *Organometallics* **2009**, *28*, 5489. (e) Feng, Y. Lail, M. Barakat, K. A. Cundari, T. R. Gunnoe, B. Petersen, J. L. *J. Am. Chem. Soc.* **2005**, *127*, 14174. (f) Santos, L. L. Mereiter, K. Paneque, M. Slugovc, C. Carmona, E. *New J. Chem.* **2003**, *27*, 107.
- ⁵⁵ Bernskoetter, W. H.; Hanson, S. K.; Buzak, S. K.; Davis, Z.; White, P. S.; Swartz, R.; Goldberg, K. I.; Brookhart, M. *J. Am. Chem. Soc.* **2009**, *131*, 8603.
- ⁵⁶ Baya, M.; Eguillor, B.; Esteruelas, M. A.; Lledós, A.; Oliván, M.; Oñate, E. *Organometallics*, **2007**, *26*, 5140.
- ⁵⁷ Tanabe, T.; Evans, M. E.; Brennessel, W. W.; Jones, W. D. *Organometallics* **2011**, *30*, 834.
- ⁵⁸ Campos J.; López-Serrano, J.; Álvarez, E.; Carmona, E. *J. Am. Chem. Soc.* **2012**, *134*, 7165.
- ⁵⁹ (a) Iron, M. A.; Ben-Ari, E.; Cohen, R.; Milstein, D. *Dalton Trans.* **2009**, 9433. (b) Findlater, M.; Bernskoetter, W. H.; Brookhart, M. *J. Am. Chem. Soc.* **2010**, *132*, 4534.
- ⁶⁰ See for example: (a) Crabtree, R. H. *Angew. Chem. Int. Ed.* **1993**, *32*, 789. (b) Kubas, G. J. *Metal Dihydrogen and sigma-Bond Complexes*; Publishers, K. A., Ed.; New York, **2001**. (c) Kubas, G. J. *Chem. Rev.* **2007**, *107*, 4152.
- ⁶¹ Jellema, E.; Jongerius, A. L.; Reek, J. N. H.; de Bruin, B. *Chem. Soc. Rev.* **2010**, *39*, 1706.
- ⁶² Campos, J.; Esqueda, A. C.; López-Serrano, J.; Sánchez, L.; Cossio, F. P.; de Cózar, A.; Álvarez, E.; Maya, C.; Carmona, E. *J. Am. Chem. Soc.* **2010**, *132*, 16765.
- ⁶³ (a) Klahn, A. H.; Moore, M. H.; Perutz, R. N. *J. Chem. Soc. Chem. Commun.* **1992**, 1699. (b) Fairchild, R. M.; Holman, K. T. *Organometallics* **2008**, *27*, 1823. (c) Fan, L.; Turner, M. L.; Hursthouse, M. B.; Malik, K. M. A.; Gusev, O. V.; Maitlis, P. M. *J. Am. Chem. Soc.* **1994**, *116*, 385. (d) Fan, L.; Wei, C.; Aigbirhio, F. I.; Turner, M. L.; Gusev, O. V.; Morozova, L. N.; Knowles, D. R. T.; Maitlis, P. M. *Organometallics* **1996**, *15*, 98. (e) Kölle, U.; Kang, B.-S.; Thewalt, U. *J. Organomet. Chem.* **1990**, *386*, 267. (f) Yamamoto, Y.; Arakawa, T.; Itoh, K. *Organometallics* **2004**, *23*, 3610.

- ⁶⁴ (a) Braga, A. A. C.; Caballero, A.; Urbano, J.; Díaz-Requejo, M. M.; Pérez, P. J.; Maseras, F. *ChemCatChem* **2011**, 3, 1646. (b) Hansen, J. H.; Parr, B. T.; Pelphrey, P.; Jin, Q.; Autschbach, J.; Davies, H. M. L. *Angew. Chem. Int. Ed.* **2011**, 50, 2544.
- ⁶⁵ (a) Schrock, R. R. *Acc. Chem. Res.* **1986**, 19, 342. (b) Schrock, R. R. *Reactions of Coordinated Ligands*, **1986**, ed. P. R. Braterman, Plenum, New York. (c) Schrock, R. R. *J. Chem. Soc., Dalton Trans.* **2001**, 2541. (d) Fellmann, J. D.; Rupprecht, G. A.; Wood C. D.; Schrock, R. R. *J. Am. Chem. Soc.* **1978**, 100, 5964.
- ⁶⁶ Cotton F. A., Murillo, C. A.; Stiriba, S.-E.; Wang, X.; Yu, R. *Inorg. Chem.* **2005**, 44, 8223.
- ⁶⁷ White, C.; Yates, A.; Maitlis, P. M.; Heinekey, D. M. *Inorg. Synth.* **1992**, 29, 228.
- ⁶⁸ Yakelis, N. A.; Bergman, R. G. *Organometallics*, **2005**, 24, 3579.
- ⁶⁹ Brookhart, M.; Grant, B.; Volpe, Jr. A. F. *Organometallics*, **1992**, 11, 3920.
- ⁷⁰ White, C.; Yates, A.; Maitlis, P. M.; Heinekey, D. M. *Inorg. Synth.* **1992**, 29, 228.
- ⁷¹ Yakelis, N. A.; Bergman, R. G. *Organometallics*, **2005**, 24, 3579.
- ⁷² Baratta, W.; Mealli, C.; Herdtweck, E.; Ienco, A.; Mason, S. A.; Rigo, P. *J. Am. Chem. Soc.* **2004**, 126, 5549.

CONCLUSIONES

CONCLUSIONES

1. El complejo de rodio $[(\eta^5\text{-C}_5\text{Me}_5)\text{Rh}\{\overline{\text{PMe}(2,6\text{-CH}_2(\text{Me})\text{C}_6\text{H}_3)(2,6\text{-Me}_2\text{C}_6\text{H}_3)}\}][\text{BAr}_\text{F}]^+$, **1-BAr_F**, es un catalizador muy eficaz para el intercambio isotópico de hidrógeno en hidrosilanos (Si–H/Si–D/Si–T). Sus reacciones catalíticas pueden llevarse a cabo tanto empleando diversos disolventes orgánicos como en ausencia de disolvente. Se requieren concentraciones de catalizador bajas, y éste puede reciclarse muchas veces sin pérdida de actividad. El catalizador es también muy activo en la hidrosililación de enlaces múltiples C–O y C–N, y estas propiedades han permitido la incorporación de D y T en numerosas moléculas orgánicas mediante procedimientos que en la terminología sajona se conocen como reacciones *one-flask*. Todas estas propiedades convierten a este nuevo método en una técnica experimental simple, benigna desde el punto de vista medioambiental, y robusta desde el técnico. La “economía atómica” en la incorporación de deuterio y tritio en moléculas orgánicas es muy elevada, lo que le confiere mayor importancia.

2. Se ha demostrado que el complejo ciclometalado **1-Cl**, de sencilla preparación, es un excelente precursor para la síntesis de los complejos análogos de tipo haluro (o pseudohaluro), hidruro y alquilo. Se ha constatado el intercambio isotópico H/D en todas las posiciones bencílicas de los complejos **1-Cl** y **1-Br** en presencia de CD₃OD, mientras que en el caso del hidruro **1-H** se ha observado una inusual reacción, catalizada por ácidos, que permite la incorporación selectiva de deuterio en las posiciones Ir-H e Ir-CH₂.

La eliminación del cloruro de **1-Cl** llevó a la formación del compuesto catiónico de Ir(III) **1**⁺, el cual contiene un ligando fosfina, monometalado en uno de los dos grupos 2,6-dimetilfenil, y coordinado a través del átomo de fósforo y de tres átomos de carbono benzílicos (κ^4 -*P,C,C',C''*). Este complejo experimenta una reacción de acoplamiento C-C deshidrogenante catalizada por bases, cuyo resultado es la generación de una mezcla equimolar del complejo hidruro-fosfepina **4**⁺ y el correspondiente dihidruro catiónico de Ir(V) (**1-H**₂⁺). Los estudios realizados permiten concluir que la especie **4**⁺ proviene de un intermedio catiónico que presenta una estructura de alquilo-alquilideno (**6**⁺), el cual experimenta la inserción migratoria del grupo alquilo en el alquilideno, y la posterior eliminación de H_β. Se han preparado además otros alquilidenos de Ir(III) similares y se han estudiado sus estructuras y reactividad.

3. Con objeto de aislar complejos catiónicos estables de Ir(III), conteniendo simultáneamente ligandos hidruro y alquilideno, se prepararon compuestos ciclotmetalados de rodio e iridio con fosfinas del tipo $\text{PR}_2(\text{Xyl})$ ($\text{R} = \text{Me}, \text{Ph}, ^i\text{Pr}, \text{Cy}$). De acuerdo con los precedentes encontrados en la literatura química, se observó que las fosfinas menos voluminosas como $\text{PMe}_2(\text{Xyl})$ y $\text{PPh}_2(\text{Xyl})$ condujeron a los correspondientes aductos catiónicos de CH_2Cl_2 , mientras que las fosfinas más voluminosas, $\text{P}^i\text{Pr}_2(\text{Xyl})$ y $\text{PCy}_2(\text{Xyl})$, permitieron el aislamiento de los correspondientes alquilidenos, los cuales experimentan de manera reversible el desplazamiento 1,2 de un átomo de H en la agrupación $[\text{Ir}](\text{H})(=\text{CRR}')$, es decir, los procesos de inserción migratoria y eliminación de un átomo de hidrógeno H_α . El carácter electrófilo de los nuevos alquilidenos de Ir se demostró mediante su reactividad frente a diversas bases de Lewis, en particular con PMe_3 , que condujo a la formación del correspondiente iluro de trimetilfosfonio, el cual evoluciona con el tiempo para formar el aducto catiónico de trimetilfosfina, termodinámicamente más estable que el iluro.

